frontiers | Research Topics

Biofilm formation and quorum sensing of foodborne microorganism

Edited by
Tao Yu, Lili Li, Lei Yuan, Agapi Doulgeraki and Ramona Iseppi

Published in
Frontiers in Microbiology

ISSN 1664-8714
ISBN 978-2-83251-180-0
DOI 10.3389/978-2-83251-180-0

About Frontiers

Frontiers is more than just an open access publisher of scholarly articles: it is a pioneering approach to the world of academia, radically improving the way scholarly research is managed. The grand vision of Frontiers is a world where all people have an equal opportunity to seek, share and generate knowledge. Frontiers provides immediate and permanent online open access to all its publications, but this alone is not enough to realize our grand goals.

Frontiers journal series

The Frontiers journal series is a multi-tier and interdisciplinary set of open-access, online journals, promising a paradigm shift from the current review, selection and dissemination processes in academic publishing. All Frontiers journals are driven by researchers for researchers; therefore, they constitute a service to the scholarly community. At the same time, the *Frontiers journal series* operates on a revolutionary invention, the tiered publishing system, initially addressing specific communities of scholars, and gradually climbing up to broader public understanding, thus serving the interests of the lay society, too.

Dedication to quality

Each Frontiers article is a landmark of the highest quality, thanks to genuinely collaborative interactions between authors and review editors, who include some of the world's best academicians. Research must be certified by peers before entering a stream of knowledge that may eventually reach the public - and shape society; therefore, Frontiers only applies the most rigorous and unbiased reviews. Frontiers revolutionizes research publishing by freely delivering the most outstanding research, evaluated with no bias from both the academic and social point of view. By applying the most advanced information technologies, Frontiers is catapulting scholarly publishing into a new generation.

What are Frontiers Research Topics?

Frontiers Research Topics are very popular trademarks of the *Frontiers journals series*: they are collections of at least ten articles, all centered on a particular subject. With their unique mix of varied contributions from Original Research to Review Articles, Frontiers Research Topics unify the most influential researchers, the latest key findings and historical advances in a hot research area.

Find out more on how to host your own Frontiers Research Topic or contribute to one as an author by contacting the Frontiers editorial office: frontiersin.org/about/contact

Biofilm formation and quorum sensing of foodborne microorganism

Topic editors

Tao Yu — Xinxiang University, China

Lili Li — Jinan University, China

Lei Yuan — Yangzhou University, China

Agapi Doulgeraki — Institute of Technology of Agricultural Products, Hellenic Agricultural Organization, Greece

Ramona Iseppi — University of Modena and Reggio Emilia, Italy

Citation

Yu, T., Li, L., Yuan, L., Doulgeraki, A., Iseppi, R., eds. (2023). *Biofilm formation and quorum sensing of foodborne microorganism*. Lausanne: Frontiers Media SA. doi: 10.3389/978-2-83251-180-0

Table of contents

frontiers | Frontiers in Microbiology

TYPE Editorial
PUBLISHED 13 December 2022
DOI 10.3389/fmicb.2022.1107603

OPEN ACCESS

EDITED AND REVIEWED BY
Giovanna Suzzi,
University of Teramo, Italy

*CORRESPONDENCE
Tao Yu
✉ yutao7777@hotmail.com
Lei Yuan
✉ leiyuan@yzu.edu.can

SPECIALTY SECTION
This article was submitted to Food Microbiology, a section of the journal Frontiers in Microbiology

RECEIVED 25 November 2022
ACCEPTED 01 December 2022
PUBLISHED 13 December 2022

CITATION
Li L, Yu T, Yuan L, Doulgeraki AI and Iseppi R (2022) Editorial: Biofilm formation and quorum sensing of foodborne microorganism. *Front. Microbiol.* 13:1107603. doi: 10.3389/fmicb.2022.1107603

Editorial: Biofilm formation and quorum sensing of foodborne microorganism

Lili Li[1], Tao Yu[2]*, Lei Yuan[3]*, Agapi I. Doulgeraki[4] and Ramona Iseppi[5]

[1]Institute of Food Safety and Nutrition, Jinan University, Guangzhou, China, [2]School of Life Sciences and Basic Medicine, Xinxiang University, Xinxiang, China, [3]School of Food Science and Technology, Yangzhou University, Yangzhou, China, [4]Institute of Technology of Agricultural Products, Hellenic Agricultural Organization Lycovrissi, Lycovrissi, Greece, [5]Institute of Technology of Agricultural Products, Hellenic Agricultural Organization – DIMITRA, Lycovrissi, Attica, Greece

KEYWORDS

biofilm, quorum sensing, food safety, control, pathogen

Editorial on the Research Topic
Biofilm formation and quorum sensing of foodborne microorganism

Biofilms are a self-protection growth pattern of microorganisms and are commonly defined as communities of microbial cells enclosed in hydrated extracellular polymeric substances and adherent to surfaces (Sauer et al., 2007). Biofilm cells are more resistant to cleaning and disinfection processes in the food industry (Yuan et al., 2021). Therefore, biofilms represent an important source of contamination of raw materials and processed products, posing a serious threat to food safety.

Biofilm formation is a complex process influenced by many factors. Quorum sensing (QS) is a cell-to-cell communication process that allows microorganisms to behave coordinately in response to environmental changes by producing, secreting, and detecting signal molecules (Bassler, 1999; Subramani and Jayaprakashvel, 2019). Previous studies have confirmed that QS plays a significant role in biofilm formation (Zhou et al., 2020) and is vital for food spoilage and food-related pathogenesis (Machado et al., 2020). Understanding of mechanisms behind QS and biofilm formation and exploring control strategies are important to enhance food safety.

In this context, this Research Topic aims to collect recent studies on the following themes:(1) The mechanisms underlying biofilm formation of food microbiology; (2) The role of QS in biofilm formation, food spoilage, and food-related pathogenesis; (3) The novel strategies for biofilm control in food microbiology; (4) Identification of QS inhibitors in food microbiology; (5) QS interfering mechanisms in food microbiology. This Research Topic comprises 8 original research articles from Israel, China, Mexico, Ireland, Iran, and Finland, contributed by 58 authors. Most of contributions focused on the mechanisms underlying biofilm formation, one developed a novel natural antimicrobial substance for biofilm control and one overviewed the literature relating to QS from the perspective of the interactions between the food and human gut microbiome.

The mechanisms underlying biofilm formation of a large number of important foodborne pathogens are still largely unknown. Li et al. investigated the mechanism of biofilm formation in emetic *Bacillus cereus* strains by random mutagenesis and confirmed the dual role of the flagellar hook gene *flgE* in the biofilm formation and cereulide production in emetic *B. cereus*. Cheng et al. determined the role of SdiA in biofilm formation and pathogenicity in *Cronobacter sakazakii* by gene editing technology. They revealed that SdiA enhanced the drug resistance of *C. sakazakii* and suppressed biofilm formation, as well as motility and adhesion. Moreover, Zhang et al. investigated the regulatory function of RpoS on spoilage activity and adhesion ability in *Shewanella baltica* and demonstrated that RpoS is a primary regulator involved in flagellar assembly mediated biofilm formation and cold adaptation-related spoilage activity of *S. baltica*. The results of these studies provide significant insights into the mechanisms underlying biofilm formation and control of bacterial infection.

Biofilm formation is influenced by many factors. Suissa et al. systematically compared five *Lactobacillaceae* strains for the effects of different carbohydrates on their free-living and biofilm lifestyles and indicated that the formation of biofilms and aggregation capacity were responsive to the carbohydrate provided. Avila-Novoa et al. demonstrated that the proportion of components that make up the extracellular matrix are associated with factors such as culture media (less nutrient-rich laboratory medium and supplements of medium) and genetic characteristics of the *Staphylococcus aureus* isolates. Moreover, Zarei et al. analyzed interaction between different foodborne pathogens in dual-species biofilms and illustrated that *Pseudomonas* biofilms may attract and/or shelter other spoilage or pathogenic bacteria, which is of great concern for the dairy industry.

Regarding the role of QS in biofilm formation, Falà et al. summarized and critically discussed the literature, providing a general overview of the current understanding of the prevalence and influence of QS on biofilms, interactions with components of food matrices and host-associated factors in the human gut.

From all the above it seems that novel strategies for biofilm control in food microbiology are urgently needed. To this point, Liu and Wang explored the effects of protocatechuic aldehyde on the biofilm formation and adhesion capabilities of *Vibrio parahaemolyticus*. The results of this study demonstrated that protocatechuic aldehyde can be used to control *V. parahaemolyticus* biofilm to ensure food safety.

The above studies have expanded our understanding on this topic; however, relevant studies about (1) the mechanisms underlying biofilm formation of different bacterial species, (2) the role of QS in biofilm formation and (3) novel strategies for QS interfering and biofilm control still needed for a better understanding of bacterial biofilms.

Author contributions

All authors listed have made a substantial, direct, and intellectual contribution to the work and approved it for publication.

Funding

This work was supported by the National Natural Science Foundation of China (Grant Nos. 31901789 and 32001796), the National Natural Science Foundation of Guangdong Province (Grant No. 2022A1515011685), the call Research-Create-Innovate of Greece (Grant No. T1EDK-03446), and COST Action EuroMicropH (Grant No. CA18113).

Acknowledgments

We deeply thank all the authors and reviewers who have participated in this Research Topic. Finally, we thank all the researchers around the world devote their valuable time into biofilm studies.

Conflict of interest

The authors declare that the research was conducted in the absence of any commercial or financial relationships that could be construed as a potential conflict of interest.

Publisher's note

References

Bassler, B. L. (1999). How bacteria talk to each other: regulation of gene expression by quorum sensing. *Curr. Opin. Microbiol.* 2, 582–587. doi: 10.1016/S1369-5274(99)00025-9

Machado, I., Silva, L. R., Giaouris, E. D., Melo, L. F., and Simões, M. (2020). Quorum sensing in food spoilage and natural-based strategies for its inhibition. *Food Res. Int.* 127, 108754. doi: 10.1016/j.foodres.2019.108754

Sauer, K., Rickard, A. H., and Davies, D. G. (2007). Biofilms and biocomplexity. *Microbe Am. Soc. Microbiol.* 2, 347. doi: 10.1128/microbe.2.347.1

Subramani, R., and Jayaprakashvel, M. (2019). "Bacterial quorum sensing: biofilm formation, survival behaviour and antibiotic resistance," in *Implication of Quorum Sensing and Biofilm Formation in Medicine, Agriculture and Food Industry* (Singapore: Springer), 21–37.

Yuan, L., Sadiq, F. A., Wang, N., Yang, Z., and He, G. (2021). Recent advances in understanding the control of disinfectant-resistant biofilms by hurdle technology in the food industry. *Crit. Rev. Food Sci. Nutr.* 61, 3876–3891. doi: 10.1080/10408398.2020.1809345

Zhou, L., Zhang, Y., Ge, Y., Zhu, X., and Pan, J. (2020). Regulatory mechanisms and promising applications of quorum sensing-inhibiting agents in control of bacterial biofilm formation. *Front. Microbiol.* 11, 589640. doi: 10.3389/fmicb.2020.589640

frontiers | Frontiers in Microbiology

ORIGINAL RESEARCH
published: 06 May 2022
doi: 10.3389/fmicb.2022.901912

SdiA Enhanced the Drug Resistance of *Cronobacter sakazakii* and Suppressed Its Motility, Adhesion and Biofilm Formation

Chuansong Cheng, Xiaotong Yan, Binxiong Liu, Tao Jiang, Ziwen Zhou, Fengting Guo, Qianwen Zhang, Changcheng Li and Ting Fang**

College of Food Science, Fujian Agriculture and Forestry University, Fuzhou, China

Cronobacter sakazakii is a common foodborne pathogen, and the mortality rate of its infection is as high as 40–80%. SdiA acts as a quorum sensing regulator in many foodborne pathogens, but its role in *C. sakazakii* remains unclear. Here, we further determined the effect of the *sdiA* gene in *C. sakazakii* pathogenicity. The *SdiA* gene in *C. sakazakii* was knocked out by gene editing technology, and the biological characteristics of the Δ*sdiA* mutant of *C. sakazakii* were studied, followed by transcriptome analysis to elucidate its effects. The results suggested that *SdiA* gene enhanced the drug resistance of *C. sakazakii* but diminished its motility, adhesion and biofilm formation ability and had no effect on its growth. Transcriptome analysis showed that the Δ*sdiA* upregulated the expression levels of D-galactose operon genes (including *dgoR*, *dgoK*, *dgoA*, *dgoD* and *dgoT*) and flagella-related genes (*FliA* and *FliC*) in *C. sakazakii* and downregulated the expression levels of related genes in the type VI secretion system (*VasK* gene was downregulated by 1.53-fold) and ABC transport system (downregulated by 1.5-fold), indicating that *SdiA* gene was related to the physiological metabolism of *C. sakazakii*. The results were useful for clarifying the pathogenic mechanism of *C. sakazakii* and provide a theoretical basis for controlling bacterial infection.

Keywords: *Cronobacter sakazakii*, quorum sensing receptor, SdiA, transcriptomics, multidrug resistance, biofilm

OPEN ACCESS

Edited by:
Ramona Iseppi, University of Modena and Reggio Emilia, Italy

Reviewed by:
Tom Defoirdt, Ghent University, Belgium
Qingli Dong, University of Shanghai for Science and Technology, China

****Correspondence:***
Changcheng Li
changcheng_li@fafu.edu.cn
Ting Fang
fangting930@163.com

Specialty section:
This article was submitted to Food Microbiology, a section of the journal Frontiers in Microbiology

Received: *22 March 2022*
Accepted: *19 April 2022*
Published: *06 May 2022*

Citation:
Cheng C, Yan X, Liu B, Jiang T, Zhou Z, Guo F, Zhang Q, Li C and Fang T (2022) SdiA Enhanced the Drug Resistance of Cronobacter sakazakii and Suppressed Its Motility, Adhesion and Biofilm Formation. Front. Microbiol. 13:901912. doi: 10.3389/fmicb.2022.901912

INTRODUCTION

Cronobacter sakazakii, a spiral-shaped flagellated Gram-negative rod-shaped bacilli bacterium, is an emerging food-borne opportunistic pathogen that is primarily parasitic in human and animal intestines (Farmer et al., 1980; Guo et al., 2019). *Cronobacter sakazakii* comes from a wide range of sources, and Powdered Infant Formula (PIF) is considered the primary source of infection and medium for transmission (Chap et al., 2009; Ogrodzki and Forsythe, 2017; Odeyemi and Sani, 2019). In addition, *C. sakakazaki* was also isolated from cheese, grains, fruits, vegetables, herbs and meats (Jung and Park, 2006; Jaradat et al., 2009). Neonates and young infants are susceptible to the bacterium that could cause severe clinical presentations of septicemia, meningitis and necrotizing enterocolitis and produce possible life-threatening chronic neurologic sequelae (Hariri et al., 2013; Hunter and Bean, 2013). Unfortunately, the death rate is as high as 40–80% (Wang et al., 2019).

In 2022, the U. S. FDA reported four infant illnesses from three states, and found the four cases related to PIF produced in Abbott nutrition's facility in Sturgis, Michigan. Four hospitalizations resulted from PIF produced environmental contamination by *C. sakakazaki*, and *C. sakakazaki* may have contributed to an infant death in one case (U.S. FDA, 2022).

Quorum sensing (QS) is a collaborative regulation system of bacterial density dependent on multi-gene expression, an environmental signal sensing system for bacteria to monitor their own population density, an important regulatory mechanism involved in adhesion, biofilm formation, virulence and so on (Williams et al., 2000; Anetzberger et al., 2009; Almeida et al., 2016; Stefany et al., 2017). In most Gram-negative bacteria, two major QS systems are autoinducer-1 (AI-1) and autoinducer-2 (AI-2). The AI-1-type QS system is mainly responsible for communication between Gram-negative bacteria. LuxI and LuxR are two key proteins: LuxI synthase produces *N-acyl* homoserine lactones (AHLs) as its own inducers, and the LuxR transcription factor is their homologous receptor (Lars et al., 2001; Assia et al., 2017; Vadakkan et al., 2018; Wang et al., 2018; Pacheco et al., 2021). The AI-2-type QS system is present in both Gram-negative and Gram-positive bacteria, and LuxS is a key protein (Ahmer, 2010; Papenfort and Bassler, 2016).

Interestingly, some Gram-negative bacteria encode LuxR receptors but do not produce AHLs because they lack LuxI synthase. For instance, *Klebsiella pneumoniae*, *Salmonella* and *Enterobacterium* do not have the LuxI synthase gene, and they do not produce AHL signaling molecules (Almeida et al., 2016; Pacheco et al., 2021). However, there is a chromosomal LuxR homolog called SdiA of these bacteria; these bacteria can use the SdiA sensor to sense the signaling molecules produced by other bacteria in the environment and then regulate the expression of their own related genes (Sharma and Bearson, 2013).

SdiA was identified as "a quorum-sensing regulator" that regulates the transcription of *ftsQAZ* operons involved in cell division of *klebsiella pneumoniae*. It has been noted that in *enterohemorrhagic Escherichia coli* (EHEC) and *Enterobacteriaceae*, SdiA is involved in the regulation of many virulence factors, such as pili production, biofilm formation, adhesion and motility of cells (Sharma and Bearson, 2013; Culler et al., 2018; Ma et al., 2020). In addition, *Salmonella* utilizes SdiA proteins to detect AHLs synthesized by other species and enhances *srgE* and *RCK* operon expression (Ahmer, 2010; Almeida et al., 2016). Recent studies have reported that SdiA has an effect on the survival of *C. sakazakii* under different environmental stresses, with improvement of *C. sakazakii* tolerance to heat, desiccation, osmotic and acid stress conditions (Cao et al., 2021). Nevertheless, the function of the QS receptor SdiA in *C. sakazakii* and its underlying mechanisms remain largely unknown. More studies are required to elucidate the exact functions of SdiA on the physiology of these microorganisms since a great level of complexity is observed as revealed by these previous works.

In this study, gene editing technology was used for the construction of an *SdiA* gene deletion mutant to investigate the role of SdiA in *C. sakazakii* pathogenicity by assessing the growth, biofilm formation, motility, adhesion and multidrug resistance of the QS receptor SdiA in *C. sakazakii*. Meanwhile, transcriptome analysis was conducted to elucidate the expression of *SdiA*-related genes.

MATERIALS AND METHODS

Bacterial Strains and Culture Conditions

Cronobacter sakazakii CICC 21550 was obtained from the China Center of Industrial Culture Collection (CICC). *Cronobacter sakazakii* CICC 21550 wild-type (WT) and its mutant (Δ*sdiA*) strains were grown in trypticase soy broth (TSB) or on trypticase soy agar (TSA) at 37°C. Stock cultures of *C. sakazakii* CICC 21550 (WT) and mutant (Δ*sdiA*) strains were maintained in brain heart infusion (BHI) broth with 20% glycerol at −80°C. Activation of the strains was achieved by streaking the stock culture onto violet red bile glucose agar (VRBGA) and incubating for 24 h at 37°C. The WT and Δ*sdiA* strains were stored on VRBGA at 4°C to maintain cell viability.

Equations Sequence Alignment, Construction and Identification of the *SdiA* Deletion Mutant

The nucleotide sequences of the *SdiA* gene and its upstream and downstream genes were obtained based on the whole genome sequencing results of *C. sakazakii* CICC 21550. Primers were designed using Primer 5.0 software (as shown in **Table 1**). All primers were synthesized by Sangon Biotech Co., Ltd. (Shanghai, China). *Cronobacter sakazakii* CICC 21550 genomic DNA was isolated using an Ezup Column Bacteria Genomic DNA Purification kit (Sangon Biotech Co., Ltd, Shanghai, China) according to the manufacturer's recommended protocol and stored at −20°C.

The *SdiA* in-frame deletion mutant was constructed using the suicide plasmid pCVD442, plasmid pKD3 of the chloramphenicol resistance gene and *E. coli* strain β2155. These plasmids and *E. coli* strain β2155 were purchased from BioVector (Biovector NTCC Inc., China). The gene deletion construct was generated according to homologous recombination as previously described (Sharma and Bearson, 2013; Zhang et al., 2018; Cao et al., 2021). Briefly, *SdiA* gene upstream and downstream homologous recombination arms were amplified by PCR from *C. sakazakii* CICC 21550 genomic DNA using primers *SdiA*-5F/*SdiA*-5R and *SdiA*-3F/*SdiA*-3R (**Table 1**). The Cm resistance cassette from plasmid pKD3 was PCR amplified with primers CmSeqF2 and CmSeqR2 (**Table 1**).

The fusion PCR approach was used to construct the *SdiA* gene-targeting vector Δ*SdiA*:Cm (2650 bp, **Figure 1A**), and the fusion PCR product was transformed into the suicide plasmid pCVD442. The plasmids were introduced by electroporation into *E. coli* strain β2155 and plated on TSA containing ampicillin (100 μg/ml) and 0.5 mM 2,6-diaminoheptanedioic acid (DAP) for selection at 37°C. After ligation, the pCVD442-Δ*SdiA*:Cm plasmid was transformed from β2155 into *C. sakazakii* CICC 21550 through conjugation (Zhang et al., 2018). Finally, 100 μL was plated on TSA containing chloramphenicol (17 μg/ml)

TABLE 1 | Primers used in this study.

Primers	Primer Sequence (5′-3′)	Use	References
SdiA-5F	CACCAGTTCGTGGTCATCAACAAG	Upstream homologous recombination arm primers	This study
SdiA-5R	ATTGGACTGATTTGAGCGGATCATTTG		This study
SdiA-3F	CGAAACTCCTGTCGTGCTGTAAG	Downstream homologous recombination arm primers	This study
SdiA-3R	GTGATATCACCATTGATACTGCCAGATC		This study
SdiA-CmF	CAAATGATCCGCTCAAATCAGTCCAATgagctgcttcgaagttccta	Primers amplification of chloramphenicol resistance genes	This study
SdiA-CmR	CTTACAGCACGACAGGAGTTTCGcatatgaatatcctccttagttcctattc		This study
SdiA-outF	CTTCATATCTTCAAGTATGCGTCGTATCC	Lateral identification primers	This study
SdiA-outR	GTAGTATTAACCTGCTGGAACAGCC		This study
SdiA-inF	GCTGAAGTCGCAACGCCAGTTCG	Internal identification primers	This study
SdiA-inR	CTCTCCTGGAACGACGCGCTGTTC		This study
CmSeqF2	ggtgagctggtgatatgggatagtg	Internal primers of chloramphenicol resistance genes	This study
CmSeqR2	cactatcccatatcaccagctcacc		This study

agar plates and cultured in an incubator at 30°C until colonies formed.

The mutant strain was confirmed by PCR analysis using the **Table 1** primer pair. Resistant colonies were streaked onto TSA plates without NaCl but supplemented with 10% sucrose (wt/vol) and chloramphenicol (17 μg/ml) to select for cells in which recombination and loss of the pCVD442 vector occurred. The chloramphenicol resistance gene was removed from the selected mutant using the pCP20 plasmid (Biovector NTCC Inc., China). Transformants were selected at 30°C on TSA plates containing 100 μg/ml ampicillin, and integration was confirmed by PCR with primers *SdiA*-outF/*SdiA*-outR (**Table 1**).

Growth Study

The powdered infant formula (PIF, 0–6 months, Yili Jinlingguanzhenhu) was sterilized by Co60 irradiation (8 kGy, Fujian Compton Irradiation Technology Co., Fuzhou, China) and then sealed and preserved. A single colony of each strain from VRBGA was grown in 10 ml of TSB on a shaker at 130 rpm for 18–20 h at 37°C. Bacterial cells were harvested by centrifugation at 5000 rpm for 15 min at 4°C. Ten milliliters of 0.1% (wt/vol) peptone water (PW)-resuspended bacterial cells were washed off their surface toxins, and the supernatant was discarded. Then, the samples were resuspended in 10 ml of PW, and the bacterial washing step was repeated once (Xie et al., 2020). Subsequently, the solution was resuspended in 5 ml of PW and then diluted with PW to obtain an inoculum containing approximately $10^{4.0-4.5}$ CFU/ml or 4.0–4.5 log CFU/ml of *C. sakazakii*. According to the instructions of PIF, sterilized deionized water was used at high temperature and high pressure (121°C, 20 min) to prepare recovered milk powder. Then, 10 mL of milk was added to sterilizated empty test tubes with 0.1 mL aliquots of WT and Δ*sdiA* mutant cultures.

According to the growth parameters of *C. sakazakii* (Fang et al., 2012), the growth experiment with WT and Δ*sdiA* mutant strains was conducted at fluctuating temperatures. The inoculated samples were incubated at fluctuating temperatures of 8.4°C–48°C, 10°C–47.8°C, and 11°C–35°C. Samples were taken at predesignated time intervals and then serially diluted and plated on TSA plates overnight and enumerated.

Scanning Electron Microscopy

Cells were grown and harvested by the above methods, resuspended in 2.5% glutaraldehyde fixative and fixed at 4°C for 10 h. Subsequently, the cells were washed in 0.1 M phosphate buffered saline (PBS) and dehydrated through graded ethanol solutions. Before EM-30AX scanning electron microscopy (SEM, COXEM, Daejeon, South Korea) observation, the samples were freeze-dried for 8 h and coated with gold.

Swimming and Swarming Motility Assays

The effect of WT and Δ*sdiA* mutant strains on swimming motility was assessed by examining swimming motility on TSA containing 0.3% (wt/vol) agar. *Cronobacter sakazakii* was cultivated in TSB overnight at 37°C in a shaking incubator at 130 rpm. Bacterial cells were diluted to 10^6 CFU/ml after stab-inoculation into 0.3% (wt/vol) TSA agar plates and incubated for 6 h–24 h at 30°C. Motility was assessed quantitatively by measuring the circular swimming motion of the growing motile *C. sakazakii* every 3 h. The effect of WT and Δ*sdiA* mutant strains on swarming motility was assessed by examining swarming motility on TSA containing 0.5% (wt/vol) agar. The same dilution (as mentioned above) was used to inoculate 0.5% (wt/vol) TSA agar plates and incubated for 6 h–36 h at 30°C. Motility was assessed quantitatively by measuring the circular swarming motion of the growing motile *C. sakazakii* every 6 h. The motility assays were repeated in three separate experiments.

Crystal Violet Staining Biofilm Assay

The biofilm forming capacities of the WT and Δ*sdiA* mutant strains were assessed by a crystal violet staining assay (Liu et al., 2018) with slight modifications. Bacterial cells were cultivated in TSB overnight at 37°C until an optical density at 595 nm (OD_{595}) of 0.5 or 10^9 CFU/ml was reached. Thirty microliters of bacterial overnight culture was inoculated into 150 μL of TSB liquid broth in sterile 96-well plates and incubated for 24 h at 37°C. Then, 200 μL of 99% methanol (vol/vol) was added to each well for 15 min to fix the biofilms. After washing three times with 200 μL of 0.1 M PBS and dried in a hot air oven at 55°C for 1 h. The plates were stained with 200 μL of 1% crystal violet for 30 min, washed with 0.1 M PBS two times and then air dried at 37°C.

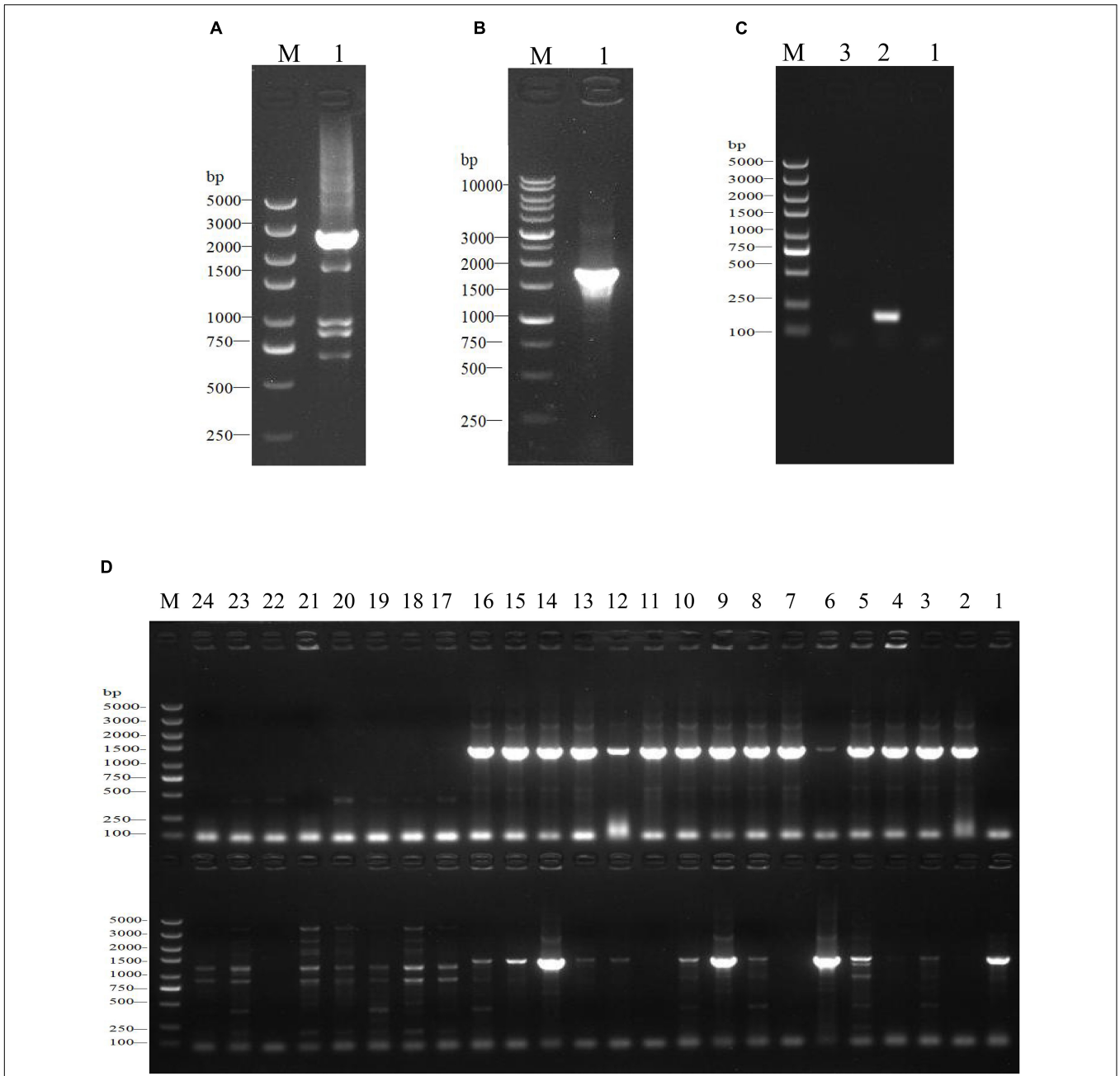

FIGURE 1 | Construction and identification of the *SdiA* deletion mutant of *C. sakazakii* by gel electrophoresis. **(A)** Construction of *SdiA* gene target shooting fragment. M: DL5000 DNA marker; 1: *SdiA* gene target shooting fragment Δ*sdiA*:Cm (2650 bp). **(B,C)** Chloramphenicol resistance gene removal. **(B)** M: DL10000 DNA Marker; 1: Results of identification of lateral primers for colonies growing on non-resistant a TSA plates. **(C)** M: DL5000 DNA marker; 1: Identification results of lateral primers for colonies growing on non-resistant a LB plates; 2: Internal primer amplification results of the original strain (193 bp); 3: No template negative control amplification results. **(D)** Screening of *SdiA* gene knockout strain. M: DL5000 DNA marker; 1–24: Amplification results of primer pairs on both sides of 24 single colonies (Amplification results on both sides of 5′ endpoints above; Amplification results on both sides of the 3′ endpoint are shown below).

Finally, the remaining crystal violet was resuspended in 200 μL of 95% ethanol and measured at 570 nm (OD_{570}) using a microplate reader (SpectraMax®i3x, Molecular Devices, United States). In addition, 200 μL of TSB was used as a blank control, and each sample was set up with six replicates. The biofilm assay was repeated in four separate experiments.

Cell Adhesion Assay

The cell adhesion capacities were measured according to the method of Fabíola (Cacciatore et al., 2020) with slight modifications. The bacterial cells were diluted with PW to 10^8 CFU/mL. The 2 cm × 2 cm samples (made of glass, plastic, silicone hydrogel and stainless steel) were soaked in 10 ml of

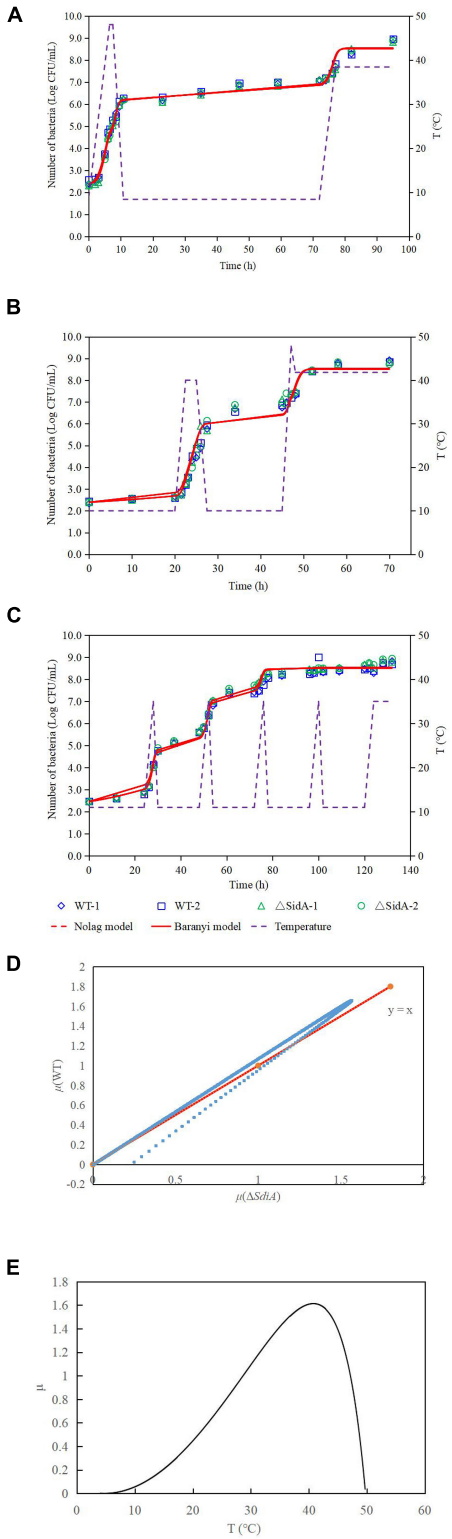

FIGURE 2 | One-step analysis for *C. sakazakii* wild-type and Δ*sdiA* mutant strains. **(A–C)** One-step fitting analysis of the growth curve of *C. sakazakii* WT and Δ*sdiA* mutant strains in powdered infant formula recovery. **(D)** Growth rate distribution of Δ*sdiA* mutant and WT strains. **(E)** One-step analysis: Effect of temperature on growth rate of WT and Δ*sdiA* mutant strains.

bacterial solution, incubated for 15 min at 30°C, and then washed three times with 10 ml of 0.01 M PBS to remove unbound cells. Then, 10 ml of 0.01 M sterile PBS was added for full oscillation to release the adhered cells into the PBS. The adhesion value was determined by counting viable cells on TSA plates. The cell adhesion assay was repeated in three separate experiments.

Tolerance and Resistance Assays

The susceptibility of the WT and Δ*sdiA* mutant strains to different antibiotics was evaluated by the disc diffusion method. The bacterial cells were diluted with PW to 10^8 CFU/mL, and 0.1 mL of bacterial culture was plated onto a TSA plate. The antibiotic resistance was checked against 6 different antibiotics (200 μg/mL and 500 μg/mL): kanamycin, chloramphenicol, rifampicin, erythromycin, tetracycline hydrochloride and penicillin (Macklin Inc., Shanghai, China). Sterilized deionized water was used as a blank control. The sterilized circular filter paper ($\Phi = 8$ mm) was soaked in antibiotic solutions and deionized water for 10 min. Then, the filter papers were removed with sterile tweezers, affixed to a dried TSA plate and incubated for 24 h at 37°C, and the diameter of the antibacterial coil was measured. The tolerance and resistance assay was repeated in three separate experiments. Results are presented as the mean ± SD.

RNA-Seq Analysis

Cronobacter sakazakii WT (W1) and Δ*sdiA* mutant strains (S1) were selected for RNA-Seq analysis. Total RNA was extracted by a UNIQ-10 column TRIzol total RNA extraction kit (Sangon Biotech Co., Ltd, China) using cultures (130 rpm at 37°C) from the logarithmic growth stage. A Ribo-off rRNA Depletion Kit (Bacteria) (Vazyme Biotech Co., Ltd, Nanjing, China) was used to remove rRNA from total RNA samples. The cDNA libraries of RNA samples were constructed using the VAHTS^{TM} Stranded mRNA-seq V2 Library Prep Kit for Illumina® (Vazyme Biotech Co., Ltd, Nanjing, China). The amplified cDNA library was visualized by 8% polyacrylamide gel electrophoresis (PAGE) (Shanghai Furi Technology Co., Ltd, China).

High-throughput sequencing was performed using the Illumina HISeq^{TM} 2500 Platform.

Illumina HISeq^{TM} raw image data files were analyzed by CASAVA Base calling and transformed into sequenced reads. The resulting sequences were then referred to as Raw Data or Raw Reads, and the results were stored in FASTQ file format. Trimmomatic software was used for data processing, the original data quality value and other information were counted, and FastQC software was used for visual evaluation of the sequencing data quality of the samples. Reference to the whole genome sequencing information of the *C. sakazakii* CICC21550 strain for gene alignment analysis, gene expression level analysis and differentially expression analysis. ClusterProfiler software was used for functional enrichment analysis and the main biological functions of differential expressed genes were obtained by comparing the GO (Gene Ontology) database. The related biological system information was obtained by comparative analysis with the KEGG (Kyoto Encyclopedia

of Genes and Genomes) database. All experiments were performed in triplicate.

Statistical Analysis

All experimental results are presented as the mean ± standard deviation, and statistical analysis was performed with SPSS 18.0. The significance of the WT and Δ*sdiA* mutant strains was established through a *t*-test using P values < 0.05.

RESULTS

Construction of a *Cronobacter sakazakii* CICC 21550 Mutant Strain

In this study, we constructed a *C. sakazakii* CICC 21550 strain in which the *SdiA* gene was deleted by gene replacement. Twenty-four single colonies were randomly selected from TSA containing chloramphenicol (17 μg/ml) agar plates for PCR analysis to screen the *SdiA* gene knockout strain. At the 5′ endpoint of the target fragment, a 1368 bp fragment was generated by pairing *SdiA*-outF and CmSeqF2 primers. At the 3′ endpoint, CmSeqR2 and *SdiA*-outR primer pairs produced a 1391 bp fragment. When both fragments were present, the chloramphenicol resistance gene fragment replaced the *SdiA* gene fragment. The results indicated that both sides of clones 9 and 14 were amplified with strong specific PCR products in accordance with the expected length (**Figure 1D**). After the chloramphenicol resistance gene was deleted, the length of the amplified product of the lateral primer was shortened to 1802 bp (**Figures 1B,C**). This assay confirmed that we successfully constructed the *SdiA* deletion strain of *C. sakazakii* CICC 21550.

Growth of *Cronobacter sakazakii* Wild-Type and Δ*sdiA* Mutant Strains in Powdered Infant Formula

The growth model of the WT strain and Δ*sdiA* mutant strains at fluctuating temperatures was constructed using a one-step data analysis method (Jia et al., 2020). **Figure 2D** shows the growth rate distribution of the Δ*sdiA* mutant and WT strains at 4–50°C, and their growth parameters were very similar. There were no significant differences, in that the absence of the *SdiA* gene had no effect on the growth of *C. sakakazakii*. Therefore, we combined the data of the WT and Δ*sdiA* mutant strains to analyze their growth (a total of 260 data points) in the recovered PIF at fluctuating temperatures of 8.4–48°C based on the no lag-Cardinal model and Baranyi-Cardinal models of the one-step data analysis method (Fang and Huang, 2014; Huang, 2017). The statistical results and estimated values of each parameter are shown in **Tables 2**, **3**. The observed values and model prediction curves of the WT and Δ*sdiA* mutant strains at each temperature are shown in **Figures 2A–C**. **Figure 2E** shows the effect of temperature on the growth rate of the WT and Δ*sdiA* mutant strains. The results showed that no lag-Cardinal model and Baranyi-Cardinal model had the same fitting effect on the growth of the *C. sakazakii* WT and Δ*sdiA* mutant strains.

TABLE 2 | One-step analysis results of WT and Δ*sdiA* mutant strains.

Model	RMSE	F-Value	P-Value	AIC
No lag – Cardinal	0.271	2.97×10^4	0	−671.90
Baranyi – Cardinal	0.255	2.8×10^4	0	−703.87

RMSE: The root-mean-square error; AIC: The Akaike Information Criterion.

Hence, we further calculated the influence of *SdiA* gene deletion on the growth parameters of *C. sakazakii* and the growth changes of *C. sakazakii* in PIF. A mathematical model for the growth of *C. sakazakii* WT and Δ*sdiA* mutant strains in the recovered PIF was established by a one-step method. In this study, *C. sakazakii* WT and Δ*sdiA* mutant strain parameters were combined to be estimated by the no lag-Cardinal model and Baranyi-Cardinal model; the minimum growth temperatures estimated by the two models were 4.74°C and 4.70°C, respectively, and the highest growth temperatures were 49.87°C and 49.77°C, respectively. The optimum growth temperatures were 40.87°C and 40.73°C, respectively, and the optimum growth rates were 1.48 h^{-1} and 1.62 h^{-1}, respectively. In addition, the maximum growth concentrations estimated by the no lag-Cardinal model and Baranyi-Cardinal model were 19.67 Ln CFU/ml (8.54 log CFU/ml) and 19.60 Ln CFU/ml (8.51 log CFU/ml), respectively.

Lack of *SdiA* Increases the Swarming and Swimming Motility of *Cronobacter sakazakii*

According to **Figure 3A**, after deletion of the *SdiA* gene in *C. sakazakii*, the swimming motility of the mutant strain (Δ*sdiA*) was markedly enhanced ($p<0.01$). Nonetheless, the WT strain barely spread after 21 h of culture on TSA plates with 0.3% agar. The Δ*sdiA* mutant strain showed a trend of spreading after 6 h of culture. After incubation for 21 h, the Δ*sdiA* mutant strain spread to the entire plate, and the swimming motility of the Δ*sdiA* mutant strain showed a linear increase (**Figure 3C**). Furthermore, the Δ*sdiA* mutant strain showed significantly higher swarming motility than the WT strain and rapidly spread after 18 h of culture ($p<0.05$), showing an exponential growth trend. Although the WT strain indicated a tiny trend of outward diffusion, their movement was still not visible after 36 h of culture (**Figures 3A,D**). In the transcriptomics study of *C. sakazakii* WT and Δ*sdiA* mutant strains, we found that the expression levels of *FliA* and *FliC*-related genes regulating the flagellate of *C. sakazakii* were significantly increased (**Supplementary Tables 1, 3, 4**), which resulted in enhanced flagellate activity and significantly enhanced swarming and swimming motility of *C. sakazakii*.

Lack of *SdiA* Increases the Biofilm Formation and Surface Adhesion Capabilities of *Cronobacter sakazakii*

To evaluate whether SdiA was also involved in the biofilm formation of *C. sakazakii*, we compared the biofilm formation ability of WT and Δ*sdiA* mutant strains. Compared with the WT

TABLE 3 | Parameter estimation of No lag–Cardinal and Baranyi–Cardinal models of wild-type and Δ*sdiA* mutant strains.

Model	Parameter	Estimate	Standard error	t-Value	P-Value	95% Confidence limit	
						Upper	Lower
No lag – Cardinal	μ_{opt}	1.48	0.038	39.492	1.171×10^{-110}	1.41	1.56
	T_{min}	4.74	0.397	11.95	1.968×10^{-26}	3.96	5.52
	T_{opt}	40.87	0.454	90.002	3.080×10^{-195}	39.98	41.77
	T_{max}	49.87	0.603	82.738	3.160×10^{-186}	48.68	51.06
	Y_{max}	19.67	0.077	254.25	9.434×10^{-309}	19.51	19.82
Baranyi – Cardinal	μ_{opt}	1.61	0.043	37.489	1.64×10^{-105}	1.53	1.70
	T_{min}	4.70	0.356	13.219	1.035×10^{-30}	4.00	5.40
	T_{opt}	40.73	0.408	99.73	1.06×10^{-205}	39.93	41.54
	T_{max}	49.77	0.499	99.738	1.039×10^{-205}	48.78	50.75
	Q	−0.204	0.251	−0.812	0.417	−0.699	0.291
	Y_{max}	19.60	0.071	275.98	8.820×10^{-317}	19.46	19.74

strain of *C. sakazakii*, the amount of biofilm formation of the *SdiA* gene deletion strain increased by 77.34%, and the Δ*sdiA* mutant strain showed more biofilm formation ($p < 0.01$) (**Figure 4A**).

We found that the *SdiA* gene regulates the adhesion of *C. sakazakii* to stainless steel, glass and plastics. The adhesion of the WT strain to glass, plastic, silicone hydrogel and stainless steel surfaces was 4.71, 4.35, 4.49 and 4.83 log CFU/cm^2, respectively, at 30°C for 15 min. The adhesion of the Δ*sdiA* mutant strain to glass, plastic, silicone hydrogel and stainless steel was 6.04, 5.68, 4.95 and 6.31 log CFU/cm^2, respectively (**Figure 4B**). The *SdiA* deletion resulted in increased adhesion of *C. sakazakii* on glass, plastic and stainless steel ($p < 0.01$), but there was no significant difference in adhesion between the WT and Δ*sdiA* mutant strains on the silica hydrogel surface. The adhesion of *C. sakazakii* was affected by the dielectric surface, and the adhesion of WT on the plastic surface was lower than that of the other three dielectric materials. However, the adhesion of the Δ*sdiA* mutant strain on the silica hydrogel surface was lower than that of the other three media materials. Through our transcriptomic studies, we also found that the expression of the ATP-active membrane-associated protein *VasK* in the VI secretion system, which is important to the regulation of *C. sakazakii* adhesion, was downregulated by 1.53-fold in *SdiA* mutant strains (**Supplementary Tables 2–4**). PIF packaging, brewing and drinking bottles were mainly made of stainless steel, glass, plastic and silicone hydrogel materials, and *C. sakazakii* was the main food-borne pathogen in PIF. By studying the adhesion of the *SdiA* mutant and WT strains to these materials, we can make it clear that the key to controlling the contamination of *C. sakazakii* during the processing and brewing of PIF was the targeted regulation of the *SdiA* gene.

Lack of *SdiA* Decreases the Multidrug Resistance of *Cronobacter sakazakii*

As shown in **Figure 5**, when the *SdiA* gene was deleted, antibiotic resistance of *C. sakazakii* showed a general decrease. With the increase in antibiotic concentration, the antibacterial zone of antibiotics showing antibacterial effect was larger, among which kanamycin showed the most obvious antibacterial effect and showed relatively good antibacterial effect on WT and Δ*sdiA* mutant strains. Second, penicillin has a certain bacteriostatic effect, but compared with kanamycin, it does not show a strong bacteriostatic effect. Chloramphenicol, rifampicin and tetracycline hydrochloride exhibited approximately the same antibacterial effect, with a slight antibacterial effect. Among the 6 antibiotics, erythromycin showed poor antibacterial activity against *C. sakazakii*, and neither WT nor Δ*sdiA* mutant strains showed an antibacterial zone, showing no visible antibacterial effect. By studying the changes in the transcript level of the *C. sakazakii SdiA* mutant and the wild-type strains, we found that the expression level of related genes in the ABC transport system regulating drug resistance of *C. sakazakii* was downregulated by 1.5-fold (**Supplementary Tables 2–4**) (Wichelecki et al., 2015; Christoph and Robert, 2018), which revealed the mechanism by which the *SdiA* gene enhances drug resistance in *C. sakazakii*.

Lack of *SdiA* Alters the Expression of Genes Involved in Motility, the Virulence Factor and Antimicrobial Resistance of *Cronobacter sakazakii*

By sequencing us through the transcriptome compared with the WT strain, the Δ*sdiA* mutant strain in normal culture showed significant differences in the expression of 244 genes, including 50 genes upregulated and 194 genes downregulated (**Figure 6**). The Δ*sdiA* mutant strain showed significant expression differences in small molecule catabolic (14 genes), polysaccharide metabolic (15 genes), polysaccharide biosynthetic (15 genes), lipid metabolic (19 genes), cellular carbohydrate metabolic (23 genes) and carbohydrate metabolic (32 genes), as well as response to virus and phage shock protein (3 genes), as shown in **Figures 7A,C** ($p < 0.01$). As shown in **Figures 7B,D**, the Δ*sdiA* mutant showed significant differences in lipid and sugar metabolic pathways, including sphingolipid metabolism (2 genes), fructose and mannose metabolism (5 genes), amino sugar and nucleotide sugar metabolism (5 genes) ($p < 0.01$), drug metabolism - cytochrome P450 (2 genes), ether lipid metabolism (1 gene), retinol metabolism (2 genes) ($p < 0.05$) (**Supplementary Tables 3, 4**). These results indicate that the QS transcription

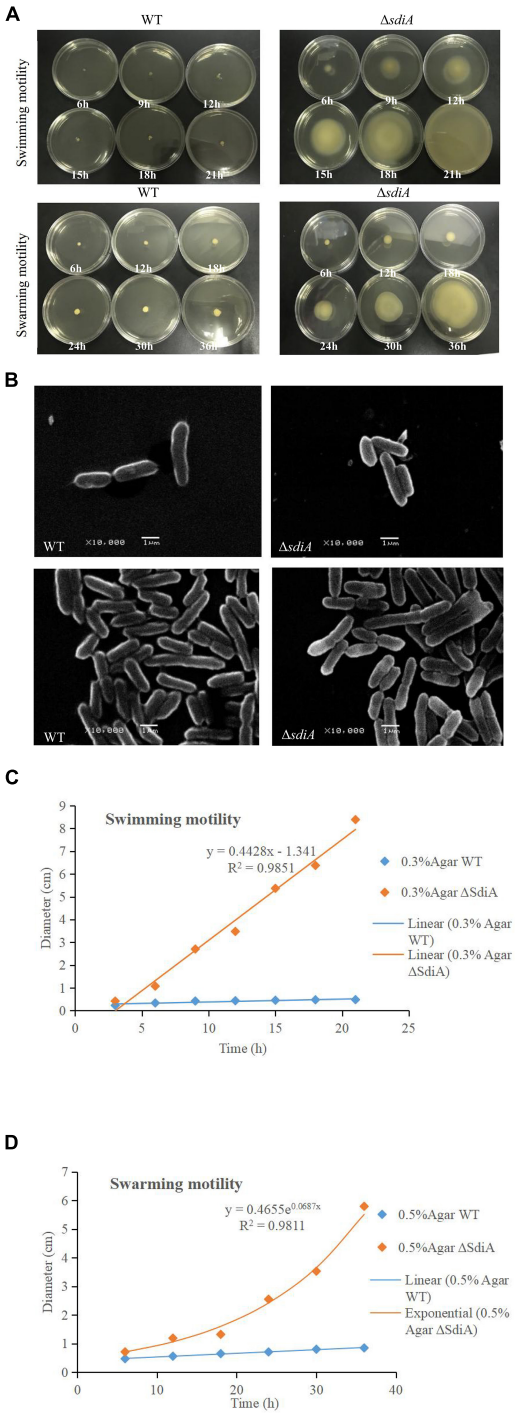

FIGURE 3 | *C. sakazakii* WT and Δ*sdiA* mutant strains cell viability and morphology differences. **(A)** WT and Δ*sdiA* mutant strains motility assay. **(B)** WT and Δ*sdiA* mutant strains scanning electron microscopy (SEM) images. **(C,D)** WT and Δ*sdiA* mutant strains motility assay curve.

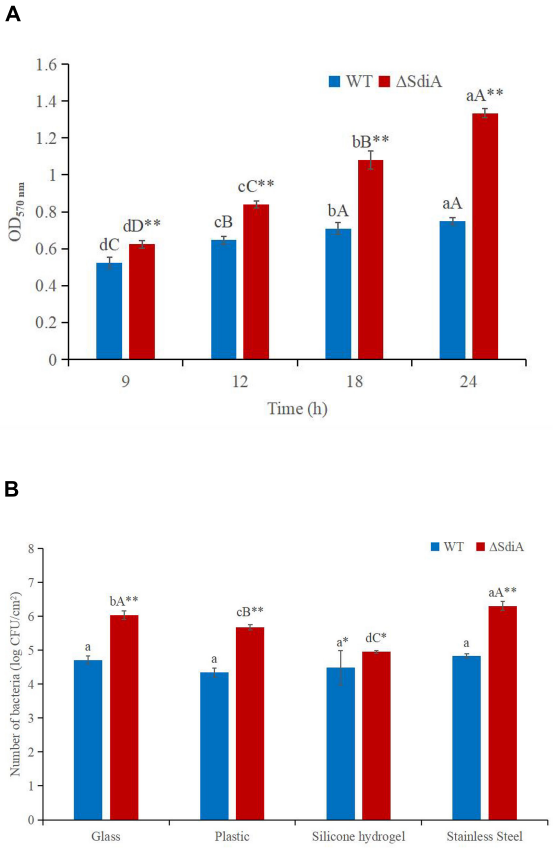

FIGURE 4 | *C. sakazakii* WT and Δ*sdiA* mutant strains biofilm formation and surface adhesion capabilities assay. **(A)** Optical density values of CV solutions obtained from biofilms of *C. sakazakii* WT and Δ*sdiA* mutant strains grown in the TSB at 37°C. $^{a-d}$Mean values differ significantly in different time of each strain ($p < 0.05$), $^{A-D}$means ($p < 0.01$); ** Mean values differ significantly between two strains in the same time ($p < 0.01$). **(B)** Number of adhered *C. sakazakii* WT and Δ*sdiA* mutant strains to different substratum. ^{a}Mean values differ significantly in different substratum of each strain ($p < 0.05$), $^{A-C}$ means ($p < 0.01$); *Mean values differ significantly between two strains in the same substratum ($p < 0.05$), **means ($p < 0.01$). Error bars represent standard deviation. All experimental data's were plotted as mean ± standard from triplicate determinations and statistical analysis was performed with SPSS 18.0 Significance of WT and Δ*sdiA* mutant strains were established through *t*-test using P values < 0.05.

regulator SdiA plays an important role in the cellular activities of *C. sakazakii*, and the mechanism of *SdiA* in each metabolic pathway of *C. sakazakii* needs to be revealed in the future.

Compared to the WT strain, the expression of D-galactose operon-related genes in the Δ*sdiA* deletion strain was markedly upregulated, including the *dgoR*, *dgoK*, *dgoA*, *dgoD* and *dgoT* genes. In addition, the expression levels of the flagellate-related genes *FliA* and *FliC* were significantly increased, and the activity of flagella was enhanced. Consequently, the Δ*sdiA* mutant strain showed significantly enhanced motor activity. Among the upregulated genes, the 6-phospho-glucosidase gene *glvA* was the most significantly upregulated by 5.24-fold (**Supplementary Tables 1, 3, 4**). 6-phosphoglucosidase has oxidoreductase activity, acting on CH-OH donors, NAD or NADP as receptors, and can bind to metal ions to express corresponding functions (Chen et al., 2018).

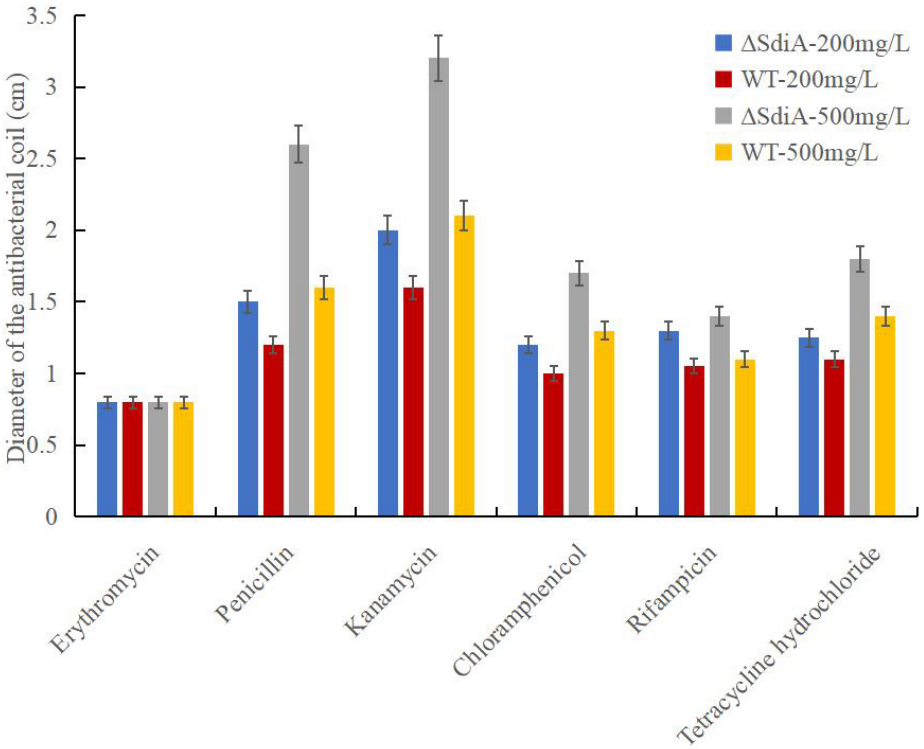

FIGURE 5 | *Cronobacter sakazakii* WT and Δ*sdiA* mutant strains antibiotic resistance assay. Error bars represent standard deviation. All experimental data's were plotted as mean ± standard from triplicate determinations and statistical analysis was performed with SPSS 18.0 Significance of WT and Δ*sdiA* mutant strains were established through *t*-test using P values < 0.05.

The differential gene expression of the *SdiA* gene deletion strain was markedly downregulated, which involved the VI secretion system and ABC transport system (Papenfort and Bassler, 2016). The type VI secretion system is a multifunctional protein secretion system that can directly deliver toxins to eukaryotic cells and other bacteria, and its function is related to virulence host immune resistance and bacterial interactions (Wang et al., 2018). In the downregulated gene expression, the key function of the VI secretory system was the ATP-active membrane-associated protein *VasK*, whose gene expression was downregulated by 1.53-fold. The type VI secretion system plays an important role in the cell adhesion, virulence, invasion and proliferation of *C. sakazakii*; this system also produces protein toxin, which is a potential toxic factor (Chen et al., 2018). Moreover, the expression level of related genes in the ABC transport system was downregulated by 1.5-fold, which may affect the pathogenesis and virulence of *C. sakazakii* and reduce its ability to infect host cells and bacteria in drug resistance (**Supplementary Tables 2–4**) (Wichelecki et al., 2015; Christoph and Robert, 2018).

DISCUSSION

Homologous recombination is a conventional method for constructing gene deletion strains. Based on the principle of DNA homologous recombination, gene knockout technology can be roughly classified as homologous recombination, site-specific recombination and transposable recombination (Zhang et al., 2018). QS is a process of communication between microbial cells, which is closely related to the secretion, colonization, invasion and infection of virulence factors of pathogenic bacteria and the formation of biofilms (Papenfort and Bassler, 2016; Stefany et al., 2017). Nonetheless, the regulatory mechanism of QS on *C. sakazakii* remains largely unknown (Cao et al., 2021). To determine the role of QS in *C. sakazakii*-induced foodborne diseases, it is necessary to construct mutant strains of QS regulatory factors. Cao et al. successfully constructed *SdiA* frame deletion mutants using the suicide T vector pLP12 plasmid and *Escherichia coli* strain β2163 by sequence alignment based on the homologous recombination principle. Additionally, the QS receptor (SdiA) of *C. sakazakii* was screened out and the survival impact of SdiA on *C. sakazakii* under different environmental stresses was verified (Sabag et al., 2015; Cao et al., 2021). In this research, a mutant strain of the *C. sakazakii SdiA* gene was successfully established by homologous recombination and electrical transformation. Moreover, the mechanism of *SdiA* action on the growth, drug resistance, motility, biofilm formation and adhesion of *C. sakazakii* was verified, which laid a foundation for *SdiA* targeted inhibition of the pathogenicity of *C. sakazakii* in PIF food.

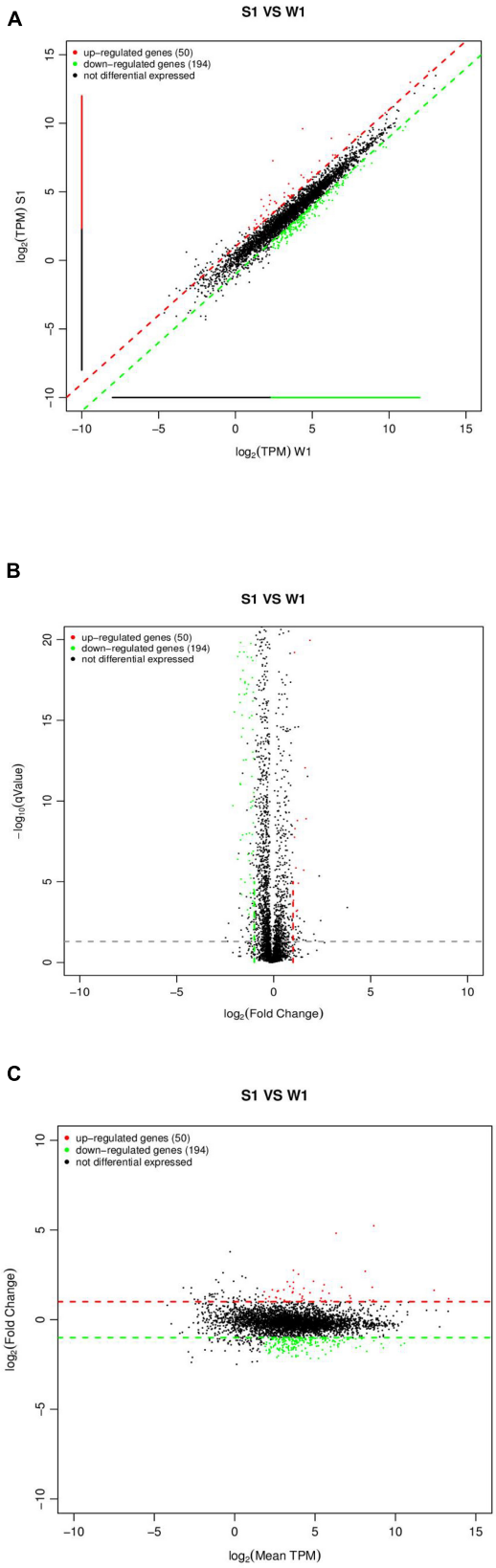

FIGURE 6 | (Continued)

FIGURE 6 | Expression difference analysis for transcriptional profiles [*C. sakazakii* Δ*sdiA* mutant (S1) compared to WT (W1) strains]. **(A)** Comparison group expression difference scatter plot. MeanTPM: Expression amount of a group. The horizontal and vertical axes are, respectively, the $\log_2$ (TPM) values of two groups of samples. Each point in the figure represents a gene, and the closer the point expression is to the origin the lower. The vertical sample is relative to the horizontal sample. **(B)** Comparison group expression difference volcano diagram. The horizontal axis represents the fold-change [$\log_2$ (B/A)] value of gene expression difference between different groups of samples. The vertical axis represents gene expression pValue, the smaller the pValue, the greater the $-\log_{10}$ (pValue), and the more significant the difference. **(C)** MA diagram of expression difference between groups was compared. The horizontal axis is the mean value of $\log_2$ (TPM) of the two groups of samples {[$\log_2$ (A) + $\log_2$ (B)]/2}. The vertical axis is $\log_2$ (Fold Change) [that is, $\log_2$ (B/A)] values.

Prediction of microbiology is a research field that applies mathematical models to predict the growth, inactivation and survival of microorganisms in food (Huang and Hwang, 2017). The two-step method is a classical method to predict microbial modeling, but due to the two-step process, large errors will accumulate in the calculation (Baranyi and Roberts, 1995). A one-step method is to construct the primary model and the secondary model simultaneously according to the observed values. Due to the one-step computation, the accumulated error is small, the fitting is excellent, and the growth parameters of microorganisms can be obtained more precisely (Huang, 2017). In recent years, the one-step predictive microbial model has been reported in the relevant literature, and a good fitting effect has been obtained. For example, the one-step kinetic analysis method was used to simultaneously analyze the growth curve of *Clostridium botulinum* in cooked beef (Huang, 2018) and the growth of *Salmonella* in liquid eggs (Huang, 2015). Fang et al. studied the growth kinetics of thermally damaged *C. sakazakii* in restored infant formula (RPIF) and established a mathematical model to forecast its growth (Fang et al., 2012). In RPIF, a logistic model was used to calculate the minimum and maximum growth temperatures of untreated cells as 6.5°C and 51.4°C, respectively. The Huang model was used to calculate the minimum and maximum growth temperatures of *C. sakazakii* with heat treatment as 6.9°C and 50.1°C, respectively. Although relevant literature has demonstrated the growth model of *C. sakazakii* in recovery PIF, the verification of the model by fluctuating temperature is deficient (Wei et al., 2017). The actual growth of microbes in food is based on practically a dynamic model. Therefore, we studied the actual growth of *C. sakazakii* WT and Δ*sdiA* mutant strains in PIF based on one-step dynamic analysis. Pacheco et al. also found that no significant changes were observed in the growth curves of *Klebsiella pneumoniae SdiA* mutant and wild-type strains. However, cell division was impaired, and cell morphology was abnormal (Pacheco et al., 2021). This is similar to the results found in this study (**Figure 3B**).

The increased motility of the *SdiA* mutant strain may be due to the influence of the *SdiA* gene on the expression of flagellate-related gene in *C. sakazakii*, which enhanced the motility of the mutant strain. Culler et al. studied the atypical *enteropathogenic*

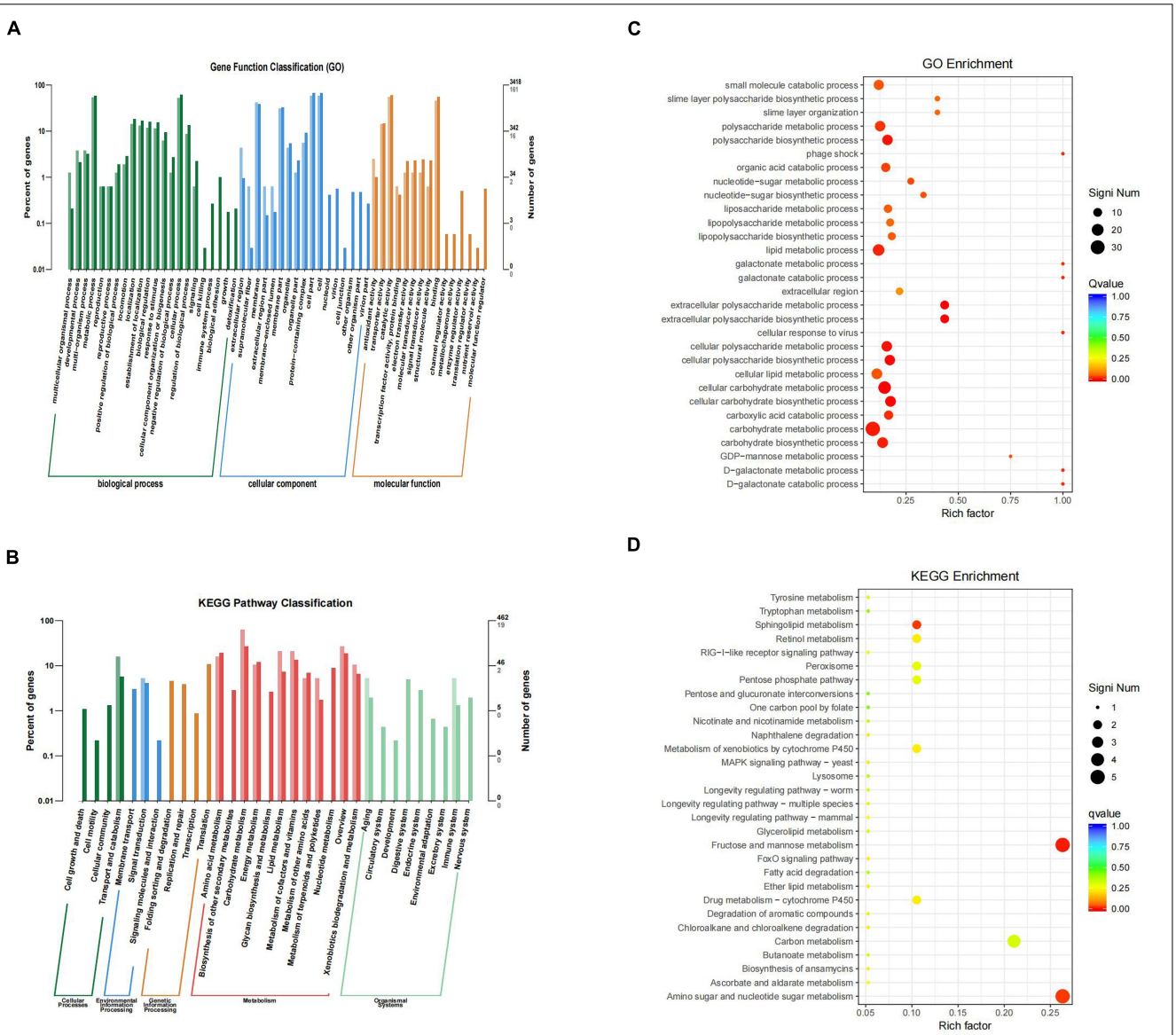

FIGURE 7 | Differential genes classification and enrichment analysis in *C. sakazakii* Δ*sdiA* mutant compared to WT strains. **(A)** Differential genes GO functional classification. **(B)** Differential genes KEGG pathway classification. For A and B, the horizontal axis is a functional classification, and the vertical axis is the number of genes in the classification (right) and their percentage in the total number of genes annotated (left). Different colors represent different categories. Light colors represent different genes and dark colors represent all genes. **(C)** GO function enrichment analysis of *C. sakazakii* Δ*sdiA* mutant compared to WT strains. **(D)** KEGG pathway enrichment of *C. sakazakii* Δ*sdiA* mutant compared to WT strains. For C, the vertical axis represents the annotation of the function; for D, the vertical axis represents the annotation of the metabolic pathway. Rich factor represents the ratio of the number of GO enriched or KEGG enriched in the pathway to the number of annotated genes. The larger the Rich factor, the greater the degree of enrichment. The size of the q value is shown by the color of the dot as shown. The number of differential genes contained under each function or metabolic pathway is shown by the size of dots. The closer q value is to 0, the more significant the enrichment (Only the top 30 GO and KEGG with the highest enrichment degree were selected to draw).

Escherichia coli SdiA gene and discovered that *SdiA* gene deletion demonstrated stronger motility (Culler et al., 2018). Kanamaru et al. showed that the flagellate-related gene *FliC* of *Escherichia coli O157:H7* was negatively regulated by the *SdiA* gene (Kanamaru et al., 2010), which was similar to the conclusion reached in this study. In addition, the cell morphology of the WT and Δ*sdiA* mutant strains was observed by scanning electron microscopy (**Figure 3B**). When the *SdiA* gene of *C. sakazakii* was removed, the overall morphology of the cells was not altered much. However, the Δ*sdiA* mutant strain was more elongated than the WT strain. This may help to enhance the swarming and swimming motility of *C. sakazakii*. In addition to quorum sensing, which can regulate cell movement, virulence factor production and biofilm formation, some similar substances also play such roles. Papenfort and Bassler showed that cyclic dimeric guanosine monophosphate (c-di-GMP) and cyclic adenosine

monophosphate (cAMP), as intracellular second-messenger signaling molecules, regulate bacterial virulence and biofilms (Papenfort and Bassler, 2016).

Culler et al. (2018) studied biofilm formation of atypical *enteropathogenic Escherichia coli* wild-type, *SdiA* mutant and complementary strains. The results showed that the *SdiA* mutant was able to form thicker biofilm structures and exhibit stronger motility. In addition, the transcription of *CsgA*, *CsgD* and *FliC* was increased in the mutant strain, and the addition of AHLs reduced biofilm formation and the transcription of *CsgD*, *CsgA* and *FimA* in the wild-type strain. Sabag et al. (2015) showed that AHL response genes and *SdiA*-dependent genes were identified in the *Enterobacter cloacae* mouse strain, and the presence of the *SdiA* gene inhibited the formation of biofilms. The conclusions from these studies are similar to those from this experiment, indicating that the *SdiA* gene may reduce the amount of bacterial biofilm formation. In this study, the expression levels of the *FliA* and *FliC* genes regulating the flagella of the *C. sakazakii SdiA* deletion strain increased at the transcriptional level, and the flagella activity was enhanced, which strengthened the adhesion process of the *SdiA* deletion strain in biofilm formation and was conducive to the formation of microcolonies. In a plant-related *Escherichia coli*, the *SdiA* mutant terminated the *csgBAC* operon, resulting in excessive pili production and increased adherence and biofilm formation of the *SdiA* mutant strain (Tavío et al., 2010). Sharma and Bearson studied the effect of the QS transcriptional regulator SdiA on the retention of *Escherichia coli O157:H7* in weaned calves and found that SdiA could sense AHLs in the rumen of cattle and enhance the acid resistance of *Escherichia coli O157:H7* to allow *Escherichia coli O157:H7* to persist and colonize the bovine intestine for a period of time (Sharma and Bearson, 2013).

Stefany et al. (2017) showed that bacteria sense environmental changes by secreting their own inducers or receiving external environmental signals through the QS system to cope with the influence of bacterial population density, external pH and antibiotics, such as the antibiotic stress response. Tavío et al. (2010) studied the role of *SdiA* in multidrugresistant strains of *E. coli* and found that the expression of the *SdiA* gene promoted the expression of the multidrug resistance-related gene *acrAB*, leading to the strengthening of drug resistance in *E. coli*. In addition, amplification of *SdiA* can enhance resistance to *mitomycin C* by increasing the ability of chromosome replication and repair.

Carneiro et al. (2020) examined the expression of *SdiA* and genes associated with the nucleotide salvage pathway in *Salmonella* by qRT-PCR and found that *SdiA* affects glucose consumption, metabolism and gene expression in *Salmonella* and is closely related to metabolic pathways associated with glycine, purine, amino acid and aminoacyl tRNA biosynthesis. It plays a role in metabolic optimization under a high population density of *Salmonella*. Cao et al. (2022) found that SdiA may inhibit the formation of *C. sakazakii* biofilms by regulating biosynthesis of flagella and extracellular polymers. Pacheco et al. (2021) that *Klebsiella pneumoniae SdiA* binds to the promoter regions *imA*, LuxS, LSR-LSRA and *ftsQAZ*, and this binding is independent of AHLs. In addition, a lack of *SdiA* can increase the formation of *Klebsiella pneumoniae* biofilms and agglutination of yeast cells and lead to downregulation of type 3 and upregulation of type 1 pili expression. More importantly, *SdiA* inhibits bacterial adhesion and biofilm aggregation (Papenfort and Bassler, 2016; Stefany et al., 2017; Pacheco et al., 2021).

SUMMARY

In summary, we constructed a mutant strain with the *SdiA* gene deletion of *C. sakazakii* CICC21550 using the principle of homologous recombination. The function of the QS-related gene *SdiA* in *C. sakazakii* was analyzed to obtain the relationship between the *SdiA* gene and pathogenicity. The results demonstrated that *SdiA* enhanced the drug resistance of *C. sakazakii* but diminished its motility, adhesion and biofilm formation ability and had no effect on its growth. It can regulate the expression of D-galactose operon genes and flagellum-related gene upregulation and VI secretory system and ABC transport system-related gene expression downregulation. These results are helpful to further explore the function of the *SdiA* gene, revealing the pathogenic mechanism of *C. sakazakii*. Our data provide a new target for therapeutic interventions targeting the pathogenicity of *C. sakazakii* and developing quorum-sensing inhibitors.

DATA AVAILABILITY STATEMENT

The datasets presented in this study can be found in online repositories. The names of the repository/repositories and accession number(s) can be found below: NCBI BioProject – PRJNA820965.

AUTHOR CONTRIBUTIONS

CC conceptualized the experiments, draft preparation, and analyzed the data. XY performed the experiments and collected the experimental data. BL supervised the experimentation and analyzed the data. TJ and ZZ collected and interpretated the data. FG and QZ assisted with critical revision of the manuscript. CL designed the experiment, analyzed data, and revised the manuscript. TF designed the experiment, secured funding, and revised the manuscript. All authors reviewed, revised, and approved the final manuscript.

FUNDING

This work was financially supported by the National Natural Science Foundation of China (NSFC 31601393, 31401597), the National and Science Foundation of Fujian Province (2018J01696), Fujian Agricultural and Forestry University (KXb16012A) and Fujian Education Department (JAT160147), 13th Five-year Plan on Fuzhou Marine Economic Innovation and Development Demonstration City Project.

ACKNOWLEDGMENTS

We would like thank Yanhong Liu and Lihan Huang at the U.S. Department of Agriculture for critical review of the manuscript.

SUPPLEMENTARY MATERIAL

The Supplementary Material for this article can be found online at: https://www.frontiersin.org/articles/10.3389/fmicb.2022.901912/full#supplementary-material

REFERENCES

Ahmer, B. (2010). Cell-to-cell signalling in *Escherichia coli* and *Salmonella enterica*. *Mol. Microbiol.* 52, 933–945. doi: 10.1111/j.1365-2958.2004.04054.x

Almeida, F., Pinto, U. M., and Vanetti, M. (2016). Novel insights from molecular docking of SdiA from *Salmonella enteritidis* and *Escherichia coli* with quorum sensing and quorum quenching molecules. *Microb. Pathog.* 99, 178–190. doi: 10.1016/j.micpath.2016.08.024

Anetzberger, C., Pirch, T., and Jung, K. (2009). Heterogeneity in quorum sensing-regulated bioluminescence of *Vibrio harveyi*. *Mol. Microbiol.* 73, 267–277. doi: 10.1111/j.1365-2958.2009.06768.x

Assia, G., Laure, P., Janek, B., Pauline, J., Benjamin, R., Mikael, E., et al. (2017). Effect of quorum quenching lactonase in clinical isolates of *Pseudomonas aeruginosa* and comparison with quorum sensing inhibitors. *Front. Microbiol.* 8:227. doi: 10.3389/fmicb.2017.00227

Baranyi, J., and Roberts, T. A. (1995). Mathematics of predictive food microbiology. *Int. J. Food Microbiol.* 26, 199–218. doi: 10.1016/0168-1605(94)00121-L

Cacciatore, F. A., Dalmás, M., Maders, C., Isaía, H. A., and Malheiros, P. D. S. (2020). Carvacrol encapsulation into nanostructures: characterization and antimicrobial activity against foodborne pathogens adhered to stainless steel. *Food Res. Int.* 133:109143. doi: 10.1016/j.foodres.2020.109143

Cao, Y., Li, L., Zhang, Y., Liu, F., Xiao, X., Li, X., et al. (2022). Evaluation of *Cronobacter sakazakii* biofilm formation after sdiA knockout in different osmotic pressure conditions. *Food Res. Int.* 151:110886. doi: 10.1016/j.foodres.2021.110886

Cao, Y., Li, L., Zhang, Y., Liu, F., and Yu, Y. (2021). SdiA plays a crucial role in stress tolerance of *C. sakazakii* CICC 21544. *LWT Food Sci. Technol.* 143:111189. doi: 10.1016/j.lwt.2021.111189

Carneiro, D. G., Almeida, F. A. D., Aguilar, A. P., Nívea, M. V., and Vanetti, M. C. D. (2020). *Salmonella enterica* optimizes metabolism after addition of acyl-homoserine lactone under anaerobic conditions. *Front. Microbiol.* 11:1459. doi: 10.3389/fmicb.2020.01459

Chap, J., Jackson, P., Siqueira, R., Gaspar, N., Quintas, C., Park, J., et al. (2009). International survey of *Cronobacter sakazakii* and other *Cronobacter* spp. in follow up formulas and infant foods. *Int. J. Food Microbiol.* 136, 185–188. doi: 10.1016/j.ijfoodmicro.2009.08.005

Chen, Q., Zhu, Y., Qin, Z., Qiu, Y., and Zhao, L. (2018). *Cronobacter* spp., foodborne pathogens threatening neonates and infants. *Front. Agric. Sci. Eng.* 5:330–339. doi: 10.15302/J-FASE-2018208

Christoph, T., and Robert, T. (2018). Multifaceted structures and mechanisms of ABC transport systems in health and disease. *Curr. Opin. Struct. Biol.* 51, 116–128. doi: 10.1016/j.sbi.2018.03.016

Culler, H. F., Couto, S. C. F., Higa, J. S., Ruiz, R. M., and Sircili, M. P. (2018). Role of sdiA on biofilm formation by atypical enteropathogenic *Escherichia coli*. *Genes* 9:253. doi: 10.3390/genes9050253

Fang, T., Gurtler, J. B., and Huang, L. (2012). Growth kinetics and model comparison of *Cronobacter sakazakii* in reconstituted powdered infant formula. *J. Food Sci.* 77, 1–9. doi: 10.1111/j.1750-3841.2012.02873.x

Fang, T., and Huang, L. (2014). Growth and survival kinetics of *Listeria monocytogenes* in cooked egg whites. *Food Control* 36, 191–198. doi: 10.1016/j.foodcont.2013.08.034

Farmer, J. J., Asbury, M. A., Hickman, F. W., and Brenner, D. J. (1980). *Enterobacter sakazakii*: a new species of "Enterobacteriaceae" isolated from clinical specimens. *Int. J. Syst. Bacteriol.* 30, 569–584. doi: 10.1099/00207713-30-3-569

Guo, D., Wang, S., Li, J., Bai, F., and Shi, C. (2019). The antimicrobial activity of coenzyme Q0 against planktonic and biofilm forms of *Cronobacter sakazakii*. *Food Microbiol.* 86:e103337. doi: 10.1016/j.fm.2019.103337

Hariri, S., Joseph, S., and Forsythe, S. J. (2013). *Cronobacter sakazakii* ST4 strains and neonatal meningitis United States. *Emerg. Infect. Dis.* 19, 175–177. doi: 10.3201/eid1901.120649

Huang, L. (2015). Direct construction of predictive models for describing growth of *Salmonella enteritidis* in liquid eggs – a one-step approach. *Food Control* 57, 76–81. doi: 10.1016/j.foodcont.2015.03.051

Huang, L. (2017). Dynamic identification of growth and survival kinetic parameters of microorganisms in foods. *Curr. Opin. Food Sci.* 14, 85–92. doi: 10.1016/j.cofs.2017.01.013

Huang, L. (2018). Growth of non-toxigenic *Clostridium botulinum* mutant LNT01 in cooked beef: one-step kinetic analysis and comparison with *C. sporogenes* and *C. perfringens*. *Food Res. Int.* 107, 248–256. doi: 10.1016/j.foodres.2018.02.028

Huang, L., and Hwang, A. (2017). *Practical Methods in Predictive Food Microbiology*. Boca Raton, FL: CRC Press.

Hunter, C. J., and Bean, J. F. (2013). *Cronobacter*: an emerging opportunistic pathogen associated with neonatal meningitis, sepsis and necrotizing enterocolitis. *J. Perinatol.* 33, 581–585. doi: 10.1038/jp.2013.26

Jaradat, Z. W., Ababneh, Q. O., Saadoun, I. M., Samara, N. A., and Rashdan, A. M. (2009). Isolation of *Cronobacter* spp. (formerly *Enterobacter sakazakii*) from infant food, herbs and environmental samples and the subsequent identification and confirmation of the isolates using biochemical, chromogenic assays, PCR and 16S rRNA sequencing. *BMC Microbiol.* 9:225. doi: 10.1186/1471-2180-9-225

Jia, Z., Bai, W., Li, X., Tfa, B., and Cla, B. (2020). Assessing the growth of *Listeria monocytogenes* in salmon with or without the competition of background microflora-A one-step kinetic analysis. *Food Control* 114:107139. doi: 10.1016/j.foodcont.2020.107139

Jung, M. K., and Park, J. H. (2006). Prevalence and thermal stability of *Enterobacter sakazakii* from unprocessed ready-to-eat agricultural products and powdered infant formulas. *Food Sci. Biotechnol.* 15, 152–157. doi: 10.1016/j.foodpol.2005.08.003

Kanamaru, K., Tatsuno, I., Tobe, T., and Sasakawa, C. (2010). SdiA, an *Escherichia coli* homologue of quorum-sensing regulators, controls the expression of virulence factors in enterohaemorrhagic *Escherichia coli* O157:H7. *Mol. Microbiol.* 38, 805–816. doi: 10.1046/j.1365-2958.2000.02171.x

Lars, R. A., Allan, B. C. B., Sren, M. B., Michael, G. B., and Lone, G. A. (2001). Methods for detecting acylated homoserine lactones produced by gram-negative bacteria and their application in studies of AHL-production kinetics. *J. Microbiol. Methods* 44, 239–251. doi: 10.1016/S0167-7012(01)00217-2

Liu, L., Yan, Y., Feng, L., and Zhu, J. (2018). Quorum sensing asaI mutants affect spoilage phenotypes, motility, and biofilm formation in a marine fish isolate of *Aeromonas salmonicida*. *Food Microbiol.* 76, 40–51. doi: 10.1016/j.fm.2018.04.009

Ma, X., Zhang, S., Xu, Z., Li, H., and Lu, Y. (2020). SdiA improves the acid tolerance of *E. coli* by regulating GadW and GadY expression. *Front. Microbiol.* 11:1078. doi: 10.3389/fmicb.2020.01078

Odeyemi, O. A., and Sani, N. A. (2019). Antibiotic resistance, putative virulence factors and curli fimbrination among *Cronobacter* species. *Microb. Pathog.* 136:103665. doi: 10.1016/j.micpath.2019.103665

Ogrodzki, P., and Forsythe, S. J. (2017). DNA-sequence based typing of the *Cronobacter* genus using MLST, CRISPR-cas array and capsular profiling. *Front. Microbiol.* 8:1875. doi: 10.3389/fmicb.2017.01875

Pacheco, T., Ana, R. I. G., Nathália, M. G. S., Assoni, L., Lúcio, F., and Caldas, F. (2021). SdiA, a quorum-sensing regulator, suppresses fimbriae expression, biofilm formation, and quorum-sensing signaling molecules production in *Klebsiella pneumoniae*. *Front. Microbiol.* 12:597735. doi: 10.3389/fmicb.2021.597735

Papenfort, K., and Bassler, B. (2016). Quorum sensing signal–response systems in gram-negative bacteria. *Nat. Rev. Microbiol.* 14, 576–588. doi: 10.1038/nrmicro.2016.89

Sabag, D. A., Dyszel, J. L., Gonzalez, J. F., Ali, M. M., and Ahmer, B. (2015). Identification of sdiA-regulated genes in a mouse commensal strain of *Enterobacter cloacae*. *Front. Cell Infect. Microbiol.* 5:47. doi: 10.3389/fcimb.2015.00047

Sharma, V. K., and Bearson, S. M. D. (2013). Evaluation of the impact of quorum sensing transcriptional regulator sdiA on long-term persistence and fecal shedding of *Escherichia coli* O157: H7 in weaned calves. *Microb. Pathog.* 57, 21–26. doi: 10.1016/j.micpath.2013.02.002

Stefany, M. G., Sorg, R. A., Domenech, A., Kjo, M., Weissing, F. J., Doorn, G. S. V., et al. (2017). Quorum sensing integrates environmental cues, cell density and cell history to control bacterial competence. *Nat. Commun.* 8, 1–12. doi: 10.1038/s41467-017-00903-y

Tavío, M. M., Aquili, V. D., Poveda, J. B., Antunes, N. T., and Sánchez, C. J. (2010). Quorum-sensing regulator sdiA and marA overexpression is involved in in vitro-selected multidrug resistance of *Escherichia coli*. *J. Antimicrob. Chemother.* 65, 1178–1186. doi: 10.1093/jac/dkq112

U. S. FDA (2022). *FDA Warns Consumers not to Use Certain Powdered Infant Formula Produced in Abbott Nutrition's Facility in Sturgis, Michigan*. Available online at: https://www.fda.gov/news-events/press-announcements/fda-warns-consumers-not-use-certain-powdered-infant-formula-produced-abbott-nutritions-facility (accessed February 20, 2022).

Vadakkan, K., Choudhury, A. A., Gunasekaran, R., Janarthanam, H. B., and Selvaraj, V. A. (2018). Quorum sensing intervened bacterial signaling: pursuit of its cognizance and repression. *J. Genet. Eng. Biotechnol.* 16, 239–252. doi: 10.1016/j.jgeb.2018.07.001

Wang, M., Wang, L., Wu, P., Chen, T. T., Zhu, Y. M., Zhang, Y., et al. (2019). Genomics and experimental analysis reveal a novel factor contributing to the virulence of *Cronobacter sakazakii* strains associated with neonate infection. *J. Infect. Dis.* 220, 306–315. doi: 10.1093/infdis/jiz098

Wang, Y., Wang, Y., Sun, L., Daniel, G., and Li, Y. (2018). The LuxS/AI-2 system of *Streptococcus suis*. *Appl. Microbiol. Biotechnol.* 102, 7231–7238. doi: 10.1007/s00253-018-9170-7

Wei, Q., Gong, X. L., Lin, J. Y., Zhang, X. Y., Jiang, Y. J., and Fang, T. (2017). The biological properties of *Cronobacter sakazakii* and its predictive model in infant formula. *J. Chin. Food Sci. Technol.* 17, 58–64. doi: 10.16429/j.1009-7848.2017.04.008

Wichelecki, D. J., Vetting, M. W., Chou, L., Al-Obaidi, N., Bouvier, J. T., Almo, S. C., et al. (2015). TP-binding cassette (ABC) transport system solute-binding protein-guided identification of novel d-Altritol and galactitol catabolic pathways in *Agrobacterium tumefaciens* C58. *J. Biol. Chem.* 290, 28963–28976. doi: 10.1074/jbc.M115.686857

Williams, P., Camara, M., Hardman, A., Swift, S., Hope, V. J., Winzer, K., et al. (2000). Quorum sensing and population-dependent control of virulence. *Philos. Trans. R. Soc. Lond. B Biol. Sci.* 355, 667–680. doi: 10.1098/rstb.2000.0607

Xie, Z. P., Peng, Y. B., Li, C. C., Luo, X. J., Fang, T., and Huang, L. (2020). Growth kinetics of *Staphylococcus aureus* and background microorganisms in camel milk. *J. Dairy Sci.* 103, 9958–9968. doi: 10.3168/jds.2020-18616

Zhang, X., Cai, X., Yi, Q., Liu, Y., Qi, C., Wang, X., et al. (2018). Improvement in the efficiency of natural transformation of *Haemophilus parasuis* by shuttle-plasmid methylation. *Plasmid* 98, 8–14. doi: 10.1016/j.plasmid.2018.07.001

Conflict of Interest: The authors declare that the research was conducted in the absence of any commercial or financial relationships that could be construed as a potential conflict of interest.

Publisher's Note: All claims expressed in this article are solely those of the authors and do not necessarily represent those of their affiliated organizations, or those of the publisher, the editors and the reviewers. Any product that may be evaluated in this article, or claim that may be made by its manufacturer, is not guaranteed or endorsed by the publisher.

frontiers | Frontiers in Microbiology

ORIGINAL RESEARCH
published: 10 June 2022
doi: 10.3389/fmicb.2022.897836

A Flagella Hook Coding Gene *flgE* Positively Affects Biofilm Formation and Cereulide Production in Emetic *Bacillus cereus*

Yangfu Li[1,2†], Nuo Chen[1,2†], Qingping Wu[2], Xinmin Liang[1,2], Xiaoming Yuan[1,2], Zhenjun Zhu[1], Yin Zheng[1], Shubo Yu[2], Moutong Chen[2], Jumei Zhang[2], Juan Wang[3] and Yu Ding[1,2]**

[1] Department of Food Science and Technology, Institute of Food Safety and Nutrition, Jinan University, Guangzhou, China, [2] State Key Laboratory of Applied Microbiology Southern China, Key Laboratory of Agricultural Microbiomics and Precision Application, Ministry of Agriculture and Rural Affairs, Guangdong Provincial Key Laboratory of Microbial Safety and Health, Institute of Microbiology, Guangdong Academy of Sciences, Guangzhou, China, [3] College of Food Science, South China Agricultural University, Guangzhou, China

OPEN ACCESS

Edited by:
Lei Yuan,
Yangzhou University, China

Reviewed by:
Hongshun Yang,
National University of Singapore, Singapore
Xiaodong Xia,
Dalian Polytechnic University, China

***Correspondence:**
Juan Wang
wangjuan@scau.edu.cn
Yu Ding
dingyu@jnu.edu.cn

[†]These authors have contributed equally to this work

Specialty section:
This article was submitted to Food Microbiology, a section of the journal Frontiers in Microbiology

Received: 16 March 2022
Accepted: 10 May 2022
Published: 10 June 2022

Citation:
Li Y, Chen N, Wu Q, Liang X, Yuan X, Zhu Z, Zheng Y, Yu S, Chen M, Zhang J, Wang J and Ding Y (2022) A Flagella Hook Coding Gene flgE Positively Affects Biofilm Formation and Cereulide Production in Emetic Bacillus cereus. Front. Microbiol. 13:897836. doi: 10.3389/fmicb.2022.897836

Bacillus cereus, an important foodborne pathogen, poses a risk to food safety and quality. Robust biofilm formation ability is one of the key properties that is responsible for the food contamination and food poisoning caused by *B. cereus*, especially the emetic strains. To investigate the mechanism of biofilm formation in emetic *B. cereus* strains, we screened for the mutants that fail to form biofilms by using random mutagenesis toward *B. cereus* 892-1, an emetic strain with strong biofilm formation ability. When knocking out *flgE*, a flagellar hook encoding gene, the mutant showed disappearance of flagellar structure and swimming ability. Further analysis revealed that both pellicle and ring presented defects in the null mutant compared with the wild-type and complementary strains. Compared with the flagellar paralytic strains Δ *motA* and Δ *motB*, the inhibition of biofilm formation by Δ *flgE* is not only caused by the inhibition of motility. Interestingly, Δ *flgE* also decreased the synthesis of cereulide. To our knowledge, this is the first report showing that a flagellar component can both affect the biofilm formation and cereulide production in emetic *B. cereus*, which can be used as the target to control the biohazard of emetic *B. cereus*.

Keywords: *Bacillus cereus*, biofilm, flagella, cereulide, motility

INTRODUCTION

Bacillus cereus, a Gram-positive, spore-forming, and facultative anaerobe with flagella, is an important pathogen associated with foodborne outbreaks worldwide and causing clinical manifestations like gastroenteritis, emesis, fulminant bacteremia, bone infection, and brain abscess (Majed et al., 2016; Enosi Tuipulotu et al., 2021). Two types of food poisoning can be caused by *B. cereus*, including diarrhea and vomiting (Zhou et al., 2019), with the latter one triggered by cereulide, which is preformed in food (Naranjo et al., 2011). Although symptoms caused by cereulide are usually self-limiting (Rouzeau-Szynalski et al., 2020), fatal cases have been reported (Mahler et al., 1997; Dierick et al., 2005; Shiota et al., 2010; Naranjo et al., 2011).

Cereulide is synthesized by enzymes encoded by the *ces* gene cluster located on a 270-kb mega-plasmid, named pCER270, which displayed a high similarity in sequence with the plasmid pXO1 in *Bacillus anthracis* (Rasko et al., 2007). After ingestion, cereulide is absorbed in the intestine and distributed throughout the body, which can be detected in the stomach, spleen, liver, kidney, muscles, and fat tissues, or even crossed the blood-brain barrier (Bauer et al., 2018). Chronic cereulide exposure induced endoplasmic reticulum stress response, intestinal inflammation, dysregulation of intestinal flora, and inhibition of serotonin biosynthesis (Lin et al., 2021). Notably, cereulide is stable to trypsin, acid, and heat (121°C for 2 h) (Dommel et al., 2010; Jovanovic et al., 2021), so conventional food processing conditions are unable to inactivate it. Emetic strains that produce cereulide are ubiquitous in different kinds of food, of which dairy products account for a relatively high proportion (Shaheen et al., 2006; Messelhäusser et al., 2010; Owusu-Kwarteng et al., 2017; Gao et al., 2018), e.g., emetic strains are found in 21% raw milk samples, in which 1,140 ng/mL cereulide can be detected (Rajkovic et al., 2006; Owusu-Kwarteng et al., 2017). It was reported cereulide caused food poisoning to an adult and rapid death of a healthy 1-year-old boy (Shiota et al., 2010) at a very low concentration (4 ng/mL in the serum). Since food poisoning outbreaks caused by emetic *B. cereus* resulted in severe cases, the presence of emetic *B. cereus* in the food and food processing chain is of great concern to food safety. Therefore, it is very important to eliminate emetic *B. cereus* in food.

Biofilm is a sessile community of microbes that adhere to the surface of abiotic or living tissue and are coated with the extracellular polymer matrix (EPS) produced by the microbes to adapt to the living environment (Costerton et al., 1999). Because of the shelter of EPS, bacteria can survive under stress conditions, including disinfectants and antimicrobials (biocides) in the biofilm lifestyle than in the planktonic form (Alvarez-Ordóñez et al., 2019). Biofilm is also the reservoir of spores, which are more resistant to heat, acid, and low water activity, and the biofilm lifestyle provides a higher proportion of spores than in planktonic culture (Ribeiro et al., 2019; Rouzeau-Szynalski et al., 2020). Since the clean-in-place (CIP) system commonly used in the food processing chain cannot eliminate spores (Thomas and Sathian, 2014), *Bacillus* becomes the dominant taxa in the milk processing chain (Kable et al., 2019). Once the biofilm is formed, it is inevitable to cause contamination in the processing environments and final products (Ostrov et al., 2016; Silva et al., 2018).

Bacillus subtilis is a model organism for studying regulatory networks directing biofilm formation among Gram-positive and spore-forming bacteria. Genes and regulatory pathways controlling biofilm formation have been well studied in *B. subtilis* (Vlamakis et al., 2013; Mielich-Süss and Lopez, 2015). In contrast to *B. subtilis*, few genes were involved in biofilm formation have been characterized in *B. cereus* and the regulatory mechanisms that control biofilm formation are poorly understood. *Bacillus cereus* produces different forms of biofilms including submerged biofilm, pellicle, and ring, that differ in their architecture and may be regulated by different genetic determinants (Wijman et al., 2007; Caro-Astorga et al., 2014; Gao et al., 2015). Previous studies showed that Spo0A and CodY act as key regulators in biofilm formation in *B. cereus* (Lindbäck et al., 2012; Gao et al., 2015). Besides, motility and flagella may involve in biofilm formation in *B. cereus* (Houry et al., 2010). Although a variety of genes were found by a genome-wide investigation with random mutagenesis and RNA sequencing, current knowledge about *B. cereus* biofilm formation, especially in the emetic strains, is still largely unknown (Yan et al., 2017).

In this study, we constructed a transposon mutagenesis library of an emetic *B. cereus* strain 892-1 with strong biofilm-forming ability, which was isolated from pasteurized milk (Gao et al., 2018). By high-throughput screening of biofilm-defective mutants, we successfully identified a mutant named 3-86, which showed a significant defect in biofilm formation. Further analysis found that the insertion site of the transposon is a flagellar hook encoding gene *flgE*, which not only has a positive regulation function in biofilm formation but also affects cereulide production. To our knowledge, this is the first time to illustrate the function of a flagellar hook encoding gene *flgE* on both biofilm formation and cereulide production in emetic *B. cereus*. Therefore, this study may provide a new strategy for the control of food contamination and poisoning incidents caused by emetic *B. cereus*.

MATERIALS AND METHODS

Bacterial Strains and Culture Condition

Bacillus cereus 892-1 and its derivatives were cultured in tryptic soy broth (TSB; Guangdong Huankai Co., Ltd., Guangzhou, China) at 37°C, 200 rpm, or on nutrient agar plates (Guangdong Huankai Co., Ltd.) at 37°C. *Escherichia coli* strains were grown at 37°C in luria-bertani broth (LB; Guangdong Huankai Co., Ltd.). When needed, antibiotics were added at the following concentrations: 5 μg/mL of erythromycin, 17 μg/mL chloramphenicol for the growth of *B. cereus*, and 100 μg/mL of ampicillin for the growth of *E. coli*. A list of strains and plasmids used in this work is provided in **Supplementary Table 1**. Oligonucleotides are listed in **Supplementary Table 2**.

Construction of Transposon Mutagenesis Library

The construction and screening steps of a transposon mutagenesis library were depicted in **Figure 1**. The plasmid pMarA (Gao et al., 2019) carrying a mariner-based transposon Tn*YLB*-1 was used as the backbone. To replace the selectable marker kanamycin resistance cassette, the chloromycin resistance cassette was amplified from pBAD33 (Guzman et al., 1995). The newly generated plasmid, named pMarA-cat, was transformed into the strain 892-1 by electroporation, followed by the selection for both Erm^R (erythromycin-resistant) and $Chlo^R$ (chloramphenicol-resistant) colonies at 28°C. Positive transformants were inoculated at 37°C, 200 rpm overnight to induce transposon-mediated mutagenesis. Fifty microliters of diluted cultures (1:100,000, v:v) were then spread onto LB agar plates containing chloramphenicol and incubated at 48°C for 10 h to induce plasmid suicide. The biofilm phenotypes of

each mutant was screened by a microplate reader (Gen5^{TM}, BioTek, Winooski, VT, United States). Then, potential mutants with altered phenotypes were verified by antibiotic selection, which are resistant to chloramphenicol (Chlo^{R}) and sensitive to erythromycin (Erm^{S}). To select mutants containing a transposon insertion, a quick DNA extraction method was used. Briefly, a single colony was suspended into 30 μL ddH_2O in a 1.5 mL tube and then ultrasonically treated at 40 kHz at 25°C for 5 min. Then, the mixture was centrifuged at 10,000 *g*, 25°C for 1 min. Afterward, the upper aqueous phase was carefully transferred to a new 1.5 mL tube without disturbing the pellet. The DNA samples was tested by the polymerase chain reaction (PCR). To confirm the transposon insertion site, restriction endonuclease *Taq* I (ER0671, Thermo Fisher Scientific Inc., Waltham, MA, United States) was used to cut the genomic DNA.The genome fragments were self-ligated by T4 DNA ligase at 25°C for 10 min (EL0014, Thermo Fisher Scientific, Waltham, MA, United States), and reverse PCR was performed using primer OIPCR-1/2 to amplify the sequence inserted by Tn*YLB*-1 transposon. After sequencing, the insertion sites were identified by local blast (ncbi-blast-2.12.0+ -win64).

Construction of Deletion Mutant and Complementary Strain

Different strains was constructed as described previously (Qi et al., 2011). Plasmid pHT304-TS (Zhu et al., 2011) was used to construct mutants by homologous recombination. Recombinant plasmids were generated by in-fusion cloning (Ma et al., 2019). Briefly, the vector was linearized by restriction endonuclease *EcoR* I and *Sal* I (1611 and 1636, Takara, Shiga, Japan) digestion. The upstream and downstream fragments were amplified by using genome DNA as the template. 5′ end of the forward and reverse primers of inserts were amplified by PCR with 15-20 bp homolog fragments of linearized vector. Then, the mixture of inserts, linearized vector, and 2 × Hieff Clone® Enzyme Premix (10912 and 10911, Yeasen, Shanghai, China) was incubated at 50°C for 1 h by using a thermo-cycler (C1000 Touch, Bio-Rad, Hercules, CA, United States). The mixture was then transformed into *E. coli* DH5α by thermal shock directly.

For the construction of mutants, including Δ*flgE*, Δ*motA*, and Δ*motB*, recombinant plasmids were transformed into *B. cereus* 892-1 by electroporation as mentioned above. One milliliter SOC media was immediately added to suspend the bacteria and the mixture was then incubated at 30°C, 200 rpm for 3 h. After incubation, the bacteria were collected by centrifugation at 25°C 5,000 *g* for 2 min and then spread on an LB agar plate with erythromycin. Plates were incubated overnight in an incubator at 30°C and potential transformants were confirmed by PCR. For gene knockout, positive transformants were transferred to media with erythromycin and incubated at 42°C, 200 rpm for 6–12 h, and this process was repeated 6 times. Then, strains were incubated at 30°C, 200 rpm for 6–12 h for 9–12 times and spread on LB agar plates without antibiotics. Colonies were then transferred on LB agar plates with antibiotics, and the ones that could not grow on the plates were detected by PCR and sent for sequencing. For the construction of complementary strains, plasmid pHT304 (Arantes and Lereclus, 1991) was used. The gene was cloned into plasmid pHT304 by in-fusion cloning as described above. Recombinant plasmids and electroporation were followed as described above and positive transformants were used for the following experiments.

Growth Curve of Different Strains

To evaluate the effect of gene deletion and complementation on bacterial growth, overnight cultures were diluted 1,000-fold (v:v) into fresh TSB broth, and then 200 μL of bacterial suspension was added to the wells of a 96-well plate. In total, three biological repeats with six technical repeats each were performed. Bacterial growth was monitored by measuring the optical density at OD_{600} of each well at 37°C every 30 min for 12 h by using a microplate spectrophotometer (EPOCH2, Biotek, Vermont, United States) and the data were analyzed by GraphPad Prism (v8.0.2) to generate XY plots.

Biofilm Formation Assay

For pellicle formation analysis, *B. cereus* strains were grown overnight at 37°C, 200 rpm. Five microliters of overnight culture were inoculated into 5 mL TSB medium in a test tube, which was then statically incubated at 37°C for 12 h. The formation of the pellicle was recorded by a Nikon D750 camera. Evaluation of the ring part was performed as previously described with minor modifications (Stepanović et al., 2000). Briefly, Bacteria (3.3×10^5 cfu/mL) were inoculated into 200 μL fresh TSB medium in 96-well polystyrene plates (Costar, Washington, DC, United States), and incubated at 37°C for 12 h statically. Then, planktonic cells were poured out, and plates were washed three times with ddH_2O. The remaining attached biofilms were dried and fixed with 210 μL of 95% methanol per well for 15 min. After drying, 210 μL of crystal violet (0.1%; w/v) was added to each well and incubated for 15 min to stain biofilms attached to the well surface. After briefly washing three times and drying, the crystal violet was dissolved in 220 μL of 30% acetic acid, and staining levels were assessed by measuring absorbance at 590 nm (A_{590}).

Scanning Electron Microscopy

Overnight cultures were diluted to an OD_{600} of 0.001 in TSB broth and biofilms were grown on 8 mm × 8 mm glass coverslips (WHB-48-CS, WHB, Shanghai, China) in 12-well plates (Costar, Washington, DC, United States) for 12 h at 37°C. Biofilms formed on the surface of the cell slide were fixed with 3% (w/v) glutaraldehyde overnight at 4°C. Samples were then dehydrated with a graded ethanol series, dried, sputter-coated with gold, and imaged by a scanning electron microscope (Hitachi S-3000N, Tokyo, Japan) operating at 20 kV and 83 μA.

Confocal Laser Scanning Microscopy Analysis

The biofilm structure was visualized by confocal laser scanning microscopy (CLSM) as described previously (Zhao et al., 2022) with minor modifications. Overnight cultures were diluted 1,000 (v:v) times in 50 mL fresh TSB broth and biofilms were grown in a beaker (100 mL volume), which were then observed

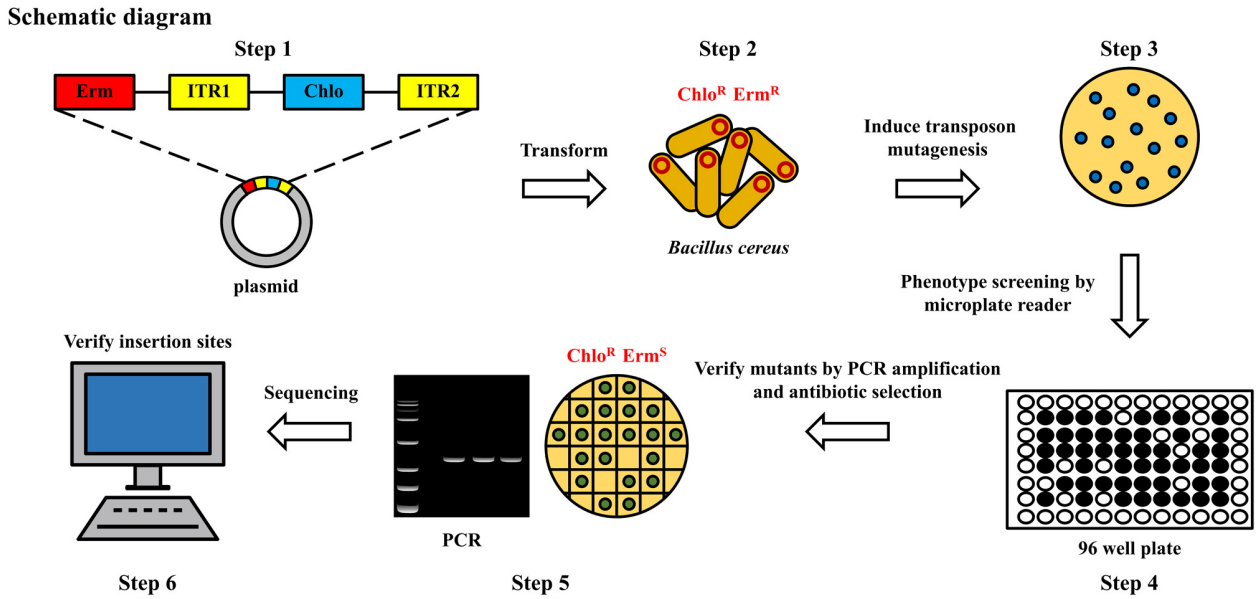

FIGURE 1 | Flow chart of construction of random mutagenesis library to screen the potential mutants with defects in biofilm formation. Erm, erythromycin; Chlo, chloromycin; R, resistant; S, sensitive; ITR1/ITR2, transposon.

using a confocal laser scanning microscope (ZEISS LSM700, Oberkochen, Germany). Biofilms without planktonic cells were stained using SYTO® 9 (Thermo Fisher Scientific Inc., Waltham, MA, United States) at 25°C in the dark for 2 min. Biofilms were then visualized using a CLSM by a 20× objective lens with excitation at 488 nm and emission at 500–550 nm. The images were processed by using the Zeiss ZEN (v3.5).

Transmission Electron Microscopy

Different samples were examined by transmission electron microscopy (TEM; Tecnai G2 F20 S-TWIN, Thermo Fisher Scientific Inc., Waltham, MA, United States) for the appearance of flagella. Overnight cultures were diluted 1,000 (v:v) times with fresh TSB broth and statically cultured at 37°C for 7 h. The bacterial suspension was spotted onto a copper grid and air-dried. Then, the samples were stained using 3% phosphotungstic acid for 2 min and observed using the TEM.

Bacterial Motility Assay

The swimming assay was performed according to a previous study (Singh et al., 2016) with some modifications. Swimming plates contained 1% tryptone, 0.5% NaCl, and 0.25% agar. For conducting the swimming assays, 1 μL overnight cultures were spotted on the agar plate and incubated at 37°C statically for 12 h. After that, the plate was imaged by using a camera (Nikon D750, Japan).

Bioinformatic Analysis

Query amino acid sequences of MotA (Houry et al., 2010) (*B. cereus* ATCC14579) and MotB (Cairns et al., 2013) (*B. subtilis* NCIB3610) by BLASTP (ncbi-blast-2.12.0+ -win64). Alignment of amino acid sequences (**Supplementary Figure 1**) was performed by CLUSTALW[1] and ESPript 3.0[2] (Robert and Gouet, 2014).

Total RNA Isolation, cDNA Synthesis and Reverse Transcription-qPCR Analysis

RNA isolation and purification were performed using the RNeasy Mini Kit (74104, Qiagen, Hilden, Germany) according to the manufacturer's instructions. RNA concentration and purification were measured with a NanoDrop One Spectrophotometer (Thermo Fisher Scientific, Waltham, MA, United States). For RT-qPCR (reverse transcription-qPCR), purified RNA was used to synthesize cDNA according to the instructions of the PrimeScript™ RT reagent Kit with gDNA Eraser (RR047A, Takara, Shiga, Japan). Primers listed in **Supplementary Table 2** were designed by SnapGene® 2.3.2. *udp* (encoding a UDP-*N*-acetylglucosamine 2-epimerase) was used as a reference gene (Reiter et al., 2011). TB Green® *Premix Ex Taq*™ II (Tli RNaseH Plus) (RR820A, Takara, Shiga, Japan) was used for all qPCR reactions. qPCR reactions were performed on a Roche LightCycler® 96 in eight tubes (PCR-0108-LP-RT-C, Axygen, Glendale, AZ, United States) using three-step PCR amplification reaction as follows: 30 s preincubation at 95°C by 1 cycle followed by 45 cycles of denaturation at 95°C for 5 s, annealing at 58°C for 30 s and elongation at 72°C for 30 s, for melting at 95°C for 10 s, 65°C for 60 s, 97°C for 1 s by 1 cycle. The specificity of the reactions was affirmed by melting peaks analysis of the amplified products. Relative expression of *flgE* was calculated by the $2^{-\Delta\Delta CT}$ (Livak) method (Livak and Schmittgen, 2001) using the difference in Cq (quantification cycle) values of the sample

[1]https://www.genome.jp/tools-bin/clustalw

[2]https://espript.ibcp.fr/ESPript/cgi-bin/ESPript.cgi

and a calibrator for the target gene and *udp*. Triplicates RT-qPCR reactions were performed for each sample with negative control for three biological repetitions.

Quantification of Cereulide via Liquid Chromatography Tandem Mass Spectrometry

Cereulide was extracted as described previously with some modifications (Tian et al., 2019). In brief, overnight cultures of *B. cereus* 892-1 were inoculated into 50 mL of LB medium (1:1,000; v:v) and cells were grown at 30°C, 200 rpm for 24 h. Bacteria were collected by centrifugation at 4°C, 8,000 *g* for 5 min, and resuspended in 5 mL methanol (HPLC grade, Guangdong Huankai Co., Ltd., Guangzhou, China). The suspension was cultivated in a shaker at 28°C, 200 rpm overnight. Then, the supernatant was filtered through a 0.22 μm filter, filled with methanol into equal volume, and diluted into a suitable concentration for LC-MS analysis. A Q Exactive Plus Orbitrap LC-MS/MS System (Thermo Fisher Scientific., Waltham, CA, United States) was equipped with an H-ESI (electrospray ionization) II probe source and positive mode was chosen to determine cereulide concentration according to a previous method (In't Veld et al., 2019). Mass spectrometric characterization of cereulide was performed using a C18 column (ACQUITY UPLC® Peptide BEH, 300A, 1.7 μm, 2.1 mm × 100 mm, 1/pkg). Mass spectrometric detection the ammonium adducts of cereulide at m/z 1,170.7 ($[M + NH_4]^+$) and potassium adducts of valinomycin at m/z 1,128.6 ($[M + K]^+$) (**Supplementary Figure 4**; Seyi-Amole et al., 2020). Methanol and ultrapure water containing 10 mM ammonium formate, both of which contained 0.1% formic acid, were used as eluents A and B. The gradient elution conditions were exhibited in **Supplementary Table 3**. An injection volume of 5 μL and a flow rate of 10 μL/min were used. MS runtime was 13 min and the retention time (RT) for cereulide and valinomycin was 5.00 and 5.10, respectively. The spray voltage was 3.50 kV. The flow rate for sheath gas was 45 and 10 for aux gas. The temperature for capillary and aux gas heater was 300 and 350°C, respectively. The concentration of cereulide in analytes is calculated by calibration curve, which was obtained by plotting the area ratios of cereulide to valinomycin (internal standard) for different dilutions. Linear regression was applied to give the equation $y = 0.00783839x + 0.0686906$ with $R^2 = 0.9952$; y is the area ratios of cereulide to valinomycin; x is the concentration of cereulide; R^2 determined the coefficient of the linear regression. The data was acquired and processed by Thermo Xcalibur (v3.5).

RESULTS

Identification of Biofilm-Defected Mutants of Emetic *Bacillus cereus* 892-1

In total, 500 chloromycetin-resistant and erythromycin-sensitive mutants were identified, which were then screened for the identification of potential mutants with defects in biofilm formation. Among them, one mutant, designated 3-86, presented an obvious biofilm formation defect (**Figure 2A**). After reverse PCR, sequencing, and local blast, the transposon was proved to insert into the gene *flgE* (**Figure 2B**).

flgE Positively Regulates Biofilm Formation in Emetic *Bacillus cereus* 892-1

To further illustrate the role of *flgE* in biofilm formation, we compared the pellicle formation of wild-type strain with Δ*flgE* and complementary strain. Wild-type cells can form a pellicle in the air-liquid interface, while Δ*flgE* strain cannot (**Figure 3A**). As expected, the complementary strain restored a comparable level in its ability to form a pellicle. Furthermore, the amount of the ring was significantly reduced in Δ*flgE*; however, the ring of the complementary strain (Δ*flgE*:pHT304-*flgE*) was largely restored, although it did not reach the wild-type level (**Figure 3B**). Through observation by an SEM, the wild-type and complementary strains showed a dense biofilm community (**Figure 3C**). In contrast, only sparse cells of the mutant strain remained on the grid. Besides, biofilms were imaged by CLSM. The results are the same as SEM. The wild-type and complementary strains had dense biofilm structure, while Δ*flgE* only had scattered bacteria (**Figure 3D**).

flgE Is Necessary for Flagella Synthesis and Swimming Ability

To exclude the possibility that the biofilm formation defect is due to the differential growth rate, we monitored the growth of different bacteria for 12 h and found that the growth rate of Δ*flgE* had no obvious difference compared with wild-type and Δ*flgE*:pHT304-*flgE* at the early stage and was a little bit faster than other strains at the stationary stage (**Figure 4A**). To verify the role of *flgE* in flagella synthesis or assembly in *B. cereus* 892-1, the cells of wild-type, Δ*flgE*, and Δ*flgE*:pHT304-*flgE* were inspected by a TEM. No flagella could be found in Δ*flgE*. In contrast, either the wild-type or Δ*flgE*:pHT304-*flgE* had obvious flagella (**Figure 4B**), and there was no difference in quantity between the wild-type and Δ*flgE*:pHT304-*flgE* (**Figure 4C**). Due to the loss of flagella, Δ*flgE* could not swim as no outward movement can be observed (**Figure 4D**).

Swimming Ability Is Not Necessary for Biofilm Formation in Emetic *Bacillus cereus* 892-1

To test the swimming ability or flagella itself is important for biofilm formation in emetic *B. cereus*, two flagellar paralytic strains were constructed and the biofilm formation ability was measured. As expected, Δ*motA* and Δ*motB* lost swimming ability in motility assay (**Figure 5A**). Surprisingly, pellicle could also be formed in Δ*motA* instead of in Δ*motB* (**Supplementary Figure 2**). The amount of ring in Δ*motA* was also significantly higher than that in Δ*flgE* or Δ*motB*, but lower than that in the wild-type strain (**Figure 5B**), demonstrating that swimming ability contributes to biofilm formation but is not necessary for biofilm formation. Δ*motB* completely lost the ability to form a biofilm, and has no significant difference in biofilm formation

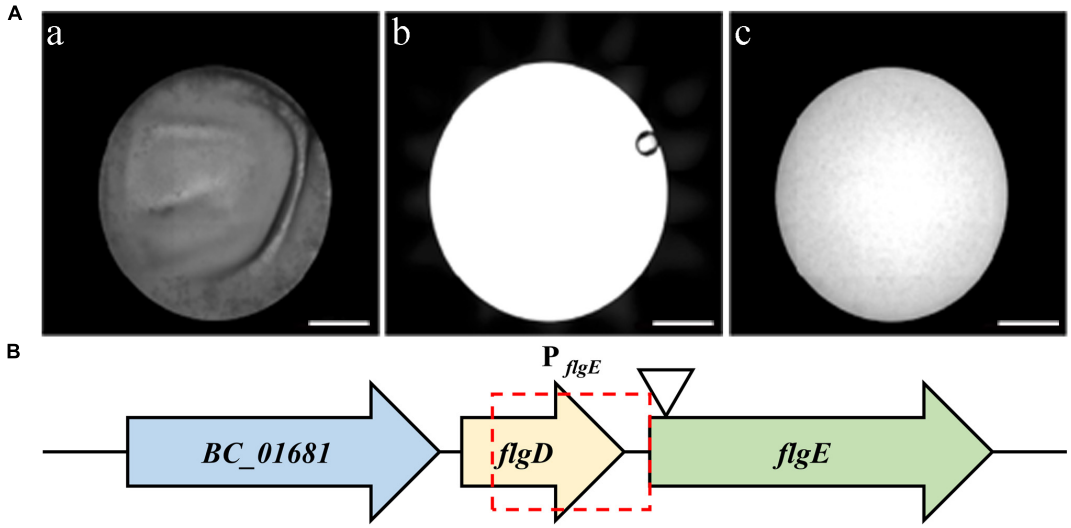

FIGURE 2 | Screening of mutants with biofilm formation defects. **(A)** microplate reader images of wild-type strain (a), only TSB medium (b), and the mutant 3-86 (c). Scale bar = 2 millimeters. **(B)** Diagram showing the transposon insertion site of the defective mutant. Potential promoter of *flgE* is indicated by the red frame. The position of the TnYLB-1 transposon in *flgE* on the chromosome of *B. cereus* 892-1 is indicated by the triangle.

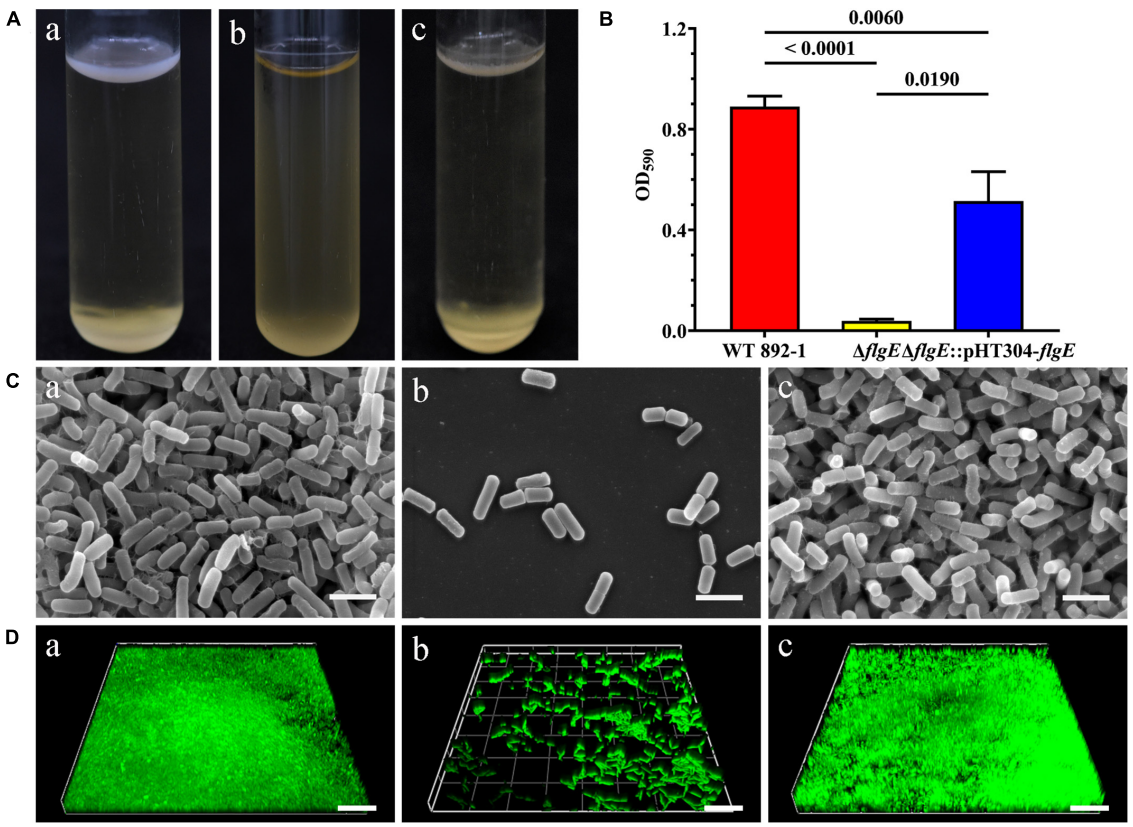

FIGURE 3 | *flgE* is essential for biofilm formation in emetic *B. cereus* 892-1. **(A)** Pellicle formation by wild-type strain (a), Δ*flgE* (b), and Δ*flgE*:pHT304-*flgE* (c). **(B)** Ring formation by wild-type strain 892-1, Δ*flgE*, and Δ*flgE*:pHT304-*flgE*. *P* values were calculated using the Student's *t*-test. Error bars represent the standard deviation of the mean. **(C)** SEM images of biofilms formed by (a) wild-type, (b) Δ*flgE*, and (c) Δ*flgE*:pHT304-*flgE*. The scale bars represent three microns. **(D)** CLSM images of biofilms formed by wild-type (a), Δ*flgE* (b), and Δ*flgE*:pHT304-*flgE* (c). The scale bars represent 30 microns.

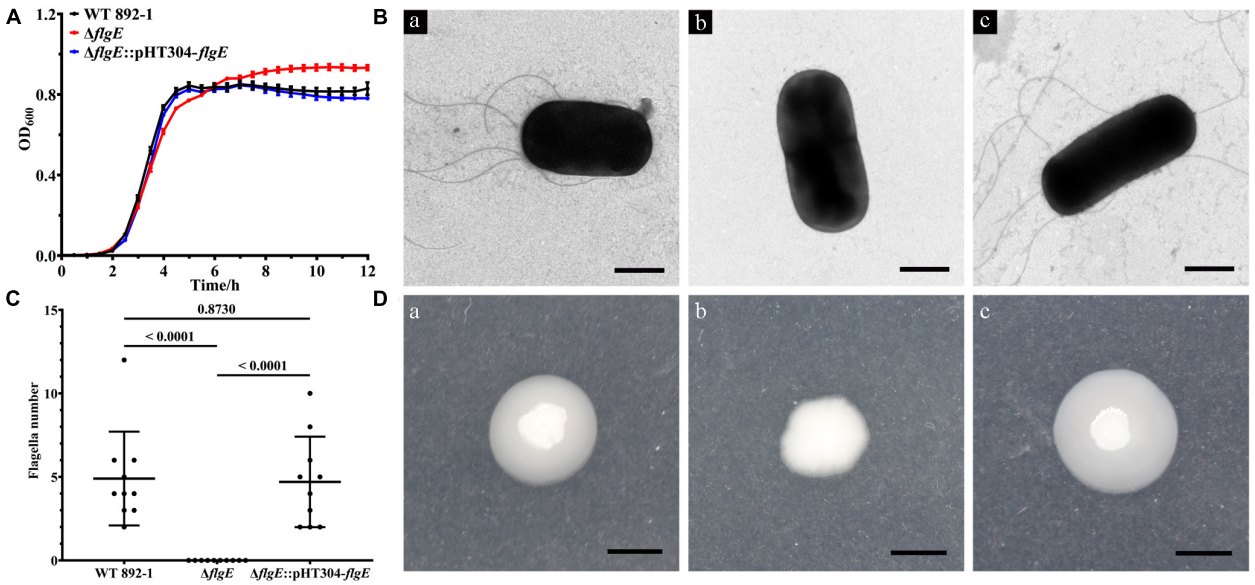

FIGURE 4 | *flgE* is important for flagella synthesis and function. **(A)** Growth curves of wild-type, Δ*flgE*, and Δ*flgE*:pHT304-*flgE*. **(B)** TEM images of flagella produced in the wild-type (a), Δ*flgE* (b), and Δ*flgE*:pHT304-*flgE* (c). Scale bars represent one micron. **(C)** The number of flagella in wild-type strain, Δ*flgE*, and Δ*flgE*:pHT304-*flgE*. The number of flagella was calculated by 10 bacteria. **(D)** Swimming motility of wild-type (a), Δ*flgE* (b), and Δ*flgE*:pHT304-*flgE* (c). Scale bars represent zero point five centimeter.

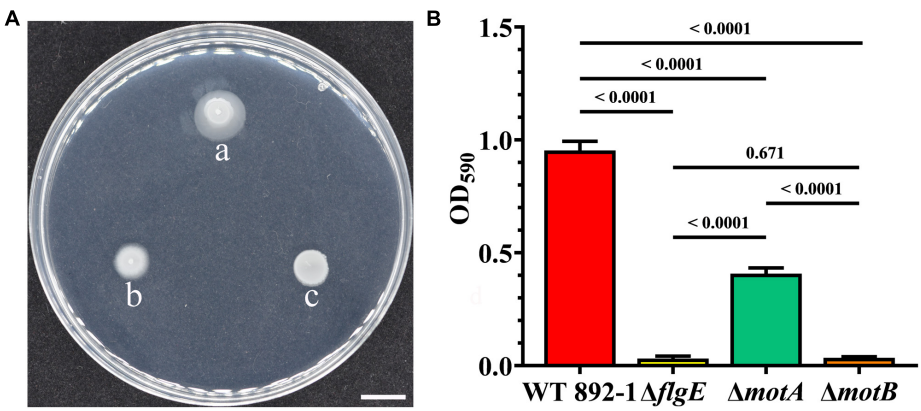

FIGURE 5 | Swimming ability is not necessary for biofilm formation. **(A)** Swimming motility of wild-type (a), Δ*motB* (b), and Δ*motA* (c). Scale bars represent one centimeter. **(B)** Ring formation by wild-type strain, Δ*flgE*, Δ*motA*, and Δ*motB*. *P* values were calculated using the Student's *t*-test, and used to determine statistical significance between each mutant and the wild-type strain. Error bars represent the standard deviation of the mean.

compared with Δ*flgE*, indicating that flagellar structure itself does not play a scaffold-role in emetic *B. cereus* 892-1.

Loss of *flgE* Significantly Decreased Cereulide Production in *Bacillus cereus* 892-1

Since 892-1 is an emetic strain, we also evaluated cereulide production in different strains by LC-MS/MS. The concentration range of cereulide was 19.327–22.757, 8.1586–10.312, and 32.417 to 35.294 μg/mL in WT 892-1, Δ*flgE* and Δ*flgE*:pHT304-*flgE*, respectively (**Figure 6A**; **Supplementary Table 4**). In conclusion, cereulide production was significantly decreased in Δ*flgE*, with a reduction of approximately 60% compared with the wild-type strain. In addition, Δ*flgE*:pHT304-*flgE* produced more cereulide; therefore, the transcriptional levels of *flgE* were monitored in the bacterial logarithmic phase. The relative expression level of *flgE* was obviously increased in Δ*flgE*:pHT304-*flgE* compared with wild-type (**Figure 6B**).

DISCUSSION

Bacillus cereus can contaminate different type of foods (Messelhäusser et al., 2010; Kim et al., 2016; Esteban-Cuesta et al., 2018; Fasolato et al., 2018; Park et al., 2018; Yu et al., 2019, 2020).

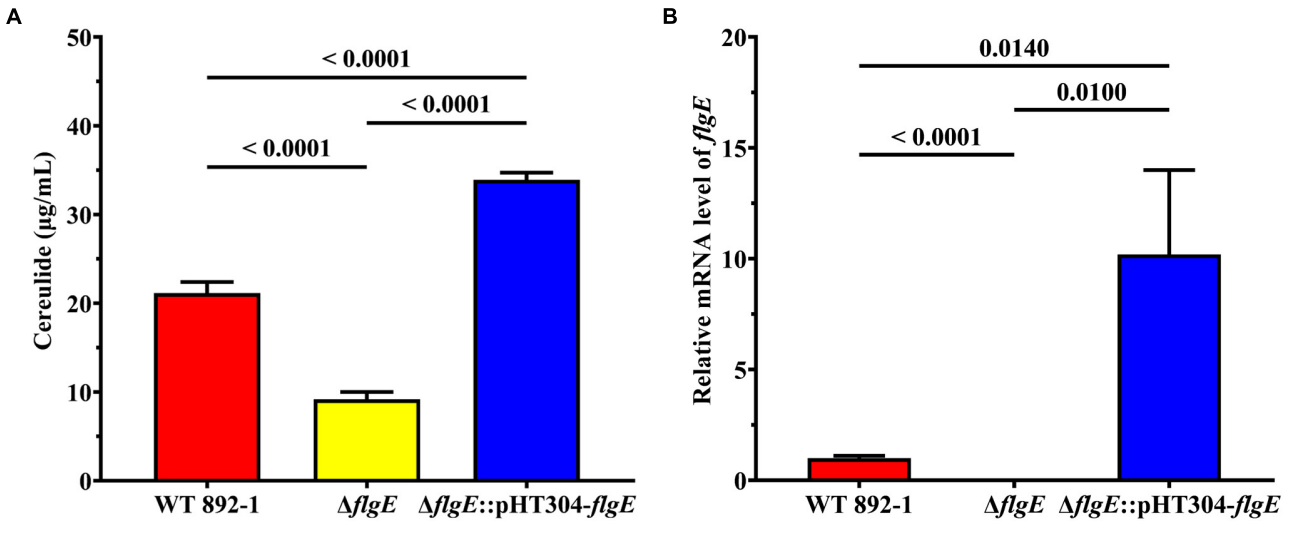

FIGURE 6 | Deletion of *flgE* significantly decreased cereulide production. **(A)** Cereulide production by wild-type strain, Δ*flgE* and Δ*flgE*:pHT304-*flgE*. **(B)** Relative mRNA levels of *flgE* in wild-type strain, Δ*flgE*, and Δ*flgE*:pHT304-*flgE*. *P* values were calculated using the Student's *t*-test. Error bars represent the standard deviation of the mean.

Notably, a relatively high prevalence of emetic strains exists in dairy products, including cow milk, and pasteurized and ultrahigh-temperature treated milk products (Wijnands et al., 2006; Messelhäusser et al., 2014; Chaves et al., 2017; Owusu-Kwarteng et al., 2017; Gao et al., 2018; Walser et al., 2021). Emetic strains can produce highly heat resistant and acid-stable cereulide which brings a great threat to human health (Rouzeau-Szynalski et al., 2020). It is worth noting that *B. cereus* contamination occurred in dairy production was largely due to the biofilm formation (Teh et al., 2012; Yobouet et al., 2014; Reda, 2019; Wang et al., 2019), indicating a possible transmission of emetic *B. cereus* from food processing environment to human infection (Kuroki et al., 2009). Besides, cereulide showed a heightened affinity to lipid components of milk samples (Walser et al., 2021). Therefore, it is important to analyze the mechanism of emetic *B. cereus* biofilm formation which can be used to inhibit the formation of emetic *B. cereus* biofilms in the food industry, especially in dairy production.

In this study, we showed that *flgE* identified by the transposon mutagenesis is essential for the biofilm formation of emetic *B. cereus* 892-1. In the stationary phase, the growth rate of *flgE* knockout strain was higher than that of the wild-type strain and complementary strain. It was speculated that flagella synthesis needed energy, so bacterial growth was promoted in Δ*flgE* which cannot form flagella (Hölscher et al., 2015). Bacterial flagella are closely related to biofilm formation (Guttenplan and Kearns, 2013). In *E. coli*, half of the mutants with defects in biofilm formation are defective in flagellar function (Pratt and Kolter, 1998). Plenty of studies demonstrated that the destruction of flagella affects the phenotype of biofilm by affecting flagella-mediated motility in different species (O'Toole and Kolter, 1998; Pratt and Kolter, 1998; Lee et al., 2004; Hossain and Tsuyumu, 2006). Besides, it is proved that the signal transmitted by flagella can stimulate biofilm formation (Belas, 2014). In *B. subtilis*, inhibiting flagellar movement by destroying flagellar stator protein MotB, over-expressing site-directed EpsE mutant, or using flagellin antibody can stimulate the generation of biofilm matrix, and the appearance of colony biofilm phenotype by activating DegS-DegU two-component system (Cairns et al., 2013). In *V. cholerae*, the deletion of flagellar filament structure can stimulate the biofilm formation by increasing the level of second-messenger cyclic diguanylate (c-di-GMP), which requires the participation of flagellar stator protein (Wu et al., 2020). In *P. aeruginosa*, c-di-GMP plays an important role in the regulation of flagella and biofilm. The flagellar stator protein MotCD has been proved to interact with diguanylate cyclase SadC to activate the activity of SadC, thus stimulating the production of c-di-GMP, inhibiting the swarm movement, and promoting the formation of biofilm (Caiazza et al., 2007; Baker et al., 2019). In contrast, it has also been suggested that flagella-mediated motility is not necessary for biofilm formation. In *B. subtilis*, the immobile cells caused by destroying flagellin protein Hag can reach the gas-liquid interface by Brownian movement and then form a biofilm (Hölscher et al., 2015). To investigate the participation of flagella-mediated motility in the biofilm formation of emetic strain 892-1, we mutated the flagellar stator proteins which are reported to control swimming ability without affecting flagellar structure (Houry et al., 2010; Cairns et al., 2013). To our surprise, the biofilm of Δ*motA* significantly decreased when compared with the wild-type cell (**Figure 5B** and **Supplementary Figure 2**). In contrast, Δ*motB* completely lost the ability to form the biofilm. Together, these results indicated that *flgE*, apart from its flagella-mediated swimming ability, plays other unknown regulatory roles that contribute to biofilm formation in 892-1. Although the flagellar structure is considered to be able to maintain the stability of biofilm structure in many other species such as in *P. aeruginosa* (Ozer et al., 2021), *Helicobacter pylori* (Hathroubi et al., 2018), and *Geobacter sulfurreducens* (Liu et al., 2019), Δ*motB* had no

obvious difference in biofilm formation compared with Δ*flgE* (**Figure 5B** and **Supplementary Figure 2**), indicating that flagella themselves do not play a scaffold-role in 892-1.

Moreover, the deletion of *flgE* not only reduced biofilm formation, but also significantly down-regulated cereulide production (**Figure 6A**). To our surprise, the amount of cereulide in complementary strain was higher than the wild-type strain. We monitored the transcriptional levels of *flgE*, the expression level of *flgE* in the complementary strain was significantly higher than the wild-type strain (**Figure 6B**), indicating the difference in the production of cereulide between the wild-type strain and supplementary strain may be caused by the differential expression of *flgE*. Therefore, we speculated that *flgE* may serve as an important contributor to both biofilm formation and cereulide production, which suggests that the two phenotypes are possibly governed by a common system within the cell. The potential regulatory effect of flagella in mediating virulence or pathogenicity has been reported widely (Haiko and Westerlund-Wikström, 2013; Stevenson et al., 2015). In *B. cereus*, *flhF*, which controls the arrangement of flagella, is important in cell migration, especially swarming motility (Salvetti et al., 2007). Deletion of *flhF* significantly affects the pathogenicity of *B. cereus*, resulting in a reduction of infection *in vivo* (Mazzantini et al., 2016). Quorum sensing (QS) is an important system in cell-cell communication that is involved in many biological processes, including biofilm formation and virulence (Rutherford and Bassler, 2012). In *V. cholerae*, QS autoinducers cholerae autoinducer-1 (CAI-1) and autoinducer-2 (AI-2) cannot bind to the kinases CqsS and LuxPQ on the cell membrane at a low cell density, resulting in the activation of biofilm formation and virulence (Bridges and Bassler, 2019). The relationship between biofilm formation and cereulide production in the emetic strain of *B. cereus* is still unclear and the mechanism of *flgE* in these two processes needs to be further investigated in the future.

CONCLUSION

In this study, we showed that flagellar hook protein FlgE is critical in biofilm formation in emetic *B. cereus*. The potential role of FlgE does not depend on the scaffold-role of flagella in biofilm formation. Instead, swimming ability contributes to biofilm formation, but is not necessary for it. Moreover, loss of *flgE* also reduced cereulide production, demonstrating the dual role of the flagellar hook protein in emetic *B. cereus*. Therefore, FlgE can be used as a target for the control of food contamination and poisoning incidents caused by emetic *B. cereus*.

DATA AVAILABILITY STATEMENT

The original contributions presented in the study are included in the article/**Supplementary Material**, further inquiries can be directed to the corresponding authors.

AUTHOR CONTRIBUTIONS

YD, QW, JW, JZ, MC, YL, and NC conceived the project and designed the experiments. YL, NC, XY, SY, and XL performed the experiments. YD and JW supervised the project. YL, NC, JW, and YD analyzed the data and wrote the manuscript. QW, JW, ZZ, YZ, and YD complemented the writing. All authors contributed to the article and approved the submitted version.

FUNDING

We would like to acknowledge the financial support of Guangdong Major Project of Basic and Applied Basic Research (2020B0301030005), Guangdong Provincial Key Laboratory (2020B121201009), and Guangdong Province Academy of Sciences Special Project for Capacity Building of Innovation Driven Development (2020GDASYL-20200301002).

ACKNOWLEDGMENTS

We sincerely thank Qi Wang from China Agricultural University for generously providing us the plasmid pMarA. We also thank Ming Sun from Huazhong Agricultural University for kindly providing us the plasmid pHT304 and pHT304-TS.

SUPPLEMENTARY MATERIAL

The Supplementary Material for this article can be found online at: https://www.frontiersin.org/articles/10.3389/fmicb.2022.897836/full#supplementary-material

REFERENCES

Alvarez-Ordóñez, A., Coughlan, L. M., Briandet, R., and Cotter, P. D. (2019). Biofilms in food processing environments: challenges and opportunities. *Annu. Rev. Food Sci. Technol.* 10, 173–195. doi: 10.1146/annurev-food-032818-121805

Arantes, O., and Lereclus, D. (1991). Construction of cloning vectors for *Bacillus thuringiensis*. *Gene* 108, 115–119. doi: 10.1016/0378-1119(91)90495-w

Baker, A. E., Webster, S. S., Diepold, A., Kuchma, S. L., Bordeleau, E., Armitage, J. P., et al. (2019). Flagellar stators stimulate c-di-GMP production by *Pseudomonas aeruginosa*. *J. Bacteriol.* 201:e00741-18. doi: 10.1128/JB.00741-18

Bauer, T., Sipos, W., Stark, T. D., Käser, T., Knecht, C., Brunthaler, R., et al. (2018). First insights into within host translocation of the *Bacillus cereus* toxin cereulide using a porcine model. *Front. Microbiol.* 9:2652. doi: 10.3389/fmicb.2018.02652

Belas, R. (2014). Biofilms, flagella, and mechanosensing of surfaces by bacteria. *Trends Microbiol.* 22, 517–527. doi: 10.1016/j.tim.2014.05.002

Bridges, A. A., and Bassler, B. L. (2019). The intragenus and interspecies quorum-sensing autoinducers exert distinct control over *Vibrio cholerae* biofilm formation and dispersal. *PLoS Biol.* 17:e3000429. doi: 10.1371/journal.pbio.3000429

Caiazza, N. C., Merritt, J. H., Brothers, K. M., and O'Toole, G. A. (2007). Inverse regulation of biofilm formation and swarming motility by *Pseudomonas aeruginosa* PA14. *J. Bacteriol.* 189, 3603–3612. doi: 10.1128/JB.01685-06

Cairns, L. S., Marlow, V. L., Bissett, E., Ostrowski, A., and Stanley-Wall, N. R. (2013). A mechanical signal transmitted by the flagellum controls signalling in *Bacillus subtilis*. *Mol. Microbiol.* 90, 6–21. doi: 10.1111/mmi.12342

Caro-Astorga, J., Pérez-García, A., de Vicente, A., and Romero, D. (2014). A genomic region involved in the formation of adhesin fibers in *Bacillus cereus* biofilms. *Front. Microbiol.* 5:745. doi: 10.3389/fmicb.2014.00745

Chaves, J. Q., de Paiva, E. P., Rabinovitch, L., and Vivoni, A. M. (2017). Molecular characterization and risk assessment of *Bacillus cereus* sensu lato isolated from ultrahigh-temperature and pasteurized milk marketed in Rio de Janeiro, Brazil. *J. Food Prot.* 80, 1060–1065. doi: 10.4315/0362-028X.JFP-16-448

Costerton, J. W., Stewart, P. S., and Greenberg, E. P. (1999). Bacterial biofilms: a common cause of persistent infections. *Science* 284, 1318–1322. doi: 10.1126/science.284.5418.1318

Dierick, K., Van Coillie, E., Swiecicka, I., Meyfroidt, G., Devlieger, H., Meulemans, A., et al. (2005). Fatal family outbreak of *Bacillus cereus*-associated food poisoning. *J. Clin. Microbiol.* 43, 4277–4279. doi: 10.1128/JCM.43.8.4277-4279.2005

Dommel, M. K., Frenzel, E., Strasser, B., Blöchinger, C., Scherer, S., and Ehling-Schulz, M. (2010). Identification of the main promoter directing cereulide biosynthesis in emetic *Bacillus cereus* and its application for real-time monitoring of *ces* gene expression in foods. *Appl. Environ. Microbiol.* 76, 1232–1240. doi: 10.1128/AEM.02317-09

Enosi Tuipulotu, D., Mathur, A., Ngo, C., and Man, S. M. (2021). *Bacillus cereus*: epidemiology, virulence factors, and host–pathogen interactions. *Trends Microbiol.* 29, 458–471. doi: 10.1016/j.tim.2020.09.003

Esteban-Cuesta, I., Drees, N., Ulrich, S., Stauch, P., Sperner, B., Schwaiger, K., et al. (2018). Endogenous microbial contamination of melons (*Cucumis melo*) from international trade: an underestimated risk for the consumer? *J. Sci. Food Agric.* 98, 5074–5081. doi: 10.1002/jsfa.9045

Fasolato, L., Cardazzo, B., Carraro, L., Fontana, F., Novelli, E., and Balzan, S. (2018). Edible processed insects from e-commerce: food safety with a focus on the *Bacillus cereus* group. *Food Microbiol.* 76, 296–303. doi: 10.1016/j.fm.2018.06.008

Gao, T., Ding, M., Yang, C., Fan, H., Chai, Y., and Li, Y. (2019). The phosphotransferase system gene *ptsH* plays an important role in MnSOD production, biofilm formation, swarming motility, and root colonization in *Bacillus cereus* 905. *Res. Microbiol.* 170, 86–96. doi: 10.1016/j.resmic.2018.10.002

Gao, T., Ding, Y., Wu, Q., Wang, J., Zhang, J., Yu, S., et al. (2018). Prevalence, virulence genes, antimicrobial susceptibility, and genetic diversity of *Bacillus cereus* isolated from pasteurized milk in China. *Front. Microbiol.* 9:533. doi: 10.3389/fmicb.2018.00533

Gao, T., Foulston, L., Chai, Y., Wang, Q., and Losick, R. (2015). Alternative modes of biofilm formation by plant-associated *Bacillus cereus*. *Microbiologyopen* 4, 452–464. doi: 10.1002/mbo3.251

Guttenplan, S. B., and Kearns, D. B. (2013). Regulation of flagellar motility during biofilm formation. *FEMS Microbiol. Rev.* 37, 849–871. doi: 10.1111/1574-6976.12018

Guzman, L. M., Belin, D., Carson, M. J., and Beckwith, J. (1995). Tight regulation, modulation, and high-level expression by vectors containing the arabinose PBAD promoter. *J. Bacteriol.* 177, 4121–4130. doi: 10.1128/jb.177.14.4121-4130.1995

Haiko, J., and Westerlund-Wikström, B. (2013). The role of the bacterial flagellum in adhesion and virulence. *Biology* 2, 1242–1267. doi: 10.3390/biology2041242

Hathroubi, S., Zerebinski, J., and Ottemann, K. M. (2018). *Helicobacter pylori* biofilm involves a multigene stress-biased response, including a structural role for flagella. *mBio* 9:e01973-18. doi: 10.1128/mBio.01973-18

Hölscher, T., Bartels, B., Lin, Y. C., Gallegos-Monterrosa, R., Price-Whelan, A., Kolter, R., et al. (2015). Motility, chemotaxis and aerotaxis contribute to competitiveness during bacterial pellicle biofilm development. *J. Mol. Biol.* 427, 3695–3708. doi: 10.1016/j.jmb.2015.06.014

Hossain, M. M., and Tsuyumu, S. (2006). Flagella-mediated motility is required for biofilm formation by *Erwinia carotovora* subsp. *carotovora*. *J. Gen. Plant Pathol.* 72, 34–39. doi: 10.1007/s10327-005-0246-8

Houry, A., Briandet, R., Aymerich, S., and Gohar, M. (2010). Involvement of motility and flagella in *Bacillus cereus* biofilm formation. *Microbiology* 156, 1009–1018. doi: 10.1099/mic.0.034827-0

In't Veld, P., van der Laak, L., Van Zon, M., and Biesta-Peters, E. (2019). Elaboration and validation of the method for the quantification of the emetic toxin of *Bacillus cereus* as described in EN-ISO 18465-Microbiology of the food chain–quantitative determination of emetic toxin (cereulide) using LC-MS/MS. *Int. J. Food Microbiol.* 288, 91–96. doi: 10.1016/j.ijfoodmicro.2018.03.021

Jovanovic, J., Ornelis, V. F., Madder, A., and Rajkovic, A. (2021). *Bacillus cereus* food intoxication and toxicoinfection. *Compr. Rev. Food Sci. Food Saf.* 20, 3719–3761. doi: 10.1111/1541-4337.12785

Kable, M. E., Srisengfa, Y., Xue, Z., Coates, L. C., and Marco, M. L. (2019). Viable and total bacterial populations undergo equipment-and time-dependent shifts during milk processing. *Appl. Environ. Microbiol.* 85:e00270-19. doi: 10.1128/AEM.00270-19

Kim, Y. J., Kim, H. S., Kim, K. Y., Chon, J. W., Kim, D. H., and Seo, K. H. (2016). High occurrence rate and contamination level of *Bacillus cereus* in organic vegetables on sale in retail markets. *Foodborne Pathog. Dis.* 13, 656–660. doi: 10.1089/fpd.2016.2163

Kuroki, R., Kawakami, K., Qin, L., Kaji, C., Watanabe, K., Kimura, Y., et al. (2009). Nosocomial bacteremia caused by biofilm-forming *Bacillus cereus* and *Bacillus thuringiensis*. *Intern. Med.* 48, 791–796. doi: 10.2169/internalmedicine.48.1885

Lee, J. H., Rho, J. B., Park, K. J., Kim, C. B., Han, Y. S., Choi, S. H., et al. (2004). Role of flagellum and motility in pathogenesis of *Vibrio vulnificus*. *Infect. Immun.* 72, 4905–4910. doi: 10.1128/IAI.72.8.4905-4910.2004

Lin, R., Li, D., Xu, Y., Wei, M., Chen, Q., Deng, Y., et al. (2021). Chronic cereulide exposure causes intestinal inflammation and gut microbiota dysbiosis in mice. *Environ. Pollut.* 288:117814. doi: 10.1016/j.envpol.2021.117814

Lindbäck, T., Mols, M., Basset, C., Granum, P. E., Kuipers, O. P., and Kovács, Á. T. (2012). CodY, a pleiotropic regulator, influences multicellular behaviour and efficient production of virulence factors in *Bacillus cereus*. *Environ. Microbiol.* 14, 2233–2246. doi: 10.1111/j.1462-2920.2012.02766.x

Liu, X., Zhuo, S., Jing, X., Yuan, Y., Rensing, C., and Zhou, S. (2019). Flagella act as *Geobacter* biofilm scaffolds to stabilize biofilm and facilitate extracellular electron transfer. *Biosens. Bioelectron.* 146:111748. doi: 10.1016/j.bios.2019.111748

Livak, K. J., and Schmittgen, T. D. (2001). Analysis of relative gene expression data using real-time quantitative PCR and the $2^{-\Delta\Delta CT}$ method. *Methods* 25, 402–408. doi: 10.1006/meth.2001.1262

Ma, X., Liang, H., Cui, X., Liu, Y., Lu, H., Ning, W., et al. (2019). A standard for near-scarless plasmid construction using reusable DNA parts. *Nat. Commun.* 10:3294. doi: 10.1038/s41467-019-11263-0

Mahler, H., Pasi, A., Kramer, J. M., Schulte, P., Scoging, A. C., Bär, W., et al. (1997). Fulminant liver failure in association with the emetic toxin of *Bacillus cereus*. *N. Engl. J. Med.* 336, 1142–1148. doi: 10.1056/NEJM199704173361604

Majed, R., Faille, C., Kallassy, M., and Gohar, M. (2016). *Bacillus cereus* biofilms-same, only different. *Front. Microbiol.* 7:1054. doi: 10.3389/fmicb.2016.01054

Mazzantini, D., Celandroni, F., Salvetti, S., Gueye, S. A., Lupetti, A., Senesi, S., et al. (2016). FlhF is required for swarming motility and full pathogenicity of *Bacillus cereus*. *Front. Microbiol.* 7:1644. doi: 10.3389/fmicb.2016.01644

Messelhäusser, U., Frenzel, E., Blöchinger, C., Zucker, R., Kämpf, P., and Ehling-Schulz, M. (2014). Emetic *Bacillus cereus* are more volatile than thought: recent foodborne outbreaks and prevalence studies in Bavaria (2007–2013). *Biomed Res. Int.* 2014:465603. doi: 10.1155/2014/465603

Messelhäusser, U., Kämpf, P., Fricker, M., Ehling-Schulz, M., Zucker, R., Wagner, B., et al. (2010). Prevalence of emetic *Bacillus cereus* in different ice creams in Bavaria. *J. Food Prot.* 73, 395–399. doi: 10.4315/0362-028X-73.2.395

Mielich-Süss, B., and Lopez, D. (2015). Molecular mechanisms involved in *Bacillus subtilis* biofilm formation. *Environ. Microbiol.* 17, 555–565. doi: 10.1111/1462-2920.12527

Naranjo, M., Denayer, S., Botteldoorn, N., Delbrassinne, L., Veys, J., Waegenaere, J., et al. (2011). Sudden death of a young adult associated with *Bacillus cereus* food poisoning. *J. Clin. Microbiol.* 49, 4379–4381. doi: 10.1128/JCM.05129-11

Ostrov, I., Harel, A., Bernstein, S., Steinberg, D., and Shemesh, M. (2016). Development of a method to determine the effectiveness of cleaning agents in removal of biofilm derived spores in milking system. *Front. Microbiol.* 7:1498. doi: 10.3389/fmicb.2016.01498

O'Toole, G. A., and Kolter, R. (1998). Flagellar and twitching motility are necessary for *Pseudomonas aeruginosa* biofilm development. *Mol. Microbiol.* 30, 295–304. doi: 10.1046/j.1365-2958.1998.01062.x

Owusu-Kwarteng, J., Wuni, A., Akabanda, F., Tano-Debrah, K., and Jespersen, L. (2017). Prevalence, virulence factor genes and antibiotic resistance of *Bacillus cereus* sensu lato isolated from dairy farms and traditional dairy products. *BMC Microbiol.* 17:65. doi: 10.1186/s12866-017-0975-9

Ozer, E., Yaniv, K., Chetrit, E., Boyarski, A., Meijler, M. M., Berkovich, R., et al. (2021). An inside look at a biofilm: *Pseudomonas aeruginosa* flagella biotracking. *Sci. Adv.* 7:eabg8581. doi: 10.1126/sciadv.abg8581

Park, K. M., Jeong, M., Park, K. J., and Koo, M. (2018). Prevalence, enterotoxin genes, and antibiotic resistance of *Bacillus cereus* isolated from raw vegetables in Korea. *J. Food Prot.* 81, 1590–1597. doi: 10.4315/0362-028X.JFP-18-205

Pratt, L. A., and Kolter, R. (1998). Genetic analysis of *Escherichia coli* biofilm formation: roles of flagella, motility, chemotaxis and type I pili. *Mol. Microbiol.* 30, 285–293. doi: 10.1046/j.1365-2958.1998.01061.x

Qi, G., Lu, J., Zhang, P., Li, J., Zhu, F., Chen, J., et al. (2011). The *cry1Ac* gene of *Bacillus thuringiensis* ZQ-89 encodes a toxin against long-horned beetle adult. *J. Appl. Microbiol.* 110, 1224–1234. doi: 10.1111/j.1365-2672.2011.04974.x

Rajkovic, A., Uyttendaele, M., Ombregt, S. A., Jaaskelainen, E., Salkinoja-Salonen, M., and Debevere, J. (2006). Influence of type of food on the kinetics and overall production of *Bacillus cereus* emetic toxin. *J. Food Prot.* 69, 847–852. doi: 10.4315/0362-028X-69.4.847

Rasko, D. A., Rosovitz, M., Økstad, O. A., Fouts, D. E., Jiang, L., Cer, R. Z., et al. (2007). Complete sequence analysis of novel plasmids from emetic and periodontal *Bacillus cereus* isolates reveals a common evolutionary history among the *B. cereus*-group plasmids, including *Bacillus anthracis* pXO1. *J. Bacteriol.* 189, 52–64. doi: 10.1128/JB.01313-06

Reda, F. M. (2019). Antibacterial and anti-adhesive efficiency of *Pediococcus acidilactici* against foodborne biofilm producer *Bacillus cereus* attached on different food processing surfaces. *Food Sci. Biotechnol.* 28, 841–850. doi: 10.1007/s10068-018-0518-7

Reiter, L., Kolstø, A. B., and Piehler, A. P. (2011). Reference genes for quantitative, reverse-transcription PCR in *Bacillus cereus* group strains throughout the bacterial life cycle. *J. Microbiol. Methods* 86, 210–217. doi: 10.1016/j.mimet.2011.05.006

Ribeiro, M. C. E., da Silva Fernandes, M., Kuaye, A. Y., and Gigante, M. L. (2019). Influence of different cleaning and sanitisation procedures on the removal of adhered *Bacillus cereus* spores. *Int. Dairy J.* 94, 22–28. doi: 10.1016/j.idairyj.2019.02.011

Robert, X., and Gouet, P. (2014). Deciphering key features in protein structures with the new ENDscript server. *Nucleic Acids Res.* 42, W320–W324. doi: 10.1093/nar/gku316

Rouzeau-Szynalski, K., Stollewerk, K., Messelhäusser, U., and Ehling-Schulz, M. (2020). Why be serious about emetic *Bacillus cereus*: cereulide production and industrial challenges. *Food Microbiol.* 85:103279. doi: 10.1016/j.fm.2019.103279

Rutherford, S. T., and Bassler, B. L. (2012). Bacterial quorum sensing: its role in virulence and possibilities for its control. *Cold Spring Harb. Perspect. Med.* 2:a012427. doi: 10.1101/cshperspect.a012427

Salvetti, S., Ghelardi, E., Celandroni, F., Ceragioli, M., Giannessi, F., and Senesi, S. (2007). FlhF, a signal recognition particle-like GTPase, is involved in the regulation of flagellar arrangement, motility behaviour and protein secretion in *Bacillus cereus*. *Microbiology* 153, 2541–2552. doi: 10.1099/mic.0.2006/005553-0

Seyi-Amole, D. O., Onilude, A. A., Rani, D. S., and Halami, P. M. (2020). Evaluation of growth and cereulide production by *Bacillus cereus* isolated from cooked rice. *Int. J. Food Stud.* 9, 135–145. doi: 10.7455/ijfs/9.1.2020.a1

Shaheen, R., Andersson, M. A., Apetroaie, C., Schulz, A., Ehling-Schulz, M., Ollilainen, V. M., et al. (2006). Potential of selected infant food formulas for production of *Bacillus cereus* emetic toxin, cereulide. *Int. J. Food. Microbiol.* 107, 287–294. doi: 10.1016/j.ijfoodmicro.2005.10.007

Shiota, M., Saitou, K., Mizumoto, H., Matsusaka, M., Agata, N., Nakayama, M., et al. (2010). Rapid detoxification of cereulide in *Bacillus cereus* food poisoning. *Pediatrics* 125, e951–e955. doi: 10.1542/peds.2009-2319

Silva, H. O., Lima, J. A. S., Aguilar, C. E. G., Rossi, G. A. M., Mathias, L. A., and Vidal, A. M. C. (2018). Efficiency of different disinfectants on *Bacillus cereus* sensu stricto biofilms on stainless-steel surfaces in contact with milk. *Front. Microbiol.* 9:2934. doi: 10.3389/fmicb.2018.02934

Singh, A., Gupta, R., and Pandey, R. (2016). Rice seed priming with picomolar rutin enhances rhizospheric *Bacillus subtilis* CIM colonization and plant growth. *PLoS One* 11:e0146013. doi: 10.1371/journal.pone.0146013

Stepanović, S., Vuković, D., Dakić, I., Savić, B., and Švabić-Vlahović, M. (2000). A modified microtiter-plate test for quantification of staphylococcal biofilm formation. *J. Microbiol. Methods* 40, 175–179. doi: 10.1016/S0167-7012(00)00122-6

Stevenson, E., Minton, N. P., and Kuehne, S. A. (2015). The role of flagella in *Clostridium difficile* pathogenicity. *Trends Microbiol.* 23, 275–282. doi: 10.1016/j.tim.2015.01.004

Teh, K. H., Flint, S., Palmer, J., Andrewes, P., Bremer, P., and Lindsay, D. (2012). Proteolysis produced within biofilms of bacterial isolates from raw milk tankers. *Int. J. Food Microbiol.* 157, 28–34. doi: 10.1016/j.ijfoodmicro.2012.04.008

Thomas, A., and Sathian, C. (2014). Cleaning-in-place (CIP) system in dairy plant-review. *IOSR J. Environ. Sci. Toxicol. Food Technol.* 3:6.

Tian, S., Xiong, H., Geng, P., Yuan, Z., and Hu, X. (2019). CesH represses cereulide synthesis as an alpha/beta fold hydrolase in *Bacillus cereus*. *Toxins* 11:231. doi: 10.3390/toxins11040231

Vlamakis, H., Chai, Y., Beauregard, P., Losick, R., and Kolter, R. (2013). Sticking together: building a biofilm the *Bacillus subtilis* way. *Nat. Rev. Microbiol.* 11, 157–168. doi: 10.1038/nrmicro2960

Walser, V., Kranzler, M., Dawid, C., Ehling-Schulz, M., Stark, T. D., and Hofmann, T. F. (2021). Distribution of the emetic toxin cereulide in cow milk. *Toxins* 13:528. doi: 10.3390/toxins13080528

Wang, B., Tan, X., Du, R., Zhao, F., Zhang, L., Han, Y., et al. (2019). Bacterial composition of biofilms formed on dairy-processing equipment. *Prep. Biochem. Biotechnol.* 49, 477–484. doi: 10.1080/10826068.2019.1587623

Wijman, J. G., de Leeuw, P. P., Moezelaar, R., Zwietering, M. H., and Abee, T. (2007). Air-liquid interface biofilms of *Bacillus cereus*: formation, sporulation, and dispersion. *Appl. Environ. Microbiol.* 73, 1481–1488. doi: 10.1128/aem.01781-06

Wijnands, L. M., Dufrenne, J. B., Rombouts, F. M., In't Veld, P. H., and Van Leusden, F. M. (2006). Prevalence of potentially pathogenic *Bacillus cereus* in food commodities in The Netherlands. *J. Food Prot.* 69, 2587–2594. doi: 10.4315/0362-028X-69.11.2587

Wu, D. C., Zamorano-Sánchez, D., Pagliai, F. A., Park, J. H., Floyd, K. A., Lee, C. K., et al. (2020). Reciprocal c-di-GMP signaling: incomplete flagellum biogenesis triggers c-di-GMP signaling pathways that promote biofilm formation. *PLoS Genet.* 16:e1008703. doi: 10.1371/journal.pgen.1008703

Yan, F., Yu, Y., Gozzi, K., Chen, Y., Guo, J. H., and Chai, Y. (2017). Genome-wide investigation of biofilm formation in *Bacillus cereus*. *Appl. Environ. Microbiol.* 83:e00561-17. doi: 10.1128/aem.00561-17

Yobouet, B. A., Kouamé-Sina, S. M., Dadié, A., Makita, K., Grace, D., Djè, K. M., et al. (2014). Contamination of raw milk with *Bacillus cereus* from farm to retail in Abidjan, Côte d'Ivoire and possible health implications. *Dairy Sci. Technol.* 94, 51–60. doi: 10.1007/s13594-013-0140-7

Yu, P., Yu, S., Wang, J., Guo, H., Zhang, Y., Liao, X., et al. (2019). *Bacillus cereus* isolated from vegetables in China: incidence, genetic diversity, virulence genes, and antimicrobial resistance. *Front. Microbiol.* 10:948. doi: 10.3389/fmicb.2019.00948

Yu, S., Yu, P., Wang, J., Li, C., Guo, H., Liu, C., et al. (2020). A study on prevalence and characterization of *Bacillus cereus* in ready-to-eat foods in China. *Front. Microbiol.* 10:3043. doi: 10.3389/fmicb.2019.03043

Zhao, L., Poh, C. N., Wu, J., Zhao, X., He, Y., and Yang, H. (2022). Effects of electrolysed water combined with ultrasound on inactivation kinetics and metabolite profiles of *Escherichia coli* biofilms on food contact surface. *Innov. Food Sci. Emerg. Technol.* 76:102917. doi: 10.1016/j.ifset.2022.102917

Zhou, P., Xie, G., Liang, T., Yu, B., Aguilar, Z., and Xu, H. (2019). Rapid and quantitative detection of viable emetic *Bacillus cereus* by PMA-qPCR assay in milk. *Mol. Cell. Probes* 47:101437. doi: 10.1016/j.mcp.2019.101437

Zhu, Y., Ji, F., Shang, H., Zhu, Q., Wang, P., Xu, C., et al. (2011). Gene clusters located on two large plasmids determine spore crystal association (SCA) in *Bacillus thuringiensis* subsp. finitimus strain YBT-020. *PLoS One* 6:e27164. doi: 10.1371/journal.pone.0027164

Conflict of Interest: The authors declare that the research was conducted in the absence of any commercial or financial relationships that could be construed as a potential conflict of interest.

Publisher's Note: All claims expressed in this article are solely those of the authors and do not necessarily represent those of their affiliated organizations, or those of the publisher, the editors and the reviewers. Any product that may be evaluated in

this article, or claim that may be made by its manufacturer, is not guaranteed or endorsed by the publisher.

frontiers | Frontiers in Microbiology

TYPE Original Research
PUBLISHED 02 September 2022
DOI 10.3389/fmicb.2022.993237

OPEN ACCESS

EDITED BY
Lei Yuan,
Yangzhou University,
China

REVIEWED BY
Tong Gao,
Fox Chase Cancer Center, United States
Hongshun Yang,
National University of Singapore, Singapore
Yanfu He,
Hainan University,
China

*CORRESPONDENCE
Yanlong Liu
liuyanlong314@163.com

SPECIALTY SECTION
This article was submitted to Food Microbiology, a section of the journal Frontiers in Microbiology

RECEIVED 13 July 2022
ACCEPTED 15 August 2022
PUBLISHED 02 September 2022

CITATION
Zhang C, Chen J, Pan X, Liu H and Liu Y (2022) Sigma factor RpoS positively affects the spoilage activity of *Shewanella baltica* and negatively regulates its adhesion effect.
Front. Microbiol. 13:993237.
doi: 10.3389/fmicb.2022.993237

Sigma factor RpoS positively affects the spoilage activity of *Shewanella baltica* and negatively regulates its adhesion effect

Caili Zhang, Jiaqi Chen, Xiaoming Pan, Haimei Liu and Yanlong Liu*

School of Food Engineering, Ludong University, Yantai, China

Shewanella baltica is the dominant bacterium that causes spoilage of seafood. RpoS is an alternative sigma factor regulating stress adaptation in many bacteria. However, the detailed regulatory mechanism of RpoS in *S. baltica* remains unclear. This study aims to investigate the regulatory function of RpoS on spoilage activity and adhesion ability in *S. baltica*. Results revealed that RpoS had no effect on the growth of *S. baltica*, but positively regulated the spoilage potential of *S. baltica* accompanied by a slower decline of total volatile basic nitrogen, lightness, and the sensory score of fish fillets inoculated with *rpoS* mutant. RpoS negatively regulated the adhesion ability, which was manifested in that the bacterial number of *rpoS* mutant adhered to stainless steel coupon was higher than that of the *S. baltica* in the early stage, and the biofilm formed on glass slide by *rpoS* mutant was thicker and tighter compared with *S. baltica*. Transcriptomic analysis showed that a total of 397 differentially expressed genes were regulated by RpoS. These genes were mainly enrichment in flagellar assembly, fatty acid metabolism/degradation, and RNA degradation pathways, which were associated with motility, biofilm formation and cold adaptation. This study demonstrated that RpoS is a primary regulator involved in flagellar assembly mediated biofilm formation and cold adaptation-related spoilage activity of *S. baltica*. Our research will provide significant insights into the control of microbiological spoilage in seafood.

KEYWORDS

food microbiology, *Shewanella* spp., RpoS, spoilage activity, adhesion, biofilm

Introduction

Microbial spoilage of seafood during processing, storage and sales lead to massive economic losses in the aquatic industry (Odeyemi et al., 2020; Zhuang et al., 2021). The psychrotolerant *Shewanella baltica* is a well-known spoilage bacterium frequently detected in chilled fish and seafood (Vogel et al., 2005). Studies indicated that *S. baltica* was the

specific spoilage microorganism in raw salmon, chilled shrimp, and large yellow croaker (Macé et al., 2013; Zhu et al., 2015, 2016). *S. baltica* is a gram-negative, motile, rod-shaped bacterium, which is capable of producing H_2S. *S. baltica* possesses a strong spoilage potential by the formation of spoilage-associated metabolites, such as utilizing trimethylamine-N-oxide as an electronic receptor to produce trimethylamine, dimethylamine and formaldehyde, thus bringing the unpleasant off-flavors (Broekaert et al., 2011; Wright et al., 2019). *S. baltica* decomposed nutrients in fish mainly *via* nitrogen and nucleotide pathways and thereby caused the production of amines, organic acids, etc. (Serio et al., 2014; Lou et al., 2021). Generally, diverse microbiota is discovered on newly caught fish, among which *S. baltica* only accounts for a fraction of the initial microflora, but *S. baltica* dominates and becomes the spoilage microorganism during low-temperature storage (Parlapani et al., 2014). It indicates that *S. baltica* has a robust ability to accommodate rapidly changing conditions. The response of bacteria to different environmental stresses requires complex coordination and overlapping regulatory networks (Zhuang et al., 2021). Adhesion is an important way for bacteria to adapt to the environment, which is a key step in the spoilage process of seafood. *S. baltica* has the potential to attach to seafood and form biofilm on the surface (Zhu et al., 2019). Understanding the environmental adaptation mechanism of *S. baltica* will provide guidelines for the storage of seafood.

Sigma factor is a constituent of bacterial RNA polymerase responsible for recognizing promoters and initiating transcription. Previous studies have shown that the sigma factor regulates a large regulon in Gram-negative bacteria, accounting for about 10% of the genome (Schellhorn, 2014; Wong et al., 2017). RpoS is associated with stress adaptation and response to changeable environments (Dodd and Aldsworth, 2002; Dong and Schellhorn, 2010). The function of RpoS has been widely explored in *Escherichia coli*, *Serratia plymuthica*, and *Vibrio cholerae* (Vidovic et al., 2011; Liu et al., 2016; Wölflingseder et al., 2022), and the results showed that RpoS enhanced their adaptation to various environmental stresses (starvation, acidic pH, oxidative stress, etc.). Recent studies found that RpoS can also regulate virulence factor expression, such as adhesion, biofilm-forming, antibiotic tolerance, etc. Mata et al. (2017) showed that the adherence to epithelial cells of *E. coli* was upregulated by RpoS. RpoS also revealed a positive effect on the expression of T6SS gene and flagellum formation with the increased synthesis of exopolysaccharides in *Y. pseudotuberculosis* (Guan et al., 2015). The role of RpoS played in stress adaptation and toxin factor expression indicated that RpoS might be involved in the environmental adaptation and spoilage ability of *S. baltica*. Feng et al. (2021) demonstrated that sigma factors RpoS/RpoN regulated the stress response and spoilage activity of *S. baltica*. Our previous study indicated that RpoS controlled the stress resistance, quorum sensing and biofilm formation in *S. baltica* (Zhang et al., 2021), however, the detailed genes regulated by RpoS remain unknown.

Recently, many emerging omics methods, such as genomics, metabolomics, and transcriptomics, have been widely applied in the study of food safety with the rapid development of science and technology (Zhao et al., 2020; Li et al., 2021). For instance, the stress responses of *Salmonella enterica* to thermal and essential oils were clarified by metabolomics and transcriptomics (Chen et al., 2022b). Transcriptomics was a feasible technique, which uses the RNA-seq high-throughput sequencing technology to investigate the gene expression level and regulation of food microorganisms at the overall level. Therefore, transcriptomics was applicable to analyze the function of RpoS in *S. baltica*.

For a better understanding of the role of RpoS in *S. baltica*, the difference between *S. baltica* and *rpoS* mutant in spoilage potential and adhesion effect was compared. We further explored the differentially expressed genes (DEGs) in *S. baltica* and *rpoS* mutant using a transcriptome technology. This study aims to clarify the regulatory mechanism of RpoS in *S. baltica*, which will provide new ideas for the control of spoilage microorganisms.

Materials and methods

Strains and culture conditions

The *S. baltica* X7 was previously isolated from large yellow croaker. The corresponding *rpoS* mutant was constructed in the previous study (Zhang et al., 2021). Both of these two bacterial species were cultured in LB broth.

Spoilage activity determination

The spoilage activity of two bacterial strains was evaluated by sterile large yellow croaker fillets. The sterile fish fillets were prepared as described by Macé et al. (2013). The overnight culture of *S. baltica* and *rpoS* mutant were centrifuged and re-suspended in sterile water to OD600 ≈ 0.2. Then 5 ml of the corresponding bacterial suspension was added to 500 ml of sterile water. After that, all the fish fillets were divided into three groups. Two groups were immersed with the bacterial suspension of *S. baltica* and *rpoS* mutant for 10 min, respectively, and the initial bacterial count of fish fillets was approx. 4 log CFU/g. The other group was immersed in sterile water for 10 min as a control (Wang et al., 2017). The fillets were then individually packed in polyvinyl chloride bags and stored at 4 ± 0.5°C. Three fillets from each group were randomly selected for analysis every day. Total viable counts (TVC) were detected as reported by Ozogul et al. (2017). Approximately 25 g of fish fillets were diluted by 225 ml of 0.85% NaCl solution, and the plate count agar was poured onto the dilution and cultured for 48 h at 30°C. The sensory evaluation was conducted based on the studies of Parlapani et al. (2014) and Chen et al. (2022a) with some modifications (Supplementary Table S1). Five trained panelists assessed the fish quality from three aspects: color, texture, and odor. The spoilage level of the fish fillets was

scored on a continuous scale from 0 to 10. The total scores of 8–10 points are fresh; 5–7 points are slight spoilage; and 0–4 points are spoilage. The total volatile basic nitrogen (TVB-N) of fish fillets was measured by the Conway and Byrne method using Semi-trace Kevlar Nitrometer (Parlapani et al., 2014). The lightness of fish fillets was determined by a chroma meter (CR-400, Konica Minolta, INC, Japan).

Bacterial adhesion assays

Bacterial adhesion to stainless steel

The adhesion assay of bacterial strains was performed on the stainless steel coupon in LB broth. The 304 stainless steel coupons (10 mm × 10 mm, 1.5 mm thickness) were washed with 75% ethanol and distilled water, and then they were sterilized (Yuan et al., 2018). One milliliter of an overnight culture of *S. baltica* wild-type and *rpoS* mutant was inoculated into a centrifugal tube containing 5 ml LB broth, respectively. Each centrifugal tube contained one stainless steel coupon and was cultured for 24 h at 30°C. The number of colonies attached to stainless steel coupon was determined at 0 and 15 min, 1, 2, 4, 7, 10, and 24 h. The stainless steel coupon was taken out with sterile tweezers and washed with sterile distilled water. The stainless steel coupon was immersed in 5 ml distilled water, handled with ultrasonic for 10 min, and homogenized for 2 min. The determination of the total viable count is the same as described above.

Microscopic analysis

For scanning electron microscopy (SEM) observation, the sterilized stainless steel coupons were incubated in LB broth containing *S. baltica* or *rpoS* mutant for 24 h, then the stainless steel coupon was washed with sterile distilled water three times and fixed with 2.5% glutaraldehyde overnight. The coupons were dehydrated by immersing in 30%, 50%, 70%, 80%, and 90% ethanol for 10 min, respectively. Then further dehydration was carried out in 100% ethanol for 15 min twice. Finally, the coupons were dried, gold sputtered and observed using a scanning electron microscope (Hitachi Model SU8010, Japan).

For light microscopic observation, the bacterial cells attached to glass were investigated according to Santhakumari et al. (2018). The sterilized glass slides were plated in LB and cultured for 24 h. Then the glass slides were washed with sterile distilled water and stained with crystal violet for 15 min. The glass slides were examined under a light microscope (Olympus CX22, Tokyo, Japan) after drying.

Transcriptome samples preparation and analyze

RNA extraction and library preparation

Strains of both *S. baltica* and *rpoS* mutant were incubated to OD600 = 1.5, and the bacterial pellet was obtained by centrifugation (4,000 rpm, 15 min). RNA was extracted using a RNeasy Mini Kit (Qiagen, Germany). The rRNA was removed and mRNA was left. The fragmentation was obtained by divalent cations in NEBNext First Strand Synthesis Reaction Buffer. First-strand of cDNA was synthesized with a random hexamer primer. Second strand cDNA synthesis was carried out by DNA Polymerase I and RNase H. The library fragments were purified by an AMPure XP system (Beckman, United States). Afterward, PCR was performed and PCR products were analyzed with the Agilent Bioanalyzer 2100 system. The library preparations were sequenced with an Illumina Novaseq platform.

Analysis of RNA-seq

The reads containing adapter, ploy-N (*N* rate > 10%) and low-quality reads were removed and clean reads were collected. The Q20 and Q30 indicated the data were of high quality with values of >98 and 95%, respectively. The clean reads were mapped to *S. baltica* OS678 complete genome in the NCBI database using Bowtie2-2.2.3. Gene expression levels were analyzed by fragments Per Kilobase of transcript sequence per Millions of base pairs sequenced (FPKM; Trapnell et al., 2013). DEGs were analyzed according to the false discovery rate (FDR) values (<0.05), *p* values (<0.05), and the |log2 (fold change)| values (>0.5). The biological functions and metabolic pathways of the DEGs were classified according to the Gene Ontology (GO) and Kyoto Encyclopedia of Genes and Genomes (KEGG) databases. GO terms with adjusted $p < 0.05$ were regarded as significantly enriched by DEGs. The statistical enrichment of DEGs in KEGG pathways was analyzed by KOBAS software.

qRT-PCR validation

Bacterial strains were cultured to the end of the exponential phase. RNA was obtained by trizol reagent (Sangon Biotech, China). The EasyScript One-step gDNA Removed and cDNA Synthesis Supermix kit (Transgen, China) was used to compose cDNA. The primers were listed in Supplementary Table S2. TransStart Tip Green qPCR supermix kit (Transgen, China) was used for qPCR amplification. The threshold cycles (CT) were recorded and the relative expression level of genes was obtained by the $2^{-\triangle\triangle Ct}$ method (Li et al., 2019).

Data analysis

Each analysis was conducted in triplicate. The results were recorded as the mean ± standard deviation. The significance between samples ($p < 0.05$) was analyzed by SPSS 19.0 software with one-way analysis of variance (ANOVA).

Results and discussion

RpoS positively regulated spoilage activity

The spoilage activity of bacterial strains was estimated on sterile yellow croaker fillets. The initial viable count for control

was below 2.0 log CFU/g. The initial number for fillets that were inoculated with *S. baltica* or *rpoS* mutant was about 4.8 log CFU/g. The number of bacteria increased with storage time, and the growth curves of the two strains were very close, which almost overlapped after 4 days of storage with a viable count of about 8.2 log CFU/g, indicating that RpoS did not affect the growth of *S. baltica* (Figure 1A). Our previous study has shown that the deletion of *rpoS* does not affect the growth of *S. baltica* at neither 30 nor 4°C in LB broth (Zhang et al., 2021). Similarly, the growth of *P. fluorescens* did not change without *rpoS* (Liu et al., 2018). RpoS regulator was first identified as a growth phase-dependent regulator, and it usually plays a role in stress regulation at the stationary phase (Schellhorn, 2014). Therefore, RpoS does not affect the growth of *S. baltica*.

Sensory scores of all samples decreased with the prolonging of storage time because of the production of spoilage metabolite and change in appearance (Figure 1B). TVB-N is one of the typical spoilage metabolites, which is usually used to evaluate the process of fish spoilage. The TVB-N of samples inoculated with *S. baltica* and *rpoS* mutant increased quickly after 3 days of storage, and the group inoculated with *S. baltica* reached a maximum TVB-N value exceeding 30 mg/100 g at day 6 (Figure 1C). The lightness of fish fillets inoculated with *S. baltica* declined quickly compared with that inoculated with *rpoS* mutant (Figure 1D), which was in accordance with the sensory scores. The sensory score of the fish fillets inoculated with *rpoS* mutant was significantly lower than that of *S. baltica* after 3 days of storage ($p < 0.05$), suggesting that RpoS positively regulated the spoilage activity of *S. baltica*. Similar results were also found in *P. fluorescens* and *S. baltica* SB02, the spoilage activities of which decreased when the *rpoS* gene was deleted, which is in agreement with the result in this study. It was inferred that this phenomenon might be attributed to the decrease of extracellular enzyme activity or the down-regulation of quorum sensing in *rpoS* mutant (Liu et al., 2018, 2019; Feng et al., 2021; Hai et al., 2022). The regulatory mechanism of RpoS on bacterial spoilage needs to be thoroughly explored in the future.

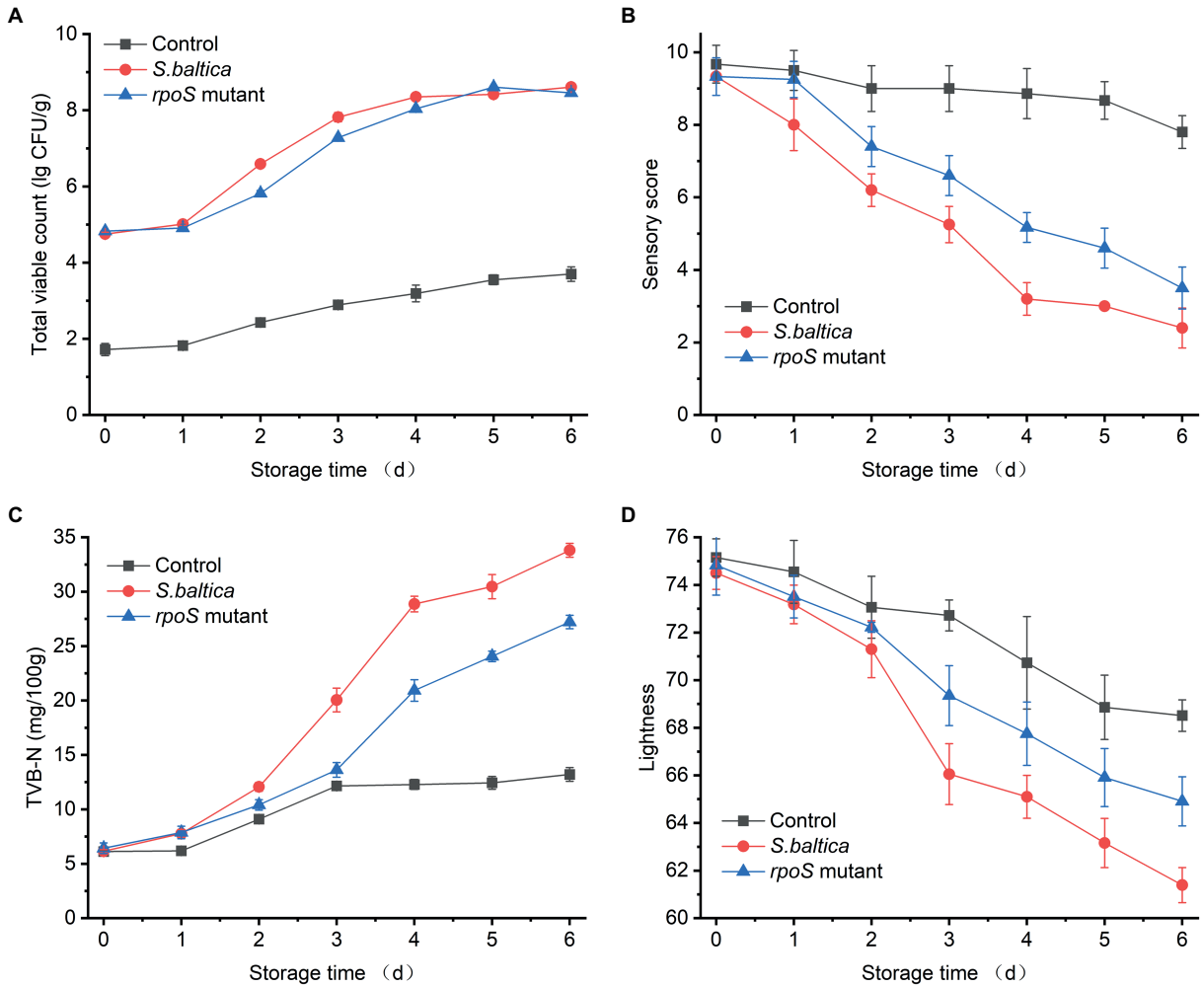

FIGURE 1
Changes in total viable counts **(A)**, sensory score **(B)**, TVB-N **(C)**, and lightness **(D)** of yellow croaker fillets inoculated with *Shewanella baltica* and *rpoS* mutant during storage at 4°C.

RpoS negatively regulated the adhesion

Bacteria mediated seafood spoilage is a complex process, involving in adhesion, proliferation, and forming biofilm (Sun et al., 2022). Once bacteria attach to seafood, biofilms will gradually form, thereby causing seafood spoilage (Zhao et al., 2022). The result of bacterial adhesion ability on stainless steel coupon was displayed in Figure 2A. In the early stage of adhesion (0–4 h), *S. baltica* wild type showed a very slow adhesion to the stainless steel, but the number of *rpoS* mutant on stainless steel coupon was higher than that of *S. baltica*. After 2 h of incubation, the number of *rpoS* mutant colonies that adhered to the coupon was nearly 100-fold higher than *S. baltica*. After 24 h, the number of colonies in both strains reached 6.6 CFU/cm^2, and no significant difference between *S. baltica* and the *rpoS* mutant was observed. It can be observed that the *rpoS* mutant exhibited an earlier and stronger adhesion ability than that of *S. baltica* wild type. For the SEM visualization (Figures 2B,C), similar biofilm morphology of *rpoS* mutant and *S. baltica* on stainless steel coupon was observed, which was in accordance with the attached bacterial count at 24 h. For the glass slides, the biofilm formed by *S. baltica* wild type was relatively loose (Figure 2D), while *rpoS* mutant formed more compact biofilm (Figure 2E). Compared with *S. baltica* wild type, *rpoS* mutant showed earlier adhesion ability on stainless steel coupon and thicker biofilm on the glass slide, indicating that RpoS negatively regulated the adhesion related characteristics of *S. baltica* in a time-dependent and condition-dependent manner.

RpoS usually had a positive response to the changes in the external environment or living state, for example, the motility of *Vibrio cholerae* decreased when the *rpoS* was deleted (Wölflingseder et al., 2022). However, RpoS also manifested some negative regulations. RpoS was found to negatively regulate the swimming motility in *E. coli* and *S. plymuthica* G3 (Ojima et al., 2012; Liu et al., 2016), suggesting that the regulatory mechanism of RpoS may be species-dependent. Consistent with our result, Feng et al. (2021) reported that the deletion of RpoS enhanced the swimming motility in *S. baltica* SB02, and the flagella of the *rpoS* mutant was thicker than that of the wild type observed by transmission electron microscopy. In addition, the biofilm production in *Cronobacter sakazakii* with a defect of *rpoS* only declined in 24 h, and there was no significant difference after 48 h of incubation, revealing that the regulation of RpoS on biofilm formation only showed a delayed effect rather than a complete inhibition (Fernández-Gómez et al., 2020). It revealed that RpoS has a growth-stage dependence on the regulation of biofilm, which provides important insights into the control of *S. baltica* during seafood processing.

RNA sequencing analysis

In this study, to further investigate the regulatory role of RpoS, a comparative transcriptome analysis of the *rpoS* gene-deficient strain (981 bp segment) and the *S. baltica* wild-type was performed. The total RNA obtained from *S. baltica* and *rpoS* mutant cells were analyzed to identify the DEGs. After filtration, there were on average 7,775,014 and 7,509,599 raw reads for *S. baltica* and *rpoS* mutant, respectively (Supplementary Table S3). A total of 7,638,874 and 7,369,249 high-quality reads from *S. baltica* and *rpoS* mutant, respectively, were mapped on the reference genome of *S. baltica* OS678 (Supplementary Table S3). Approximately 85% of short reads were successfully mapped on the *S. baltica* OS678 genome (Supplementary Table S4).

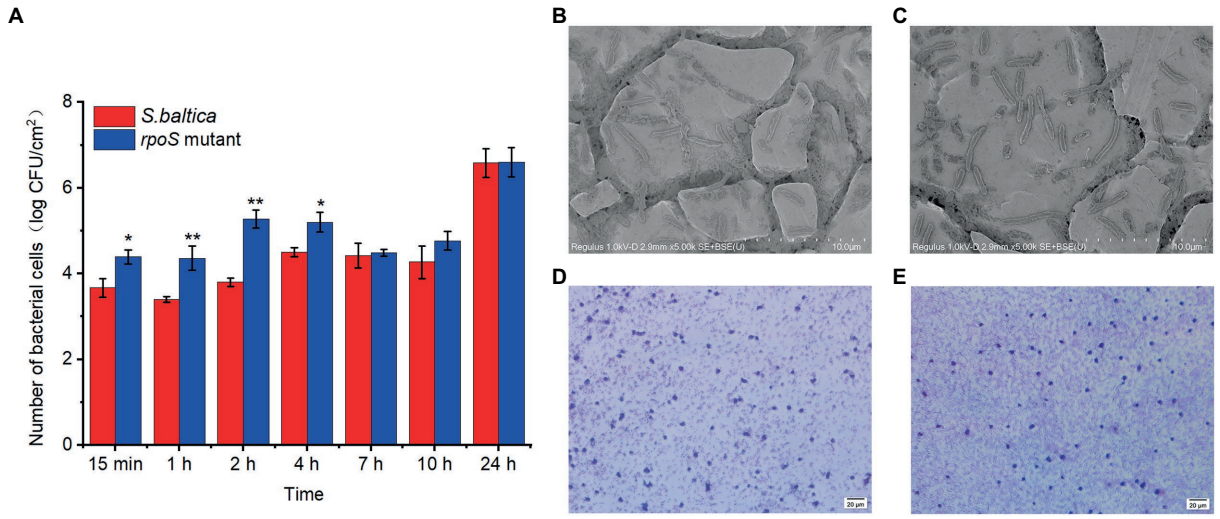

FIGURE 2
Number of bacterial count on stainless steel coupon, "*" and "**" indicate the significant difference at $p < 0.05$ and $p < 0.01$, respectively **(A)**. Scanning electron microscopy images of biofilm formed on stainless steel coupon by *Shewanella baltica* **(B)**, and *rpoS* mutant **(C)**. Microscopic visualization of biofilm formed on glass slide by *S. baltica* **(D)**, and *rpoS* mutant **(E)**.

To reduce the impact of sequencing depth and gene length, the corrected FPKM is usually used for describing the gene expression value of RNA-seq. The correlation coefficients indicate the correlations of gene expression between samples. As exhibited in Figure 3A, the squares of the Pearson correlation coefficients (R^2) were all greater than or equal to 0.8, signifying that the expression patterns of genes were very similar between samples (Garber et al., 2011). A total of 397 DEGs was observed, which accounted for almost 10% of the genome (Figure 3B; Supplementary Table S5). The expression of 248 genes (approximately 62%) increased in *rpoS* mutant, while the other 149 genes (approximately 38%) decreased.

Hierarchical clustering was performed according to the 397 DEGs, in which the intuitive changes of DEGs between samples were observed (Figure 4). The unsupervised clustering formed two major gene clusters. Cluster 1 (red color) and cluster 2 (green color) indicated the upregulated and downregulated genes, respectively.

GO analysis

Gene Ontology enrichment analysis was conducted based on the DEGs. Among the up-regulated DEGs in *rpoS* mutant (Figure 5; Supplementary Table S6), it showed that several categories of biological processes were enriched in the DEGs of *rpoS* mutant, including flagellum-dependent cell motility (GO:0001539, GO:0071973, and GO:0097588), movement of cell component, cell motility (GO:0006928, GO:0048870, and GO:0040011), localization of cell (GO:0051674), and oxidation–reduction process (GO:0055114). As to molecular function, oxidoreductase activity (GO:0016491, GO:0016627), cofactor and coenzyme binding (GO:0048037, GO:0050662), heme binding (GO:0020037), flavin adenine dinucleotide (GO:0050660), tetrapyrrole binding (GO:0046906), and electron transfer activity (GO:0009055) were over-represented. The oxidoreductase activity and cofactor binding were the most represented. The increased motility has been observed in *rpoS* mutant (Zhang et al., 2021), which was mediated by flagellum. The changes in oxidoreductase indicated that RpoS may be involved in the activation of oxidative stress response of *S. baltica*. Therefore, cell motility and oxidoreductase activity were considered to be the main regulation pathways of RpoS.

Among downregulated DEGs in *rpoS* mutant, membrane (GO:0016020) in cellular component, nucleic acid binding (GO:0003676), and RNA binding (GO:0003723) involved in molecular function were representive. In terms of the membrane, the expressions of major facility superfamily (MFS) genes (RS23645, RS43790, and RS29395) were significantly declined in *rpoS* mutant. MFS family transporters are not only related to the absorption of nutrients but also involved in response to external stress. It can be inferred that membrane is one of the main targets of RpoS (Costa et al., 2014).

KEGG analysis

To comprehensively analyze the regulatory function of DEGs, these DEGs were further subjected to KEGG analysis. For the upregulation of DEGs, they were principally focused on flagellar assembly, bacterial chemotaxis, fatty acid metabolism, and two-component system. The downregulation of DEGs were

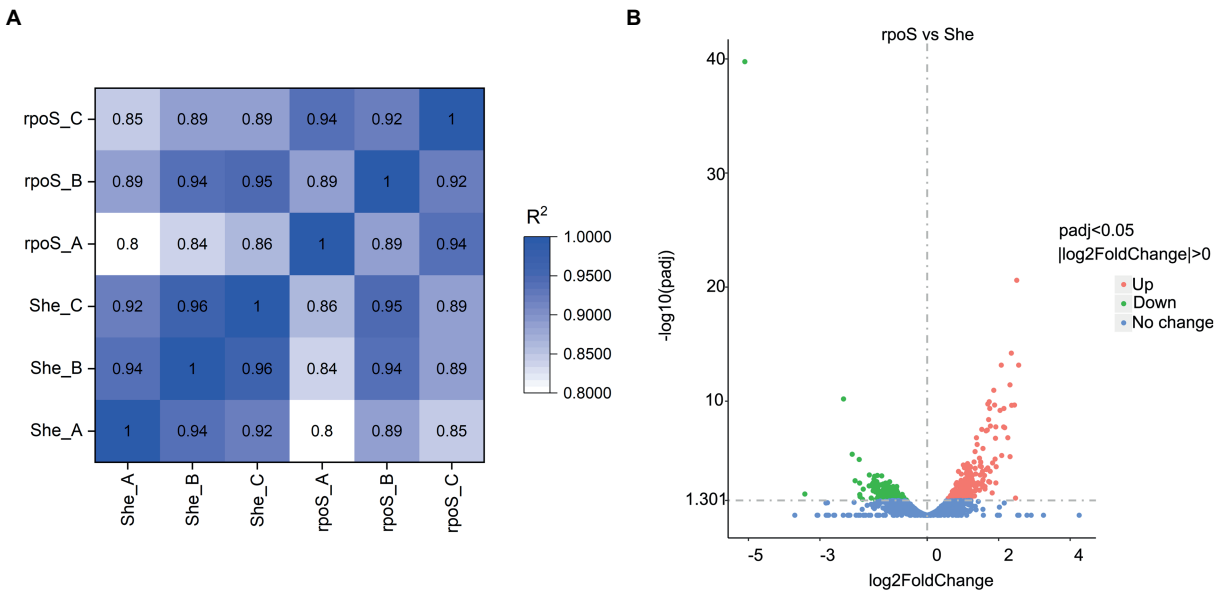

FIGURE 3
The heat-map of Pearson correlation coefficients based on gene expression levels **(A)**. Volcano plots of different expressed genes **(B)**. "She" indicates *Shewanella baltica* wild type, "*rpoS*" indicates the *rpoS* mutant.

enriched in the RNA degradation and quorum sensing pathways (Figure 6; Supplementary Table S7).

Flagellar assembly and biofilm formation

Flagella is an important motor organ in bacteria. It was reported to have three functional characteristics: motility, chemotaxis, and adhesion, which contribute to responding to the adverse environment quickly and timely for bacteria (Lund et al., 2020). The motility can promote the adhesion of bacteria on host cells, thus realizing infection (Colin et al., 2021). Previous studies indicated that flagella played a crucial role in the adhesion for bacteria, as the *flic* subunit promoted bacteria move to the attachment site in the early stage of adhesion (Sun et al., 2022). It has been observed in our previous study that RpoS negatively regulated the motility of *S. baltica* and the diameter of the *rpoS* mutant increased by 46.6% more than *S. baltica* wild type on the plate (Zhang et al., 2021). The flagella structure consists of three parts: a body basel, hook, and filament (Chilcott and Hughes, 2010). The synthesis and assembly of flagellum are usually involved in more than 50 genes (Chevance and Hughes, 2008). As shown in Table 1, the high expression levels of flagellar body basel-related genes (*flgF, flgG, flgH, flgI, flgC, fliF, fliN*, and *motB*) and flagella hook associated genes (*flgK*, *fliK*, and *flgD*) were found in *rpoS* mutant. The *flgM* and *flgE* showed 1.21 and 0.72 $\log_2$ (fold change) expression levels, respectively (Figure 7). FlgM protein regulates the transcription level of flagellum-related genes, thus affecting the length and quantity of flagellum. The secretion of FlgM indicates the accomplishment of the Hook-basal body (Wosten et al., 2010). The function of FlgE is to connect the flagellum filament and hook, which changes the angle of flagellum rotation (Shen et al., 2017; Li et al., 2022). Previous studies showed that the enhanced motility of *rpoS* mutant required the RpoN, and about 60% of genes were simultaneously oppositely regulated by RpoS and RpoN (Dong and Schellhorn, 2010). Feng et al. (2021) found that the deficiency of RpoN leads to a decrease in the motility of *S. baltica*, which was owing to the downregulation of flagella assembly-related genes (i.e., *flgF*, *flgC*, etc). The current increased swimming motility of *rpoS* mutant of *S. baltica* might be also affected by the existence of RpoN.

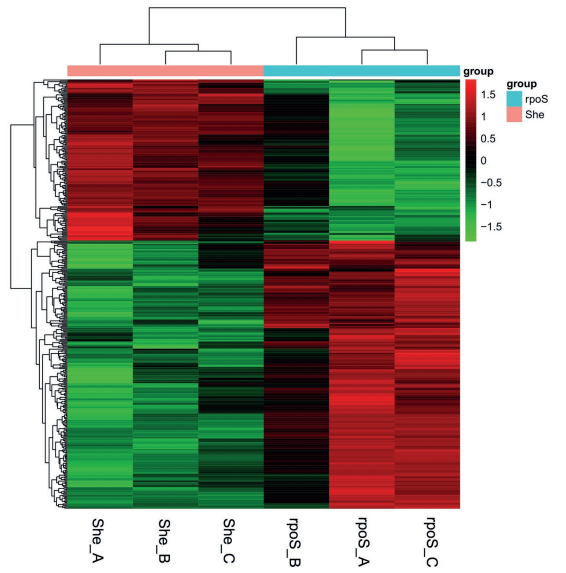

FIGURE 4
Heatmap of different expressed genes in *Shewanella baltica* and *rpoS* mutant. Each row represents the expression pattern of a single gene and each column corresponds to a single sample. "She" indicates *S. baltica* wild type, "*rpoS*" indicates the *rpoS* mutant.

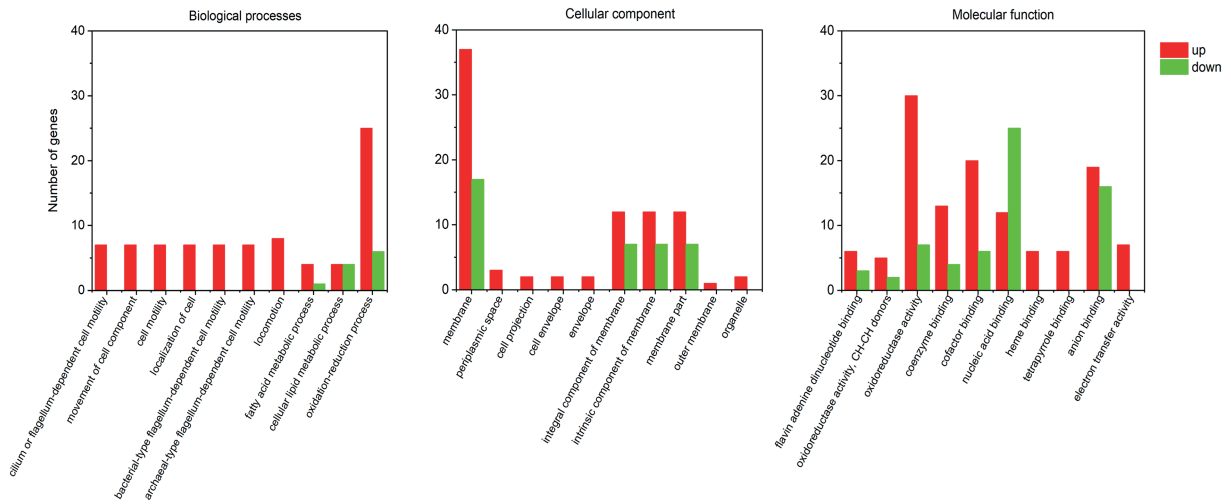

FIGURE 5
GO enrichment analysis of differently expressed genes.

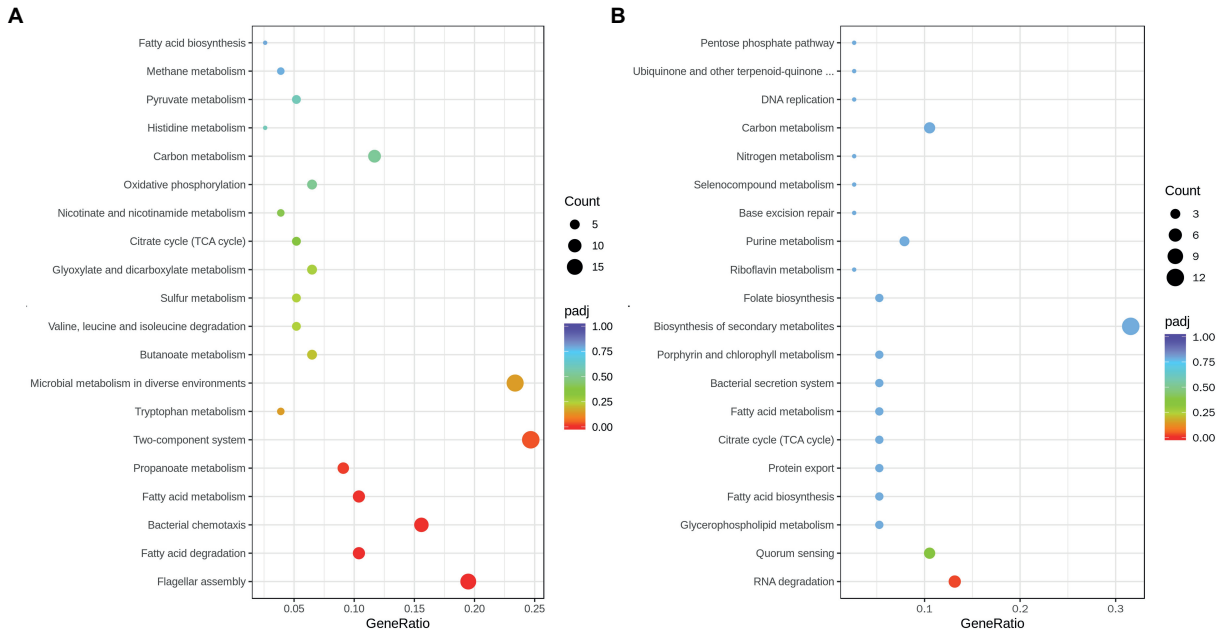

FIGURE 6
Scatterplot of upregulated genes **(A)**, and down-regulated genes **(B)**, enriched Kyoto Encyclopedia of Genes and Genomes (KEGG) pathway. Enrichment score represents the ratio of the number of upregulated/downregulated genes and the number of all genes in the pathway.

Biofilm formation is another important flagella-dependent survival model for microorganisms. When the number of bacteria fixed on the surface of host cells increases, the bacteria can secrete extracellular compounds, such as polysaccharides and protein, eventually forming stable biofilms (Voglauer et al., 2022). Zhao et al. (2022) exhibited that acidic electrolysed water disturbed the biofilm formation of *E.coli* by decreasing the nucleotide-related and carbohydrates component. This study revealed that the adhesion and biofilm-forming abilities of *rpoS* mutant were higher than that of *S. baltica* wild type (Figure 2). RNA degradation declined in *rpoS* mutant, while protein and carbohydrate metabolism had no significant change (Figure 6). We inferred that flagella assembly and RNA degradation might play a more important role in biofilm formation than nutrient metabolism The present study indicated that RpoS negatively regulated the flagellar-associated gene expression and biofilm formation. Therefore, RpoS-mediated flagellar assembly is one of the most crucial features of *S. baltica* in environmental adaptability.

Fatty acid metabolism

Fatty acid metabolism and fatty acid degradation are also important pathways regulated by RpoS (Figure 6). Fatty acids are the main components of the bacterial cell membrane. Fatty acid metabolism has been identified to be closely related to bacterial adaptation to the cold environment because the low temperature can reduce bacterial membrane fluidity and growth rate by adjusting the composition of fatty acids, especially the unsaturated fatty acids (UFAs) (Wang et al., 2020). In the fatty acid metabolism pathway, FabA plays a key role in the synthesis of UFAs. FabA is a bifunctional enzyme that can dehydrate β-hydroxy-decanoyl-ACP and isomerize trans-2-decenoyl-ACP in order to stimulate UFAs synthesis. While *fadA, fadB*, *fadD*, *fadE*, *fadF*, *fadI*, and *fadJ* are the essential genes in the fatty acid degradation pathway (Feng and Cronan, 2011). This study indicated that *fabA* was down-regulated by RpoS, while the expression of *fadA, fadB*, *fadD*, *fadI*, and *fadJ* were upregulated (Table 1), indicating that the deficiency of *rpoS* decreased the synthesis of UFAs in *S. baltica*. FabH is β-Ketoacyl-ACP synthase, which is the initiation factor of the carbon chain extension cycle, and *fabH* was down-regulated in *S. baltica* (Figure 7). Phosphatidylglycerol phosphate synthase (PgsA) catalyzes the primary reaction of phosphatidylglycerol biosynthesis, which was down-regulated in the *rpoS* mutant. *Shewanella baltica* is one of the most common specific spoilage bacteria in refrigerated fish and seafood. The strong adaptability to low temperature contributes *Shewanella* to maintaining a great growth state under refrigerated conditions. Initiation factor 1 (IF1) is encoded by *infA*, which is associated with the initiation step of protein synthsis in bacteria. The *infA* gene was positive-regulated by RpoS in *S. baltica* strain (Supplementary Table S5). Ko et al. (2006) reported that the expression of IF1 increased when *E. coli* cells were treated with cold shock, which is in accordance with our result. The deficiency of RpoS decreased the spoilage ability in *S. baltica* (Figure 1), which may be related to the decline of cold adaptation. Wang et al. (2020) reported that cell membrane

TABLE 1 Representative differently expressed genes in the *Shewanella baltica* wild type and *rpoS* mutant.

Gene ID	Gene	log2 (Fold change)	*p* value	FDR	Gene_description
Flagellar assembly					
SBAL678_RS39020	flgM	1.21	3.08×10^{-6}	1.88×10^{-4}	Flagellar biosynthesis anti-sigma factor
SBAL678_RS38990	flgD	1.08	9.39×10^{-5}	2.68×10^{-3}	Flagellar hook assembly protein
SBAL678_RS38815	fliN	0.95	1.51×10^{-3}	0.02	Flagellar motor switch protein
SBAL678_RS38975	flgG	0.89	7.80×10^{-4}	1.32×10^{-2}	Flagellar basal-body rod protein
SBAL678_RS38970	flgH	0.78	1.43×10^{-3}	0.02	Flagellar basal body L-ring protein
SBAL678_RS38995	flgC	0.76	9.30×10^{-4}	1.49×10^{-2}	Lagellar basal body rod protein
SBAL678_RS38985	flgE	0.72	1.53×10^{-3}	0.02	Flagellar hook protein
SBAL678_RS38855	fliF	0.72	2.51×10^{-3}	0.03	Flagellar basal body M-ring protein
SBAL678_RS38980	flgF	0.70	2.25×10^{-3}	0.03	Flagellar basal-body rod protein
SBAL678_RS38955	flgK	0.65	2.90×10^{-3}	0.03	Flagellar hook-associated protein
SBAL678_RS46955	flik	1.34	2.11×10^{-8}	2.62×10^{-6}	Flagellar hook-length control protein
SBAL678_RS38965	flgI	0.72	2.39×10^{-3}	0.03	Flagellar basal body P-ring protein
SBAL678_RS30420	pomA	0.81	5.62×10^{-5}	1.87×10^{-3}	Flagellar motor protein
SBAL678_RS30425	motB	0.71	2.19×10^{-3}	0.03	Flagellar motor protein
Fatty acid metabolism and degradation					
SBAL678_RS23420	fadB	2.36	8.02×10^{-13}	2.30×10^{-10}	Fatty acid oxidation complex subunit
SBAL678_RS23415	fadA	2.15	1.76×10^{-12}	4.37×10^{-10}	gene_description
SBAL678_RS37715	fadJ	1.53	1.75×10^{-10}	2.98×10^{-8}	Fatty acid oxidation complex subunit
SBAL678_RS37720	fadI	1.20	6.22×10^{-7}	5.28×10^{-5}	Acetyl-CoA C-acyltransferase
SBAL678_RS33045	fadD	1.13	9.07×10^{-6}	4.46×10^{-4}	Long-chain-fatty-acid--CoA ligase
SBAL678_RS36810	fabA	−0.83	6.25×10^{-4}	0.01	Bifunctional 3-hydroxydecanoyl-ACP dehydratase/trans-2-decenoyl-ACP isomerase
SBAL678_RS32300	fabB	−1.13	7.00×10^{-5}	2.21×10^{-3}	ketoacyl-ACP synthase III
SBAL678_RS32515	acs	1.86	2.08×10^{-14}	1.11×10^{-11}	Acetate-CoA ligase
SBAL678_RS43885	acnB	0.88	2.24×10^{-6}	1.44×10^{-4}	Bifunctional aconitate hydratase 2/2-methylisocitrate dehydratase
SBAL678_RS44375	prpC	0.71	2.94×10^{-3}	0.03	2-methylcitrate synthase
SBAL678_RS36490	sucD	−0.70	4.87×10^{-3}	0.04	Succinate--CoA ligase subunit alpha
Transport RNA					
SBAL678_RS36755		−1.90	1.24×10^{-7}	1.29×10^{-5}	tRNA-Leu
SBAL678_RS34195		−1.88	1.72×10^{-3}	0.02	tRNA-Tyr
SBAL678_RS32495		−1.81	3.75×10^{-3}	0.04	tRNA-Lys
SBAL678_RS38230		−1.62	9.34×10^{-5}	2.68×10^{-3}	tRNA-Val
SBAL678_RS36765		−1.62	5.44×10^{-6}	2.95×10^{-4}	tRNA-Gly
SBAL678_RS34190		−1.57	2.58×10^{-3}	0.03	tRNA-Tyr
SBAL678_RS37180		−1.53	5.18×10^{-5}	1.81×10^{-3}	tRNA-Ile
SBAL678_RS35065		−1.47	1.83×10^{-4}	4.55×10^{-3}	tRNA-Val
SBAL678_RS39045		−1.45	4.48×10^{-3}	0.04	tRNA-Arg
SBAL678_RS40785		−1.38	1.84×10^{-4}	4.55×10^{-3}	tRNA-Leu
SBAL678_RS39860		−1.33	1.20×10^{-3}	0.02	tRNA-Ser
SBAL678_RS37175		−1.30	1.04×10^{-3}	0.02	tRNA-Ala
SBAL678_RS31635		−1.29	3.56×10^{-3}	0.04	tRNA-Pro
SBAL678_RS38195		−1.16	4.71×10^{-3}	9.06×10^{-3}	tRNA-Ala
SBAL678_RS40675		−1.16	6.84×10^{-4}	0.01	tRNA-Met

UFAs-mediated cold adaptation was closely related to the spoilage potential. However, there are few reports on the relationship between RpoS and cold adaptation. Therefore, the cold adaptation regulatory mechanism regulated by RpoS needs to be further studied, which will contribute to clarifying the spoilage characteristics of *Shewanella* spp.

Two-component regulatory systems

Microorganism can assemble some necessary genetic circuits to sense external stimuli and respond to environmental stress. Two-component regulatory system (TCRS) is one of the most important signal transduction systems that allow bacteria to

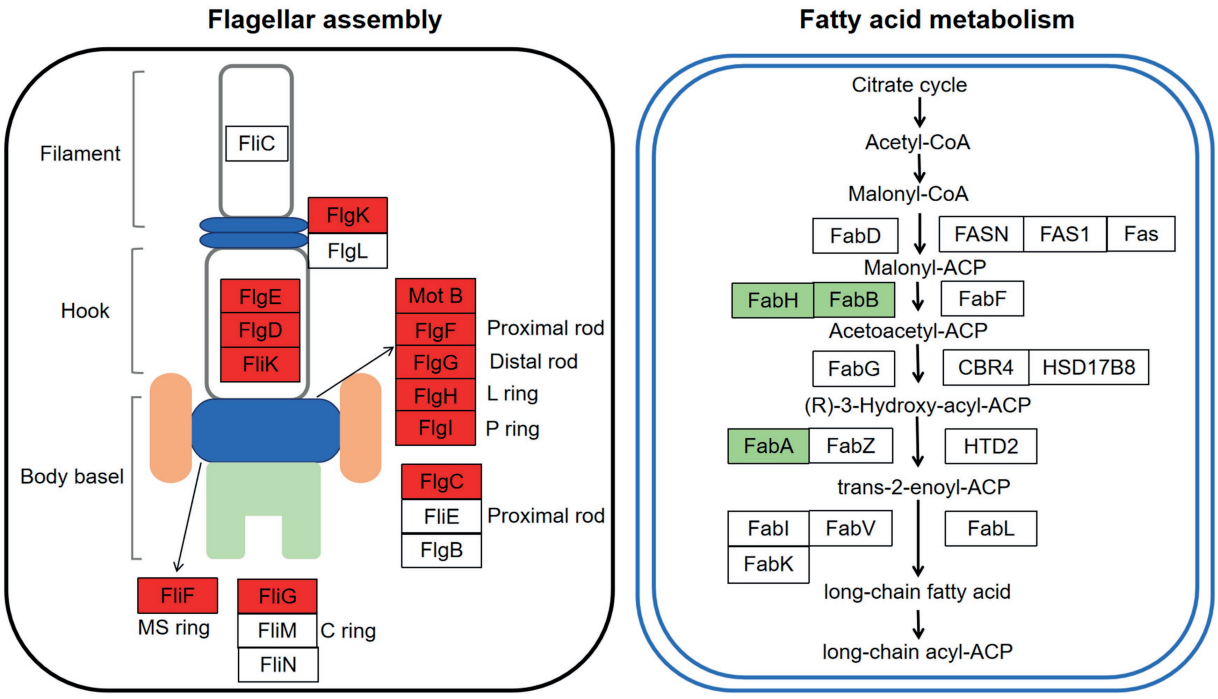

FIGURE 7
Changes of the expression levels of genes involved in flagellar assembly and fatty acid metabolism of *Shewanella baltica*. The genes marked in red and green represented upregulation and downregulation in *rpoS* mutant.

respond to stress conditions and improve their survival (Nguyen and Hong, 2008). The present study showed that TCRS was upregulated in the *rpoS* mutant of *S. baltica*. Bacterial TCRS is involved in the regulation of bacterial chemotaxis, morphological differentiation, nutrient metabolism, drug resistance, and many other physiological processes. Li et al. (2022) showed that the expression of *rpoS* can be activated by the two-component system of TorR using transcriptomics, while the effect of RpoS on TCRS was rarely studied. The up-regulated TCRS in the *rpoS* mutant indicated that TCRS is involved in the stress regulation of RpoS to *S. baltica*, but the detailed mechanism needs to be further explored.

Transport RNA

The tRNA mainly participates in the process of protein translation. Table 1 showed that 15 kinds of the transfer RNA (tRNA) were downregulated, indicating that RpoS contributes to the tRNA-mediated protein synthesis. Studies revealed that translation regulation is an important mechanism for bacteria to respond to stress quickly, and the dynamic adjustment of the total amount of tRNA is a critical regulation means for bacteria to deal with the harsh environment. Zhong et al. (2015) reported that *E. coli* slowed down the rate of translation extension by downregulating the expression of tRNA, which makes cells promptly adapt to oxidative stress.

Quorum sensing

Quorum sensing (QS) is a mechanism that microorganisms communicate to sense chemical signaling change, thus mediating the toxin factors expression, such as biofilm formation and extracellular enzyme production (Mukherjee and Bassler, 2019). Figure 6 showed that the expression of QS pathway decreased in the *rpoS* mutant. Consistent with this study, our previous study demonstrated that QS signals cyclo-(L-Pro-L-Leu) and cyclo-(L-Pro-L-Phe) declined in *rpoS* mutant, and the expression levels of QS sensing genes *luxR* were also declined in *rpoS* mutant (Zhang et al., 2021). Similar phenomena were also found in *P. fluorescens* and *S. baltica* SB02, in which the acyl homoserine lactone and diketopiperazines QS signaling decreased in the deletion of *rpoS* mutant (Liu et al., 2018; Zhang et al., 2021), indicating that RpoS usually positively regulated the QS. Therefore, QS is expected to become a new target to control the spoilage caused by *S. baltica*.

Others

Cold shock protein is an important protein that affects the ability of bacteria to adapt to low temperature. Cold shock DNA-binding domains (RS31005) were downregulated in the *rpoS* mutant (Supplementary Table S5). Cold shock protein can be used as molecular chaperones to bind with single-stranded DNA or single-stranded RNA, which prevents DNA or RNA

from forming secondary structures at low temperature, thereby promoting transcription and translation (Mihailovich et al., 2010). DNA gyrase B and *parE* (RS27555), which were the targets of antibiotics in Gram-negative bacteria, were downregulated in *rpoS* mutant. Bacterial DNA gyrase is the basic enzyme involved in the formation of DNA superhelix, and the decrease of gyrase related genes usually causes antibiotic resistance (Jogula et al., 2020). It suggests that RpoS take part in the regulation of antibiotic resistance of *S. baltica*. Previous studies indicated that the *rpoS* gene was involved in tolerance to antibiotics in *Pseudomonas aeruginosa* during the stationary phase (Keiji et al., 2010), and the deficiency of *rpoS* in *Salmonella Enteritidis* decreased the tolerance to essential oils (Cariri et al., 2019), which supports our conclusion.

Danhorn and Fuqua (2007) described that flagellum generally guides bacteria colonized on food-contact surfaces in the initial adhesive stage, then the flagella declined with the bacterial proliferation. Food gradually spoiled with the bacteria adapting to the environment and secretion of extracellular enzymes (Hai et al., 2022). Previous studies have confirmed that fatty acid synthesis and QS can enhance the growth and spoilage ability of *S. baltica* (Zhu et al., 2015; Wang et al., 2020). In this study, the fatty acid synthesis and QS pathways were downregulated in *rpoS* mutant, and its spoilage ability also decreased, but the gene expression related to flagellum assembly increased. Therefore, we speculated that RpoS might improve the survival strategy and spoilage activity through early adhesion mediated by flagella assembly pathway as a crucial target. Overall, RpoS is an important regulator involved in the environmental adaptation and spoilage potential of *S. baltica*.

qPCR validation

To validate the RNA-seq data, qPCR was conducted on four genes (RS37220, RS42925, RS34240, and RS32515) regulated by RpoS. These selected genes showed up-regulation in *rpoS* mutant compared with *S. baltica*. The expression levels were very close in RNA-seq and qPCR results (Figure 8), which indicated that the transcriptome results were reliable.

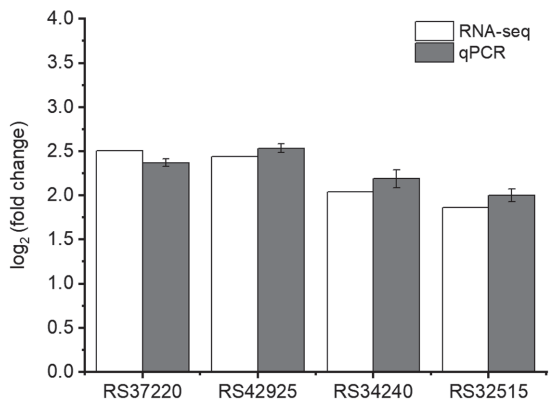

FIGURE 8
Validation of RNA-seq data of selected genes by qPCR.

Conclusion

This study revealed that RpoS positively regulated the spoilage activities of *S. baltica* while negatively regulated the adhesion and biofilm formation. Transcriptome analysis indicated that large numbers of genes were regulated by RpoS, mainly including flagellar assembly, fatty acid metabolism, two-component regulatory systems, and RNA degradation. These biological pathways might be involved in colonization, stress response, cold adaptation, and spoilage potential of *S. baltica*. Meanwhile, some other pathways such as quorum sensing were also mediated by RpoS, indicating that RpoS has a wide range of regulatory functions in cell processes. The transcriptome results are reliable through qPCR validation. The present results deepened our understanding of the bacterial spoilage mechanisms. RpoS might be used as a new target for food preservation in the future.

Data availability statement

The datasets presented in this study can be found in online repositories. The names of the repository/repositories and accession number(s) can be found at: NCBI BioProject—PRJNA858939.

Author contributions

CZ and YL designed the research. CZ and JC performed the experiments. CZ and HL analyzed the data. CZ, JC, and YL wrote the manuscript. CZ, HL, XP, and YL revised the manuscript. All authors contributed to the article and approved the submitted version.

Funding

This work was supported by Key Research and Development of Shandong Province, China (2019GNC106085) and A Project of Shandong Province Higher Educational Science and Technology Program, China (J18KA140).

Acknowledgments

The authors gratefully acknowledge laboratory colleagues for their help.

Conflict of interest

The authors declare that the research was conducted in the absence of any commercial or financial relationships that could be construed as a potential conflict of interest.

Publisher's note

All claims expressed in this article are solely those of the authors and do not necessarily represent those of their affiliated organizations, or those of the publisher, the editors and the reviewers. Any product that may be evaluated in this article, or claim that may be made by its manufacturer, is not guaranteed or endorsed by the publisher.

Supplementary material

The Supplementary material for this article can be found online at: https://www.frontiersin.org/articles/10.3389/fmicb.2022.993237/full#supplementary-material

References

Broekaert, K., Heyndrickxa, M., Hermana, L., Devlieghereb, F., and Vlaemyncka, G. (2011). Seafood quality analysis: molecular identifiification of dominant microbiota after ice storage on several general growth media. *Food Microbiol.* 28, 1162–1169. doi: 10.1016/j.fm.2011.03.009

Cariri, M. L., de Melo, A. N. F., Mizzi, L., Ritter, A. C., Tondo, E., De Souza, E. L., et al. (2019). Quantitative assessment of tolerance response to stress after exposure to oregano and rosemary essential oils, carvacrol and 1,8-cineole in *salmonella Enteritidis* 86 and its isogenic deletion mutants Δdps, ΔrpoS and ΔompR. *Food Res. Int.* 122, 679–687. doi: 10.1016/j.foodres.2019.01.046

Chen, L., Zeng, W., Rong, Y., and Lou, B. (2022a). Compositions, nutritional and texture quality of wild-caught andcage-cultured small yellow croaker. *J. Food Compos. Anal.* 107:104370. doi: 10.1016/j.jfca.2021.104370

Chen, L., Zhao, X., Li, R., and Yang, H. (2022b). Integrated metabolomics and transcriptomics reveal the adaptive responses of *salmonella enterica* serovar Typhimurium to thyme and cinnamon oils. *Food Res. Int.* 157:111241. doi: 10.1016/j.foodres.2022.111241

Chevance, F. F. V., and Hughes, K. T. (2008). Coordinating assembly of a bacterial macromolecular machine. *Nat. Rev. Microbiol.* 6, 455–465. doi: 10.1038/nrmicro1887

Chilcott, G. S., and Hughes, K. T. (2010). The type III secretion determinants of the flagellar anti-transcription factor, FlgM, extend from the amino-terminus into the anti-sigma 28 domain. *Mol. Microbiol.* 30, 1029–1040. doi: 10.1046/j.1365-2958.1998.01131.x

Colin, R., Ni, B., Laganenka, L., and Sourjik, V. (2021). Multiple functions of flagellar motility and chemotaxis in bacterial physiology. *FEMS Microbiol. Rev.* 45, fuab038. doi: 10.1093/femsre/fuab038

Costa, C., Dias, P. J., Sá-Correia, I., and Teixeira, M. C. (2014). MFS multidrug transporters in pathogenic fungi: do they have real clinical impact? *Front. Physiol.* 5:197. doi: 10.3389/fphys.2014.00197

Danhorn, T., and Fuqua, C. (2007). Biofilm formation by plant-associated bacteria. *Annu. Rev. Microbiol.* 61, 401–422. doi: 10.1146/annurev.micro.61.080706.093316

Dodd, C. E., and Aldsworth, T. G. (2002). The importance of RpoS in the survival of bacteria through food processing. *Int. J. Food Microbiol.* 74, 189–194. doi: 10.1016/S0168-1605(01)00679-1

Dong, T., and Schellhorn, H. E. (2010). Role of RpoS in virulence of pathogens. *Infect. Immun.* 78, 887–897. doi: 10.1128/IAI.00882-09

Feng, L., Bi, W., Chen, S., Zhu, J., and Liu, X. (2021). Regulatory function of sigma factors RpoS/RpoN in adaptation and spoilage potential of *Shewanella baltica*. *Food Microbiol.* 97:103755. doi: 10.1016/j.fm.2021.103755

Feng, Y., and Cronan, J. E. (2011). Complex binding of the FabR repressor of bacterial unsaturated fatty acid biosynthesis to its cognate promoters. *Mol. Microbiol.* 80, 195–218. doi: 10.1111/j.1365-2958.2011.07564.x

Fernández-Gómez, P., López, M., Prieto, M., González-Raurich, M., and Alvarez-Ordóñez, A. (2020). The role of the general stress response regulator RpoS in *Cronobacter sakazakii* biofilm formation. *Food Res. Int.* 136:109508. doi: 10.1016/j.foodres.2020.109508

Garber, M., Grabherr, M. G., Guttman, M., and Trapnell, C. (2011). Computational methods for transcriptome annotation and quantification using RNA-seq. *Nat. Methods* 8, 469–477. doi: 10.1038/nmeth.1613

Guan, J., Xiao, X., Xu, S., Gao, F., Wang, J., Wang, T., et al. (2015). Roles of RpoS in *Yersinia pseudotuberculosis* stress survival, motility, biofilm formation and type VI secretion system expression. *J. Microbiol.* 53, 633–642. doi: 10.1007/s12275-015-0099-6

Hai, Y., Zhou, D., Lam, Y. L. N., Li, X., Chen, G., Bi, J., et al. (2022). Nanoemulsified clove essential oils-based edible coating controls *pseudomonas* spp.-causing spoilage of tilapia (*Oreochromis niloticus*) fillets: working mechanism and bacteria metabolic responses. *Food Res. Int.* 159:111594. doi: 10.1016/j.foodres.2022.111594

Jogula, S., Krishna, V. S., Meda, N., Balraju, V., and Sriram, D. (2020). Design, synthesis and biological evaluation of novel *Pseudomonas aeruginosa* DNA gyrase B inhibitors. *Bioorg. Chem.* 100:103905. doi: 10.1016/j.bioorg.2020.103905

Keiji, M., Tsuneko, O., Darija, V., Shizuo, K., Makiko, M., Katsuhiko, H., et al. (2010). Role for rpoS gene of *Pseudomonas aeruginosa* in antibiotic tolerance. *FEMS Microbiol. Lett.* 242, 161–167. doi: 10.1016/j.femsle.2004.11.005

Ko, J., Lee, S., Cho, B., and Lee, Y. (2006). Differential promoter usage of *infA* in response to cold shock in *Escherichia coli*. *FEBS Lett.* 580, 539–544. doi: 10.1016/j.febslet.2005.12.066

Li, Y., Chen, N., Wu, Q., Liang, X., Yuan, X., Zhu, Z., et al. (2022). A flagella hook coding gene *flgE* positively affects biofilm formation and cereulide production in emetic *Bacillus cereus*. *Front. Microbiol.* 13:897836. doi: 10.3389/fmicb.2022.897836

Li, S., Tian, Y., Jiang, P., Lin, Y., Liu, X., and Yang, H. (2021). Recent advances in the application of metabolomics for food safety control and food quality analyses. *Crit. Rev. Food Sci.* 61, 1448–1469. doi: 10.1080/10408398.2020.1761287

Li, J., Yang, X., Shi, G., Chang, J., Liu, Z., and Zenget, M. (2019). Cooperation of *lactic acid bacteria* regulated by the AI-2/LuxS system involve in the biopreservation of refrigerated shrimp. *Food Res. Int.* 120, 679–687. doi: 10.1016/j.foodres.2018.11.025

Liu, X., Ji, L., Wang, X., Li, J., Zhu, J., and Sun, A. (2018). Role of RpoS in stress resistance, quorum sensing and spoilage potential of *Pseudomonas fluorescens*. *Int. J. Food Microbiol.* 270, 31–38. doi: 10.1016/j.ijfoodmicro.2018.02.011

Liu, X., Wu, Y., Chen, Y., Xu, F., Halliday, N., Gao, K., et al. (2016). RpoS differentially affects the general stress response and biofilm formation in the endophytic *Serratia plymuthica* G3. *Res. Microbiol.* 167, 168–177. doi: 10.1016/j.resmic.2015.11.003

Liu, X., Xu, J., Zhu, J., Du, P., and Sun, A. (2019). Combined transcriptome and proteome analysis of RpoS regulon reveals its role in spoilage potential of *Pseudomonas fluorescens*. *Front. Microbiol.* 10:94. doi: 10.3389/fmicb.2019.00094

Lou, X., Zhai, D., and Yang, H. (2021). Changes of metabolite profiles of fish models inoculated with *Shewanella baltica* during spoilage. *Food Control* 123:107697. doi: 10.1016/j.foodcont.2020.107697

Lund, P. A., Biase, D. D., Liran, O., Scheler, O., Mira, N. P., Cetecioglu, Z., et al. (2020). Understanding how microorganisms respond to acid pH is central to their control and successful exploitation. *Front. Microbiol.* 11:556140. doi: 10.3389/fmicb.2020.556140

Macé, S., Joffraud, J. J., Cardinal, M., Malcheva, M., Cornet, J., Lalanne, V., et al. (2013). Evaluation of the spoilage potential of bacteria isolated from spoiled raw salmon (*Salmo salar*) fillets stored under modified atmosphere packaging. *Int. J. Food Microbiol.* 160, 227–238. doi: 10.1016/j.ijfoodmicro.2012.10.013

Mata, G. M. S. C., Ferreira, G. M., and Spira, B. (2017). RpoS role in virulence and fitness in enteropathogenic *Escherichia coli*. *PLoS One* 12:e0180381. doi: 10.1371/journal.pone.0180381

Mihailovich, M., Militti, C., Gabaldón, T., and Gebauer, F. (2010). Eukaryotic cold shock domain proteins: highly versatile regulators of gene expression. *BioEssays* 32, 109–118. doi: 10.1002/bies.200900122

Mukherjee, S., and Bassler, B. L. (2019). Bacterial quorum sensing in complex and dynamically changing environments. *Nat. Rev. Microbiol.* 17, 371–382. doi: 10.1038/s41579-019-0186-5

Nguyen, T. V. A., and Hong, S. H. (2008). Whole genome-based phylogenetic analysis of bacterial two-component systems. *Biotechnol. Bioproc. E.* 13, 288–292. doi: 10.1007/S12257-008-0017-4

Odeyemi, O. A., Alegbeleby, O. O., Strateva, M., and Stratev, D. (2020). Understanding spoilage microbial community and spoilage mechanisms in foods of animal origin. *Compr. Rev. Food Sci. F.* 19, 311–331. doi: 10.1111/1541-4337.12526

Ojima, Y., Hakamada, K., Nishinoue, Y., Nguyen, M. H., Miyake, J., and Taya, M. (2012). Motility behavior of *rpoS*-deficient *Escherichia coli* analyzed by individual cell tracking. *J. Biosci. Bioeng.* 114, 652–656. doi: 10.1016/j.jbiosc.2012.06.014

Ozogul, Y., Yuvka, İ., Ucar, Y., Durmus, M., Kösker, A. R., Öz, M., et al. (2017). Evaluation of effects of nanoemulsion based on herb essential oils (*rosemary, laurel, thyme and sage*) on sensory, chemical and microbiological quality of rainbow trout (*Oncorhynchus mykiss*) fillets during ice storage. *LWT Food Sci. Technol.* 75, 677–684. doi: 10.1016/j.lwt.2016.10.009

Parlapani, F. F., Mallouchos, A., Haroutounian, S. A., and Boziaris, I. S. (2014). Microbiological spoilage and investigation of volatile profile during storage of sea bream fillets under various conditions. *Int. J. Food Microbiol.* 189, 153–163. doi: 10.1016/j.ijfoodmicro.2014.08.006

Santhakumari, S., Jayakumar, R., Logalakshmi, R., Prabhu, N. M., Nazar, A. K. A., Pandian, S. K., et al. (2018). *In vitro* and *in vivo* effect of 2,6-Di-*tert*-butyl-4-methylphenol as an antibiofilm agent against quorum sensing mediated biofilm formation of *vibrio* spp. *Int. J. Food Microbiol.* 281, 60–71. doi: 10.1016/j.ijfoodmicro.2018.05.024

Schellhorn, H. E. (2014). Elucidating the function of the RpoS regulon. *Future Microbiol.* 9, 497–507. doi: 10.2217/fmb.14.9

Serio, A., Fusella, G. C., López, C. C., Sacchetti, G., and Paparella, A. (2014). A survey on bacteria isolated as hydrogen sulfifide-producers from marine fish. *Food Control* 39, 111–118. doi: 10.1016/j.foodcont.2013.11.003

Shen, Y., Chen, L., Wang, M., Lin, D., Liang, Z., Song, P., et al. (2017). Flagellar hooks and hook protein FlgE participate in host microbe interactions at immunological level. *Sci. Rep.* 7:1433. doi: 10.1038/s41598-017-01619-1

Sun, Y., Ma, Y., Guan, H., Liang, H., Zhao, X., and Wang, D. (2022). Adhesion mechanism and biofilm formation of *Escherichia coli* O157:H7 in infected cucumber (*Cucumis sativus* L.). *Food Microbiol.* 105:103885. doi: 10.1016/j.fm.2021.103885

Trapnell, C., Hendrickson, D. G., Sauvageau, M., Goff, L., Rinn, J. L., and Pachter, L. (2013). Differential analysis of gene regulation at transcript resolution with RNA-seq. *Nat. Biotechnol.* 31, 46–53. doi: 10.1038/nbt.2450

Vidovic, S., Mangalappalli-Illathu, A. K., and Korber, D. R. (2011). Prolonged cold stress response of *Escherichia coli* O157 and the role of *rpoS*. *Int. J. Food Microbiol.* 146, 163–169. doi: 10.1016/j.ijfoodmicro.2011.02.018

Vogel, B. F., Venkateswaran, K., Satomi, M., and Gram, L. (2005). Identification of *Shewanella baltica* as the most important H_2S-producing species during iced storage of danish marine fish. *Appl. Environ. Microbiol.* 71, 6689–6697. doi: 10.1128/AEM.71.11.6689-6697.2005

Voglauer, E. M., Zwirzitz, B., Thalguter, S., Selberherr, E., Wagner, M., and Rychli, K. (2022). Biofilms in water hoses of a meat processing environment harbor complex microbial communities. *Front. Microbiol.* 13:832213. doi: 10.3389/fmicb.2022.832213

Wang, H., Liu, X., Zhang, Y., Lu, H., Xu, Q., Shi, C., et al. (2017). Spoilage potential of three different bacteria isolated from spoiled grass carp (*Ctenopharyngodon idellus*) fillets during storage at 4°C. *LWT Food Sci. Technol.* 81, 10–17. doi: 10.1016/j.lwt.2016.11.010

Wang, Y., Zhang, X., Cen, C., and Fu, L. (2020). Transcription factors FabR and FadR regulate cold adaptability and spoilage potential of *Shewanella baltica*. *Int. J. Food Microbiol.* 331:108693. doi: 10.1016/j.ijfoodmicro.2020.108693

Wölflingseder, M., Tutzal, S., Fenglera, V. H., Schild, S., and Reidl, J. (2022). Regulatory interplay of RpoS and RssB controls motility and colonization in *vibrio cholerae*. *Int. J. Med. Microbiol.* 312:151555. doi: 10.1016/j.ijmm.2022.151555

Wong, G. T., Bonocora, R. P., Schep, A. N., Beeler, S. M., Lee Fong, A. J., Shull, L. M., et al. (2017). Genome-wide transcriptional response to varying RpoS levels in *Escherichia coli* K-12. *J. Bacteriol.* 199, e00755–e00816. doi: 10.1128/JB.00755-16

Wosten, M. M. S. N., van Dijk, L., Veenendaal, A. K. J., de Zoete, M. R., Bleumink-Pluijm, N. M. C., and van Putten, J. P. M. (2010). Temperature-dependent FlgM/FliA complex formation regulates *Campylobacter jejuni* flagella length. *Mol. Microbiol.* 75, 1577–1591. doi: 10.1111/j.1365-2958.2010.07079.x

Wright, M. H., Shalom, J., Matthews, B., Greene, A. C., and Cock, I. E. (2019). *Terminalia ferdinandiana* Exell: extracts inhibit *Shewanella* spp. growth and prevent fish spoilage. *Food Microbiol.* 78, 114–122. doi: 10.1016/j.fm.2018.10.006

Yuan, L., Burm, M., Sadiq, F. A., Wang, N., and He, G. (2018). Interspecies variation in biofilm-forming capacity of psychrotrophic bacterial isolates from Chinese raw milk. *Food Control* 91, 47–57. doi: 10.1016/j.foodcont.2018.03.026

Zhang, C., Wang, C., Jatt, A., Liu, H., and Liu, Y. (2021). Role of RpoS in stress resistance, biofilm formation and quorum sensing of *Shewanella baltica*. *Lett. Appl. Microbiol.* 72, 307–315. doi: 10.1111/lam.13424

Zhao, X., Chen, L., Wu, J., He, Y., and Yang, H. (2020). Elucidating antimicrobial mechanism of nisin and grape seed extract against *listeria monocytogenes* in broth and on shrimp through NMR-based metabolomics approach. *Int. J. Food Microbiol.* 319:108494. doi: 10.1016/j.ijfoodmicro.2019.108494

Zhao, L., Poh, C. N., Wu, J., Zhao, X., He, Y., and Yang, H. (2022). Effects of electrolysed water combined with ultrasound on inactivation kinetics and metabolite profiles of *Escherichia coli* biofilms on food contact surface. *Innov. Food Sci. Emerg.* 76:102917. doi: 10.1016/j.ifset.2022.102917

Zhong, J., Xiao, C., Wei, G., Du, G., Sun, X., He, Q. Y., et al. (2015). Transfer RNAs mediate the rapid adaptation of *Escherichia coli* to oxidative stress. *PLoS Genet.* 11:e1005302. doi: 10.1371/journal.pgen.1005302

Zhu, S., Wu, H., Zeng, M., Liu, Z., and Wang, Y. (2015). The involvement of bacterial quorum sensing in the spoilage of refrigerated *Litopenaeus vannamei*. *Int. J. Food Microbiol.* 192, 26–33. doi: 10.1016/j.ijfoodmicro.2014.09.029

Zhu, J., Yan, Y., Wang, Y., and Qu, D. (2019). Competitive interaction on dual-species biofilm formation by spoilage bacteria, *Shewanella baltica* and *Pseudomonas fluorescens*. *J. Appl. Microbiol.* 126, 1175–1186. doi: 10.1111/jam.14187

Zhu, J., Zhao, A., Feng, L., and Gao, H. (2016). Quorum sensing signals affect spoilage of refrigerated large yellow croaker (*Pseudosciaena crocea*) by *Shewanella baltica*. *Int. J. Food Microbiol.* 217, 146–155. doi: 10.1016/j.ijfoodmicro.2015.10.020

Zhuang, S., Hong, H., Zhang, L., and Luo, Y. (2021). Spoilage-related microbiota in fish and crustaceans during storage: research progress and future trendsa. *Compr. Rev. Food Sci. F.* 20, 252–288. doi: 10.1111/1541-4337.12659

frontiers | Frontiers in Microbiology

TYPE Original Research
PUBLISHED 24 October 2022
DOI 10.3389/fmicb.2022.949932

OPEN ACCESS

EDITED BY
Lei Yuan,
Yangzhou University,
China

REVIEWED BY
Wenyi Zhang,
Inner Mongolia Agricultural University,
China
Hasan Ufuk Celebioglu,
Bartin University,
Turkey

*CORRESPONDENCE
Ilana Kolodkin-Gal
ilana.kolodkin@mail.huji.ac.il

SPECIALTY SECTION
This article was submitted to
Food Microbiology,
a section of the journal
Frontiers in Microbiology

RECEIVED 21 May 2022
ACCEPTED 20 September 2022
PUBLISHED 24 October 2022

CITATION
Suissa R, Oved R, Maan H, Hadad U, Gilhar O, Meijler MM, Koren O and Kolodkin-Gal I (2022) Context-dependent differences in the functional responses of Lactobacillaceae strains to fermentable sugars.
Front. Microbiol. 13:949932.
doi: 10.3389/fmicb.2022.949932

Context-dependent differences in the functional responses of Lactobacillaceae strains to fermentable sugars

Ronit Suissa[1,2], Rela Oved[1], Harsh Maan[1], Uzi Hadad[3], Omri Gilhar[1], Michael M. Meijler[2], Omry Koren[4] and Ilana Kolodkin-Gal[1,5]*

[1]Department of Molecular Genetics, Weizmann Institute of Science, Rehovot, Israel, [2]Department of Chemistry, Ben-Gurion University of the Negev, Be'er Sheva, Israel, [3]Ilse Katz Institute for Nanoscale Science and Technology, Ben-Gurion University of the Negev, Be'er Sheva, Israel, [4]Azrieli Faculty of Medicine, Bar-Ilan University, Safed, Israel, [5]Department of Plant Pathology and Microbiology, Faculty of Agriculture, Food and Environment, The Hebrew University of Jerusalem, Rehovot, Israel

Lactobacillaceae are Gram-positive rods, facultative anaerobes, and belong to the lactic acid bacteria (LAB) that frequently serve as probiotics. We systematically compared five LAB strains for the effects of different carbohydrates on their free-living and biofilm lifestyles. We found that fermentable sugars triggered an altered carrying capacity with strain specificity during planktonic growth. In addition, heterogeneous response to fermentable sugar was manifested in microbial aggregation (measured by imaging flow cytometry), colony development, and attachment to mucin. The acid production capacities of the strains were compatible and could not account for heterogeneity in their differential carrying capacity in liquid and on a solid medium. Among tested LAB strains, *L. paracasei, and L. rhamnosus GG* survived self-imposed acid stress while *L. acidophilus* was extremely sensitive to its own glucose utilization acidic products. The addition of a buffering system during growth on a solid medium significantly improved the survival of most tested probiotic strains during fermentation, but the formation of biofilms and aggregation capacity were responsive to the carbohydrate provided rather than to the acidity. We suggest that the optimal performance of the beneficial microbiota members belonging to Lactobacillaceae varies as a function of the growth model and the dependency on a buffering system.

KEYWORDS

aggregation, acid stress, glucose, probiotics, lactobacillacea, flow cytometry, biofilms

Introduction

Firmicutes are a dominant phylum in the human microbiota, and the proportions of members of this phylum vary between individuals and are greatly influenced by the local pH (Spor et al., 2011). Accordingly, the stomach is the least diverse growth niche within the human gastrointestinal tract (due to its extreme acidity). In the microbiome, the

presence of probiotic strains varies between healthy individuals. Probiotics are defined simply as "microorganisms that, when administered in adequate amounts, confer a health benefit to the host" (Qin et al., 2010). Probiotic strains are consumed either as fresh fermentation products or as dried bacterial supplements, with Lactobacillaceae and Bifidobacteria, being the two most widely used probiotic species (Didari et al., 2014; Azad et al., 2018). The main strains currently used for probiotic formulation were originally isolated from fermented products or humans (Fontana et al., 2004; Vijaya Kumar et al., 2015; Zielińska et al., 2018).

Lactobacillaceae are Gram-positive rods, facultative anaerobes, and belong to the lactic acid bacteria (LAB) group, as lactic acid is their main end-product of carbohydrate metabolism (Bintsis, 2018; Wang et al., 2021). This family is naturally found in the gastrointestinal tract (GIT) of humans and animals as well as in the urogenital tract of females (Turroni et al., 2014). LAB are considered efficient fermenters, proficient in the production of energy under anaerobic conditions, or when oxygen is limited. The fermentation process involves the oxidation of carbohydrates to generate a range of products including organic acids, alcohol, and carbon dioxide (Hofvendahl and Hahn-Hägerdal, 2000). In general, the response of all LAB strains to fermentation is considered to be uniform and primarily depends on the capacity to utilize glucose and its products (Qin et al., 2010).

In LAB, a phosphotransferase system (PTS) transports glucose across the membrane that is then used by the glycolysis pathway to produce pyruvate. This pathway generates energy and consumes NAD^+. Pyruvate is then converted into L-and D-lactate by the stereospecific NAD-dependent lactate dehydrogenases (LDHs), LdhL and LdhD, respectively, which regenerate NAD^+ and maintain the redox balance (Ferain et al., 1994). In the presence of oxygen and following the depletion of glucose, lactate is oxidized to pyruvate *via* the enzyme lactate oxidase followed by the production of acetate using pyruvate oxidase and acetate kinase (ACK) enzymes. The formation of acetate as the major fermentation end product results in homoacetic fermentation (Hols, 2004). Depending on the utilized saccharide and the environmental conditions, carbohydrate catabolism can differ between the LAB species and specific strains. LGG can catabolize glucose and mannose but not raffinose and xylose (Hedberg et al., 2008). *Lacticaseibacillus casei* ATCC 393 and *Lactiplantibacillus plantarum* ATCC 8014 can utilize glucose (Paucean et al., 2013), while *Lactobacillus acidophilus* ATCC 4356 and *L. casei* ATCC 393 can catabolize both glucose and raffinose from soymilk (Yeo and Liong, 2010). In contrast, *Lacticaseibacillus paracasei* fermentation capacity was higher with glucose compared with raffinose (Hedberg et al., 2008; Palacio et al., 2014).

In addition to the importance of glucose utilization to microbial energy production, different regulatory effects for fermentable and non-fermentable carbohydrates were episodically reported. Glucose and fructose induce biofilm formation in *Lacticaseibacillus rhamnosus GG,* together with changes in protein abundance and surface proteome (Savijoki et al., 2019). *L. plantarum* increases biofilm formation when supplemented with manganese and glucose (Salas-Jara et al., 2016) and *Lactobacillus acidophilus* NCFM improves its adhesive properties upon raffinose utilization together with changing its proteome architecture (Celebioglu et al., 2016). Altogether, these findings indicate that changes in carbon sources and their concentrations induce more complex adaptations than alterations in microbial growth and that these adaptations need to be systematically explored, characterized, and compared to predict accurately the optimal compositions and formulations of probiotics.

To map adaptations to carbohydrates that are growth-dependent and independent, we systematically compared the response to metabolic stress in microaerophilic (CO_2 >3%) conditions of the five probiotic Lactobacillaceae species: *Lacticaseibacillus rhamnosus GG* (Segers and Lebeer, 2014), *Lacticaseibacillus casei* (Karapetsas et al., 2010), *Lactobacillus acidophilus* (Huang et al., 2022), *Lacticaseibacillus paracasei,* and *Lactiplantibacillus plantarum* (Rocchetti et al., 2021) during planktonic growth and colony biofilm formation. *Bacillus coagulans*, a probiotic *Bacilli* belonging to the same phylum (Cao et al., 2020), was studied as a non-Lactobacillaceae LAB control strain. Under our conditions, similar glucose utilization efficiencies were observed between the species (as judged by the levels of the end products: lactate and acetate). Our results indicate that a differential response to carbohydrates is correlated with a differential acid tolerance, rather than a differential production of organic acids. Thereof, LAB bacteria significantly differ in their response to their own self-imposed acid stress from glucose utilization products and can be clustered into fermentation resistant and fermentation sensitive strains. The differential adaptation to acidic products included reversible changes in cellular organization and colony formation.

Results

Fermentable sugars specifically but heterogeneously affect the carrying capacity during planktonic growth

To test whether fermentable sugars affect growth differently than non-fermentable sugars, five probiotic Lactobacillaceae species were grown on a rich medium (TSB) in a shaking culture either with glucose (fermentable) or with raffinose (non-fermentable).

All bacteria grew similarly in the rich medium. The addition of glucose induced growth as judged by an increased carrying capacity (reflected by the maximal OD measured) of LGG and *L. acidophilus* compared to TSB alone, but its effect on growth in *L. casei*, *L. paracasei*, *L. plantarum*, and *B. coagulans* was extremely noisy (Figure 1). To better distinguish between the growth patterns of the different probiotic strains, we further analyzed growth with the software GrowthRates 3.0. We extracted the length of the lag phase, the growth rate, and the

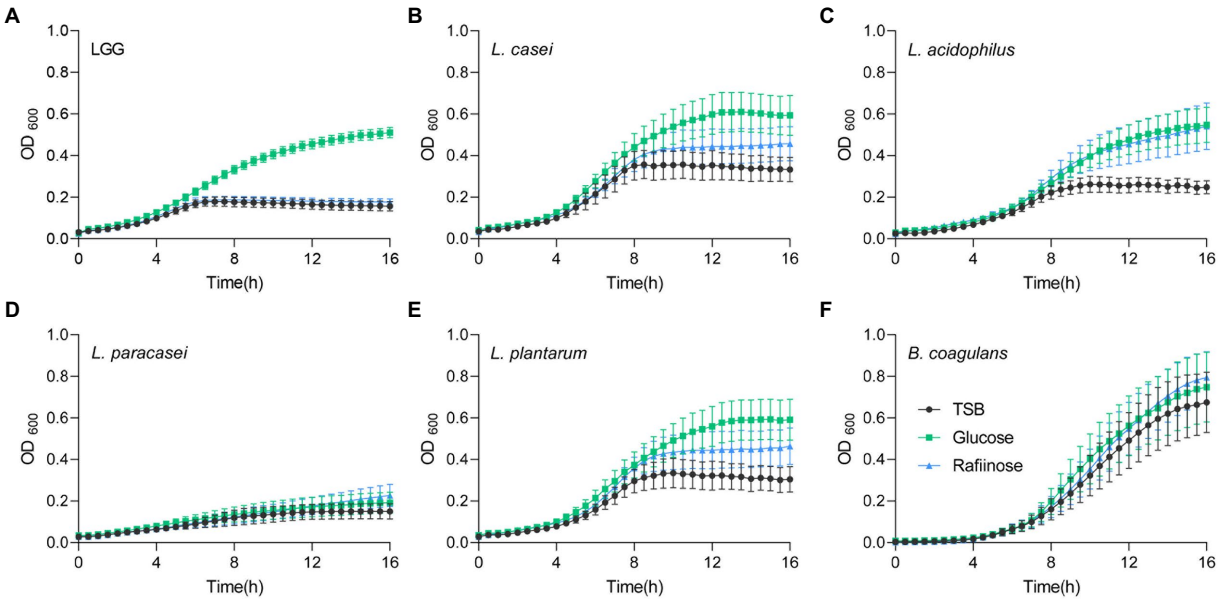

FIGURE 1
Heterogeneous alterations in planktonic growth of LAB strains during glucose utilization. Planktonic growth of the indicated species **(A)** LGG; **(B)** *L. casei*; **(C)** *L. acidophilus*; **(D)** *L. paracasei*; **(E)** *L. plantarum*, and **(F)** *B. coagulans* in TSB medium (control) either supplemented or not with glucose (1% W/V) and raffinose (1% W/V). Graphs represent mean±SEM from six independent experiments (n =24).

carrying capacity of all LAB strains with the different treatments (Hall et al., 2014). Our results indicated that the heterogeneous response was primarily manifested in an altered carrying capacity (e.g., the maximal OD of the cultures; Figure 2A). Strains showed varied carrying capacities from each other, and indeed LGG and *L. acidophilus* had enhanced carrying capacity in response to Glucose, while other probiotic strains did not exhibit a significant response. In all species, the growth rate and lag time were not significantly altered by glucose addition (Figures 2B,C).

We then asked whether the induction of growth is an outcome of fermentable sugar utilization, as fermentation is a metabolic process allowing the production of energy under anaerobic conditions. To answer this, we assessed the growth of the bacteria on media supplemented with raffinose, a sugar source less compatible with fermentation, as it was indicated that alpha-galactosidase, responsible for the hydrolysis of this sugar, is not enzymatically active (Garro et al., 1998; Hedberg et al., 2008; Zartl et al., 2018). Raffinose did not induce the growth of LGG, suggesting that the induction of growth depends on the fermentable nature of the sugar (Figures 1, 2A). In contrast, the carrying capacity of *L. acidophilus* cultures increased with both glucose and raffinose (Figure 1) but failed to meet the statistical significance of each parameter of growth (Figures 2B,C). In general, the addition of raffinose failed to induce significant alterations in growth parameters in all strains. Similar results were observed when the bacteria were grown with mannose (fermentable) which induced enhanced carrying capacity and xylose non-fermentable), which failed to induce significant alterations of growth (Supplementary Figure S1). With the exception of carrying capacity, other parameters of growth remained unaltered by sugar application in all strains (Figures 1, 2; Supplementary Figure S1).

Differential response of Lactobacillaceae to fermentation is not a result of organic acid production

To compare the fermentation efficiency, we measured the acidity of the medium after growth in the presence and absence of glucose. Indeed, after 24 h the pH of the medium decreased in both glucose and raffinose compared to TSB alone (Figure 3A). The acidity of Lactobacillaceae conditioned medium grown in the absence of glucose and the addition of raffinose was approximately 4.5–5, while the addition of glucose to the medium lowered the pH to 4 or less confirming that upon application of glucose, the acidification of the growth media was enhanced in all Lactobacillaceae that were tested. Compared with other tested strains, *B. coagulans* altered the pH the least, e.g., to 4.5 in the presence of glucose and 6 in its absence (Figure 3A). The pH drop in the growth medium source was comparable between all Lactobacillaceae strains in glucose and raffinose, except in LGG which was inert to raffinose.

To confirm that the uniform drop in pH levels resulted from the differential accumulation of organic acids among the tested LAB species, we measured the accumulation of glucose utilization products (organic acids), focusing on the levels of key organic acids, lactate, and acetate using high-performance liquid chromatography

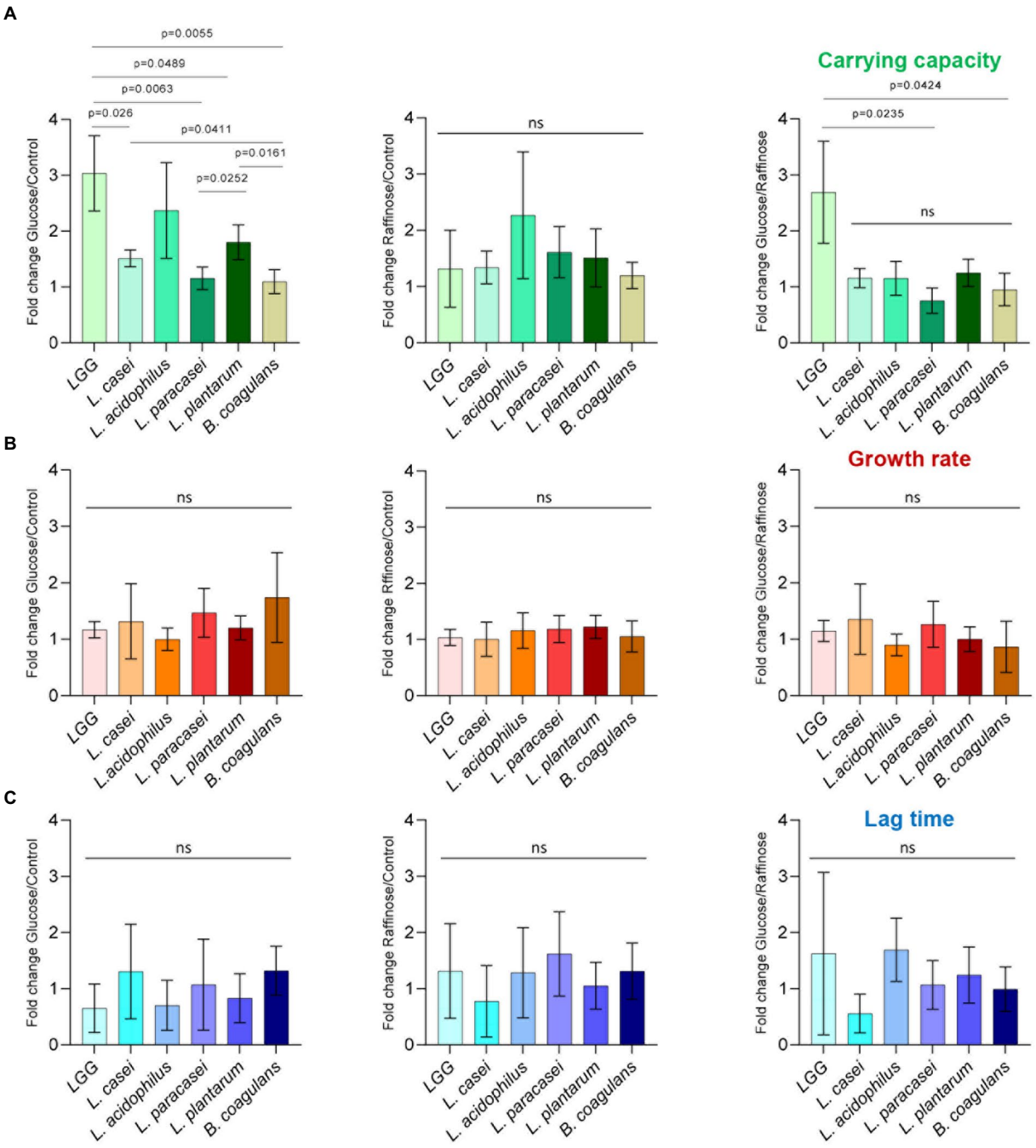

FIGURE 2
Carbon-dependent growth induction is specifically manifested by an altered carrying capacity. Analysis of planktonic growth from the data shown in Figure 1 using GrowthRates 3.0. **(A)** Fold change, in carrying capacity, **(B)** growth rate, and **(C)** lag time of indicated species between glucose/control, raffinose/control, and glucose/raffinose. Graphs represent mean±SD from six independent experiments (n =24). Statistical analysis was performed using Brown-Forsythe and Welch's ANOVA with Dunnett's T3 multiple comparisons test. p <0.05 was considered statistically significant.

(HPLC; Supplementary Figure S2). In general, lactic acid was ten times more abundant than acetic acid in the growth media. When we statistically analyzed the concentration of lactate produced by the bacteria, there was no single species that was significantly different from the other group members, indicating that the production of organic acids and thereby glucose utilization is performed similarly under our conditions (Figures 3B,C) and cannot account for the differential carrying capacity.

To exclude that the differential response to fermentation is a result of different enzymatic activities of enzymes involved in the process, we studied *in silico* the presence of lactate dehydrogenase from different LAB strains. Alignment of LDH proteins from

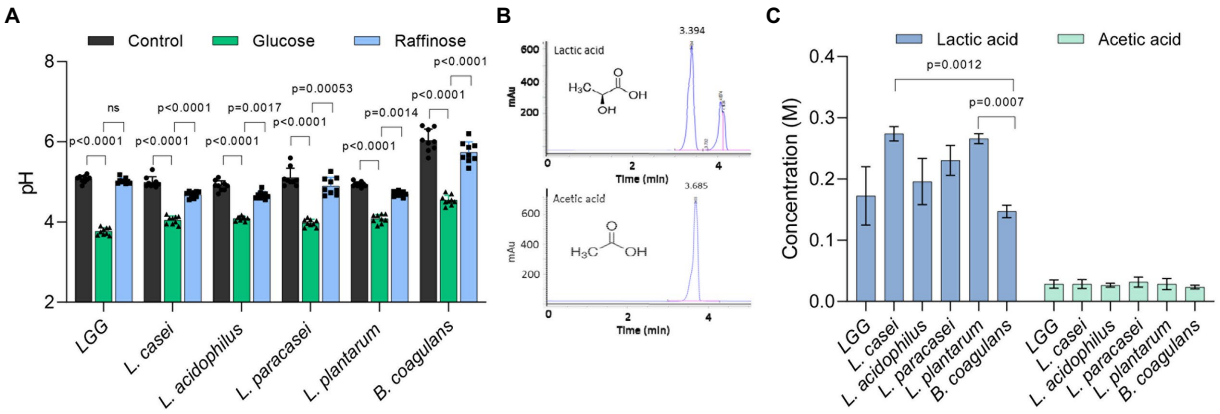

FIGURE 3
The variation at the species level in growth enhancement is not due to glucose catabolism. **(A)** The pH of the conditioned media of indicated species in TSB medium (control) and TSB medium supplemented with glucose (1% W/V) and raffinose (1% W/V). Statistical analysis was performed using two-way ANOVA followed by Dunnett's multiple comparison test. p <0.05 was considered statistically significant. **(B)** HPLC chromatograms indicate an exclusive peak and stable retention time for the pure standards of lactic acid and acetic acid. **(C)** The concertation of lactic acid and acetic acid produced by the indicated species. Bacteria were grown on an MSgg medium supplemented with glucose (1% W/V) for 24h. The conditioned medium from the cultures was collected and analyzed using the C-18 column. Statistical analysis was performed using Brown-Forsythe and Welch's ANOVA with Dunnett's T3 multiple comparisons test. p <0.05 was considered statistically significant.

different Lactobacillaceae members (Supplementary Figure S3) indicated that LGG *L. paracasei* and *L. casei* have two groups of homologues LDH proteins with more than 90% identity. 16S rRNA gene sequence alignment showed that all species have at least 89% similarity, and the evolutionary closest species are LGG *L. casei* and *L. paracasei* based on 16S rRNA gene sequences. Therefore, the key differences revealed by growth analysis on fermentable sugars are despite the high evolutionary closeness of all five species.

Self-imposed acid stress in biofilm colonies of LAB species

To further study the differential response to fermentation in Lactobacillaceae, we examined the growth on a solid medium under static conditions [frequently correlated with biofilm formation (Povolotsky et al., 2021)], we assessed the colony morphology with the addition of glucose and raffinose (Figure 4A). In all strains, the application of glucose induced the formation of asymmetric, smaller, and morphologically different colonies. Raffinose did not induce the same morphological changes in colony structure, suggesting glucose metabolism has a role also in shaping the colony architecture (Figure 4A). Solid growth media from bacteria grown on TSB or TSB with raffinose had similar pH values of approximately 5.5 (Figure 4B; Supplementary Table S1). The addition of glucose to the growth media lowered the pH significantly suggesting that glucose induced fermentation in all tested strains under these conditions. To test whether acid stress is related to the alterations in colony morphology we monitored cell death using flow cytometry in the presence and absence of a buffering system. As shown, in all strains, with the exception of *L. paracasei*, the buffering system significantly enhanced the survival of the cells, and acid-dependent cell death during fermentation significantly varied between the strains (Figures 4C,D). The addition of a buffer also resulted in colony morphology comparable to the morphology of strains grown without glucose. While cell death was reduced, the buffer did not fully restore the viability of the cells within a colony but was sufficient to restore colony morphologies to those observed in a glucose-free solid medium (Figure 4A). These results may suggest that cell death on solid biofilm media primarily but not solely results from differential acid sensitivity, and that the alterations in biofilm formation capacities occur independently of cell counts.

Glucose acts as a broad-spectrum regulator of aggregation and adhesion properties while raffinose specifically affects *Lactiplantibacillus plantarum* and *Lactiplantibacillus acidophilus*

To better assess the level of changes on the single-cell level we grew the bacteria on solid growth media (TSB), TSB with glucose, and TSB with raffinose in the presence and absence of a buffering system. Colony cells grown without glucose are rod-shaped, divide normally, and are arranged in short chains (Figure 5A). While all the species looked similar in TSB, glucose-induced noticeable alterations in the morphology of LGG and *L. paracasei* cells were consistent with the observed alterations in cell aggregation properties. Noticeable clumps were induced in both species, which also lost their characteristic elongated rod shape. Alteration in cell shape upon glucose treatment could be partially rescued with the

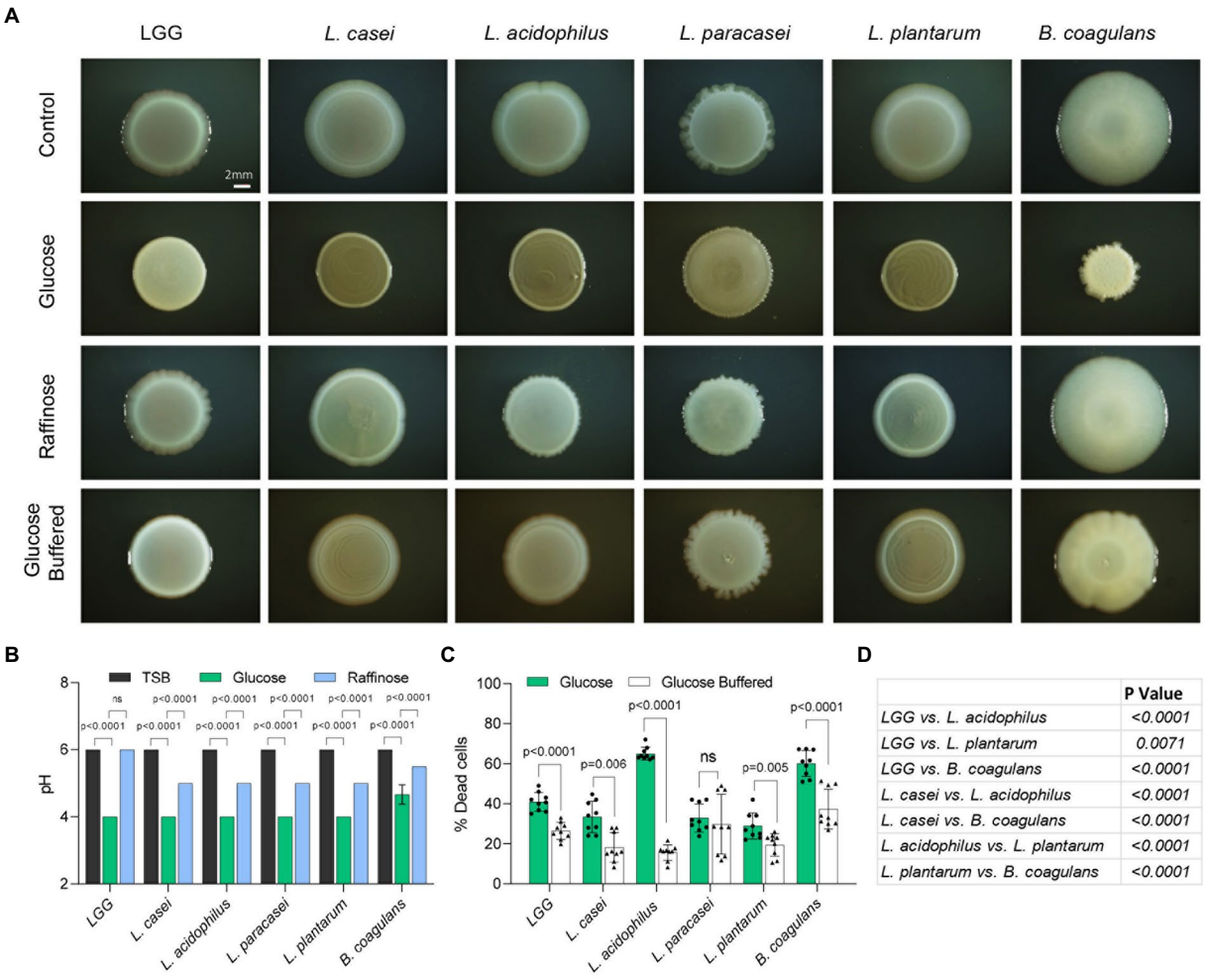

	P Value
LGG vs. L. acidophilus	*<0.0001*
LGG vs. L. plantarum	*0.0071*
LGG vs. B. coagulans	*<0.0001*
L. casei vs. L. acidophilus	*<0.0001*
L. casei vs. B. coagulans	*<0.0001*
L. acidophilus vs. L. plantarum	*<0.0001*
L. plantarum vs. B. coagulans	*<0.0001*

FIGURE 4
Self-imposed acid stress has a role in the formation of structured microbial colonies. **(A)** Shown are the indicated biofilm colonies grown on TSB medium (control), TSB medium supplemented with glucose and raffinose (1% W/V), and TSB medium supplemented with glucose (1% W/V)+buffer. Biofilms were grown at 37°C in a CO_2 enriched environment. Biofilm colonies were imaged at 72h post inoculation. Scale bar = 2mm. **(B)** Measurement of pH of the indicated species shown in A. Statistical analysis was performed using two-way ANOVA followed by Dunnett's multiple comparison test. p <0.05 was considered statistically significant. **(C)** Flow cytometry analysis of the number of dead cells of the indicated species shown in **(A)**. Colonies were grown on TSB medium supplemented with glucose (1% W/V), and TSB medium supplemented with glucose (1% W/V)+buffer. Data were collected 72h post inoculation; 100,000 cells were counted. Y-axis represents the % of dead cells, graphs represent mean±SD from 3 independent experiments (n =9). Statistical analysis was performed between glucose and glucose + buffer using unpaired two tailed t test with Welch's correction. p <0.05 was considered statistically significant. **(D)** Table showing multiple comparison tests between the dead cell populations of the indicated species grown in TSB medium supplemented with glucose (1% W/V). Statistical analysis was performed using Brown-Forsythe and Welch's ANOVA with Dunnett's T3 multiple comparisons test. p <0.05 was considered statistically significant.

application of buffer, supporting a differential response of probiotic bacteria to fermentation and its acidic products. Interestingly, alterations in cell clumping did not perfectly correlate with the response to acid stress as judged by cell growth as LGG had pronounceable growth upon utilization of glucose, while *L. paracasei* failed to increase it carrying capacity with glucose. To further assess whether alterations in cell properties account for the differential colony morphology, we used imaging flow cytometry (Narayana et al., 2020; Maan et al., 2021). While imaging flow cytometry was sporadically used to monitor aggregation (Konieczny et al., 2021), it was never applied to probiotic bacteria.

For each bacterium, we could easily differentiate between single cells and small aggregates vs. larger aggregates (Supplementary Figures S4–S9), and to confirm with high accuracy the % of aggregation evens out of the total measured events. As each bacterium has different aggregation properties, the population of aggregates was determent based on the area value. In LGG, *L. paracasei* and *B. coagulans* we could not fully separate aggregates from bacterial chains. Our results indicated (Figures 5B,C) that LAB strains greatly differ in their basal aggregation properties as judged by the portion of the population capable to aggregate and the average size of the observed aggregates (Figure 5B; Supplementary Figures S4–S9). Overall, the

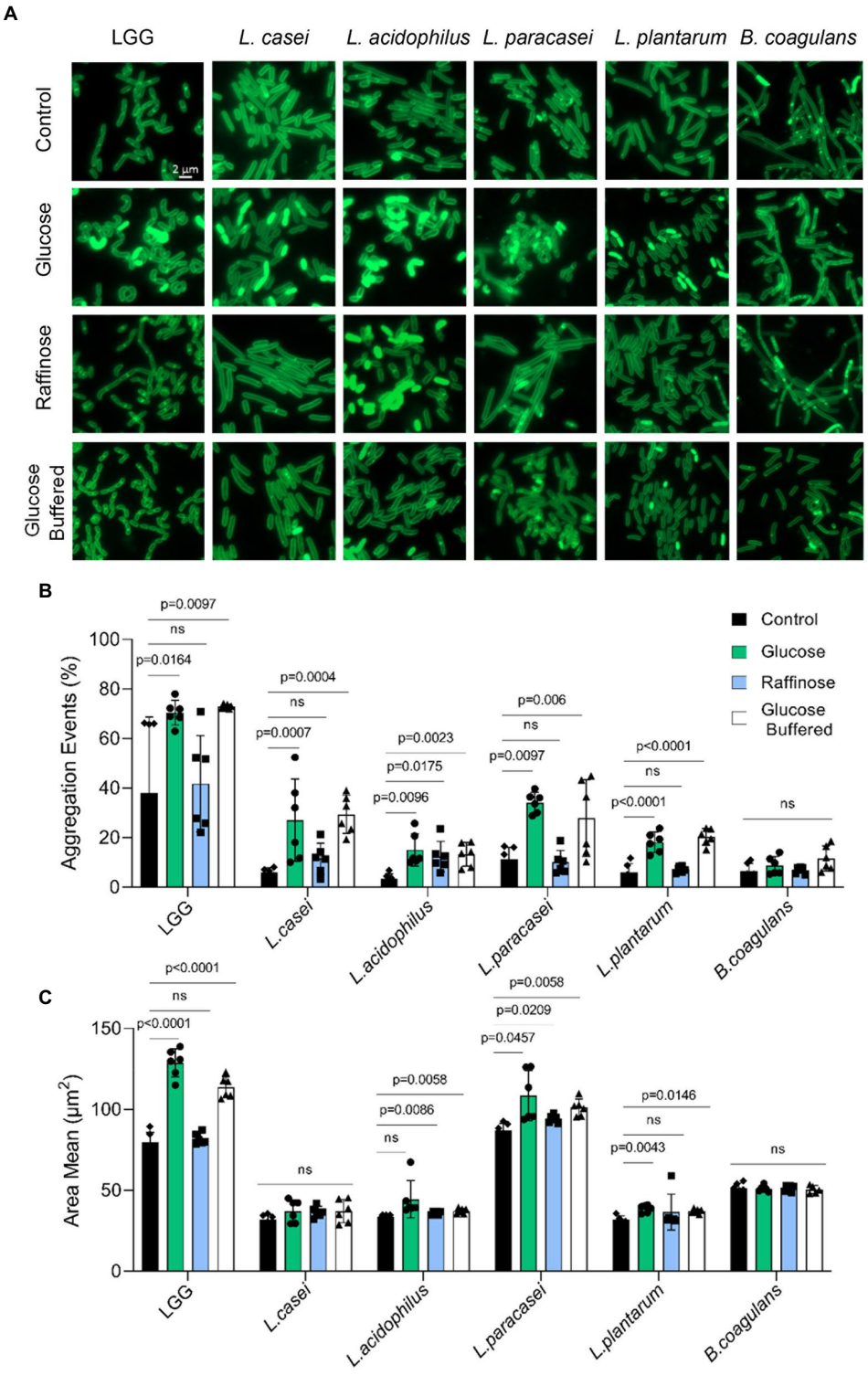

FIGURE 5
Carbohydrates specifically regulate microbial aggregation. **(A)** Fluorescence microscope images of cells from biofilm colonies that were grown on TSB medium (control), TSB medium supplemented with glucose and raffinose (1% W/V), and TSB medium supplemented with glucose (1% W/V)+buffer. Cells were stained using Green-membrane stain FM™ 1–43FX. Biofilms were grown at 37° C in CO_2 enriched environment. Cells were imaged at 72h post inoculation. The images represent 3 independent experiments, from each repeat at least 10 fields examined. Scale bar = 2µm. **(B)** Imaging Flow cytometry analysis of the number of aggregation events, population of the indicated species and **(C)** aggregate size-the mean of measured area of bacterial aggregates population. Cells were grown in liquid TSB medium supplemented with glucose (1% W/V), raffinose (1% W/V), and TSB medium supplemented with glucose (1% W/V)+buffer. Data were collected from overnight culture, and 20,000 cells were counted. Y-axis represents the % of aggregate events or area mean, and graphs represent mean±SD from 2 independent experiments (n =6). Statistical analysis was performed using Brown-Forsythe and Welch's ANOVA with Dunnett's T3 multiple comparisons test. p <0.05 was considered statistically significant.

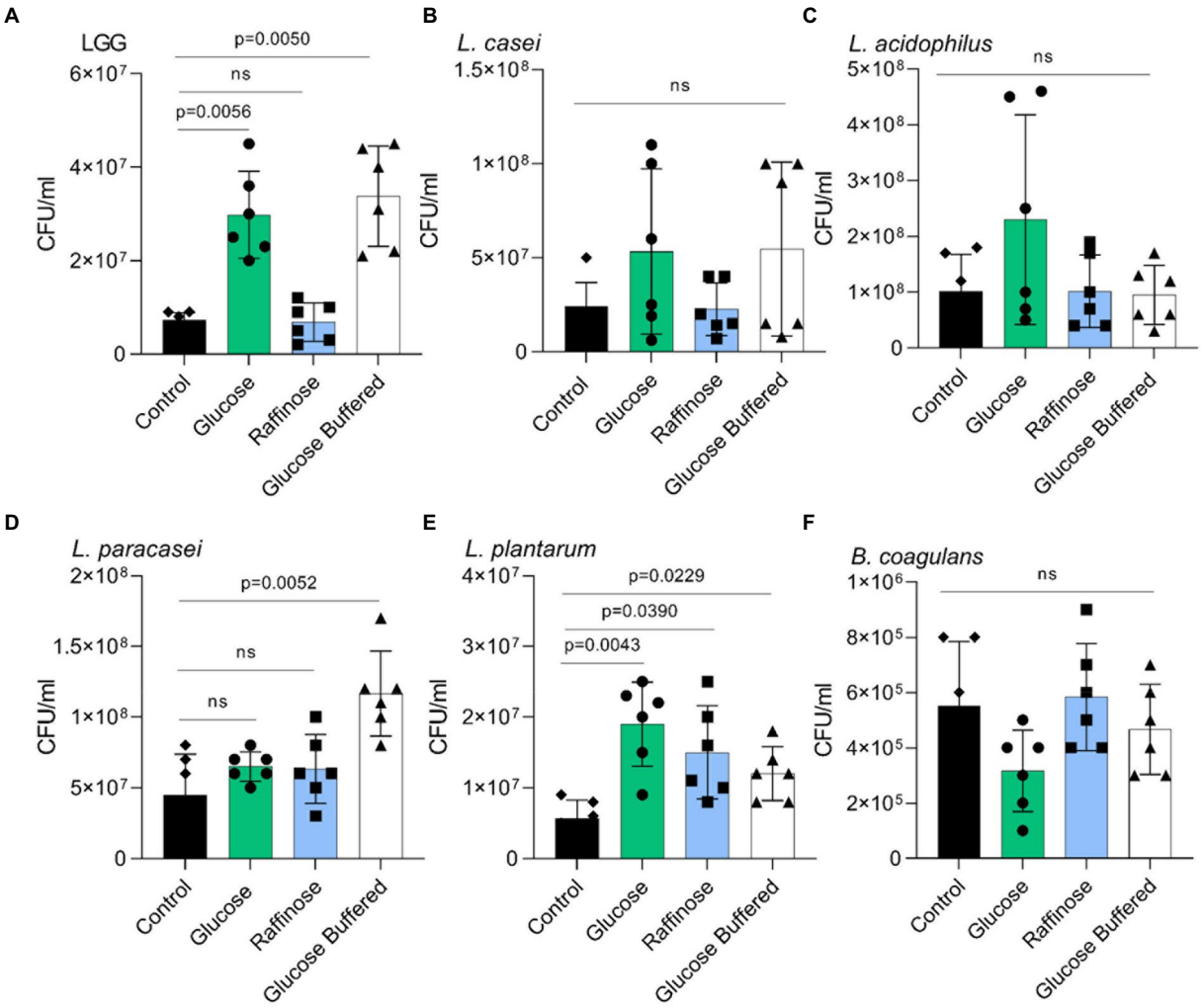

FIGURE 6
Glucose but not acid stress promotes adhesion to mucin. Adherence of the indicated species to porcine mucin in a microtiter plate. **(A) LGG**. **(B)** *L. casei*. **(C)** *L. acidophilus* **(D)** *L. paracasei*. **(E)** *L. plantarum* **(F)** *B. coagulans* Y-axis represents the number of bacteria adherent to mucin by CFU/ml, graphs represent mean ± SD from 2 independent experiments (n = 6). Statistical analysis was performed using Brown-Forsythe and Welch's ANOVA with Dunnett's T3 multiple comparisons test. $p < 0.05$ was considered statistically significant.

frequency of aggregation properties (Figure 5B) was more in response to the carbohydrate's composition than the size of the aggregate (Figure 5C) which was an intrinsic property of the probiotic strain. Glucose (but not raffinose) significantly induced aggregation in all Lactobacillaceae strains, except for *L. acidophilus*, in which both glucose and raffinose induced aggregation. For *B. coagulans*, neither glucose nor raffinose affects the formation of aggregates (Figure 5B), indicating that carbohydrate-driven aggregation is a unifying response in Lactobacillaceae that preferentially occurs with glucose. This carbohydrate-driven aggregation was not rescued with buffering, consistent with the partial effect of buffering on cell death within biofilm colonies and the 3D structure of the colonies (Figure 4).

In a host, LAB strains must adhere to the host's tissue, frequently adhering to mucins. Therefore, we tested whether the overall changes in the adhesive properties of LAB strains and, in particular, a specific response to glucose but not raffinose were observed in LGG. Interestingly, raffinose was an efficient inducer of adhesion for *L. plantarum*. The basal level of adhesion to mucin primarily differed between LAB strains, as did aggregation (Figure 6). The effect of buffering on glucose-dependent adhesion was insignificant, indicating that adhesion is not triggered by the acidification of the medium but is a specific carbohydrate-mediated response.

Discussion

Probiotic bacteria are considered a means for microbiota modulation, along with nutrition, personal hygiene, and lifestyle (Spor et al., 2011). Probiotics are found to have a beneficial effect on the consumer in the prevention of antibiotic-associated

diarrhea and acute infectious diarrhea, treatment of inflammatory bowel disease (Saez-lara et al., 2015), and other gastric disorders (O'Mahony et al., 2005). Lactobacillaceae are widely used probiotic bacteria, represented in most fermented products and supplements. Probiotic performance in the gut is dependent on nutrient composition and availability (Singh et al., 2017). Positive effects on probiotics proliferation and beneficial effects on the host have been associated with prebiotic consumption. For example, it was shown that the addition of raffinose and *L. acidophilus* to the diet of rats decreases their body weight and increases the concentration of *L. acidophilus* in the gut (1-s2.0-S027153179600231X-main). However, the responses of single LAB strains to their acidic fermentation products may vary and contribute to their physiological responses to carbohydrates.

Therefore, we systematically compared five different LAB species for their response to the utilization of glucose and raffinose model sugars. We found that glucose utilization has a general role in shaping the colony morphology under static conditions, as all species exhibit morphological colony changes upon glucose treatment. Similarly, medium acidification was generally similar during static growth (Figure 4B) and comparable for all Lactobacillaceae during planktonic growth (Figure 2). For all tested species, the final product of glucose utilization and fermentation (occurring under microaerophilic conditions) was almost exclusively the organic acid lactate alongside acetate. Analyses of the fermentation capacities of the different species revealed similar fermentation efficiencies. Lactic and acetic acid concentrations and the pH of the growth medium were all similar and stable among the different species (Figures 3,4B). In agreement, the alignment of lactate dehydrogenase proteins revealed that LGG, *L. paracasei,* and *L. casei* have two groups of almost identical protein homologs with more than 90 % identity between the different species (Supplementary Figure S3). This indicates that differential utilization of glucose may not account for the differential carrying capacities of the cultures in the presence of glucose.

Contrary to glucose utilization, organic acid accumulation, and medium acidification, which are comparable between strains, the carrying capacity of the culture is differentially enhanced during the planktonic growth of Lactobacillaceae. While LGG, *L. acidophilus L. casei* and *L. plantarum* doubled the carrying capacity following exposure to glucose exposure, *L. paracasei* had no noticeable growth induction with glucose. Interestingly, the capacity of LAB strains to utilize glucose, raffinose, mannose, and xylose for planktonic growth differed significantly (Figures 1,2, Supplementary Figure S1). A detailed analysis of the microbial growth reflected that carbon utilization is unintuitively inert to the growth rate, and does not affect the lag phase (Figure 2). Rather, it allows the bacterial community to reach a significantly higher carrying capacity that may account for changes in their proportions in the GI.

Acid stress in Lactobacillaceae is self-imposed stress, and, thus, LAB is relatively acid-tolerant, and employs several mechanisms to regulate the homeostasis of the pH level (De Angelis and Gobbetti, 2004). The mechanisms generally include the removal of protons or alkalization of the environment *via* ammonia production through arginine deiminase (ADI; Costa, 2002). In addition, glutamic acid decarboxylase (GAD) catalyzes the decarboxylation of glutamate into gamma-aminobutyric acid (GABA), which results in the alkalization of the cytoplasmic pH due to the removal of protons (Gobbetti et al., 2010). Lastly, the urease system allows the hydrolysis of urea, which enhances the survival of LAB under acid stress conditions by the production of NH_3. The urease operon was found to be positively regulated under low pH levels in the LAB *Streptococcus salivarius* (Huang et al., 2014). The F-ATPase system is another mechanism that protects LAB from acid damage. Overall, probiotic acid-tolerant species are of great value as additional encapsulation to ensure survival to transit through the acidic stomach. As the survival of LAB during acid stress is quite heterogeneous the expression of these systems during self-imposed acid stress and, in the stomach, needs to be properly evaluated while selecting formulating probiotics. Alternatively, food carriers with high buffering potential to aid gastric transit and ensure that viable cells reach the small intestine may contribute to assure a beneficial effect on the host. For example, our results indicate that *L. paracasei* in liquid (Figure 1) and *L. acidophilus* (Figure 4) grown on a solid medium exhibit poor acid tolerance during self-imposed acid stress. One immediate application of our findings for *L. paracasei* in solution (Figure 1) and *L. acidophilus* (Figure 4C) is that the probiotic performance of these strains in the gut is dependent on the availability of a suitable buffering system.

In the gut, acid-sensitive species are protected from the acidic pH of the stomach (2–4) because of the buffering properties of food, which depend on the type of food and its volume (Simonian et al., 2005; Papadimitriou et al., 2015). In parallel, self-imposed acid stress from the accumulation of organic acids following the utilization of carbohydrates may affect the performance of the ingested bacterial species. Interestingly, buffering of the colonies restored the glucose-free morphology of all strains, indicating that acid stress is involved in biofilm formation throughout the Firmicutes phylum directly or indirectly. The addition of a buffering system to the growth media of bacteria grown in the presence of glucose increased the survival of most species significantly. However, while cell death was decreased with buffering, it was still significantly higher with glucose compared with non-glucose conditions (Figure 4C). Thus, the glucose-induced change in colony morphology may be reflective of a complex adaptation and biofilm regulation, rather than a simple reflection of cell density.

Our results, observed in all LAB strains are consistent with recent findings that the stress protein Hsp plays an important role in shaping colony morphology under acidic pH in a single specie: *L. plantarum* (Rajasekharan and Shemesh, 2022). While glucose utilization capacities and medium acidification under our conditions were similar, the enhancement of carrying capacity (Figure 2), carbohydrate-mediated cell death within the colony (Figure 4C), and the adaptation to glucose utilization, are reflected

by enhanced aggregation properties (Figure 5) varied dramatically between the tested species. The observed alterations in cell shape and aggregation properties may indicate an independent adaption to fermentable carbohydrates (for example, a change in surface proteome) and not a direct reflection of acid stress as they poorly responded to buffering.

Changes in the surface proteome (Savijoki et al., 2019), quorum sensing (Di Cagno et al., 2011), and the activation of differential target genes of the stressosome (Papadimitriou et al., 2016) may differ between LAB strains. These results are consistent with pH independent changes in the aggregation and adhesion properties of the LAB strains tested with glucose. Raffinose was an efficient inducer of aggregation of *L. acidophilus* (Figure 5B) and adhesion of *L. plantarum* (Figure 6). These exceptions indicate that specific response to carbohydrates as mediators of cellular adhesive properties is not limited to glucose or highly fermentable sugars and that additional layers of carbohydrate-responsive adhesins/cell envelope components evolved in the microbiome. While the exact regulations remain to be determined, our results indicate that the overall physiological response to carbohydrate metabolism and self-imposed acid stress is not a mere reflection of microbial growth.

Materials and methods

Strains, media, and imaging

Lactobacillus acidophilus ATCC 4356, *Lacticaseibacillus casei* ATCC 393, *Lacticaseibacillus casei subsp. paracasei* ATCC BAA-52, *Lactiplantibacillus plantarum* ATCC 8014, and *Lacticaseibacillus rhamnosus GG* ATCC 53103 probiotic strains were used in the study. *Bacillus coagulans* ATCC 10545 was used as a control. A single colony of Lactobacillaceae was isolated on a solid deMan, Rogosa, Sharpe Agar (MRS) plate, inoculated into 5 ml MRS broth (Difco, Le Pont de Claix, France), and grown at 37°C, without shaking overnight. A single colony of *Bacillus coagulans* isolated on a solid LB agar plate was inoculated into 5 ml LB broth (Difco) and grown at 37°C, with shaking overnight. For biofilm colonies, these cultures were inoculated into a solid medium (1.5% agar) containing 50% Tryptic soy broth (TSB), TSB supplemented with (1% w/v) D-(+) - glucose (1% w/v) D-(+)- raffinose or (1% w/v) D-(+)- mannose or (1% w/v) D-(+)-Xylose or with (1% w/v) D-(+) - glucose buffered with MOPS (3-(N-morpholino)propane-sulfonic acid) and potassium phosphate buffer. The bacteria were incubated in a BD GasPak EZ - Incubation Container with BD GasPak EZ CO_2 Container System Sachets (260679; Becton, Sparks, MD, United States), for 72 h at 37°C. The colony images were taken using a Stereo Discovery V20″ microscope (Tochigi, Japan) with objectives Plan Apo S × 1.0 FWD 60 mm (Zeiss, Goettingen, Germany) attached to a high-resolution microscopy Axiocam camera. Data were created and processed using Axiovision suite software (Zeiss). For planktonic growth, the bacterial cultures were inoculated into a liquid medium of 50% TSB with different sugars as described above, and incubated for 24 h, at 37°C.

Growth measurement and analysis

Cultured cells grown overnight were diluted 1:100 in 200 µl liquid medium contains 50% TSB (BD), TSB supplemented with (1% w/v) D-(+)- glucose, (1% w/v) D-(+)- raffinose or (1% w/v) D-(+)- mannose or (1% w/v) D-(+)-Xylose in a 96-well microplate (Thermo Scientific, Roskilde, Denmark). Cells were grown with agitation at 37°C for 18 h in a microplate reader (Tecan, Männedorf, Switzerland), and the optical density at 600 nm (OD_{600}) was measured every 30 min. Maximum OD, growth rate, and lag time calculation were performed with GrowthRates 3.0 software.

Fluorescence microscopy

A bacterial colony grown as described above was suspended in 200 µl 1x Phosphate-Buffered Saline (PBS), and dispersed by pipetting. Samples were centrifuged briefly, pelleted, and re-suspended in 5 µl of 1x PBS supplemented with the membrane stain FM1-43 (Molecular Probes, Eugene, OR, United States) at 1 µg/ml. These cells were placed on a microscope slide and covered with a poly-L-Lysine (Sigma) treated coverslip. The cells were observed by Axio microscope (Zeiss, Germany). Images were analyzed by Zen-10 software (Zeiss).

pH measurements

After inoculation in different liquid mediums and 24 h incubation (without shaking) at 37°C, the cells were separated from the medium by centrifugation (4,000 × *g*, 20 min) followed by filtration through a 0.22 µm. The conditioned media acidity was measured by the pH meter (Mettler Toledo). pH measurements of the solid media were done using pH-indicator strips (MQuant®, Merck KGaA, Darmstadt, Germany).

Determination of organic acids

The supernatant of the bacteria grown on a defined medium-MSgg with 1% glucose for 24 h was filtered through 0.22 µm filter membranes for HPLC analysis. The contents of organic acids in each liquid sample were determined using an Infinity 1260 (Agilant Technologies, Santa Clara, CA, United States) HPLC system with C 18 column (Syncronis™ C18 Columns, 4.6 × 250 mm, 5 µm). Mobile phase A was acetonitrile and mobile phase B was 5-mM KH_2PO_4 pH 2.4. The flow rate was kept constant at 1 ml/min, with ultraviolet detection performed at 210 nm. The injection volume was 20 µl and the column temperature was maintained at 30°C. Identification and

quantification of organic acids were accomplished by comparing the retention times and areas with those of pure standards.

Notably, although quantification of organic acids in TSB was not feasible due to the high background, the comparable acidity strongly indicates similar fermentation capacities of the strains tested in rich growth media.

Flow cytometry analysis

Starter cultures were spotted on TSB with glucose or TSB with glucose buffered with MOPS and potassium phosphate buffer. The plates were then incubated as mentioned in the first section. Colonies were harvested after 72 h and separated with mild sonication. Samples were diluted in PBS and measured using an LSR-II new cytometer (Becton Dickinson, San Jose, CA, United States). PI (Propidium Iodide, 20 Mm, Invitrogen™) fluorescence was measured using laser excitation of 488 nm, coupled with 600 LP and 610/20 sequential filters. A total of 100,000 cells were counted for each sample and flow cytometry analyses were performed using BD FACSDiva software.

Imaging flow cytometry for aggregation

Strains were grown in different liquid mediums for overnight incubation (without shaking) at 37°C. Data were acquired by ImageStreamX Mark II (AMNIS, Austin, TX) using a 60× lens (NA = 0.9). The laser used was 785 nm (5 mW) for side scatter measurement. During acquisition, bacterial cells were gated according to their area (in square microns) and side scatter, which excluded the calibration beads (that run in the instrument along with the sample). For each sample, 20,000 events were collected. Data were analyzed using IDEAS 6.2 (AMNIS). Focused events were selected by the Gradient RMS, a measurement of image contrast. Singlets and small aggregates events vs. larger microbial aggregates and chain events were selected according to their area (in square microns) and aspect ratio (width divided by the length of the best fit ellipse) of the bright filed image. Aggregate event populations were determined for each bacterium, from an Area value of 55 for LGG, 25 for *L. casei*, 27 for *L. acidophilus*, 68 for *L. paracasei*, 24 for *L. plantarum* and 35 for *B. coagulans* (Supplementary Figures S4–S9). The size of the population of the aggregate event was quantified using the Area feature (the number of microns squared in a mask, in μm^2) of the brightfield image.

Mucin adhesion assay

Strains were assayed for adhesion to mucin in 96-well microtiter plates under sterile conditions. Plates were coated with 100 µl of 10 mg/ml porcine Mucin Type || (Sigma-Aldrich) in sterile Dulbecco's phosphate-buffered saline (PBS) at 4°C overnight. Wells were washed twice with sterile PBS to remove unbound mucin. Strains were grown in different liquid mediums for overnight incubation (without shaking) at 37°C. The cells grown overnight were harvested by centrifugation (10,000 × *g* for 2 min at 4°C) and the bacterial cells were resuspended in sterile PBS and adjusted to the optical density (OD_{600}) of 0.5. 100 µl of each strain was added to respective wells and allowed to adhere for 2 h at 37°C. Un-adhered bacterial cells were then withdrawn, and wells were washed 3 times with 100 µl sterile PBS each. Adhered cells were released by treatment with 100 µl 0.1% (v/v) Triton X-100 in sterile PBS for 30 min at 37°C. The released bacterial cells were plated after appropriate dilution on MRS agar, and enumeration was carried out following 48-h incubation at 37°C.

Protein alignment, phylogenetic tree

A phylogenetic tree was built based on 16S rRNA bacterial gene sequences and multiple alignment sequences of LDH proteins was performed using Clustal Omega.[1]

Statistical analysis

All experiments were performed at least three separate and independent times in triplicate unless stated otherwise. Statistical analyses were performed with GraphPad Prism 9.0 (GraphPad 234 Software, Inc., San Diego, CA). Relevant statistical tests are mentioned in the indicated legends of the figures.

Data availability statement

The original contributions presented in the study are included in the article/Supplementary material, further inquiries can be directed to the corresponding author.

Author contributions

IKG, OK, MM, RS, and RO designed the experiments. RS and RO performed the experiments. IKG, MM, OK, HM, OG, RS, and RO contributed reagents. All authors analyzed the data. IKG wrote the paper. All authors contributed to the article and approved the submitted version.

Funding

This work was funded by ImoH grant 3-15656 and ISF 119/16 to IKG.

1 https://www.ebi.ac.uk/Tools/msa/clustalo/

Conflict of interest

The authors declare that the research was conducted in the absence of any commercial or financial relationships that could be construed as a potential conflict of interest.

Publisher's note

All claims expressed in this article are solely those of the authors and do not necessarily represent those of their affiliated organizations, or those of the publisher, the editors and the reviewers. Any product that may be evaluated in this article, or claim that may be made by its manufacturer, is not guaranteed or endorsed by the publisher.

Supplementary material

The Supplementary material for this article can be found online at: https://www.frontiersin.org/articles/10.3389/fmicb.2022.949932/full#supplementary-material

References

Azad, M. A. K., Sarker, M., Li, T., and Yin, J. (2018). Probiotic species in the modulation of gut microbiota: an overview. *Biomed. Res. Int.* 2018, 1–8. doi: 10.1155/2018/9478630

Bintsis, T. (2018). Lactic acid bacteria as starter cultures: an update in their metabolism and genetics. *AIMS Microbiol.* 4, 665–684. doi: 10.3934/MICROBIOL.2018.4.665

Cao, J., Yu, Z., Liu, W., Zhao, J., Zhang, H., Zhai, Q., et al. (2020). Probiotic characteristics of Bacillus coagulans and associated implications for human health and diseases. *J. Funct. Foods* 64:103643. doi: 10.1016/J.JFF.2019.103643

Celebioglu, H. U., Ejby, M., Majumder, A., Køhler, C., Goh, Y. J., Thorsen, K., et al. (2016). Differential proteome and cellular adhesion analyses of the probiotic bacterium Lactobacillus acidophilus NCFM grown on raffinose: an emerging prebiotic. *Proteomics* 16, 1361–1375. doi: 10.1002/pmic.201500212

Costa, C. M. (2002). Formulário para parecer. *Projeto de Pesquisa* 68, 6193–6201. doi: 10.1128/AEM.68.12.6193

De Angelis, M., and Gobbetti, M. (2004). Environmental stress responses in lactobacillus: a review. *Proteomics* 4, 106–122. doi: 10.1002/pmic.200300497

Di Cagno, R., De Angelis, M., Calasso, M., and Gobbetti, M. (2011). Proteomics of the bacterial cross-talk by quorum sensing. *J. Proteome* 74, 19–34. doi: 10.1016/J.JPROT.2010.09.003

Didari, T., Solki, S., Mozaffari, S., Nikfar, S., and Abdollahi, M. (2014). A systematic review of the safety of probiotics. *Expert Opin. Drug Saf.* 13, 227–239. doi: 10.1517/14740338.2014.872627

Ferain, T., Garmyn, D., Bernard, N., Hols, P., and Jean Delcour, A. (1994). Lactobacillus plantarum ldhL gene: overexpression and deletion. *J. Bacteriol.* 176, 596–601.

Fontana, L., Bermudez-Brito, M., Plaza-Diaz, J., Muñoz-Quezada, S., and Gil, A. (2004). *Sources, isolation, characterisation and evaluation of probiotics. Br. J. Nutr. 109*:S35–S50. doi:10.1017/S0007114512004011.

Garro, M. S., De Valdez, G. F., Oliver, G., and De Giori, G. S. (1998). Growth characteristics and fermentation products of Streptococcus salivarius subsp. thermophilus, Lactobacillus casei and L. fermentum in soymilk. *Eur. Food Res. Technol.* 206, 72–75. doi: 10.1007/s002170050217

Gobbetti, M., Di Cagno, R., and de Angelis, M. (2010). Functional microorganisms for functional food quality. *Crit. Rev. Food Sci. Nutr.* 50, 716–727. doi: 10.1080/10408398.2010.499770

Hall, B. G., Acar, H., Nandipati, A., and Barlow, M. (2014). Growth rates made easy. *Mol. Biol. Evol.* 31, 232–238. doi: 10.1093/MOLBEV/MST187

Hedberg, M., Hasslöf, P., Sjöström, I., Twetman, S., and Stecksén-Blicks, C. (2008). Sugar fermentation in probiotic bacteria: an in vitro study. *Oral Microbiol. Immunol.* 23, 482–485. doi: 10.1111/j.1399-302X.2008.00457.x

Hofvendahl, K., and Hahn-Hägerdal, B. (2000). Factors affecting the fermentative lactic acid production from renewable resources. *Enzyme Microb. Technol.* 26, 87–107.

Hols, P. (2004). Major role of NAD-dependent lactate dehydrogenases in aerobic lactate utilization in Lactobacillus plantarum during early stationary phase. *Microbiology* 186, 6661–6666. doi: 10.1128/JB.186.19.6661

Huang, S. C., Burne, R. A., and Chen, Y. Y. M. (2014). The pH-dependent expression of the urease operon in Streptococcus salivarius is mediated by CodY. *Appl. Environ. Microbiol.* 80, 5386–5393. doi: 10.1128/AEM.00755-14

Huang, Y., Xin, W., Xiong, J., Yao, M., Zhang, B., and Zhao, J. (2022). The intestinal microbiota and metabolites in the gut-kidney-heart axis of chronic kidney disease. *Front. Pharmacol.* 13:734. doi: 10.3389/FPHAR.2022.837500/BIBTEX

Karapetsas, A., Vavoulidis, E., Galanis, A., Sandaltzopoulos, R., and Kourkoutas, Y. (2010). Rapid detection and identification of probiotic Lactobacillus casei ATCC 393 by multiplex PCR. *Microb. Physiol.* 18, 156–161. doi: 10.1159/000308518

Konieczny, M., Rhein, P., Czaczyk, K., Białas, W., and Juzwa, W. (2021). Imaging flow cytometry to study biofilm-associated microbial aggregates. *Molecules* 26, 1–12. doi: 10.3390/molecules26237096

Maan, H., Gilhar, O., Porat, Z., and Kolodkin-Gal, I. (2021). Bacillus subtilis colonization of Arabidopsis thaliana roots induces multiple biosynthetic clusters for antibiotic production. *Front. Cell. Infect. Microbiol.* 11, 1–10. doi: 10.3389/fcimb.2021.722778

Narayana, S. K., Mallick, S., Siegumfeldt, H., and van den Berg, F. (2020). Bacterial flow cytometry and imaging as potential process monitoring tools for industrial biotechnology. *Fermentation* 6:10. doi: 10.3390/fermentation6010010

O'Mahony, L., Mccarthy, J., Kelly, P., Hurley, G., Luo, F., Chen, K., et al. (2005). Lactobacillus and Bifidobacterium in irritable bowel syndrome: symptom responses and relationship to cytokine profiles. *Gastroenterology* 128, 541–551. doi: 10.1053/j.gastro.2004.11.050

Palacio, M. I., Etcheverría, A., Manrique, G., Palacio, M. I., Etcheverría, A. I., and Manrique, G. D. (2014). Fermentation by Lactobacillus paracasei of galactooligosaccharides and low-molecular-weight carbohydrates extracted from squash (Curcubita maxima) and lupin (Lupinus albus) seeds. *J. Microbiol. Biotechnol. Food Sci.* 3, 329–332.

Papadimitriou, K., Alegría, Á., Bron, P. A., de Angelis, M., Gobbetti, M., Kleerebezem, M., et al. (2016). Stress physiology of lactic acid bacteria. *Microbiol. Mol. Biol. Rev.* 80, 837–890. doi: 10.1128/MMBR.00076-15/ASSET/AF4F2855-634D-46C6-A58C-BAA8988DF6CC/ASSETS/GRAPHIC/ZMR0031624320005.JPEG

Papadimitriou, K., Zoumpopoulou, G., Foligné, B., Alexandraki, V., Kazou, M., Pot, B., et al. (2015). Discovering probiotic microorganisms: in vitro, in vivo, genetic and omics approaches. *Front. Microbiol.* 6:58. doi: 10.3389/fmicb.2015.00058

Paucean, A., Vodnar, D. C., Socaci, S. A., and Socaciu, C. (2013). Carbohydrate metabolic conversions to lactic acid and volatile derivatives, as influenced by Lactobacillus plantarum ATCC 8014 and Lactobacillus casei ATCC 393 efficiency during in vitro and sourdough fermentation. *Eur. Food Res. Technol.* 237, 679–689. doi: 10.1007/s00217-013-2042-6

Povolotsky, T. L., Keren-Paz, A., and Kolodkin-Gal, I. (2021). Metabolic microenvironments drive microbial differentiation and antibiotic resistance. *Trends Genet.* 37, 4–8. doi: 10.1016/J.TIG.2020.10.007

Qin, J., Li, R., Raes, J., Arumugam, M., Burgdorf, K. S., Manichanh, C., et al. (2010). A human gut microbial gene catalogue established by metagenomic sequencing. *Nature* 464, 59–65. doi: 10.1038/nature08821

Rajasekharan, S. K., and Shemesh, M. (2022). Spatiotemporal bio-shielding of bacteria through consolidated geometrical structuring. *NPJ Biofilms Microbiomes* 8:37. doi: 10.1038/s41522-022-00302-2

Rocchetti, M. T., Russo, P., Capozzi, V., Drider, D., Spano, G., and Fiocco, D. (2021). Bioprospecting antimicrobials from Lactiplantibacillus plantarum: key factors underlying its probiotic action. *Int. J. Mol. Sci.* 22:12076. doi: 10.3390/IJMS222112076

Saez-lara, M. J., Gomez-llorente, C., Plaza-diaz, J., and Gil, A. (2015). The role of probiotic lactic acid bacteria and Bifidobacteria in the prevention and treatment of inflammatory bowel disease and other related diseases: a systematic review of randomized human clinical trials. *Biomed. Res. Int.* 2015:505878. doi: 10.1155/2015/505878

Salas-Jara, M. J., Ilabaca, A., Vega, M., and García, A. (2016). Biofilm forming lactobacillus: new challenges for the development of probiotics. *Microorganisms* 4:35. doi: 10.3390/microorganisms4030035

Savijoki, K., Nyman, T. A., Kainulainen, V., Miettinen, I., Siljamäki, P., Fallarero, A., et al. (2019). Growth mode and carbon source impact the surfaceome dynamics of lactobacillus rhamnosus GG. *Front. Microbiol.* 10:1272. doi: 10.3389/FMICB.2019.01272/BIBTEX

Segers, M. E., and Lebeer, S. (2014). Towards a better understanding of Lactobacillus rhamnosus GG - host interactions. *Microb. Cell Factories* 13:S7. doi: 10.1186/1475-2859-13-S1-S7

Simonian, H. P., Vo, L., Doma, S., Fisher, R. S., and Parkman, H. P. (2005). Regional postprandial differences in pH within the stomach and gastroesophageal junction. *Dig. Dis. Sci.* 50, 2276–2285. doi: 10.1007/s10620-005-3048-0

Singh, R. K., Chang, H. W., Yan, D., Lee, K. M., Ucmak, D., Wong, K., et al. (2017). Influence of diet on the gut microbiome and implications for human health. *J. Transl. Med.* 15:17. doi: 10.1186/s12967-017-1175-y

Spor, A., Koren, O., and Ley, R. (2011). Unravelling the effects of the environment and host genotype on the gut microbiome. *Nat. Rev. Microbiol.* 9, 279–290. doi: 10.1038/nrmicro2540

Turroni, F., Ventura, M., Buttó, L. F., Duranti, S., O'Toole, P. W., Motherway, M. O. C., et al. (2014). Molecular dialogue between the human gut microbiota and the host: a Lactobacillus and Bifidobacterium perspective. *Cell. Mol. Life Sci.* 71, 183–203. doi: 10.1007/s00018-013-1318-0

Vijaya Kumar, B., Vijayendra, S. V. N., and Reddy, O. V. S. (2015). Trends in dairy and non-dairy probiotic products: a review. *J. Food Sci. Technol.* 52, 6112–6124. doi: 10.1007/s13197-015-1795-2

Wang, Y., Wu, J., Lv, M., Shao, Z., Hungwe, M., Wang, J., et al. (2021). Metabolism characteristics of lactic acid bacteria and the expanding applications in food industry. *Front. Bioeng. Biotechnol.* 9:378. doi: 10.3389/FBIOE.2021.612285/BIBTEX

Yeo, S. K., and Liong, M. T. (2010). Effect of prebiotics on viability and growth characteristics of probiotics in soymilk. *J. Sci. Food Agric.* 90, 267–275. doi: 10.1002/jsfa.3808

Zartl, B., Silberbauer, K., Loeppert, R., Viernstein, H., Praznik, W., and Mueller, M. (2018). Fermentation of non-digestible raffinose family oligosaccharides and galactomannans by probiotics. *Food Funct.* 9, 1638–1646. doi: 10.1039/c7fo01887h

Zielińska, D., Kolozyn-Krajewska, D., and Laranjo, M. (2018). Food-origin lactic acid bacteria may exhibit probiotic properties: review. *Biomed. Res. Int.* 2018, 1–15. doi: 10.1155/2018/5063185

frontiers | Frontiers in Microbiology

TYPE Original Research
PUBLISHED 26 October 2022
DOI 10.3389/fmicb.2022.1053239

OPEN ACCESS

EDITED BY
Agapi Doulgeraki,
Hellenic Agricultural Organization,
Greece

REVIEWED BY
Steve Flint,
Massey University,
New Zealand
Qingli Dong,
University of Shanghai for Science and Technology, China

*CORRESPONDENCE
Mehdi Zarei
zarei@scu.ac.ir
Amin Yousefvand
amin.yousefvand@helsinki.fi

SPECIALTY SECTION
This article was submitted to Food Microbiology, a section of the journal Frontiers in Microbiology

RECEIVED 25 September 2022
ACCEPTED 13 October 2022
PUBLISHED 26 October 2022

CITATION
Zarei M, Rahimi S, Saris PEJ and Yousefvand A (2022) *Pseudomonas fluorescens* group bacterial strains interact differently with pathogens during dual-species biofilm formation on stainless steel surfaces in milk.
Front. Microbiol. 13:1053239.
doi: 10.3389/fmicb.2022.1053239

Pseudomonas fluorescens group bacterial strains interact differently with pathogens during dual-species biofilm formation on stainless steel surfaces in milk

Mehdi Zarei[1]*, Saeid Rahimi[1], Per Erik Joakim Saris[2] and Amin Yousefvand[1,2]*

[1]Department of Food Hygiene, Faculty of Veterinary Medicine, Shahid Chamran University of Ahvaz, Ahvaz, Iran, [2]Department of Microbiology, Faculty of Agriculture and Forestry, University of Helsinki, Helsinki, Finland

In order to develop strategies for preventing biofilm formation in the dairy industry, a deeper understanding of the interaction between different species during biofilm formation is necessary. Bacterial strains of the *P. fluorescens* group are known as the most important biofilm-formers on the surface of dairy processing equipment that may attract and/or shelter other spoilage or pathogenic bacteria. The present study used different strains of the *P. fluorescens* group as background microbiota of milk, and evaluated their interaction with *Staphylococcus aureus*, *Bacillus cereus*, *Escherichia coli* O157:H7, and *Salmonella* Typhimurium during dual-species biofilm formation on stainless steel surfaces. Two separate scenarios for dual-species biofilms were considered: concurrent inoculation of *Pseudomonas* and pathogen (CI), and delayed inoculation of pathogen to the pre-formed *Pseudomonas* biofilm (DI). The gram-positive pathogens used in this study did not form dual-species biofilms with *P. fluorescens* strains unless they were simultaneously inoculated with *Pseudomonas* strains. *E. coli* O157:H7 was able to form dual-species biofilms with all seven *P. fluorescens* group strains, both in concurrent (CI) and delayed (DI) inoculation. However, the percentage of contribution varied depending on the *P. fluorescens* strains and the inoculation scenario. *S. Typhimurium* contributed to biofilm formation with all seven *P. fluorescens* group strains under the CI scenario, with varying degrees of contribution. However, under the DI scenario, *S.* Typhimurium did not contribute to the biofilm formed by three of the seven *P. fluorescens* group strains. Overall, these are the first results to illustrate that the strains within the *P. fluorescens* group have significant differences in the formation of mono-or dual-species biofilms with pathogenic bacteria. Furthermore, the possibility of forming dual-species biofilms with pathogens depends on whether the pathogens form the biofilm simultaneously with the *P. fluorescens* group strains or whether these strains have already formed a biofilm.

10.3389/fmicb.2022.1053239

KEYWORDS

Biofilm, *Pseudomonas fluorescens*, *Staphylococcus aureus*, *Bacillus cereus*, *Escherichia coli* O157:H7, *Salmonella* Typhimurium

Introduction

More than 50 validly named species and a large number of unclassified isolates make up *Pseudomonas fluorescens* complex group, one of the most diverse groups within the *Pseudomonas* genus (Mulet et al., 2010; Gomila et al., 2015; Garrido-Sanz et al., 2016). There are nine subgroups within this complex group, including *P. fluorescens*, *P. jessenii*, *P. fragi*, *P. gessardii*, *P. corrugata*, *P. chlororaphis*, *P. mandelii*, *P. koreensis* and *P. protegens* (Garrido-Sanz et al., 2016). Bacterial strains of the *P. fluorescens* group are among the most important spoilage bacteria in milk and dairy products, and have been frequently isolated from fresh milk and cheese (Wang and Jayarao, 2001; De Jonghe et al., 2011; Martin et al., 2011; Carrascosa et al., 2015). Their ability to grow at low temperatures allows them to outgrow other bacteria in cold raw milk (Fricker et al., 2011; von Neubeck et al., 2015; Meng et al., 2017). Furthermore, *P. fluorescens* group strains have also been reported to cause repeat and sporadic post-pasteurization contamination, which results in shorter shelf life for pasteurized milk (Reichler et al., 2018).

P. fluorescens group bacterial strains are important in the dairy industry not only because of their heat-resistant enzymes, but also because of their ability to adhere to and from biofilms on the surface of milk tanks and other dairy processing equipment (Shpigel et al., 2015; Stoeckel et al., 2016). They are therefore able to withstand harsh conditions such as cleaning-in-place (CIP) processes, allowing them to remain within the dairy processing plant for extended periods of time (Cherif-Antar et al., 2016). Aside from contaminating subsequent batches of milk passing the biofilm region, *Pseudomonas* biofilms may also attract and/or provide shelter for other (spoilage or pathogenic) bacteria.

Biofilm formation by spoilage and pathogenic bacteria is a serious concern in the dairy industry, and hence has received much attention. A variety of different spoilage and pathogenic bacteria are known to attach to the internal stainless steel surfaces of the raw milk storage tanks and pipelines, where they can grow and form mono-or multi-species biofilms (Austin and Bergeron, 1995; Sharma and Anand, 2002; Latorre et al., 2010; Marchand et al., 2012; Anand et al., 2014; Cherif-Antar et al., 2016). Although biofilms in the dairy industry are more likely to be formed by spoilage bacteria (due to the higher population), pathogenic bacteria may also participate in the biofilm formation process, which may result in dual-or multi-species biofilms (Shi and Zhu, 2009; van Houdt and Michiels, 2010; Schirmer et al., 2013; Makovcova et al., 2017). In such cases, the cooperative interspecies interactions within dual-or multi-species biofilms are likely increase their resistance to adverse conditions compared to single-species biofilms. On the contrary, interspecific competition may occur and cause antagonistic effects (Yang et al., 2011; Elias and Banin, 2012; Rendueles and Ghigo, 2012; Liu et al., 2016).

To our knowledge, there is no information on the interaction between *P. fluorescens* group strains and bacterial pathogens from different genera during biofilm formation. Hence, in the present study, we used different strains of the *P. fluorescens* complex group as background microbiota of milk and evaluated their interaction with *Staphylococcus aureus*, *Bacillus cereus*, *Escherichia coli* O157:H7, and *Salmonella* Typhimurium during dual-species biofilm formation on stainless steel surfaces. We considered two separate scenarios for dual-species biofilms; (i) concurrent inoculation of *Pseudomonas* and the pathogen, and (ii) delayed inoculation of the pathogen to the pre-formed *Pseudomonas* biofilm.

Materials and methods

Bacterial strains and culture conditions

This study used *P. fluorescens* ATCC 13525, six other *P. fluorescens* group bacterial strains previously isolated from cold raw milk: *P. fluorescens* 5a, *P. fluorescens* 21c, *P. fluorescens* 68a, *P. veronii* 25d, *P. cedrina* 69a, and *P. simiae* 77a (Zarei et al., 2020). *S. aureus* (ATCC 25923), *B. cereus* (PTCC 1154), *E. coli* O157:H7 (ATCC 43895), and *S.* Typhimurium (ATCC 14028) were also used in this study. Stock cultures of bacterial strains were stored at-70°C in Tryptic Soy Broth (TSB; Merck, Germany) supplemented with 25% (v/v) sterile glycerol (Merck, Germany). Bacterial strains were first activated by two successive transfers in TSB at 30°C for 48 h. To prepare the inoculum, 0.1 ml of activated culture was added to 10 ml of ultra-high temperature (UHT) milk (3.79% protein and 1.5% fat), and incubated at 30°C for 48 h. Commercial UHT milk from the same batch was used for all experiments throughout the study.

Biofilm formation on stainless steel surfaces

Single-species biofilm

To evaluate the ability of individual *Pseudomonas* strains and the pathogenic bacteria to produce a biofilm on stainless steel surfaces, overnight cultures of each strain were diluted to the final concentration of 10^6 CFU/ml in UHT milk. The inoculated UHT milk (2 ml) was added to 12-well plates containing 1 × 1 cm

10.3389/fmicb.2022.1053239

TABLE 1 Identification key tests for differentiation of the colonies.

	Identification key		
Bacterial strain	**KOH test**	**Catalase**	**Oxidase**
Pseudomonas strains	+	+	+
S. aureus	−	+	−
B. cereus	−	+	+
E. coli O157:H7	+	+	−
S. Typhimurium	+	+	−

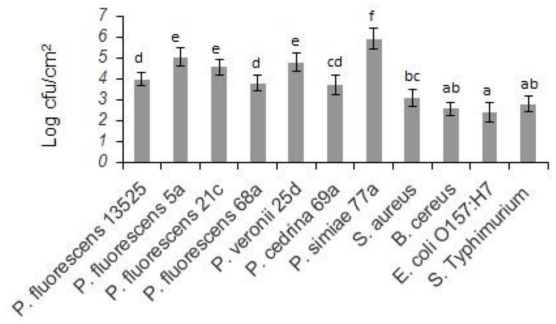

FIGURE 1
Biofilm cell counts of the selected *P. fluorescens* group strains and the pathogenic bacteria in mono-species biofilms on stainless steel surfaces after 48h of incubation in UHT milk at 7°C. Different letters indicate significant differences between the strains.

stainless steel coupons (AISI 304, 2B, Norsk Stål AS, Norway), and incubated at 7°C for 48 h before quantifying the biofilm.

Dual-species biofilms

Each of the seven *Pseudomonas* strains was tested in dual-culture with each individual pathogen. The individual strain cultures were added to UHT milk and combined to contain approximately 10^6 CFU/ml of each strain.

To investigate dual-species biofilms, two scenarios were considered. In the first scenario, an individual strain of *Pseudomonas* and the pathogen were inoculated concurrently (10^6 CFU/ml of each strain) in UHT milk samples, and the formation of dual-species biofilms was evaluated. To achieve this, (hereinafter referred to as concurrent inoculation; CI), the combined dual-cultures in UHT milk (2 ml) were added to 12-well plates containing 1 × 1 cm stainless steel coupons, and incubated at 7°C for 48 h before quantifying the biofilm.

In the second scenario, the possibility of the pathogen being added to the pre-formed *Pseudomonas* biofilms was evaluated. For this scenario, (hereinafter referred to as delayed inoculation; DI), the UHT milk inoculated with 10^6 CFU/ml of each individual *Pseudomonas* strain was added to 12-well plates containing stainless steel coupons, and incubated at 7°C. After 48 h of incubation, the wells were drained and replaced with 2 ml of UHT milk containing 10^6 CFU/ml of each individual pathogen. The plates were then incubated for another 48 h before quantifying the biofilm.

Biofilm quantification

At the end of the incubation period, the wells were drained and the plates were gently washed three times by adding sterile dH_2O (2 ml) to the coupon wells, followed by swirling of the plates and pipetting to remove non-attached bacteria. Biofilm cells were scraped into 1 ml of physiological saline solution using a cell scraper, and resuspended by vigorous pipetting for 15 s. Serial decimal dilutions of the cells were plated onto Tryptic Soy Agar (**TSA**) plates, and colonies were counted after 36 h of incubation at 30°C (Zarei et al., 2020).

Bacterial contribution to biofilm communities

To determine the percent contribution of bacterial strains to dual-species biofilms, all colonies within a zone of the TSA plates were selected and identified using KOH test, oxidase, and catalase tests, as shown in Table 1. The size of the zones for colony selection was adjusted to have approximately 30 colonies within the zone of TSA plates, with a total of 30–300 colonies (Heir et al., 2018).

Statistical analysis

All experiments were replicated at least three times on different days. Results were analyzed using One-Way ANOVA (SPSS 20, SPSS Inc., Chicago, IL). The significance levels are expressed at a 95% confidence level ($p \leq 0.05$) throughout.

Results

Single-species biofilms

Biofilm-forming ability of the selected strains of the *P. fluorescens* group and the pathogenic bacteria on stainless steel surfaces was evaluated in UHT milk. In general, after 48 h incubation at 7°C, the number of biofilm cells of the *Pseudomonas* strains was higher than the pathogens ($p < 0.05$). As shown in Figure 1, comparing *Pseudomonas* strains revealed that the highest number of biofilm cells on the stainless steel surfaces were from *P. simiae* 77a (5.89 ± 0.51 log CFU/cm²), and the lowest number was from *P. cedrina* 69a (3.66 ± 0.47 CFU/cm²). Among the pathogens, the highest and lowest number of biofilm cells were from *S. aureus* (2.87 ± 0.43 CFU/cm²) and *E. coli* O157:H7 (2.08 ± 0.31 CFU/cm²), respectively.

Dual-species biofilms

Pseudomonas fluorescens group strains and *Staphylococcus aureus*

Evaluating the formation of dual-species biofilm by different *P. fluorescens* group strains and *S. aureus* showed differences between *P. fluorescens* group strains within each scenario, and

also between scenarios. In the CI scenario, *S. aureus* was found in six of the seven biofilms, with varying degrees of contribution. As shown in Figure 2, the highest contributions were observed with *P. simiae* 77a (24.3%) and *P. veronii* 25d (20.4%), while the lowest was observed with *P. fluorescens* 5a (3.6%). In this scenario, *S. aureus* did not contribute to the biofilm formed by *P. fluorescens* 21c. Additionally, there were significantly more dual-species biofilm cells with *P. fluorescens* ATCC 13525, *P. fluorescens* 68a, *P. veronii* 25d, and *P. simiae* 77a than in their single-species biofilms ($p < 0.05$; Figure 3). In contrast, *S. aureus* did not contribute to the structure of any biofilms in the DI scenario. Biofilms formed in pure cultures of *P. fluorescens* group strains did not differ significantly from those formed in the DI scenario in terms of the number of biofilm cells ($p > 0.05$; Figure 3).

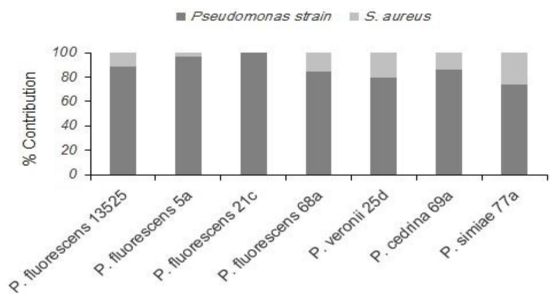

FIGURE 2
Contributions of different *P. fluorescens* group strains and *S. aureus* to dual-species biofilms on stainless steel surfaces under the CI scenario.

Pseudomonas fluorescens group strains and *Bacillus cereus*

As with *S. aureus*, *B. cereus* did not contribute to the biofilm formation in the DI scenario, and the total number of biofilm cells did not differ significantly from those formed in pure cultures of *P. fluorescens* group strains. In contrast, *B. cereus* contributed to five out of seven biofilms in the CI scenario. As shown in Figure 4, the highest contributions were observed with *P. simiae* 77a (19.4%) and *P. veronii* 25d (14.3%), while the lowest was observed with *P. fluorescens* 5a (6.9%); *B. cereus* did not contribute to the biofilm formed by *P. fluorescens* 21c and *P. cedrina* 69a. The total number of biofilm cells in dual-species biofilms with *B. cereus* and *P. fluorescens* ATCC 13525, *P. fluorescens* 5a, *P. fluorescens* 68a, *P. veronii* 25d and *P. simiae* 77a were significantly higher than those in the pure cultures of *P. fluorescens* group strains ($p < 0.05$; Figure 5).

Pseudomonas fluorescens group strains and *Escherichia coli* O157:H7

Unlike the two gram-positive bacteria that did not contribute to the biofilm structure in the DI scenario, *E. coli* O157:H7 contributed to biofilm formation with all seven *P. fluorescens* group strains in both CI and DI scenarios, to varying degrees. As shown in Figure 6, the highest percent contribution was found with *P. cedrina* 69a (27.8 and 16.7% in the CI and DI scenarios, respectively), and the lowest was found with *P. fluorescens* 5a (2.1 and 4.7% in the CI and DI scenarios, respectively).

In both scenarios, the total number of biofilm cells in dual-species biofilms with *E. coli* O157:H7 and *P. fluorescens* 68a, *P. cedrina* 69a and *P. simiae* 77a were significantly higher than those in pure cultures of *P. fluorescens* group strains (Figure 7; $p < 0.05$). For *P. veronii* 25d, the total number of biofilm cells in dual-species biofilms was significantly higher than in the pure culture ($p < 0.05$), but only in the CI scenario. No significant

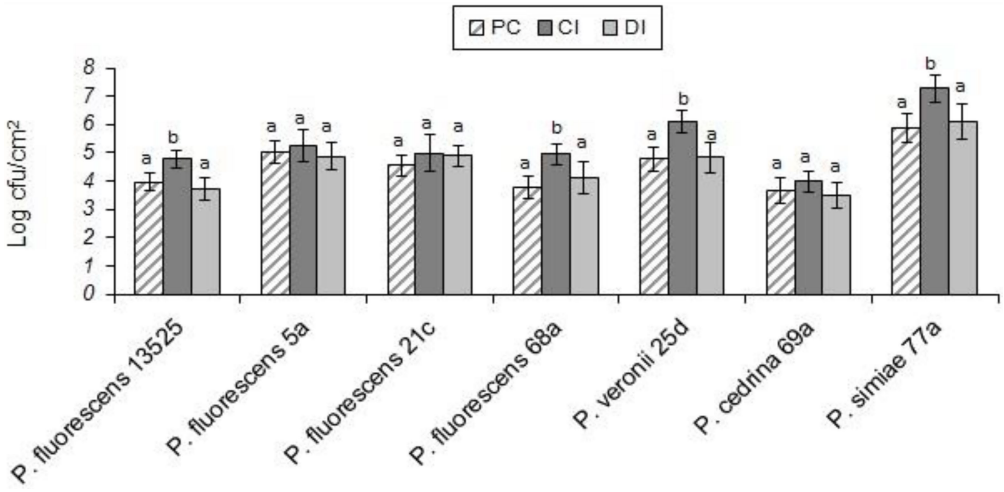

FIGURE 3
Total number of biofilm cells in mono- and dual-species biofilms of the seven *P. fluorescens* group strains with *S. aureus* on stainless steel surfaces. PC: pure culture biofilms; CI: dual-species biofilms under the CI scenario; DI: dual-species biofilms under the DI scenario. For each *P. fluorescens* strain, different letters indicate significant differences in the total number of biofilm cells.

differences were observed between CI and DI scenarios in terms of the number of biofilm cells in dual-species biofilms of the seven *P. fluorescens* group strains with *E. coli* O157:H7 ($p > 0.05$; Figure 7).

Pseudomonas fluorescens group strains and *Salmonella* Typhimurium

With *S.* Typhimurium, the situation was somewhat different from that of the other Gram-negative bacteria tested (*E. coli* O157:H7). *S.* Typhimurium contributed to biofilm formation with all seven *P. fluorescens* group strains in the CI scenario, to varying degrees. As shown in Figure 8A, the highest contribution was found with *P. fluorescens* 68a (25.2%), and the lowest was with *P. fluorescens* 5a (4.6%). However, in the DI scenario, *S.* Typhimurium did not contribute to the biofilm formed by *P. fluorescens* 5a, *P. fluorescens* 21c, or *P. veronii* 25d. It did contribute to dual-species biofilms with other *P. fluorescens* group strains, but to a lesser extent than in the CI scenario (Figure 8B).

As shown in Figure 9, in both scenarios the total numbers of biofilm cells in dual-species biofilms of *P. fluorescens* 5a, *P. fluorescens* 21c and *P. veronii* 25d were not significantly different from those in pure cultures of *P. fluorescens* group strains ($p > 0.05$). In contrast, the total number of biofilm cells in dual-species biofilms with *S.* Typhimurium and *P. fluorescens* 68a and *P. cedrina* 69a in the CI scenario were significantly higher than those in the DI scenario, and in pure cultures ($p < 0.05$). Furthermore, the total number of biofilm cells in dual-species biofilms with *S.* Typhimurium and *P. fluorescens* 13,525 and *P. simiae* 77a in the CI scenario were significantly higher than that in the DI scenario, and in the pure culture, respectively ($p < 0.05$).

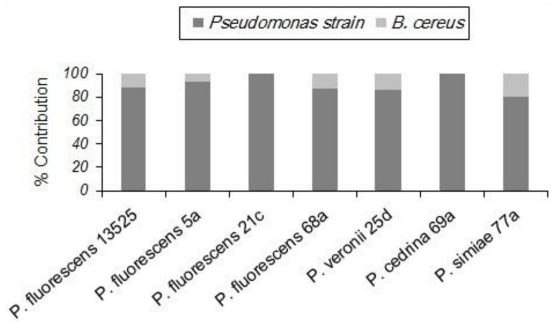

FIGURE 4
Contributions of different *P. fluorescens* group strains and *B. cereus* to dual-species biofilms on stainless steel surfaces in CI scenario.

Discussion

P. fluorescens group strains are among the bacteria most frequently isolated from surfaces in the food industry, and are characterized as quick and thick biofilm producers on various surfaces (Simoes et al., 2008; Mann and Wozniak, 2012; Marchand et al., 2012; Puga et al., 2016; Zarei et al., 2020). Results of the present study re-confirmed the high ability of these bacteria to produce biofilm on stainless steel surfaces. In general, at 7°C these bacteria produced more biofilm than the pathogenic strains tested, however the *P. fluorescens* strains differed significantly in their ability to produce biofilms on stainless steel surfaces in UHT milk.

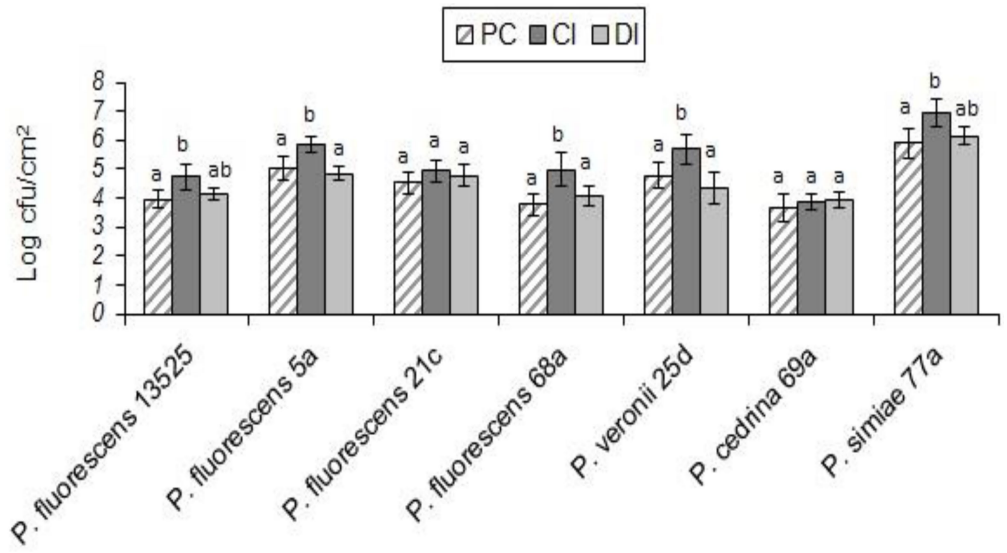

FIGURE 5
Total number of biofilm cells in mono- and dual-species biofilms of the seven *P. fluorescens* group strains with *B. cereus* on stainless steel surfaces. PC: pure culture biofilms; CI: dual-species biofilms under the CI scenario; DI: dual-species biofilms under the DI scenario. For each *P. fluorescens* strain, different letters indicate significant differences in the total number of biofilm cells.

Previous research has highlighted strain diversity of the *P. fluorescens* group isolated from dairy products and raw milk in terms of blue pigment production and lipoproteolytic activity (Chierici et al., 2016; Longhi et al., 2022). Other differences in the proteolytic activity of *P. fluorescence* group strains have also been reported previously (Zarei et al., 2020).

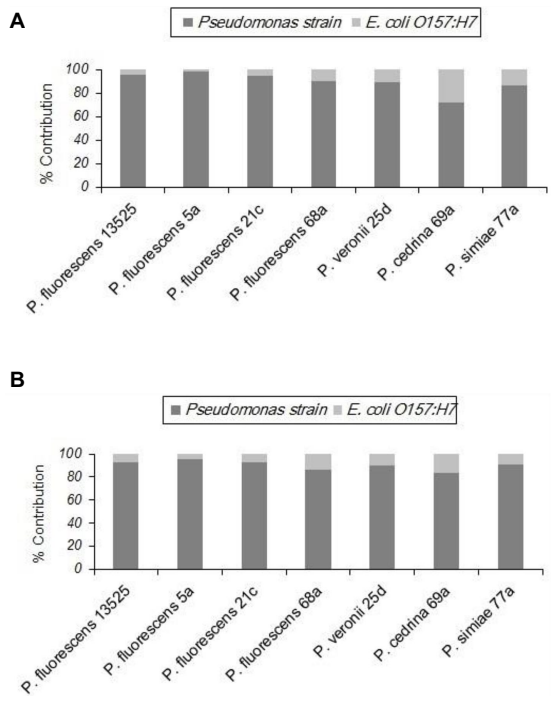

FIGURE 6
Contributions of different *P. fluorescens* group strains and *E. coli* O157:H7 to dual-species biofilms on stainless steel surfaces under CI **(A)** and DI **(B)** scenarios.

The presence of spoilage and pathogenic bacteria in milk and dairy products is a worldwide problem that not only leads to shelf-life reduction and alteration of organoleptic properties, but is also related to many disease outbreaks. The coexistence and interactions between foodborne pathogens and resident background microbiota are likely to occur on the surface of milk tanks and other dairy processing equipment between sessile cells, particularly in biofilms. It has been well documented that most naturally occurring biofilms are composed of multiple bacterial species (Yannarell et al., 2019). Hence, in terms of pathogen densities in dual-or multi-species biofilms, interactions with background microbiota strains can have neutral, positive, or antagonistic effects (Langsrud et al., 2016; Møretrø and Langsrud, 2017; Heir et al., 2018). These interactions can protect bacteria from environmental stresses, and can also influence the growth and survival of the individual members of these microbial consortia (Røder et al., 2015; Sanchez-Vizuete et al., 2015; Møretrø and Langsrud, 2017; Papaioannou et al., 2018).

In the present study, the interactions between *P. fluorescens* group bacterial strains and *S. aureus*, *B. cereus*, *E. coli* O157:H7, and *S.* Typhimurium during dual-species biofilm formation on stainless steel surfaces in UHT milk were evaluated. Two scenarios (concurrent inoculation and delayed inoculation of pathogens) were examined to better understand the possibility of dual-species biofilm formation. Given that all experiments in this study were performed at 7°C, the predominance of the *Pseudomonas* population in biofilms in both scenarios was expected.

In dual-species biofilms with *S. aureus*, this pathogen was found in six of the seven biofilms, with varying degrees of contributions in the CI scenario, which revealed differences

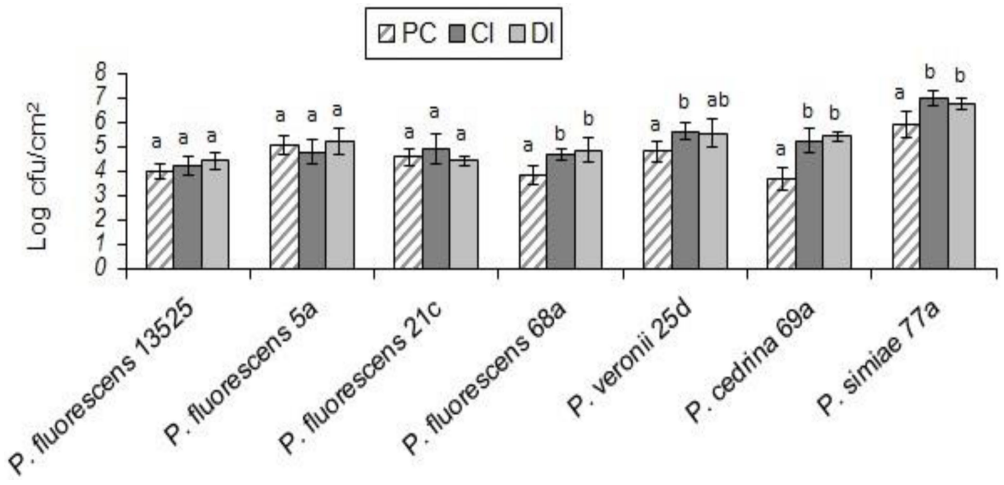

FIGURE 7
Total number of biofilm cells in mono-and dual-species biofilms of the seven *P. fluorescens* group strains with *E. coli* O157:H7 on stainless steel surfaces. PC: pure culture biofilms; CI: dual-species biofilms under the CI scenario; DI: dual-species biofilms under the DI scenario. For each *P. fluorescens* strain, different letters indicate significant differences in the total number of biofilm cells.

between various strains within the *P. fluorescens* group. Moreover, our findings indicated that although *S. aureus* could co-produce biofilms with *P. fluorescens* group bacterial strains, it could not be incorporated into the pre-formed biofilms. Almost the same results were observed for another gram-positive bacterium used in this study – *B. cereus*. This pathogen was found in five of the seven biofilms, also with varying degrees of contributions in the CI scenario, while it did not contribute to biofilm formation in the DI scenario. The metabolites secreted around the biofilm matrix of *P. fluorescens* group strains may have prevented these two gram-positive pathogens from entering the pre-formed biofilms. Insufficient places to attach to the surface can be another explanation for the lack of contribution of these two gram-positive bacteria to the biofilm formation in the DI scenario (Balaure and Grumezescu, 2020). Evidently, biofilm formation in the CI scenario was not hampered by this challenge, leading to dual-species biofilms. Simoes et al. (2008) demonstrated that dual-species biofilms of *P. fluorescens* and *B. cereus* were significantly more metabolically active than *P. fluorescens* mono-species biofilms. Furthermore, Davies and Marques (2011) found that the fatty acid cis-2-decenoic acid produced by *Pseudomonas* group strains yielded dispersion of biofilms formed by *S. aureus*.

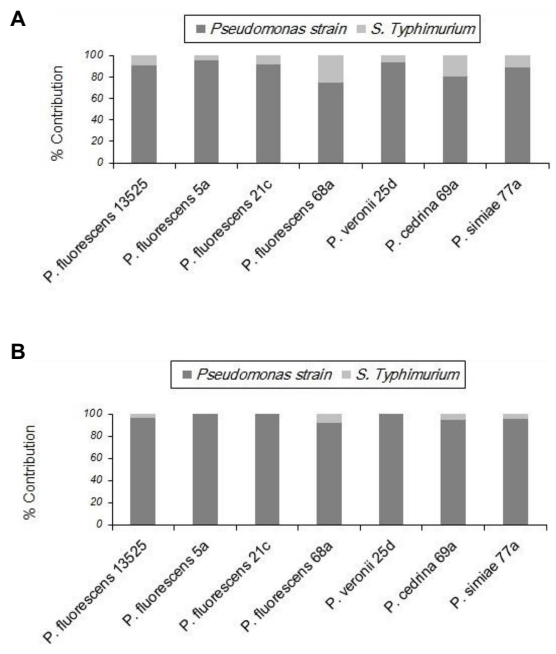

FIGURE 8
Contributions of different *P. fluorescens* strain groups and *S.* Typhimurium to dual-species biofilms on stainless steel surfaces under CI **(A)** and DI **(B)** scenarios.

In contrast to the two gram-positive bacteria, *E. coli* O157:H7 and *S.* Typhimurium formed dual-species biofilms with all seven strains of the *P. fluorescens* group in the CI scenario, and with seven (*E. coli* O157:H7) and four (*S.* Typhimurium) strains in the DI scenario. Nevertheless, for both pathogens, significant differences were observed between *P. fluorescens* group strains in both scenarios, indicating strong and weak competitor strains within the *P. fluorescens* group. It has been previously reported that the biofilm formation of *E. coli* O157:H7 increased in the presence of background microbiota of meat (Dourou et al., 2011). This might explain why *E. coli* O157:H7 had a higher percent contribution to biofilm formation in the CI scenario than the DI scenario.

Overall, this study provides the first demonstration of differences between strains of the *P. fluorescens* group in terms of the formation

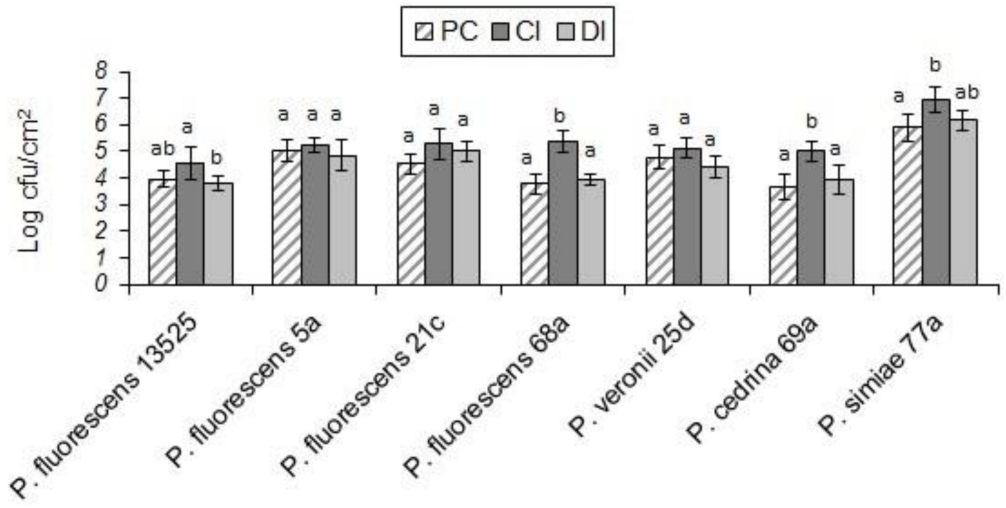

FIGURE 9
Total number of biofilm cells in mono- and dual-species biofilms of the seven *P. fluorescens* group strains with *S. typhimurium* on stainless steel surfaces. PC: pure culture biofilms; CI: dual-species biofilms under the CI scenario; DI: dual-species biofilms under the DI scenario. For each *P. fluorescens* strain, different letters indicate significant differences in the total number of biofilm cells.

of mono-or dual-species biofilms with pathogenic bacteria. Moreover, the ability to produce dual-species biofilms with pathogenic bacteria depends on whether the pathogens form the biofilm simultaneously with the *P. fluorescens* group strains or whether *P. fluorescens* group strains have already formed a biofilm. Such differences between strains and the inoculation time makes comparison of the results difficult, but also highlights the complexity of bacterial interactions involving the strains of the *P. fluorescens* group that requires further understanding for improved control of biofilms in the dairy industry. This study also contributes to the understanding of the role of different strains of the *P. fluorescens* group in the ability of four important foodborne pathogens to establish, survive and persist in dairy processing premises.

Data availability statement

The original contributions presented in the study are included in the article/supplementary material, further inquiries can be directed to the corresponding authors.

Author contributions

MZ designed the research. AY and SR performed the experiments. MZ and PS performed data analysis. MZ and AY prepared the figures. MZ wrote the manuscript, with contributions from AY and PS. All authors contributed to the article and approved the submitted version.

Funding

This study was supported by the research grant provided by Shahid Chamran University of Ahvaz (SCU.VF99.245) and open access funded by Helsinki University Library.

Conflict of interest

The authors declare that the research was conducted in the absence of any commercial or financial relationships that could be construed as a potential conflict of interest.

Publisher's note

All claims expressed in this article are solely those of the authors and do not necessarily represent those of their affiliated organizations, or those of the publisher, the editors and the reviewers. Any product that may be evaluated in this article, or claim that may be made by its manufacturer, is not guaranteed or endorsed by the publisher.

References

Anand, S., Singh, D., Avadhanula, M., and Marka, S. (2014). Development and control of bacterial biofilms on dairy processing membranes. *Compr. Rev. Food Sci.* 13, 18–33. doi: 10.1111/1541-4337.12048

Austin, J. W., and Bergeron, G. (1995). Development of bacterial biofilms in dairy processing lines. *J. Dairy Res.* 62, 509–519. doi: 10.1017/s0022029900031204

Balaure, P. C., and Grumezescu, A. M. (2020). Recent advances in surface nanoengineering for biofilm prevention and control. Part I: molecular basis of biofilm recalcitrance. Passive anti-biofouling nanocoatings. *Nano* 10:1230. doi: 10.3390/nano10061230

Carrascosa, J. M., Cuevas, R., Gonzalez, R., Azcorra, A., and Garcia, D. (2015). Quantifying the economic and cultural biases of social media through trending topics. *PLoS One* 10:e0134407. doi: 10.1371/journal.pone.0134407

Cherif-Antar, A., Moussa-Boudjemaa, B., Didouh, N., Medjahdi, K., Mayo, B., and Florez, A. B. (2016). Diversity and biofilm-forming capability of bacteria recovered from stainless steel pipes of a milk-processing dairy plant. *Dairy Sci. Technol.* 96, 27–38. doi: 10.1007/s13594-015-0235-4

Chierici, M., Picozzi, C., La Spina, M. G., Orsi, C., Vigentini, I., Zambrini, V., et al. (2016). Strain diversity of *Pseudomonas fluorescens* group with potential blue pigment phenotype isolated from dairy products. *J. Food Prot.* 79, 1430–1435. doi: 10.4315/0362-028X.JFP-15-589

Davies, D. G., and Marques, C. N. (2011). A fatty acid messenger is responsible for inducing dispersion in microbial biofilms. *J. Bacteriol.* 191, 1393–1403. doi: 10.1128/JB.01214-08

de Jonghe, V., Coorevits, A., van Hoorde, K., Messens, W., van Landschoot, A., de Vos, P., et al. (2011). Influence of storage conditions on the growth of *Pseudomonas* species in refrigerated raw milk. *Appl. Environ. Microbiol.* 77, 460–470. doi: 10.1128/AEM.00521-10

Dourou, D., Beauchamp, C. S., Yoon, Y., Geornaras, I., Belk, K. E., Smith, G. C., et al. (2011). Attachment and biofilm formation by *Escherichia coli* O157:H7 at different temperatures, on various food-contact surfaces encountered in beef processing. *Int. J. Food Microbiol.* 149, 262–268. doi: 10.1016/j.ijfoodmicro.2011.07.004

Elias, S., and Banin, E. (2012). Multi-species biofilms: living with friendly neighbors. *FEMS Microbiol. Rev.* 36, 990–1004. doi: 10.1111/j.1574-6976.2012.00325

Fricker, M., Skånseng, B., Rudi, K., Stessl, B., and Ehling-Schulz, M. (2011). Shift from farm to dairy tank milk microbiota revealed by a polyphasic approach is independent from geographical origin. *Int. J. Food Microbiol.* 145, S24–S30. doi: 10.1016/j.ijfoodmicro.2010.08.025

Garrido-Sanz, D., Meier-Kolthoff, J. P., Göker, M., Martín, M., and Rivilla, R. (2016). Genomic and genetic diversity within the *Pseudomonas fluorescens* complex. *PLoS One* 11:e0153733. doi: 10.1371/journal.pone.0153733

Gomila, M., Peña, A., Mulet, M., Lalucat, J., and García-Valdés, E. (2015). Phylogenomics and systematics in pseudomonas. *Front. Microbiol.* 6:214. doi: 10.3389/fmicb.2015.00214

Heir, E., Møretrø, T., Simensen, A., and Langsrud, S. (2018). Listeria monocytogenes strains show large variations in competitive growth in mixed culture biofilms and suspensions with bacteria from food processing environments. *Int. J. Food Microbiol.* 275, 46–55. doi: 10.1016/j.ijfoodmicro.2018.03.026

Langsrud, S., Moen, B., Møretrø, T., Loype, M., and Heir, E. (2016). Microbial dynamics in mixed culture biofilms of bacteria surviving sanitation of conveyor belts in salmon processing plants. *J. Appl. Microbiol.* 120, 366–378. doi: 10.1111/jam.13013

Latorre, A. A., van Kessel, J. S., Karns, J. S., Zurakowski, M. J., and Pradhan, A. K. (2010). Biofilm in milking equipment on a dairy farm as a potential source of bulk tank milk contamination with listeria monocytogenes. *J. Dairy Sci.* 93, 2792–2802. doi: 10.3168/jds.2009-2717

Liu, W., Røder, H. L., Madsen, L. S., Bjarnsholt, T., Sørensen, S. J., and Burmølle, M. (2016). Interspecific bacterial interactions are reflected in multispecies biofilm spatial organization. *Front. Microbiol.* 7:1366. doi: 10.3389/fmicb.2016.01366

Longhi, R., Correia, S., Bruzaroski, S., Poli-Frederico, R., Fagnani, R., and Santana, E. (2022). *Pseudomonas fluorescens* and *Pseudomonas putida* from refrigerated raw milk: genetic diversity and lipoproteolytic activity. *J. Dairy Res.* 89, 86–89. doi: 10.1017/S0022029922000048

Makovcova, J., Babak, V., Kulich, P., Masek, J., Slany, M., and Cincarova, L. (2017). Dynamics of mono-and dual-species biofilm formation and interactions between Staphylococcus aureus and Gram-negative bacteria. *Microb. Biotechnol.* 10, 819–832. doi: 10.1111/1751-7915.12705

Mann, E. E., and Wozniak, D. J. (2012). Pseudomonas biofilm matrix composition and niche biology. *FEMS Microbiol. Rev.* 36, 893–916. doi: 10.1111/j.1574-6976.2011.00322.x

Marchand, S., De Block, J., De Jonghe, V., Coorevits, A., Heyndrickx, M., and Herman, L. (2012). Biofilm formation in milk production and processing environments; influence on milk quality and safety. *Compr. Rev. Food Sci. Food Saf.* 11, 133–147. doi: 10.1111/j.1541-4337.2011.00183.x

Martin, N. H., Murphy, S. C., Ralyea, R. D., Wiedmann, M., and Boor, K. J. (2011). When cheese gets the blues: *Pseudomonas fluorescens* as the causative agent of cheese spoilage. *J. Dairy Sci.* 94, 3176–3183. doi: 10.3168/jds.2011-4312

Meng, L., Zhang, Y., Liu, H., Zhao, S., Wang, J., and Zheng, N. (2017). Characterization of *Pseudomonas* spp. and associated proteolytic properties in raw milk stored at low temperatures. *Front. Microbiol.* 8, 1–7. doi: 10.3389/fmicb.2017.02158

Møretrø, T., and Langsrud, S. (2017). Residential bacteria on surfaces in the food industry and their implications for food safety and quality. *Compr. Rev. Food Sci. Food Saf.* 16, 1022–1041. doi: 10.1111/1541-4337.12283

Mulet, M., Lalucat, J., and García-Valdés, E. (2010). DNA sequence-based analysis of the *Pseudomonas* species. *Environ. Microbiol.* 12, 1513–1530. doi: 10.1111/j.1462-2920.2010.02181.x

Papaioannou, E., Giaouris, E. D., Berillis, P., and Boziaris, I. S. (2018). Dynamics of biofilm formation by *Listeria monocytogenes* on stainless steel under mono-species and mixed culture simulated fish processing conditions and chemical disinfection challenges. *Int. J. Food Microbiol.* 267, 9–19. doi: 10.1016/j.ijfoodmicro.2017.12.020

Puga, C. H., Orgaz, B., and San Jose, C. (2016). *Listeria monocytogenes* impact on mature or old *Pseudomonas fluorescens* biofilms during growth at 4 and 20°C. *Front. Microbiol.* 7:134. doi: 10.3389/fmicb.2016.00134

Reichler, S. J., Trmčić, A. H., Martin, N. H., Boor, K. J., and Wiedmann, M. (2018). *Pseudomonas fluorescens* group bacterial strains are responsible for repeat and sporadic post pasteurization contamination and reduced fluid milk shelf life. *J. Dairy Sci.* 101, 7780–7800. doi: 10.3168/jds.2018-14438

Rendueles, O., and Ghigo, J. M. (2012). Multi-species biofilms: how to avoid unfriendly neighbors. *FEMS Microbiol. Rev.* 36, 972–989. doi: 10.1111/j.1574-6976.2012.00328.x

Røder, H. L., Raghupathi, P. K., Herschend, J., Brejnrød, A., Knøchel, S., Sørensen, S. J., et al. (2015). Interspecies interactions result in enhanced biofilm formation by co-cultures of bacteria isolated from a food processing environment. *Food Microbiol.* 51, 18–24. doi: 10.1016/j.fm.2015.04.008

Sanchez-Vizuete, P., Orgaz, B., Aymerich, S., Le Coq, D., and Briandet, R. (2015). Pathogens protection against the action of disinfectants in multispecies biofilms. *Front. Microbiol.* 6:12. doi: 10.3389/fmicb.2015.00705

Schirmer, B. C. T., Heir, E., Møretrø, T., Skaar, I., and Langsrud, S. (2013). Microbial background flora in small-scale cheese production facilities does not inhibit growth and surface attachment of *Listeria monocytogenes*. *J. Dairy Sci.* 96, 6161–6171. doi: 10.3168/jds.2012-6395

Sharma, M., and Anand, S. K. (2002). Characterization of constitutive microflora of biofilms in dairy processing lines. *Food Microbiol.* 19, 627–636. doi: 10.1006/fmic.2002.0472

Shi, X., and Zhu, X. (2009). Biofilm formation and food safety in food industries. *Trends Food Sci. Technol.* 20, 407–413. doi: 10.1016/j.tifs.2009.01.054

Shpigel, N. Y., Pasternak, Z., Factor, G., and Gottlieb, Y. (2015). Diversity of bacterial biofilm communities on sprinklers from dairy farm cooling systems in Israel. *PLoS One* 10:e0139111. doi: 10.1371/journal.pone.0139111

Simoes, M., Simoes, L. C., and Vieira, M. J. (2008). Physiology and behavior of *Pseudomonas fluorescens* single and dual strain biofilms under diverse hydrodynamics stresses. *Intl. J. Food Microbiol.* 128, 309–316. doi: 10.1016/j.ijfoodmicro.2008.09.003

Stoeckel, M., Lidolt, M., Achberger, V., Glück, C., Krewinkel, M., Stressler, T., et al. (2016). Growth of *Pseudomonas weihenstephanensis*, *Pseudomonas proteolytica* and *Pseudomonas* spp. in raw milk: impact of residual heat-stable enzyme activity on stability of UHT milk during shelf-life. *Int. Dairy J.* 59, 20–28. doi: 10.1016/j.idairyj.2016.02.045

van Houdt, R., and Michiels, C. W. (2010). Biofilm formation and the food industry, a focus on the bacterial outer surface. *J. Appl. Microbiol.* 109, 1117–1131. doi: 10.1111/j.1365-2672.2010.04756.x

von Neubeck, M., Baur, C., Krewinkel, M., Stoeckel, M., Kranz, B., Stressler, T., et al. (2015). Biodiversity of refrigerated raw milk microbiota and their enzymatic spoilage potential. *Int. J. Food Microbiol.* 211, 57–65. doi: 10.1016/j.ijfoodmicro.2015.07.001

Wang, L., and Jayarao, B. M. (2001). Phenotypic and genotypic characterization of *Pseudomonas fluorescens* isolated from bulk tank milk. *J. Dairy Sci.* 84, 1421–1429. doi: 10.3168/jds.S0022-0302(01)70174-9

Yang, L., Liu, Y., Wu, H., Høiby, N., Molin, S., and Song, Z. (2011). Current understanding of multi-species biofilms. *Int. J. Oral Sci.* 3, 74–81. doi: 10.4248/IJOS11027

Yannarell, S. M., Grandchamp, G. M., Chen, S., Daniels, K. E., Shank, E. A., and Elizabeth, A. (2019). A dual-species biofilm with emergent mechanical and protective properties. *J. Bacteriol. Res.* 201:e00670-18. doi: 10.1128/JB.00670-18

Zarei, M., Yousefvand, A., Maktabi, S., Pourmahdi Borujeni, M., and Mohammadpour, H. (2020). Identification, phylogenetic characterisation and proteolytic activity quantification of high biofilm-forming *Pseudomonas fluorescens* group bacterial strains isolated from cold raw milk. *Int. Dairy J.* 109:104787. doi: 10.1016/j.idairyj.2020.104787

frontiers | Frontiers in Microbiology

TYPE Original Research
PUBLISHED 10 November 2022
DOI 10.3389/fmicb.2022.1060506

OPEN ACCESS

EDITED BY
Ramona Iseppi,
University of Modena and Reggio Emilia, Italy

REVIEWED BY
Tom Defoirdt,
Ghent University, Belgium
Steve Flint,
Massey University, New Zealand

*CORRESPONDENCE
Li Wang
wangli_scau@scau.edu.cn

SPECIALTY SECTION
This article was submitted to Food Microbiology, a section of the journal Frontiers in Microbiology

RECEIVED 03 October 2022
ACCEPTED 26 October 2022
PUBLISHED 10 November 2022

CITATION
Liu Y and Wang L (2022) Antibiofilm effect and mechanism of protocatechuic aldehyde against *Vibrio parahaemolyticus*. *Front. Microbiol.* 13:1060506. doi: 10.3389/fmicb.2022.1060506

Antibiofilm effect and mechanism of protocatechuic aldehyde against *Vibrio parahaemolyticus*

Yawen Liu and Li Wang*

Guangdong Provincial Key Laboratory of Food Quality and Safety, College of Food Science, South China Agricultural University, Guangzhou, China

This study investigated the effect of protocatechuic aldehyde (PCA) on *Vibrio parahaemolyticus* biofilm formation and its effects on gene expression. Crystal violet assay, metabolic activity assay, and fluorescence experiments were used to evaluate the antibiofilm activities of PCA and to reveal its possible antibiofilm mechanisms using transcriptomic analysis. The results indicated that the minimum antibacterial concentration of PCA against *V. parahaemolyticus* was 300 μg/mL. PCA (9.375 μg/mL) inhibited biofilm generation and adhesion of the mature biofilm. PCA (75 μg/mL) significantly reduced the metabolic viability of *V. parahaemolyticus*, reduced polysaccharide production, and inhibited cell surface flagella-mediated swimming and aggregation phenotypes. Meanwhile, transcriptome analysis showed that the key genes of *V. parahaemolyticus* expressed under PCA (75 μg/mL) inhibition were mainly related to biofilm formation (*pfkA*, *galE*, *narL*, and *oppA*), polysaccharide production and adhesion (*IF*, *fbpA*, and *yxeM*), and motility (*cheY*, *flrC*, and *fliA*). By regulating these key genes, PCA reduced biofilm formation, suppressed polysaccharide production and transport, and prevented the adhesion of *V. parahaemolyticus*, thereby reducing the virulence of *V. parahaemolyticus*. This study demonstrated that protocatechuic aldehyde can be used to control *V. parahaemolyticus* biofilm to ensure food safety.

KEYWORDS

***Vibrio parahaemolyticus*, antibiofilm, protocatechuic aldehyde, comparative transcriptome analysis, bacteriostatic activity**

Introduction

Vibrio, found in the global marine environment, includes *V. alginolyticus*, *V. vulnificus*, and *V. parahaemolyticus* (Mok et al., 2019). Among them, *V. parahaemolyticus* has become an important pathogen of sporadic, epidemic diarrhea and food poisoning in many areas, and is increasing yearly. Some pathogenic

strains of *V. parahaemolyticus* causes bacterial diseases in fish, shrimp, and shellfish, resulting in a serious economic loss (Bauer et al., 2021).

The pathogenicity of *V. parahaemolyticus* is closely related to a variety of virulence factors, including the iron absorption system, lipopolysaccharides, proteases, outer membrane proteins, the adhesion factor type III secretion system, and the type VI secretion system (He et al., 2020; Puangpee and Suanyuk, 2021). Biofilms are an important survival and pathogenic mechanism of *V. parahaemolyticus*, which are difficult to remove (Hall-Stoodley et al., 2004). Biofilms are mainly composed of proteins and polysaccharides that resist adverse environmental factors (such as UV, pH, heavy metals, and phagocytosis) and reduce sensitivity to conventional antimicrobial agents (Wang et al., 2022).

The widespread use of prophylactic antibiotics (e.g., in aquaculture) leads to increased rates of pathogen resistance, rendering many antibiotics ineffective. Cells within mature biofilms may be more resistant to antimicrobials than cells in planktonic states (Bhardwaj et al., 2021).

Therefore, new approaches are needed to treat *Vibrio* diseases or to reduce antibiotic resistance in pathogenic bacteria (Ashrafudoulla et al., 2021). Many natural compounds, including herbs, synthetic and organic plant derivatives, biosynthetic nanocomposites such as citral (Faleye et al., 2021), essential oils (Smaoui et al., 2022), blueberry extract (Sun et al., 2020), eugenol (Ashrafudoulla et al., 2020), and cationic peptide chimeras (Ning et al., 2021), have shown significant effects on biofilms. Among them, the phenols have strong antibacterial activity and have been widely verified.

PCA is a non-toxic drug excipient, preservative, and food additive that can be isolated from the water extract of *Salvia miltiorrhiza* and some as fermentation products of bacteria (Chen et al., 2021). PCA has been identified with multiple roles, including antioxidant (Guo et al., 2017), anti-inflammatory (Jieke et al., 2021), antitumor (Kyoung-Ja et al., 2008), and antimicrobial properties. Studies have found that PCA has significant effects on *Yersinia enterocolitica* (Tian et al., 2021) and *Ralstonia solanacearum* (Shili et al., 2016).

However, the antibiofilm and antivirulence activity of PCA on *V. parahaemolyticus* have not been evaluated. In this study, we explored the ability of PCA to inhibit biofilm formation and clear mature biofilms by crystal violet experiment. The inhibitory effect of PCA on the invasion and pathogenicity of *V. parahaemolyticus* was also explored by measuring bacterial motility and observing the changes in biofilm extracellular polysaccharide and bacterial numbers using Zeiss fluorescence confocal microscopy. Finally, the effect of PCA on *V. parahaemolyticus* biofilm and its possible mechanism were explored by transcriptome analysis. These results revealed for the first time the ability of PCA to inhibit the biofilm formation of *V. parahaemolyticus*, expanding the antibacterial application of PCA as a natural antioxidant food additive.

Materials and methods

Bacterial strains and growth conditions

Vibrio parahaemolyticus ATCC17802 (Guangdong Institute of Microbiology) was used as a test bacterial pathogen in this study. The cells were cultured in Tryptic Soy Broth (TSB) (3% NaCl) (Guangdong HuanKai Microbial, China) for 8 h at 37°C and then resuspended through centrifugation (2,506 × g for 10 min) in 10^8 CFU/mL. Protocatechuic aldehyde (3,4-dihydroxybenzaldehyde, 98%) was purchased from Macklin (Shanghai, China) and the stock solutions were prepared using TSB or sterile water.

Vibrio parahaemolyticus growth curves with protocatechuic aldehyde treatment

The minimum inhibitory concentrations and minimum bactericidal concentrations at different PCA concentrations were calculated using twofold dilutions. The PCA concentrations ranged from 7.8 to 1,000 μg/mL (Shili et al., 2016). The bacterial suspension was prepared using a nutrient broth containing 3% NaCl to give 10^6 CFU/mL as a final concentration. The optical density was measured at 600 nm every 1 h for 24 h at 37°C using an automatic growth curve analyzer (Oy Growthcurves Ab Ltd.). The positive control was TSB (3% NaCl) with the bacterial suspension and without PCA. The negative control was an uninoculated TSB (3% NaCl).

Biofilm formation inhibition assay and clearance of mature biofilms

Crystal violet staining was used to evaluate biofilm formation (Wang et al., 2022). Briefly, 100 μL of bacterial suspension (10^6 CFU/mL) was seeded into 96-well plates with different concentrations of PCA (0, 9.375, 18.25, and 37.5 μg/mL) to form a biofilm. Inoculated or PCA-treated TSB (3% NaCl) was used as background. In addition, PCA (0, 9.375, 18.25, and 37.5 μg/mL) was added for 24 and 48 h. The scavenging effect of PCA on mature biofilms was detected as described by Qiao et al. (2021). The plate was incubated at 37°C for 24 h. Then, the plate was washed twice with sterile saline, dried for 30 min (25°C), stained with 200 μL of crystal violet (0.1% w/v), and incubated at 25°C for 20 min. Then, we washed the plate once with sterile saline. Subsequently, we added 200 μL of 33% (v/v) glacial acetic acid and measured the absorbance at 570 nm.

Biofilm metabolic activity

Vibrio parahaemolyticus biofilm metabolic activity was determined using MTT (Wang et al., 2010). After forming biofilms in 96-well plates for 72 h, a PBS wash was used to remove the loosely attached cells and planktonic cells (Liu et al., 2022). To each well, thiazole blue (MTT) [3,4,5-dimethyl-2-thiazolyl]-2,5-diphenyl-2-H-tetrazolium bromide solution (5 mg/mL, prepared in sterile water) was added. The mixture was incubated at 37°C in the dark for 3 h. We then added 200 μL of dimethyl sulfoxide, incubated at 37°C for 30 min, and then measured the absorbance at 490 nm.

Extraction and quantification of exopolysaccharides

The extracellular polysaccharides in biofilms were determined using the phenol-sulfuric acid method (Cao et al., 2021). *V. parahaemolyticus* was treated with PCA at 37°C for 24 h. The cells were centrifuged (2,500 × g for 15 min), and the supernatant was separately mixed with a threefold volume of 95% (v/v) ethanol and precipitated at 4°C for 24 h. The mixture was then centrifuged to collect the precipitates (2,500 × g for 15 min). Then, 5% phenol and 90% H_2SO_4 were added to the precipitate, mixed, and placed in the dark for 1 h at 25°C. The final mixture was centrifuged at 9600 × g for 10 min, and the absorbance of the supernatant at 490 nm was measured.

Microscopy assay

The survival of *V. parahaemolyticus* under PCA inhibition was determined using a live/dead staining kit (Yu et al., 2022). Briefly, the PCA (0 and 75 μg/mL)-treated bacterial suspension was centrifuged (6,000 × g for 5 min), then 10 μL of NucGreen and EthD-III mix was added, and left in the dark for 15 min. Then the suspension was analyzed using a Zeiss fluorescence confocal microscopy (30×). Additionally, the bacterial suspension (200 μL, 10^6 CFU/mL) and PCA solution (200 μL) were added to the 8-well chamber slides (Bhardwaj et al., 2021). The final concentrations of PCA were 75 and 300 μg/mL. The mixture was incubated at 37°C for 48 h. Then slides were washed with PBS; FITC conA (20 μg/mL) was added and stained at 25°C in the dark (30 min). Finally, the slides were washed with PBS and visualized using a Zeiss fluorescence confocal microscope (10×). The image acquisition was performed using the ZEN software. The micrographs were analyzed using the ImageJ software to evaluate the biomass and the surface volume ratio of the biofilms (Lu et al., 2021).

Motility assay

For the swimming exercise test (Faleye et al., 2021), PCA was added to warm (45°C) TSB medium (15 mL) containing 0.3% (w/v) agar to obtain final concentrations of 0, 7.81, 15.625, 31.25, 150, and 300 μg/mL. A swarming exercise was performed using 15 mL of TSB medium containing 0.5% (w/v) agar. The plate was then dried for 1 h; then 5 μL of bacterial suspension (1×10^6 CFU/mL) was added to its center and incubated at 37°C for 12 h. The diameter of the bacterial movement zone was measured using a vernier caliper (mm), and pictures were taken with Gel DOCTM XR +. A medium without PCA was used as a control.

Transcriptome sequencing

Vibrio parahaemolyticus was treated with 75 μg/mL of PCA (B sample) or without PCA (A sample) as a control. Two samples of PCA were added to the logarithmic growth phase bacteria and shaken at 37°C and 150 rpm for 8 h. We extracted RNA using an RNA extraction kit (TIANGEN BIOTECH CO., Ltd.). Gene library sequencing was performed using the Illumina Hiseq platform, and quality screening was performed using FastQC (Zhang Q. et al., 2020). Reference genome alignments were performed at https://www.ncbi.nlm.nih.gov/nucleotide/CP014046.2 using Bowtie2. Differential expression analysis between the two groups of samples was performed with the DESeq2 R software package (1.16.1) [Sangon Biotech (Shanghai) Co., Ltd.] with a corrected *P*-value of 0.05 and an absolute fold change ≥ 2. Gene Ontology (GO) and Kyoto Encyclopedia of Genes and Genomes (KEGG) enrichment analyses were further profiled using the cluster Profiler package.

Determination of gene expression using RT-qPCR

mRNA was extracted and transcribed into cDNA using an RNA extraction kit (Vazyme, Nanjing, China) and a reverse transcription kit (HiScript II Q RT Super Mix) (Vazyme) according to the kit instructions. Primer sequences (5′–3′) were designed with Primer software (**Table 1**). In a RT-qPCR reaction, the total volume was 20μL, which contained 0.6 μL of 10 μM of each primer F/R, 10 μL of SYBR Mix (Vazyme Biotech, Nanjing, China), 1 μL of cDNA template, and 7.8 μL of nuclease-free water. The temperature was first maintained at 95°C for 1 min in the qPCR reaction. Then, 40 cycles of temperature change at 95°C for 10 s, annealing at 55°C for 34 s, and extension at 72°C for 15 s were performed. Changes in the expression levels of target mRNAs were calculated using the $2^{-\Delta\Delta CT}$ method (Zhang J. et al., 2020).

TABLE 1 The primers for the detection of *Vibrio parahaemolyticus*.

Gene name	Sequence (5′–3′) F	Sequence (5′–3′) R
Control	TATCCTTGTTTGCCAGCGAG	CTACGACGCACTTTTTGGGA
ectC	CATTCTGGACAAGCACGAC	TAGTCAACGAGCGGGTAAA
narL	AACTCAGACGCTCTTTACG	TCTTACTGCTATTGCCTTG
yxeM	TGTTTGCAGACCCTTATGT	CTTTGTCGTATTGGCGTAG
fbpA	AACCTTGCTCGTAAACCTC	TACCCAAAGAAACATCACAT
rpsR	TCTTCCGTCGTCGTAAATT	GTACCAGTGATACGGCTAG

Statistical analysis

The mean and standard deviation (SD) were calculated for triplicates. Differences between variables were tested for significance using SPSS. Standard curves and other figures were completed using Origin 2021, Graph 7, and ImageJ.

Results

Impact of protocatechuic aldehyde treatment on the viability of *Vibrio parahaemolyticus*

The ability of PCA to inhibit the growth of *V. parahaemolyticus* was determined. With an increase in PCA concentration, the inhibitory ability of PCA against *V. parahaemolyticus* gradually increased, and the growth of *V. parahaemolyticus* almost completely stopped at 1,000 μg/mL (**Figure 1**). Using SPSS software for analysis, compared with the control group, PCA concentration (300 μg/mL) had a remarkable inhibitory effect on *V. parahaemolyticus*. These results indicate that PCA dose-dependently inhibited the growth of *V. parahaemolyticus*.

Biofilm generation

Vibrio parahaemolyticus is a typical bacterium that forms biofilms (Bhardwaj et al., 2021). The two main methods of processing biofilms are to prevent their formation or eliminate already formed biofilms (Faleye et al., 2021). Therefore, the ability of PCA to disrupt prefabricated biofilms and its ability to clear mature biofilms was investigated. At different PCA concentrations (9.375, 18.75, and 37.5 μg/mL), the biofilm formation rate decreased by 73, 80, and 83%, respectively, after 24 h and by 69.3, 73.3, and 87.4%, respectively after 48 h (**Figure 2A**). Under the action of PCA (37.5 μg/mL), the clearance rates of mature biofilms at 24 and 48 h reached 76.8 and 68% (**Figure 2B**), respectively. We speculate that PCA not only inhibits the formation of biofilms but also considerably inhibits the adhesion of bacterial.

Determination of the metabolic activity

We determined the metabolic capacity of the biofilm by measuring the metabolic activity of the cells in the biofilm (Liu et al., 2022). The intensity of the MTT releases positively correlated with cellular metabolic activity. After treatment with PCA, the cell metabolic activity increased by 23.8 and 63.5% at low PCA concentrations (9.37 and 18.75 μg/mL) (**Figure 3**). As shown in **Figure 1**, the number of bacteria did not increase at the

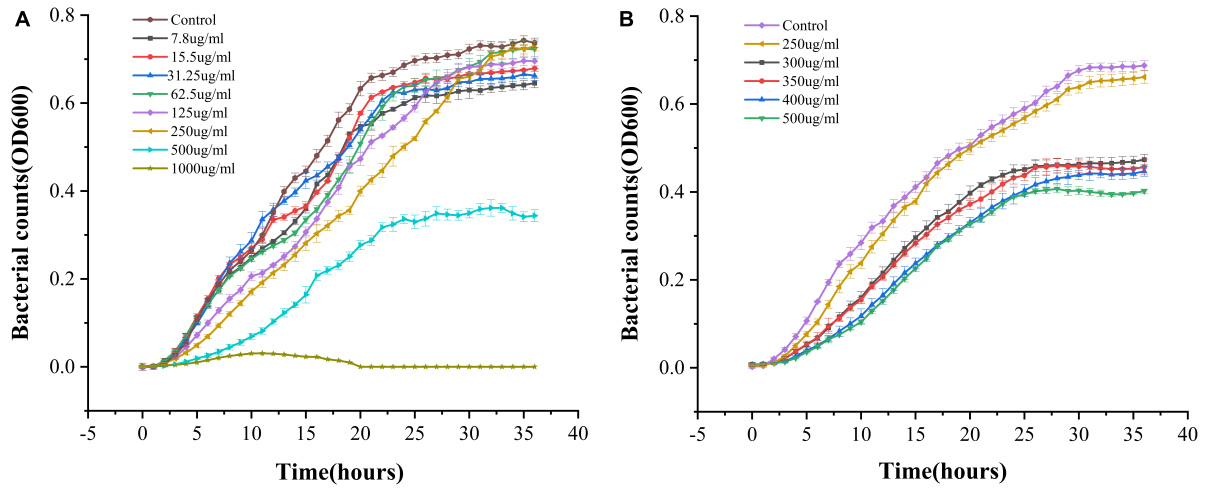

FIGURE 1
OD growth curves of *Vibrio parahaemolyticus* in the presence of different PCA concentrations at 37°C. **(A)** PCA concentrations of 7.8–1,000 μg/mL. **(B)** PCA concentration of 250–400 μg/mL.

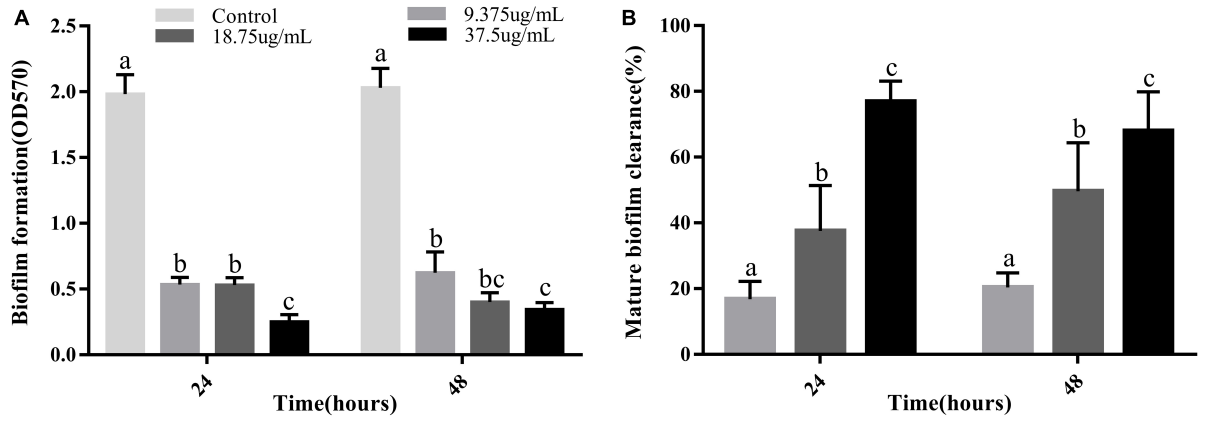

FIGURE 2
(A) Inhibitory effects of PCA at different concentrations on biofilm formation by *Vibrio parahaemolyticus* ATCC 17802. **(B)** Clearance of mature biofilms by different concentrations of PCA. The data are shown as means ± the Crystal violet of three independent experiments. Within each treatment, values marked with the same letter are not significantly different based on Duncan's multiple-range test ($p > 0.05$).

concentration of 15.5 μg/mL compared with the control group. With an increase in PCA (75 μg/mL), the inhibitory effect on the metabolic activity of the biofilm of pathogenic bacteria increased continuously, and the metabolic activity decreased sharply by 88.59%. Then, the metabolic state of the bacteria remained stable.

Extracellular polysaccharide assay

EPSs are the major part of the biofilm and directly contribute to the properties of the biofilm, especially with their strong water-binding capacity. They usually account for more than 90% of the biofilm mass (Liu et al., 2022). We used the sulfate and phenol methods to measure the polysaccharide content for evaluating the effect of PCA on EPS production. As shown, the polysaccharide content in the *V. parahaemolyticus* biofilms decreased significantly in the presence of PCA. When PCA concentration increased from 37.5 to 75 μg/mL, the polysaccharide content decreased by 27.6, 44.3, and 48% (**Figure 4**). The amount of biofilm formed, the biofilm metabolic activity, and the amount of polysaccharide produced decreased significantly at 75 μg/mL.

Mobility determination

During the initial phase of biofilm formation, movement of *V. parahaemolyticus* is critical for the attachment to host surfaces (Faleye et al., 2021). Loss of movement may affect bacterial adhesion, impairing biofilm formation (Zhu et al., 2020). As shown, PCA remarkably inhibited the swimming and swarming ability of *V. parahaemolyticus* at 75 μg/mL concentration (**Figures 5C,D**). Compared with the untreated cells, the swimming Bacterial colonies area (75 and 150 μg/mL) decreased by 81.4% (**Figure 5B**) and 93.1%, respectively. Meanwhile, the swarming Bacterial colonies area decreased by 56.9 and 73.7% (**Figure 5A**), respectively.

Microscopy inspection

As shown in the control group, the bacteria were wrapped in large amounts of polysaccharides, forming a large biofilm structure with a thick membrane structure (**Figures 6A,D**). The number of dead bacteria increased after 48 h of treating

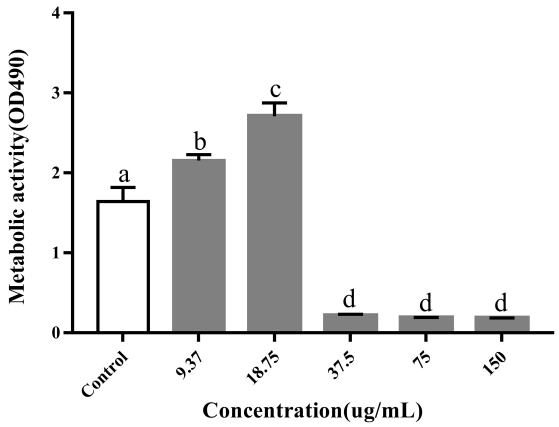

FIGURE 3
Inhibitory effects of PCA on the metabolic activity of *Vibrio parahaemolyticus* cells within biofilms. The data are shown as means ± the determination of MTT three independent experiments. Within each treatment, values marked with the same letter are not significantly different based on Duncan's multiple-range test ($p > 0.05$).

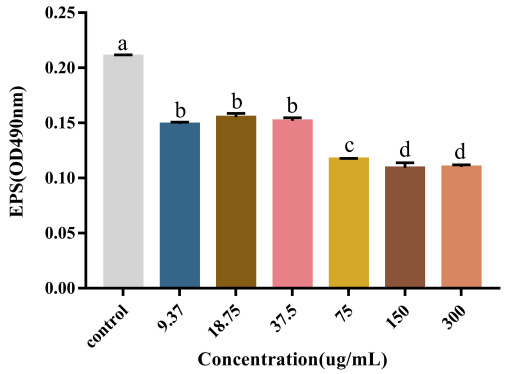

FIGURE 4
The effect of PCA on polysaccharide content in biofilm formed by *Vibrio parahaemolyticus*. The data are shown as means ± the polysaccharide three independent experiments. Within each treatment, values marked with the same letter are not significantly different based on Duncan's multiple-range test ($p > 0.05$).

the mature biofilms with a high concentration (300 μg/mL) of PCA. In addition, biofilm formation decreased by 83.5%, and the biofilms were dispersed with a substantial reduction in thickness. The fluorescence intensity in the three-dimensional optical microscopy images changed remarkably (**Figures 6C,F**; Lu et al., 2021).

The number of viable bacteria was remarkably lower than that of the dead bacteria accounting for 63.7% of the total bacteria (**Figure 6C**). Visual results obtained with a microscope indicate that PCA reduced the biofilm of *V. parahaemolyticus* accounting for 4% (**Figure 6A**; Shangguan et al., 2021). The polysaccharide matrix was considerably reduced in the biofilms formed at 75 μg/mL PCA concentration. The overall membrane structure was dispersed. The biofilm area decreased by 71%, and showed low thickness variation (**Figures 6B,E**). The number of viable bacteria decreased by 88% under PCA (75 μg/mL) inhibition (**Figure 6B**).

Transcriptome results and analysis

Global transcriptional analysis revealed a differential expression of 142 genes, approximately 8 h after exposure to 75 μg/mL PCA, with 63 genes upregulated and 79 genes downregulated. This mainly manifested in cell motility (**Figure 7A**), cell growth and death, signaling, and energy

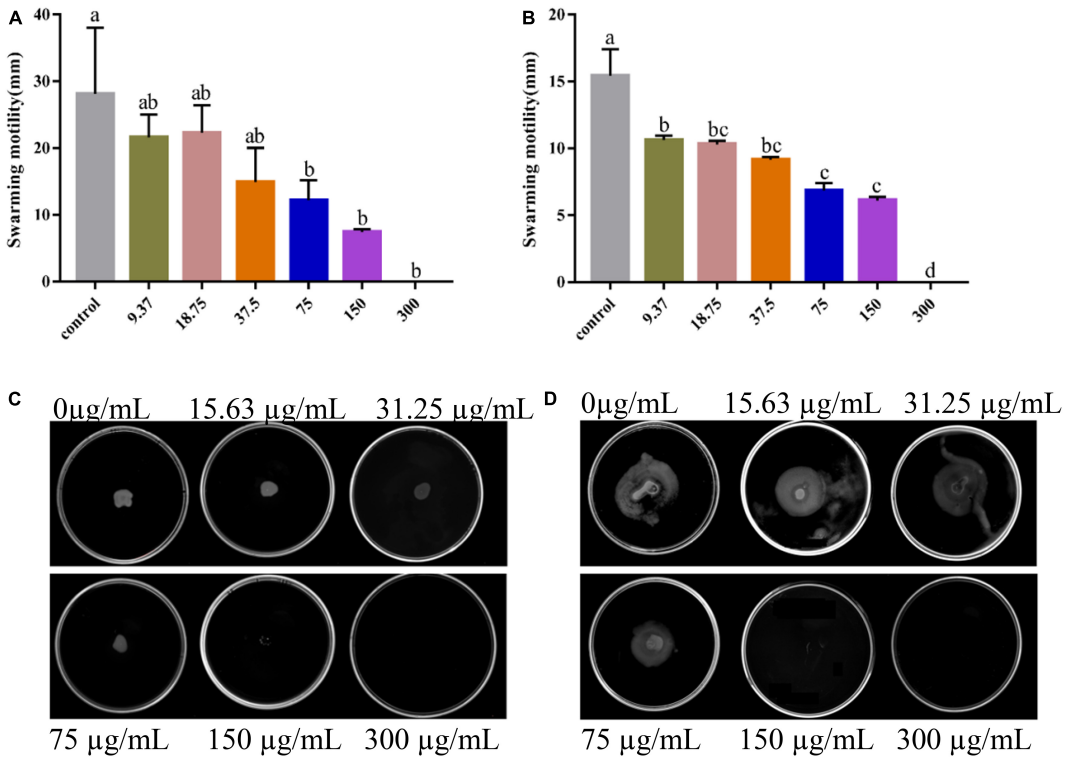

FIGURE 5
Images of swarming motility **(A)** and swimming motility **(B)** of *Vibrio parahaemolyticus* treated with PCA at different concentrations. The swarming **(C)** and swimming **(D)** areas of *Vibrio parahaemolyticus* ATCC 17802 were measured. The data are shown as means ± the motility three independent experiments. Within each treatment, values marked with the same letter are not significantly different based on Duncan's multiple-range test ($p > 0.05$).

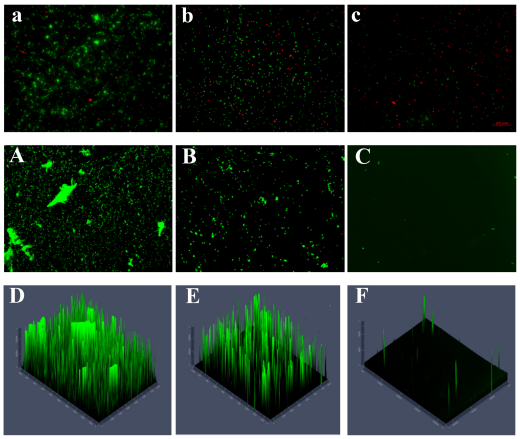

FIGURE 6
(A) The number of untreated dead and viable bacteria (40×). **(B,C)** The number of dead and viable bacteria treated with different PCA concentrations (75 and 150 μg/mL), green represents viable bacteria and red for dead bacteria. **(A)** The content and morphology of polysaccharides in the untreated biofilm, and the green distribution **(B,C)** indicate the polysaccharide content and morphology production in the biofilm treated under different PCA concentrations (75 and 150 μg/mL) (10×). **(D–F)** Fluorescence intensity of EPS in control and treated (75 and 150 μg/mL) biofilms.

metabolism. Combined with the metabolic pathways provided by the KEGG database (**Figure 7B**). We found that the pathways significantly enriched in *V. parahaemolyticus* mainly included Carbohydrate metabolism, Amino acid metabolism, ABC transport process, Ribosome, Two-component system (i.e., not complete). Up-regulated or down-regulated genes are shown in **Table 2**.

We analyzed the data by combining the metabolic pathways and GO annotations provided by the KEGG database. We found up-regulation of Nitrate/nitrite response regulator (*narL*) (**Figure 7C**) and down-regulation of ATP-dependent 6-phosphofructokinase (*pfkA*). Regulation of these two genes inhibited the expression of *frdA* and *frdB*, thereby regulating the two-component system and pentose phosphate pathway. Previous studies have found that inhibition of the bacterial two-component system (Cho and Sung-il, 2021) and pentose phosphate pathway (Kong et al., 2022) may promote carbohydrate intake and dephosphorylation of the phosphotransferase system. Kong et al. (2022) found that the inhibition of the pentose phosphate pathway may reduce the intracellular accumulation of carbohydrates such as glucose, thereby inhibiting bacterial exopolysaccharide synthesis and biofilm formation; Meanwhile, it may also reduce the efficiency of glucose transport, thereby destroying the energy metabolism of bacteria and inhibiting its cell viability.

After PCA was applied to *V. parahaemolyticus*, glycolysis and TCA cycle were also involved in the internal regulation of the bacteria. The up-regulation of isopropyl malate synthase (*IMS*) and alanine dehydrogenase (*ald*) affect acetyl-CoA formation, thereby regulating glycolysis and TCA cycle. In addition, the up-regulation of transcription factor glucose-6-phosphate 1 dehydrogenase (*G6PD*) promotes the conversion of NADP to NADPH. Tan et al. (2022) found that after antibiotic inhibition, internal carbon and nitrogen metabolism in *V. parahaemolyticus* is involved in the activation of bacterial glycolysis and TCA cycle to promote ATP accumulation, and the increase of NADPH maintains a stable cellular state and also promotes amino acid metabolism to enhance antibiotic tolerance. At the same time, we found that enoyl-CoA hydratase (*paaF*) and 3-hydroxyalkyl-CoA dehydrogenase (*fadB*) were up-regulated in *V. parahaemolyticus*, which may lead to enhanced tryptophan or β-alanine metabolism. Dukes et al. (2015) found that by promoting tryptophan or β-alanine metabolism, producing pyruvate and acetyl-CoA to activate mTOR, it would promote glycolysis and TCA cycle. However, this promotion of glycolysis and the TCA cycle by pyruvate and acetyl-CoA reaches a threshold (Yang et al., 2020).

The metabolism of amino acids in *V. parahaemolyticus* also changes after PCA inhibition. The down-regulation of L-ectoine synthase (*ectC*), aspartate kinase (*lysC*), cysteine synthetase (*cysK*), and asparagine synthetase (*asnB*) related genes involved in amino acid synthesis (**Figure 7C**) may result in the decreased amino acid synthesis of aspartic acid, glutamic acid, threonine, and cysteine. Down-regulation of small subunit ribosomal protein S18 (*rpsR*) also directly affects amino acid substitutions. In ribosomes, the small subunit ribosomal protein S15 (*IF*) responsible for adhesion and invasion is downregulated. At the same time, the iron (III) transport system substrate-binding protein (*fbpA*) and putative amino acid ABC transporter substrate-binding protein (*yxeM*) were also significantly down-regulated. In biofilm proteomics of *V. parahaemolyticus*, Guo et al. (2020) found that increased glutamate and threonine promoted the synthesis of extracellular proteins in biofilms and down-regulation of *cysK* gene may regulate the secretion of toxins by bacteria to inhibit the growth of neighboring cells. Zhu et al. (2020) found in their proteomic studies on *V. parahaemolyticus* that the ABC transport system is closely related to bacterial adhesion ability. Thereby down-regulation of genes related to the ABC transport system may hinder material transport and reduce bacterial adhesion and biofilm formation.

In addition, under the inhibition of PCA, the chemotaxis receptor response regulator (*cheY*) in the internal genes of *V. parahaemolyticus* was down-regulated, and *cheY* could directly inhibit Flageller motor switch adaptation. A gene associated with bacterial quorum sensing, oligopeptide transport system substrate-binding protein (*oppA*), was down-regulated. Upregulation of 5'-deoxynucleotides (*yfbR*) associated with eDNA synthesis in biofilms is upregulated. This can lead to reduced motility, adhesion, and biofilm production (Kong et al., 2020). Chang et al. (2020) found

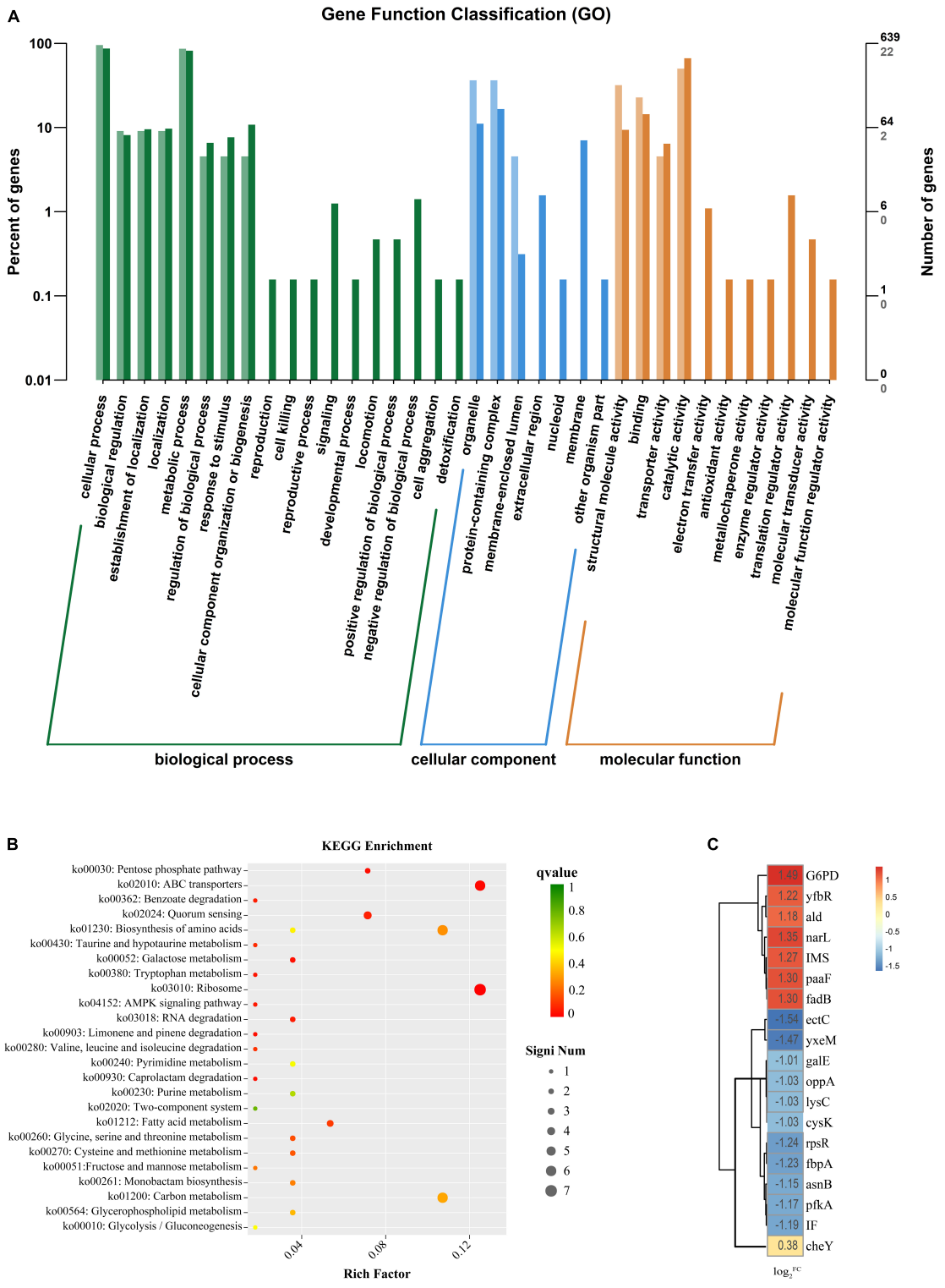

FIGURE 7

(A) The horizontal axis is the functional classification, and the vertical axis is the number of genes in the classification (right) and its percentage of the total number of annotated genes (left). Different colors represent different classifications. Light colors represent differential genes, and dark colors represent all genes. **(B)** The vertical axis in the figure represents the functional annotation information. The color of dots indicates the size of the *q* value, the smaller the *q* value the closer to red. The size of the dots indicates the number of differential genes included under each term, with larger points and more genes. **(C)** Heat map diagram of the log2^{FC} value of the *Vibrio parahaemolyticus* for gene. The darker the color, the larger the log2^{FC} value.

TABLE 2 Top 14% genes with significant expression from RNA sequencing.

Gene ID	Gene	Log_2 fold change	*P*-values (10^{-3})	Significant
AL464_14590	*yfbR*	1.22	0.456466	Up
AL464_09910	*narL*	1.35	10.248579	Up
AL464_03690	*paaF*	1.3	1.48×10^{-7}	Up
AL464_03690	*fadB*	1.3	1.48×10^{-7}	Up
AL464_11100	*G6PD*	1.49	1.78×10^{-3}	Up
AL464_02095	*IMS*	1.27	4.86×10^{-2}	Up
AL464_12510	*cheY*	0.375	9.9	Up
AL464_13825	*ald*	1.18	3.05×10^{-3}	Up
AL464_05650	*pfkA*	−1.17	1.80×10^{-10}	Down
AL464_07590	*galE*	−1.006	5.35×10^{-2}	Down
AL464_07335	*IF*	−1.19	2.270273	Down
AL464_06250	*rpsR*	−1.24	5.72×10^{-4}	Down
AL464_11050	*ectC*	−1.54	5.61×10^{-10}	Down
AL464_11055	*lysC*	−1.03	1.40×10^{-15}	Down
AL464_15200	*cysK*	−1.03	1.13×10^{-3}	Down
AL464_15075	*asnB*	−1.15	1.21×10^{-2}	Down
AL464_07135	*fbpA*	−1.23	0.257048	Down
AL464_03780	*yxeM*	−1.47	6.81×10^{-3}	Down
AL464_09010	*oppA*	−1.03	8.21×10^{-8}	Down

that *cheY* could modulate Flageller motor in bacteria, thereby affecting bacterial motility. Sun et al. (2022) hypothesized that quorum sensing may be involved in regulating pilus production to control biofilm generation. Renfei et al. (2019) and Wu et al. (2022) found that quorum-sensing regulators affect gene transcription in the lateral flagella of *V. parahaemolyticus* to regulate swarming movement. In general, PCA inhibits the biofilm of *V. parahaemolyticus* by regulating a variety of genes.

Validation of RNA-seq data by RT-qPCR

We screened biofilm-related genes by high-throughput sequencing and verified the reliability of the data by RT-qPCR. Four significantly decreased genes and one significantly increased gene were screened. The gene *narL* related to bacterial metabolism was up-regulated. The relative expression of this gene with values of 217% of the control group (**Figure 3**). The ABC transport system genes *fbpA* and *yxeM* related to biofilm clearance and production were down-regulated. *rpsR* gene related to amino acid synthesis was down-regulated. The bacterial growth-related gene *ectC* was down-regulated. The relative expression of these genes was significantly reduced with values of 1.4%, 13.5, 3.7, and 7.5% of the control group, respectively. These results demonstrated that 75 μg/mL PCA could effectively inhibit the biofilm formation of *V. parahaemolyticus*.

Discussion

It is important to control *V. parahaemolyticus* in the global outbreak of diseases and contaminated food. In recent years, the antibacterial ability of many natural antibacterial substances has been investigated. Cinnamaldehyde and some of its derivatives have been found to inhibit biofilm formation and motility, and quorum sensing-related virulence gene expression in *V. parahaemolyticus* (Faleye et al., 2021). Citral can effectively inhibit the adhesion ability and flagellar biosynthesis of *V. parahaemolyticus* (Yi et al., 2019). Tea polyphenols have been found to reduce the immune capacity of *V. parahaemolyticus* and improve the vibrio resistance of shrimp (Qin et al., 2021). As a kind of polyphenol, the application of PCA effectively reduced the incidence of bacterial wilt, and the control effect was up to 92.01% after 9 days of inoculation (Shili et al., 2016). Tian et al. (2021) showed that PCA could cause morphological changes in *Yersinia enterocolitica*, destroy intracellular ATP and pH, and significantly inhibit the growth of the bacteria. However, the inhibitory effect of PCA on *V. parahaemolyticus* has not been studied. We investigated the inhibitory effect of PCA on *V. parahaemolyticus* biofilm and its mechanism.

The results showed that the polysaccharide content was significantly reduced by 48%, the biofilm clearance rate reached 78% (**Figure 4**), and the biofilm thickness became increasingly thinner (**Figures 6D–F**), and moved from a large structure to a dispersed structure (**Figures 6A–C**). Probably

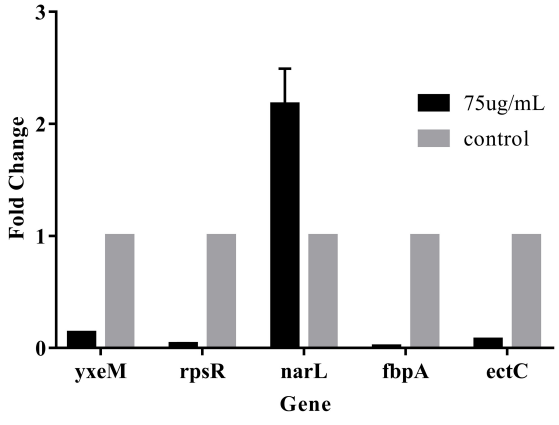

FIGURE 8
The gene expression levels were determined by RT-qPCR. The $2^{-\Delta\Delta CT}$ method was applied to determine the expression levels using 16S as the control gene. The data are shown as means ± the RT-qPCR three independent experiments. Within each treatment, values marked with the same letter are not significantly different based on Duncan's multiple-range test ($p > 0.05$).

through inhibition of carbohydrate uptake and phosphorylation (*pfkA*, *galE*, and *narL*) (Kong et al., 2020), PCA reduces exopolysaccharide secretion in *V. parahaemolyticus*, affecting bacterial surface adhesion and virulence (Hwang et al., 2012). At the same time, PCA inhibits biofilm adhesion and reduces biofilm formation by inhibiting *IF* expression and polysaccharide production or transport. In addition, PCA may also reduce the accumulation of cysteine and aspartate by regulating the expression of *ectC*, *lysC*, *cysK*, and *asnB*. Upregulation of *yfbR* may lead to reduced eDNA synthesis (Kong et al., 2020), promoting the self-organization of biofilm structural communities and promoting cell-to-cell gene transmission (Brown et al., 2015). Downregulation of *oppA* directly inhibits biofilm formation, promotes bacterial necrotivity, and stops the production of degradative enzymes (Sun et al., 2022).

At low concentrations of PCA (9.37 and 18.75 μg/mL), The metabolic activity of *V. parahaemolyticus* increased by 23.8 and 63.5%, respectively, in metabolic activity (**Figure 3**). But the bacterial numbers did not increase at these concentrations. PCA may regulate transcription factors, such as *paaF*, *fadB*, *IMS*, and *ald*, causing ATP accumulation. *G6PD* also increases NADPH and reduces bacterial stress response (Dukes et al., 2015; Gong et al., 2020). However, owing to the negative feedback regulation of the signaling pathway in bacteria, the metabolic activity decreased rapidly at 37.5 μg/mL PCA concentration (**Figure 3**). Some studies have also reported that cinnamaldehyde and eugenol significantly inhibited bacterial adhesion ability and metabolic activity (Liu et al., 2022).

We found that PCA suppresses the expression of class III flagellar system genes and biofilm formation by regulating the transcription factors *cheY*, *flrC*, and *fliA* (Li et al., 2022), thereby inhibiting Vibrio motility (McCarter, 2001). As the concentration of PCA increases, the bacterial colony area decreased, and the motility capacity of *V. parahaemolyticus* is almost lost at the 150 μg/mL PCA concentration (**Figures 5B,D**). Some substances have similar effects on bacterial motility and downregulate related genes, such as thymoquinone (Guo et al., 2019). Other virulence factors of *V. parahaemolyticus* also change under PCA inhibition, including downregulation of the *oppA*, regulation of a transcription factor involved in quorum sensing, and reduction in the adhesion of the virulence factor T6SS2 to host cells (Wu et al., 2022). In addition, PCA significantly inhibits the *fbpA* and *yxeM* genes, affecting material transport, and reducing biofilm formation (**Figure 8**; Gregory et al., 2020).

Transcriptional regulation high-throughput analysis revealed that PCA mainly regulates related downstream genes. We speculate that PCA may activate the bacterial signaling system, thereby inducing transcriptional changes in downstream genes.

Conclusion

In this study, we demonstrated that 75 μg/mL of PCA had potent antibiofilm properties against *V. parahaemolyticus*. At a PCA concentration of 37.5 μg/mL, biofilm production was greatly reduced (**Figure 2A**). Meanwhile, PCA regulated the expression of biofilm-related genes *oppA*, *fbpA*, and *yxeM*. With the increase of concentration, PCA greatly inhibited the metabolism of *V. parahaemolyticus* (**Figure 3**) and up-regulated the expression of *G6PD*, *ald*, *paaF*, and *fadB*. In addition, PCA decreased the production of exopolysaccharides and regulated the expression of related genes *pfkA*, *galE*, and *IF*. The clearance rate of *V. parahaemolyticus* increased with the increase in PCA concentration. The motility of *V. parahaemolyticus* was also dose-dependent on the concentration of PCA. Taken together, PCA significant inhibited the biofilm formation, adhesion and motility of *V. parahaemolyticus*.

Therefore, PCA may be developed as commercially more efficient and safer antimicrobial additives to curb *V. parahaemolyticus* biofilms in food systems and to alleviate foodborne diseases caused by such pathogens, which is of great importance in ensuring food safety.

Data availability statement

The original contributions presented in the study are included in the article/supplementary material, further inquiries can be directed to the corresponding author.

Author contributions

YL was responsible for the conception and filling of the manuscript. LW was responsible for the review and feasibility analysis of the manuscript. Both authors contributed to the article and approved the submitted version.

Acknowledgments

This research was supported by the Natural Science Foundation of Guangdong Province (2020A1515011561).

Conflict of interest

The authors declare that the research was conducted in the absence of any commercial or financial relationships that could be construed as a potential conflict of interest.

Publisher's note

References

Ashrafudoulla, M., Mizan, M. F. R., Ha, A. J., Park, S. H., and Ha, S. D. (2020). Antibacterial and antibiofilm mechanism of eugenol against antibiotic resistance *Vibrio parahaemolyticus*. *Food Microbiol.* 91:103500. doi: 10.1016/j.fm.2020.103500

Ashrafudoulla, M., Na, K. W. M., Hossain, I., Mizan, M. F. R., Nahar, S., Toushik, S. H., et al. (2021). Molecular and pathogenic characterization of *Vibrio parahaemolyticus* isolated from seafood. *Mar. Pollut. Bull.* 172:112927. doi: 10.1016/j.marpolbul.2021.112927

Bauer, J., Teitge, F., Neffe, L., Adamek, M., Jung, A., and Peppler, C. (2021). Impact of a reduced water salinity on the composition of *Vibrio* spp. in recirculating aquaculture systems for Pacific white shrimp (*Litopenaeus vannamei*) and its possible risks for shrimp health and food safety. *J. Fish Dis.* 44, 89–105. doi: 10.1111/jfd.13270

Bhardwaj, D. K., Taneja, N. K., Dp, S., Chakotiya, A., Patel, P., Taneja, P., et al. (2021). Phenotypic and genotypic characterization of biofilm forming, antimicrobial resistant, pathogenic *Escherichia coli* isolated from Indian dairy and meat products. *Int. J. Food Microbiol.* 336:108899. doi: 10.1016/j.ijfoodmicro.2020.108899

Brown, H. L., Kate, H., Mark, R., Roy, P. B., and Arnoud, H. M. V. (2015). Campylobacter jejuni biofilms contain extracellular DNA and are sensitive to DNase I treatment. *Front. Microbiol.* 6:699. doi: 10.3389/fmicb.2015.00699

Cao, J., Liu, H., Wang, Y., He, X., Jiang, H., Yao, J., et al. (2021). Antimicrobial and antivirulence efficacies of citral against foodborne pathogen *Vibrio parahaemolyticus* RIMD2210633. *Food Control* 120:107507. doi: 10.1016/j.foodcont.2020.107507

Chang, Y. J., Zhang, K., Carroll, B. L., Zhao, X. W., Charon, N. W., Norris, S. J., et al. (2020). Molecular mechanism for rotational switching of the bacterial flagellar motor. *Nat. Struct. Mol. Biol.* 27, 1041–1047. doi: 10.1038/s41594-020-0497-2

Chen, X., Yuan, M., Wang, Y., Zhou, Y., and Sun, X. (2021). Influence of fermentation with different lactic acid bacteria and *in vitro* digestion on the change of phenolic compounds in fermented kiwifruit pulps. *Int. J. Food Sci. Technol.* 57, 2670–2679. doi: 10.1111/ijfs.15316

Cho, S. Y., and Sung-il, Y. (2021). Structural analysis of the activation and DNA interactions of the response regulator VbrR from *Vibrio parahaemolyticus*. *Biochem. Biophys. Res. Commun.* 555, 102–108. doi: 10.1016/j.bbrc.2021.03.114

Dukes, A., Davis, C., Refaey, E. M., Upadhyay, S., Mork, S., and Arounleut, P. (2015). The aromatic amino acid tryptophan stimulates skeletal muscle IGF1/p70s6k/mTor signaling *in vivo* and the expression of myogenic genes *in vitro*. *Nutrition* 31, 1018–1024. doi: 10.1016/j.nut.2015.02.011

Faleye, O. S., Sathiyamoorthi, E., Lee, J. H., and Lee, J. (2021). Inhibitory effects of cinnamaldehyde derivatives on biofilm formation and virulence factors in *Vibrio* species. *Pharmaceutics* 13:2176. doi: 10.3390/pharmaceutics13122176

Gong, Q. Y., Yang, M. J., Yang, L. F., Chen, Z. G., Jiang, M., and Peng, B. (2020). Metabolic modulation of redox state confounds fish survival against *Vibrio alginolyticus* infection. *Microb. Biotechnol.* 13, 796–812. doi: 10.1111/1751-7915.13553

Gregory, G. J., Dutta, A., Parashar, V., and Boyd, E. F. (2020). Investigations of dimethylglycine, glycine betaine, and ectoine uptake by a betaine-carnitine-choline transporter family transporter with diverse substrate specificity in *Vibrio* species. *J. Bacteriol.* 202, 314–320. doi: 10.1128/jb.00314-20

Guo, C., Wang, S., Duan, J., Jia, N., Zhu, Y., Ding, Y., et al. (2017). Protocatechuic aldehyde protects against cerebral ischemia-reperfusion-induced oxidative injury via protein kinase cepsilon/Nrf2/HO-1 pathway. *Mol. Neurobiol.* 54, 833–845. doi: 10.1007/s12035-016-9690-z

Guo, D., Yang, Z., Zheng, X., Kang, S., Yang, Z., Xu, Y., et al. (2019). Thymoquinone inhibits biofilm formation and attachment-invasion in host cells of *Vibrio parahaemolyticus*. *Foodborne Pathog. Dis.* 16, 671–678. doi: 10.1089/fpd.2018.2591

Guo, L. X., Wang, J. J., Yi, G., Ling, T., Haiquan, L., Yingjie, P., et al. (2020). Comparative proteomics reveals stress responses of *Vibrio parahaemolyticus* biofilm on different surfaces: Internal adaptation and external adjustment. *Sci. Total Environ.* 731:138386. doi: 10.1016/j.scitotenv.2020.138386

Hall-Stoodley, L., Costerton, J. W., and Stoodley, P. (2004). Bacterial biofilms: From the natural environment to infectious diseases. *Nat. Rev. Microbiol.* 2, 95–108. doi: 10.1038/nrmicro821

He, Y. U., Wang, S., Yin, X., Sun, F., He, B., and Liu, X. (2020). Comparison of extracellular proteins from virulent and avirulent *Vibrio parahaemolyticus* strains to identify potential virulence factors. *J. Food Prot.* 83, 155–162. doi: 10.4315/0362-028x.jfp-19-188

Hwang, G., Kang, S., El-Din, M. G., and Liu, Y. (2012). Impact of an extracellular polymeric substance (EPS) precoating on the initial adhesion of *Burkholderia cepacia* and *Pseudomonas aeruginosa*. *Biofouling* 28, 525–538. doi: 10.1080/08927014.2012.694138

Jieke, Y., Jianchun, L., Ruizhi, T., Xingcan, H., Xiao, L., Xia, Z., et al. (2021). Protocatechuic aldehyde attenuates obstructive nephropathy through inhibiting lncRNA9884 induced inflammation. *Phytother. Res.* 35, 1521–1533. doi: 10.1002/ptr.6919

Kong, T., Lin, S., Ren, X., Li, S., and Gong, Y. (2020). Transcriptome and metabolome integration analysis of mud crab Scylla paramamosain challenged to *Vibrio parahaemolyticus* infection. *Fish Shellfish Immunol.* 103, 430–437. doi: 10.1016/j.fsi.2020.05.069

Kong, X., Li, C., Sun, X., Niu, B., Guo, D., Jiang, Y., et al. (2022). The maltose transporter subunit IICB of the phosphotransferase system: An important factor for biofilm formation of *Cronobacter*. *Int. J. Food Microbiol.* 370:109517. doi: 10.1016/j.ijfoodmicro.2021.109517

Kyoung-Ja, K., Mi-Ae, K., and Jee-Hyung, J. (2008). Antitumor and antioxidant activity of protocatechuic aldehyde produced from *Streptomyces lincolnensis* M-20. *Arch. Pharm. Res.* 31, 1572–1577. doi: 10.1007/s12272-001-2153-7

Li, L., Lu, J., Zhan, P., Qiu, Q., Chen, J., and Xiong, J. (2022). RNA-seq analysis unveils temperature and nutrient adaptation mechanisms relevant for pathogenicity in *Vibrio parahaemolyticus*. *Aquaculture* 558:738397. doi: 10.1016/j.aquaculture.2022.738397

Liu, H., Zhu, W., Cao, Y., Gao, J., Jin, T., Qin, N., et al. (2022). Punicalagin inhibits biofilm formation and virulence gene expression of *Vibrio parahaemolyticus*. *Food Control* 139:109045. doi: 10.1016/j.foodcont.2022.109045

Lu, C., Liu, H., Shangguan, W., Chen, S., and Zhong, Q. (2021). Antibiofilm activities of the cinnamon extract against i and *Escherichia coli*. *Arch. Microbiol.* 203, 125–135. doi: 10.1007/s00203-020-02008-5

McCarter, L. L. (2001). Polar flagellar motility of the *Vibrionaceae*. *Microbiol. Mol. Biol. Rev.* 65, 445–462. doi: 10.1128/mmbr.65.3.445-462.2001

Mok, J. S., Ryu, A., Kwon, J. Y., Park, K., and Shim, K. B. (2019). Abundance, antimicrobial resistance, and virulence of pathogenic *Vibrio* strains from molluscan shellfish farms along the Korean coast. *Mar. Pollut. Bull.* 149:1105590. doi: 10.1016/j.marpolbul.2019.110559

Ning, H., Cong, Y., Lin, H., and Wang, J. (2021). Development of cationic peptide chimeric lysins based on phage lysin Lysqdvp001 and their antibacterial effects against *Vibrio parahaemolyticus*: A preliminary study. *Int. J. Food Microbiol.* 358:109396. doi: 10.1016/j.ijfoodmicro.2021.109396

Puangpee, S., and Suanyuk, N. (2021). *In vitro* and *in vivo* evaluation of antimicrobial activity of Zooshikella marina against pathogenic bacteria causing *vibriosis* in aquaculture. *Aquac. Res.* 52, 4996–5007. doi: 10.1111/are.15371

Qiao, Y., Jia, R., Luo, Y., and Feng, L. (2021). The inhibitory effect of Ulva fasciata on culturability, motility, and biofilm formation of *Vibrio parahaemolyticus* ATCC17802. *Int. Microbiol.* 24, 301–310. doi: 10.1007/s10123-021-00165-1

Qin, G., Chunyan, Z., Qingguo, C., Jiahui, C., and Hui, C. (2021). Synergistic inhibition effects of tea polyphenols as adjuvant of oxytetracycline on *Vibrio*

parahaemolyticus and enhancement of *Vibriosis* resistance of *Exopalaemon carinicauda*. *Aquac. Res.* 52, 3900–3910. doi: 10.1111/are.15234

Renfei, L., Hao, T., Yue, Q., Wenhui, Y., Huiying, Y., Dongsheng, Z., et al. (2019). Quorum sensing regulates the transcription of lateral flagellar genes in *Vibrio parahaemolyticus*. *Future Microbiol.* 50, 795–810. doi: 10.2217/fmb-2019-0048

Shangguan, W., Xie, T., Zhang, R., Lu, C., Han, X., and Zhong, Q. (2021). Anti-biofilm potential of kefir-derived *Lactobacillus paracasei* L10 against *Vibrio parahaemolyticus*. *Lett. Appl. Microbiol.* 73, 750–758. doi: 10.1111/lam.13568

Shili, L., Yanmei, Y., Juanni, C., Bing, G., Liang, Y., and Wei, D. (2016). Evaluation of the antibacterial effects and mechanism of action of protocatechuic aldehyde against *Ralstonia solanacearum*. *Molecules* 21:754.

Smaoui, S., Hlima, H. B., Tavares, L., Ennouri, K., Braiek, O. B., Mellouli, L., et al. (2022). Application of essential oils in meat packaging: A systemic review of recent literature. *Food Control* 132:108566. doi: 10.1016/j.foodcont.2021.108566

Sun, J., Li, X., Qiu, Y., Xue, X., Zhang, M., Yang, W., et al. (2022). Quorum sensing regulates transcription of the pilin gene mshA1 of MSHA pilus in *Vibrio parahaemolyticus*. *Gene* 807:145961. doi: 10.1016/j.gene.2021.145961

Sun, X., Hao, L., Xie, Q., Lan, W., Zhao, Y., Pan, Y., et al. (2020). Antimicrobial effects and membrane damage mechanism of blueberry (*Vaccinium corymbosum* L) extract against *Vibrio parahaemolyticus*. *Food Control* 1111:107020.

Tan, X., Qiao, J., Wang, J. L., Li, H. D., and Wang, X. Y. (2022). Characterization of ampicillin-resistant genes in *Vibrio parahaemolyticus*. *Microb. Pathog.* 168:105573. doi: 10.1016/j.micpath.2022.105573

Tian, L., Wang, X., Zhang, D., Wu, M., Xue, Z., Liu, Z., et al. (2021). Evaluation of the membrane damage mechanism of protocatechuic aldehyde against Yersinia enterocolitica and simulation of growth inhibition in pork. *Food Chem.* 363:130340. doi: 10.1016/j.foodchem.2021.130340

Wang, H., Cheng, H., Wang, F., Wei, D., and Wang, X. (2010). An improved 3-(4,5-dimethylthiazol-2-yl)-2, 5-diphenyl tetrazolium bromide (MTT) reduction assay for evaluating the viability of *Escherichia coli* cells. *J. Microbiol. Methods* 82, 330–333. doi: 10.1016/j.mimet.2010.06.014

Wang, H., Zou, H., Wang, Y., Jin, J., Wang, H., and Zhou, M. (2022). Inhibition effect of epigallocatechin gallate on the growth and biofilm formation of *Vibrio parahaemolyticus*. *Lett. Appl. Microbiol.* 5, 81–88. doi: 10.1111/lam.13712

Wu, K., Long, Y., Liu, Q., Wang, W., Fan, G., Long, H., et al. (2022). CqsA-introduced quorum sensing inhibits type VI secretion system 2 through an OpaR-dependent pathway in *Vibrio parahaemolyticus*. *Microb. Pathog.* 162:105334. doi: 10.1016/j.micpath.2021.105334

Yang, M. J., Xu, D., Yang, D. X., Li, L., Peng, X. X., Chen, Z. G., et al. (2020). Malate enhances survival of zebrafish against *Vibrio alginolyticus* infection in the same manner as taurine. *Virulence* 11, 349–364. doi: 10.1080/21505594.2020.1750123

Yi, S., Du, G., Zi, H., Huihui, S., Zhanwen, Z., Xiaodong, X., et al. (2019). Attenuation of multiple *Vibrio parahaemolyticus* virulence factors by citral. *Front. Microbiol.* 10:894. doi: 10.3389/fmicb.2019.00894

Yu, H., Pei, J., Qiu, W., Mei, J., and Xie, J. (2022). The antimicrobial effect of *Melissa officinalis* L. Essential oil on *Vibrio parahaemolyticus*: Insights based on the cell membrane and external structure. *Front. Microbiol.* 13:812792. doi: 10.3389/fmicb.2022.812792

Zhang, J., Wang, L., Shi, L., Chen, X., Chen, C., Hong, Z., et al. (2020). Survival strategy of *Cronobacter sakazakii* against ampicillin pressure: Induction of the viable but nonculturable state. *Int. J. Food Microbiol.* 334:108819. doi: 10.1016/j.ijfoodmicro.2020.108819

Zhang, Q., Wang, L., Liu, Z., Zhao, Z., Zhao, J., Wang, Z., et al. (2020). Transcriptome and metabolome profiling unveil the mechanisms of *Ziziphus jujuba* mill. peel coloration. *Food Chem.* 312:125903. doi: 10.1016/j.foodchem.2019.125903

Zhu, Z., Yang, L., Yu, P., Wang, Y., Peng, X., and Chen, L. (2020). Comparative proteomics and secretomics revealed virulence and antibiotic resistance-associated factors in *Vibrio parahaemolyticus* recovered from commonly consumed aquatic products. *Front. Microbiol.* 11:1453. doi: 10.3389/fmicb.2020.01453

frontiers | Frontiers in Microbiology

TYPE Review
PUBLISHED 25 November 2022
DOI 10.3389/fmicb.2022.1002185

OPEN ACCESS

EDITED BY
Tao Yu,
Xinxiang University,
China

REVIEWED BY
Shengbo Wu,
Tianjin University,
China
Tung Truong,
Phenikaa Institute for Advanced Study,
Vietnam

*CORRESPONDENCE
Paul D. Cotter
paul.cotter@teagasc.ie

SPECIALTY SECTION
This article was submitted to Food Microbiology, a section of the journal Frontiers in Microbiology

RECEIVED 24 July 2022
ACCEPTED 17 October 2022
PUBLISHED 25 November 2022

CITATION
Falà AK, Álvarez-Ordóñez A, Filloux A, Gahan CGM and Cotter PD (2022) Quorum sensing in human gut and food microbiomes: Significance and potential for therapeutic targeting. *Front. Microbiol.* 13:1002185. doi: 10.3389/fmicb.2022.1002185

Quorum sensing in human gut and food microbiomes: Significance and potential for therapeutic targeting

A. Kate Falà[1,2,3], Avelino Álvarez-Ordóñez[4], Alain Filloux[5], Cormac G. M. Gahan[1,2,6] and Paul D. Cotter[1,3]*

[1]APC Microbiome Ireland, University College Cork, Cork, Ireland, [2]School of Microbiology, University College Cork, Cork, Ireland, [3]Food Bioscience Department, Teagasc Food Research Centre, Fermoy, Ireland, [4]Department of Food Hygiene and Technology and Institute of Food Science and Technology, Universidad de León, León, Spain, [5]MRC Centre for Molecular Bacteriology and Infection, Department of Life Sciences, Imperial College London, London, United Kingdom, [6]School of Pharmacy, University College Cork, Cork, Ireland

Human gut and food microbiomes interact during digestion. The outcome of these interactions influences the taxonomical composition and functional capacity of the resident human gut microbiome, with potential consequential impacts on health and disease. Microbe-microbe interactions between the resident and introduced microbiomes, which likely influence host colonisation, are orchestrated by environmental conditions, elements of the food matrix, host-associated factors as well as social cues from other microorganisms. Quorum sensing is one example of a social cue that allows bacterial communities to regulate genetic expression based on their respective population density and has emerged as an attractive target for therapeutic intervention. By interfering with bacterial quorum sensing, for instance, enzymatic degradation of signalling molecules (quorum quenching) or the application of quorum sensing inhibitory compounds, it may be possible to modulate the microbial composition of communities of interest without incurring negative effects associated with traditional antimicrobial approaches. In this review, we summarise and critically discuss the literature relating to quorum sensing from the perspective of the interactions between the food and human gut microbiome, providing a general overview of the current understanding of the prevalence and influence of quorum sensing in this context, and assessing the potential for therapeutic targeting of quorum sensing mechanisms.

KEYWORDS

quorum sensing, quorum quenching, quorum sensing inhibition, gut microbiome, food microbiome, food matrix

Introduction

The interactions between human, animal and plant microbiomes and their ultimate impact on the assembly and maintenance of community structure and functionality is the focus of intense research efforts (Jagadeesan et al., 2019). In food microbiology, the influence of ingested food microbiomes on the human gut is a particular focus in recent years. The human gut harbours the greatest microbial load of all body sites – estimated to

be in the order of 10^{13} bacterial cells (along with eukaryotic microorganisms and phage; Sender et al., 2016). This resident microbiota plays a significant role in human health and is amenable to outside influences imposed by diet and organisms that are resident in raw and minimally processed foods (Janssens et al., 2018; Walter et al., 2020). Nevertheless, many knowledge gaps persist regarding the dynamics of colonisation, resistance and succession in the food and gut microbiomes and how these may be modulated.

The genetic repertoire of bacteria enables them to perceive and adapt to environmental factors in flux. Environmental sensing and signalling in bacteria is primarily achieved through secondary nucleotide messengers, such as cyclic adenosine monophosphate (cAMP), cyclic diguanylate (c-di-GMP) and the hyperphosphorylated guanosine derivatives collectively referred to as (p)ppGpp (Hengge et al., 2019), as well as Two-Component Systems (TCSs) – pairs of sensory histidine kinases and response regulators that perceive extracellular signals and modulate gene expression accordingly (Liu et al., 2018a). In addition, many bacterial species possess dedicated Quorum Sensing (QS) systems that involve the secretion, extracellular accumulation and subsequent import and processing of specific small chemical signal molecules (Eickhoff and Bassler, 2018). At threshold concentrations, these signal molecules in the extracellular environment induce transcriptional changes that trigger phenotypic adaptation to changing social contexts. These include the coordination of biofilm regulation, expression of virulence or food spoilage traits and social choices such as cooperation, competition and cheating within micro-ecological contexts (Li and Tian, 2012; Allen et al., 2016; Defoirdt, 2018).

QS systems can provide information on the local population of 'self' and 'other'; and it has been also proposed that QS could enable bacteria to detect diffusion-limited situations through an integrated model of efficiency sensing (Hense et al., 2007; Liu et al., 2018a). QS systems are described in both Gram-negative (Papenfort and Bassler, 2016) and Gram-positive bacteria (Verbeke et al., 2017), as well as fungi (Nogueira et al., 2019) and some viruses (Silpe and Bassler, 2019). Furthermore, next-generation sequencing and comparative genomic approaches have identified homologues of known quorum sensing circuits across genus and species boundaries (Whiteley et al., 2017), suggesting its importance in the regulation of survival strategies.

This review summarises the fundamental and translational research to date relating to the targeting of bacterial quorum sensing to produce foods with enhanced safety and quality profiles and the modulation of gut microbiomes for human health. An updated catalogue of quorum sensing activity and its inhibition in foods and the human gut is provided. Finally, we identify and discuss gaps in the literature that can be addressed in order to progress research in this field specifically with a view to the bioprotection of foods and the therapeutic targeting of the gut microbiome. As this review demonstrates, there is great promise for direct applications in food production systems, particularly in the context of functional foods, as well as biotherapeutics in the clinical sphere. On the other hand, some of the gaps identified within have the potential, if addressed, to benefit broader research in the field of microbial ecology in a cross-disciplinary manner.

Quorum sensing in bacteria

As per the original system first identified in *Vibrio fischeri*, the simplest QS circuit consists of regulatory gene pairs responsible for the production of signalling molecules (*luxI*) and transcriptional activation (*luxR*) of regulated genes responsible for phenotypes such as bioluminescence (Nealson et al., 1970). In addition to global phenotypic regulation based on local population density, QS can also contribute to managing the production of public goods including both the signal molecules themselves (auto-induction) and co-regulated products relevant to the context of foods and the human gut, such as extracellular enzymes, exopolysaccharides, surfactants, antimicrobial compounds, virulence factors and siderophores (Heilmann et al., 2015). An overview of the principal systems found in bacteria is presented in Figure 1. Public goods, in the context of microbiology, refers to molecular components of the secretome produced by individual cells and transferred to the extracellular milieu, potentially benefiting the population as a whole. Public goods are distinct from private goods, which are generally cytosolic or membrane-bound and hence confer an exclusive benefit upon producer cells.

Understanding the relative contribution of quorum sensing to microbiome structure and functionality is complicated by heterogeneous distribution of QS producers and responders, even within clonal populations (Striednig and Hilbi, 2022). For instance, one study reported that just 68% of *V. fischeri* cells responded to exogenous QSM (Pérez and Hagen, 2010). Further, receptor promiscuity and divergence in ligand binding of quorum sensing receptors towards non-canonical substrates is suggestive of a system that can be tuned and can adapt over time to changing environmental conditions and competitors (Hawver et al., 2016; Prescott and Decho, 2020). Mapping QS systems in complex ecological environments is complicated by their tendency to follow hierarchical and combinatorial structures (Ng and Bassler, 2009; Cornforth et al., 2014) and to modulate gene expression programs through asymmetry (Hurley and Bassler, 2017), thought to facilitate the management of metabolic trade-offs (Dinh and Prather, 2019). This is perhaps best exemplified by the Qrr sRNAs (Quorum Regulatory sRNAs) of the *Vibrio* genus and the multifunctional RNAIII which coordinates several stacked regulatory circuits managing the accessory gene regulator (*agr*) system in *Staphylococcus aureus* (Bronesky et al., 2016).

Quorum sensing molecules

QS systems involve the production and detection of Quorum Sensing Molecules (QSM) and understanding the synthesis,

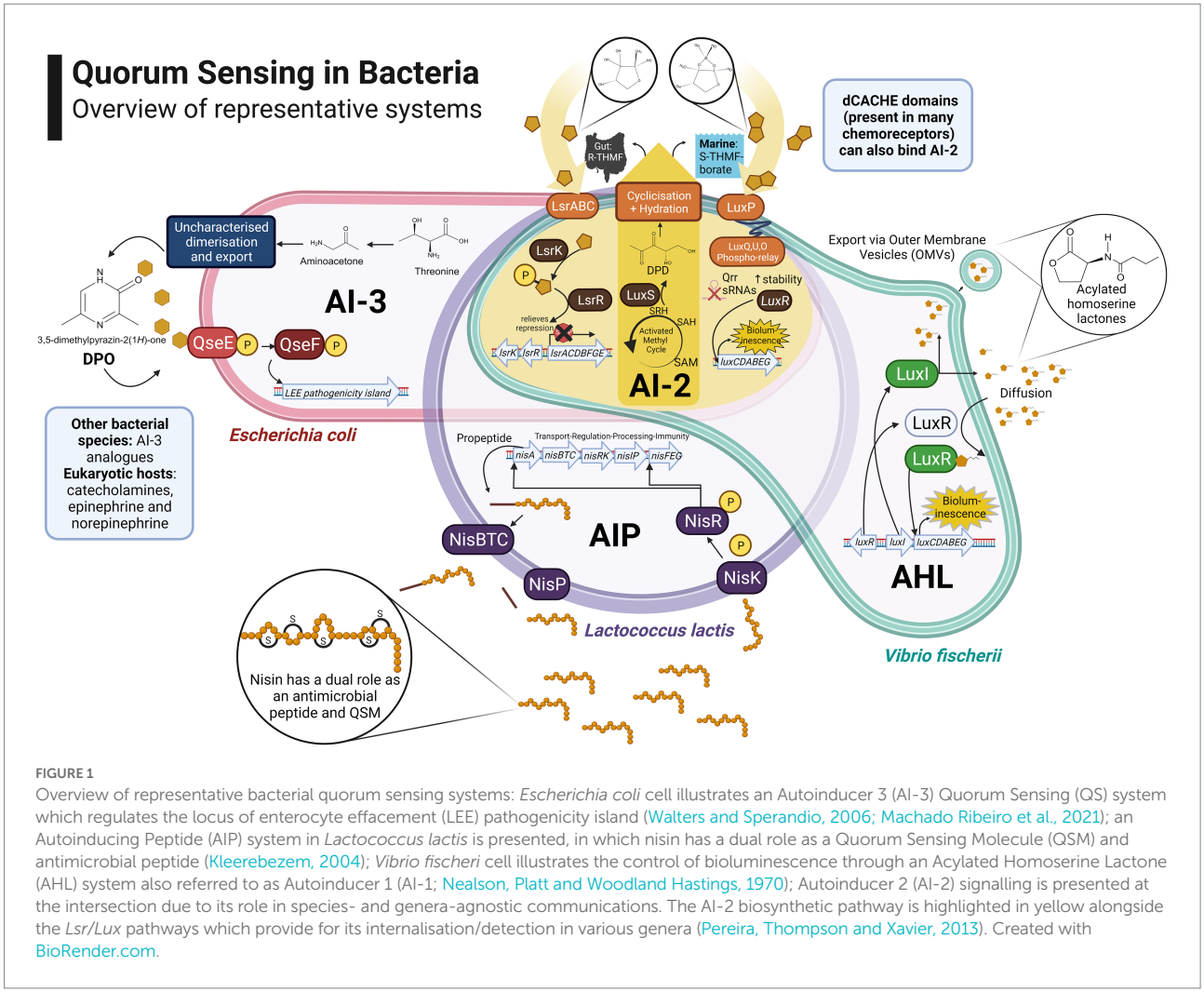

FIGURE 1
Overview of representative bacterial quorum sensing systems: *Escherichia coli* cell illustrates an Autoinducer 3 (AI-3) Quorum Sensing (QS) system which regulates the locus of enterocyte effacement (LEE) pathogenicity island (Walters and Sperandio, 2006; Machado Ribeiro et al., 2021); an Autoinducing Peptide (AIP) system in *Lactococcus lactis* is presented, in which nisin has a dual role as a Quorum Sensing Molecule (QSM) and antimicrobial peptide (Kleerebezem, 2004); *Vibrio fischeri* cell illustrates the control of bioluminescence through an Acylated Homoserine Lactone (AHL) system also referred to as Autoinducer 1 (AI-1; Nealson, Platt and Woodland Hastings, 1970); Autoinducer 2 (AI-2) signalling is presented at the intersection due to its role in species- and genera-agnostic communications. The AI-2 biosynthetic pathway is highlighted in yellow alongside the *Lsr/Lux* pathways which provide for its internalisation/detection in various genera (Pereira, Thompson and Xavier, 2013). Created with BioRender.com.

structure and stability of these compounds is important for developing strategies for therapeutic targeting of these systems. A high-level overview of the principal classes of QSM is provided in Table 1.

There are many instances in which QSM fulfil a dual role in addition to QS, such as Autoinducer 2 (AI-2) and Autoinducer Peptides (AIPs). AI-2 systems have been identified in approximately half of sequenced bacterial genomes and are considered to mediate species-agnostic communication, particularly in complex communities, presented at the intersection of the bacterial cells in Figure 1. At the same time, some argue that AI-2 biosynthesis mainly contributes to the detoxification of S-adenosylhomocysteine (SAH) produced during the activated methyl cycle (AMC) and is essential to the metabolism of cysteine and methionine, with an incidental QS role (Kang et al., 2019). Disambiguation of these contrasting theories has been explored through the construction of a LuxS-deficient *Streptococcus mutans*, followed by restoration of AMC functionality by complementation with S-adenosyl-L-homocysteine hydrolase (*sahH* from *P. aeruginosa*; Hu et al., 2018). Whilst biofilm formation and acid tolerance were restored through complementation, homocysteine and lactic acid levels remained aberrant, underlining the broader significance of *luxS* in the metabolic landscape of the cell.

Similarly, there are numerous examples of AIP QSM which, in addition to facilitating QS, act as antimicrobial peptides such as lantibiotics (bacteriocins are reviewed in greater detail in Section 2.3). In addition to the multifunctionality of QSM themselves, it bears considering that QSM can also be degraded or for instance exported in a non-specific manner through multidrug efflux pumps (Rahmati et al., 2002).

Methods for the analysis of QSM

As raised almost a decade ago (Skandamis and Nychas, 2012), a greater understanding of the relative abundance and significance of QS signalling in microbiomes is required, particularly in providing temporal resolution of QS at significant points in time and space (Donaldson et al., 2016). Accurate and rapid detection, characterisation and quantification of QSM can enhance our understanding of QS in various environments, as well as providing a real-time readout of microbial physiology within a given microbiome.

TABLE 1 Overview of major bacterial Quorum Sensing Molecules (QSM) families, examples, possible modifications, producer and/or responder bacteria utilising the QSM as well as the regulated phenotypes and specificity.

System	QSM	QSM modification	Producer (and responder) bacteria	Responder bacteria (no production)	Relevant phenotypes regulated	Specificity	Reference
Autoinducer 1 (AI-1)	Acylated-homoserine lactones (AHL/HSL)	Homoserine lactone moiety is joined to a variable length (C4-C16) acyl tail, which can bear oxo- or hydroxyl- substitutions.	Gram-negative bacteria, e.g. *Aliivibrio fischeri*	Species with LuxR solos	*las* and *rhl* systems	Generally species-specific due to AHL molecular structure (length of acyl chain; substitutions)	Fuqua, Parsek and Greenberg, (2001); Bez et al., (2021)
Autoinducer 2 (AI-2)	*S*-THMF (*2S,4S*)-2-methyl-2,3,3,4-tetra-hydroxytetrahydrofuran; *R*-THMF: (*2R,4S*)-2-methyl-2,3,3,4-tetrahydroxytetrahydro-furan)	*S*-THMF-borate predominates in marine environments; heptyl modifications are possible	~Half of sequenced bacterial genomes through *luxS*	*Pseudomonas aeruginosa*, *Bacillus subtilis* and *Rhodopseudomonas palustris* (through dCACHE domain)	Multiple and varied	Species-agnostic; enteric bacteria detect *R*-THMF through *lsr* operon; boronated *S*-THMF is detected through *lux* cascade; other bacteria detect through dCACHE domain-containing proteins	Pereira, Thompson and Xavier, (2013)
Autoinducer 3 (AI-3)	3,5-dimethylpyrazin-2-one (DPO)	Various pyrazinone analogues	Enterohemorrhagic *Escherichia coli* (EHEC)	Many Gram-negative bacteria (through QseC homologues)	Expression of locus of enterocyte effacement (LEE), Shiga-toxin production	Interspecific (differences in relative abundance of AI-3 analogues); Inter-kingdom crosstalk with mammalian hormones epinephrine and norepinephrine.	Clarke et al., (2006); Walters and Sperandio, (2006); Kim et al., (2020); Machado Ribeiro et al., (2021)
Autoinducer peptides (AIP)	Post-translationally modified peptides	Length (5–17 amino acids); Linear or cyclical structure	Gram-positive bacteria, e.g. *Lactococcus lactis*		Sporulation and competence in *Bacillus subtilis* (*phr* system); toxin production in *C. botulinum* and *C. perfringens* (*agr*-type system)	Generally species-specific due to the molecular structure	Kleerebezem et al., (1997); Novick and Muir, (1999); Cook and Federle, (2014); Monnet, Juillard and Gardan, (2016)
Small RNAs	miRNAs and siRNAs; Qrr sRNAs (Quorum Regulatory sRNAs) in *Vibrio* spp.; RNAIII in *Staphylococcus aureus*	Specificity to targeted mRNA transcripts, which are removed from circulation.	Reported in *Escherichia*, *Salmonella*, *Streptococcus*, *Pseudomonas* and *Vibrio* genera		Type III secretion genes in *Vibrio harveyi*	Specificity to the targeted mRNA transcript	Rutherford et al., (2011); Teng et al., (2011); Fu, Elena and Marquez, (2019)

(Continued)

10.3389/fmicb.2022.1002185

TABLE 1 (Continued)

System	QSM	QSM modification	Producer (and responder) bacteria	Responder bacteria (no production)	Relevant phenotypes regulated	Specificity	Reference
Diffusible Signal Factor (DSF)	*cis*-11-methyl-dodecenoic acid Derived from fatty acids with a cis-unsaturated double bond at the 2-position.	Chain length, branched/ unbranched structure	*Stenotrophomonas maltophil*ia, *Burkholderia cenocepacia* and *P. aeruginosa*	*S. aureus, B. cereus, S. enterica, E. coli*	Virulence and exopolysaccharide (EPS) production in *Xanthomonas oryza*e pv. oryzae; Biofilm dispersal in *P. aeruginosa*	Intraspecific and cross-kingdom crosstalk possible	Sepehr et al., (2014); Zhou et al., (2017); Liu et al., (2018b)
Palmitate methyl ester (PAME)	3-hydroxy palmitic acid methyl ester		*Ralstonia solanacearum*		Virulence and upregulation of AHL production	Species-specific	Flavier et al., (1997); Mole et al., (2007)
Diketopiperazines (DKP)	Amino acid-derived cyclic dipeptides	Constituent amino acids; Chirality;	*Cronobacter sakazakii*, *Bacillus cereus*, *Vibrio* spp.		Biofilm formation in *C. sakazakii*; Increased resistance to oxidative stress in *Vibrio* spp.	cyclo(Phe-Pro) is detected by both *C. sakazakii* and *B. cereus*	Bofinger et al., (2017); Kim et al., (2018); Zink et al., (2021)
Quinolones	2-heptyl-3-hydroxy-4-quinolone (PQS); 2-alkyl-4(1H)-quinolone (AHQ)		*P. aeruginosa*		Virulence factors, including pyocyanin, elastase, lectin, and rhamnolipid production	Species-specific	Rampioni et al., (2016); Lin et al., (2018)
Dialkylresorcinols	Dialkylresorcinols (DARs) and Cyclohexanediones (CHDs)	Variable R chain	116 species, including the genera *Photorhabdus, Neisseria, Capnocytophaga, Flavobacterium*		Pathogenicity against *Galleria mellonella*	Intraspecific crosstalk possible	Brameyer et al., (2015)
Photopyrones (PPYs)	α-pyrones	Variable R chain	*Photorhabdus luminescens*	*Bacillus atrophaeus*	*Photorhabdus* clumping factor (Pcf); biofilm formation	Intraspecific crosstalk possible	Brachmann et al., (2013); Hickey et al., (2021)

10.3389/fmicb.2022.1002185

Conventional methods frequently used to interrogate the physico-chemical properties of QSM include mass spectrometry (MS) and high-performance liquid chromatography (HPLC), whilst biosensor-based systems employing plasmids, chromosomes or enzymes from reporter bacterial strains can rapidly detect a colorimetric, luminescent or fluorescent signal. Chromatographic techniques are more resource-intensive but can detect QSM with a higher degree of accuracy and can also be used to validate novel biosensors (Cutignano, 2019).

Whilst several analytical techniques are available for AI-1 and AI-2 QSM, AIP are generally more difficult to quantify as they are normally found at low concentrations in complex mixtures (Kalkum et al., 2003) whilst AI-3 was only recently characterised and no methods have been developed for its routine analysis yet (Kim et al., 2020). Novel approaches for the detection and characterisation of AIP and AI-3 are needed, in addition to protocols for QSM analysis in the complex matrices associated with food and human gut microbiome samples. In this regard, analytical techniques developed and validated in the context of environmental microbiology, such as the analysis of biofilms in wastewater treatment plants (Wang et al., 2018) could be adapted. These could be combined with emerging fluorescence-based techniques such as Combinatorial Labelling And Spectral Imaging-Fluorescence *In-Situ* Hybridization (CLASI-FISH) to incorporate the spatial ecology of microbial communities (Wilbert et al., 2020).

Several biosensor strains, often plasmid-based, have been constructed to detect different QSM classes (Wen et al., 2017), however chromatographic methods tend to be preferred to detect mixes of QSM in complex microbial consortia (Gui et al., 2018). Rapid paper-based diagnostic tools containing immobilised whole cell biosensors have also been validated to nanomolar level detection of AHLs and AI-2 QSM (Wynn et al., 2018).

Biochemical analytical techniques are increasingly being paired with *in silico* studies of quorum sensing-related genes in metagenomic samples to help distinguish QS potential from active QS processes (Rezzonico et al., 2012). In addition to the established Quorumpeps database for AIP peptides (Wynendaele et al., 2013), more recent efforts have generated novel databases including the Omics Database of Fermentative Microbes (ODFM; Whon et al., 2021) and Quorum Sensing of Human Gut Microbes (QSHGM; Wu et al., 2021b). Curated and regularly updated databases are fundamental for accurate bioinformatic predictions, which will assist in modelling the effect of quorum sensing systems in complex communities as part of broader pipelines (Wynendaele et al., 2013). Accurate modelling of quorum sensing in foods and the human gut is necessary in order to establish prevalence, relevance and to evaluate potential interventions. *Ex vivo* modelling of the human gut, such as through colonic models and gut-on-a-chip approaches, can provide an opportunity to benchmark quorum sensing activity at various points in the digestive process (Garcia-Gutierrez and Cotter, 2021). Fermented foods have also been demonstrated to be tractable and convenient experimental models for studying community assemblage in food microbiomes (Wolfe and Dutton, 2015) and could be evaluated as models for QS studies.

Quorum sensing "eavesdropping"

Whilst QS was originally described in terms of autoinduction, communication through QS can occur across strains, species and even kingdoms (Kendall and Sperandio, 2016). LuxR solos are one such circuit that permit 'eavesdropping' by detecting and integrating community-level information to inform the regulation of gene expression without investing in the production of QSM (Subramoni and Venturi, 2009). The metabolic cost of QSM synthesis varies considerably – estimated in the order of 184 ATP per autoinducer peptide (AIP), 8 ATP per acyl-homoserine lactone (AHL) and 0–1 ATP per autoinducer-2 moiety (AI-2; Ruparell et al., 2016), highlighting the likely evolutionary benefit of an eavesdropping strategy.

Notable examples in an enteric context include species of the genera *Escherichia*, *Klebsiella*, and *Salmonella* that possess orthologues of the transcriptional regulatory protein SdiA – detecting AHLs produced by other species – whilst lacking the requisite genes for AHL production (Michael et al., 2001; Lindsay and Ahmer, 2005). This type of QS circuit is implicated in the suppression of *traI*-mediated conjugation between *E. coli* and *P. aeruginosa* (Lu et al., 2017), which could potentially be harnessed in applications to reduce dissemination of genetic determinants of antimicrobial resistance (AMR) by horizontal gene transfer (HGT). Similarly, several instances of food spoilage appear to be augmented by synergy between AHL-QSM producers and non-producers, presumably due to the capacity of the non-producers to detect QSM in the extracellular milieu (Yu et al., 2019; Wang and Xie, 2020).

Quorum sensing inhibition

Due to the wide range of bacterial phenotypes regulated by quorum sensing and their impact in clinical, environmental and agricultural contexts, QS systems have been proposed as a potential therapeutic target for the modulation of microbial communities (Rutherford and Bassler, 2012; Kalia, 2013; Lade et al., 2014). Indeed, the phenomenon of quorum sensing inhibition (QSI; also referred to in the literature as quorum sensing interference to describe broader modulation of QS) has been reported not just amongst bacteria, suggesting an ecological role in governance of cooperation and competition (Murugayah and Gerth, 2019), but also between bacteria and eukaryotic cells including fungi, plants and animals (Hughes and Sperandio, 2008; Joshi et al., 2021). QSI can be accomplished through several mechanisms, such as enzymatic degradation [also referred to as Quorum Quenching (QQ)], production of QSM analogues, signal sequestration or other modulation of signal flux up or downstream.

Whilst various applications in medical and industrial settings have been investigated, the use of QSI to modulate food microbiomes and gut microbiota has received relatively less attention, yet may prove useful in addressing the global threat of antibiotic resistance and enhancing the robustness of probiotic

strains (Kareb and Aïder, 2020). It is anticipated that metagenomics and metatranscriptomics will guide studies in this relatively novel area to determine the effect of QSI on microbial communities, whilst genetic engineering can be used to improve and maximise the potential of QQ enzymes derived from natural environments (Billot et al., 2020). Advances in the field of chemistry such as structure–activity studies of synthetic QSM analogues (Rajamani et al., 2008; Lyons et al., 2020) naturally complement such bioprospecting and rational design approaches.

Perhaps some of the most exciting research in the field has emerged at the interdisciplinary juncture between biology and engineering occupied by the field of synthetic biology (Wang et al., 2020). Given the close resemblance between electronic circuits and the intrinsic networks and feedback loops of quorum sensing systems, there is potential for ground-breaking interdisciplinary work. In the field of synthetic ecology, precisely engineered consortia are being used to evaluate the relative importance of quorum sensing pathways and the equilibrium between QS and QSI when targeted for therapeutic modulation (Stephens and Bentley, 2020), as well as advancing the fundamental research in the field (Wu et al., 2021a).

Biofilms as environments which favour QS

Biofilms are aggregations of microbial cells, attached to one another and typically adhered to a surface through a matrix of polymers that are at least partially microbially secreted. They are ubiquitous and considered the predominant form of living adopted by bacteria, fungi, viruses and single-celled eukaryotes (Flemming et al., 2016), with specific relevance to food and food processing environments (Alvarez-Ordóñez et al., 2019) and the human gut (Deng et al., 2020).

As well as physically shielding in-dwelling cells, the structure of the biofilm matrix includes channels and microcolonies that generate nutrient and oxygen gradients. These gradients are thought to contribute to phenotypic and genotypic plasticity and reinforce the heterogeneity generally seen in biofilm-dwelling populations (Penesyan et al., 2019). The distinct microenvironments formed and defined by biofilms are thought to favour interactions with other microorganisms due to their enforced proximity within the matrix and reduced diffusion. The resulting circulation of nutrients, metabolites, QSM and other public goods such as extracellular enzymes and siderophores are considered to influence emergent features in bacteria (Solano et al., 2014; Flemming et al., 2016). Emergent properties refer to characteristics of populations, especially multispecies and biofilm-associated, which differ from those of equivalent planktonic populations. Most commonly studied attributes include social cooperation, nutrient management and antimicrobial tolerance (Flemming et al., 2016).

More specifically, mixed biofilms containing multiple species are commonplace. They may arise due to synergy between different attachment phenotypes, such as specialised fimbriae and exopolysaccharide (EPS) production, with the structure of the latter in particular being influential on the emergent properties of biofilms beyond those of equivalent planktonic populations (Swaggerty et al., 2018).

Quorum sensing in foods and food processing environments

Advances in nucleic acid manipulation and sequencing have helped enhance our understanding of food microbiomes: the microbial communities within and upon food matrices, which become established during primary production and evolve throughout the farm-to-fork continuum (De Filippis et al., 2018; Yap et al., 2022). This field of study receives special attention in light of the emerging, cross-disciplinary approach of One Health, which recognises the interrelationship between human, animal and environmental health [One Health High-Level Expert Panel (OHHLEP) et al., 2022]. These advances have helped the collection of temporal datasets that can better describe the taxonomical and functional evolution of microbiomes across complex food chains, in order to enhance our understanding of their influence on food safety, quality, sustainability and potential impact on human health (Pasolli et al., 2020). Whilst certain species can dominate specific communities at particular times, broadly speaking food microbiomes consist of multiple strains with some degree of interaction, which may affect collective behaviours of microorganisms such as food spoilage (Qian et al., 2018). In regulating phenotypic characteristics and metabolic processes, QS is proposed to enhance microbial adaptation to dynamic environments and has been associated with food quality in both a negative sense with respect to microbial food spoilage (Yuan et al., 2018), as well as enhancing the quality of some fermented foods (Johansen and Jespersen, 2017).

The overall impact of QS in microbial succession dynamics within food microbiomes is difficult to assess due to the frequent heterogeneous responses seen in bacteria to QSM described previously. Further, relative receptor binding affinity studies have demonstrated that many QS receptors can be activated by many other small molecules produced by microorganisms or hosts (Wellington and Greenberg, 2019), as we will outline for various compounds present in foods. Finally, the accumulation, compartmentalisation and stability of QSM are likely to be highly influenced by intrinsic and extrinsic factors of the food matrix and subject to fluctuations at different points of the food production process (Skandamis and Nychas, 2012). For example, studies on AHL-QSM stability in soil established a half-life ranging from hours to days depending on pH and temperature (Delalande, 2005) and the influence of micro-environmental conditions in foods and the human gut remains to be elucidated. Recent technologies have harnessed bacterial QS activity to provide real-time monitoring of microbial activity during food production (Miller and Gilmore, 2020).

Quorum sensing molecules detected in foods

A broad range of QSM have been reported in different foods, as illustrated in Figure 2. Overall, fatty acid-derived QSM such as AHLs and DKPs in foods are predominantly associated with bacteria involved in food spoilage or food-borne illness, whilst associations with AI-2-QSM appear more evenly split between instances of benign bacterial consortia and undesirable ones.

Different foods present distinct matrix effects, which will likely impact the stability and mobility of QSM produced by the microbiota within; high AI-2 activity is reported in frozen fish, tomato, cantaloupe, carrots, tofu and cow's milk, whilst raw poultry, beef and artisanal cheeses appeared to inhibit AI-2 QS activity (Lu et al., 2004). This finding was supported by a more recent study measuring spiked AHL and AI-2 in water, skim milk and meat suspensions *via* a whole-cell biosensor assay, finding that signal was diminished only in the meat matrix (Wynn et al., 2018). The fluctuating levels of organic acids, pH and other biomolecules during food processing, especially in activities involving fermentation, are likely to influence QSM concentration and stability over time.

AI-2 appears to be particularly significant in the context of fermented food microbiomes. For instance, many bacteria isolated from the surface of smear-ripened cheeses produce AI-2, including *Arthrobacter nicotianae, Corynebacterium ammoniagenes, Corynebacterium casei, Microbacterium barkeri, Microbacterium gubbeenense and Staphylococcus equorum subsp. linens* (Novak and Fratamico, 2006; Gori et al., 2011). Another study of isolates from West African fermented foods reported AI-2 production in many Aerobic Endospore-producing Bacteria (AEB) such as *Bacillus subtilis, B. cereus, B. altitudinis, B. amyloliquefaciens, B. licheniformis, B. aryabhattai, B. safensis, Lysinibacillus macroides* and *Paenibacillus polymyxa* (Qian et al., 2015). This is supported by bioinformatic analysis of the microbiome of cocoa bean fermentations, which revealed a high prevalence of *luxS*-related genes in the core/soft-core of the lactic acid bacteria (LAB) *Limosilactobacillus fermentum, Pediococcus acidilactici* and *Lactiplantibacillus plantarum*. Additional *luxS* genes were also detected in some accessory genomes (de Almeida

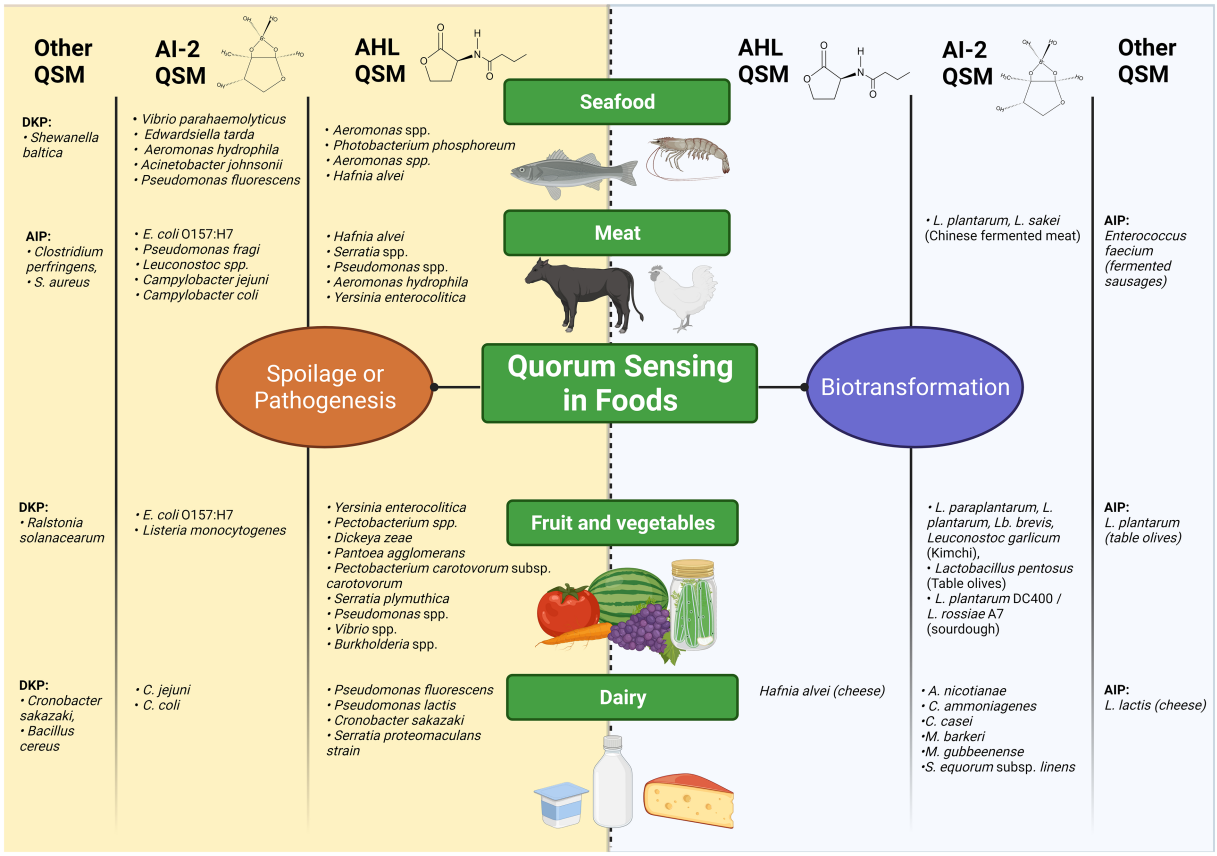

FIGURE 2
Overview of Quorum Sensing Processes as involved in food production, adapted from (Blana, Doulgeraki and Nychas, 2011; Plummer, 2012; Nahar et al., 2018; Quintieri et al., 2020; Wang and Xie, 2020). The left hand side of the figure in yellow maps food-associated bacteria reported in the literature to utilise QS for spoilage or pathogenesis, organised into columns based on the class of QSM (AHL, AI-2 and others) and by the type of food in which they are reported. This scheme is repeated on the right hand side in blue for those food-borne bacteria with positive attributes in food with respect to biopreservation and biotransformation. Created with BioRender.com.

et al., 2021) and altogether participation in AI-2 signalling was proposed to help LAB adapt to diverse niches such as food fermentations.

AI-2 QS is also emerging as a key player in supporting desirable biofilms in food processing. For instance, AI-2 is present in high concentrations in Spanish table olive biofilms produced using a sequential yeast-LAB starter culture, which controlled undesirable spontaneous microbiota and maintained organoleptic quality throughout the product shelf life (Benítez-Cabello et al., 2020). In the same study, high AI-2 levels also correlated with high LAB counts on the olive skin surface, supporting the assertion that robust biofilm-forming capacity can enable potential probiotic strains to better survive and become established in fermented food microbiomes. This phenomenon has also been reported in other beneficial members of food microbiomes such as *Lactiplantibacillus pentosus* in olives (Perpetuini et al., 2016) and *Lactiplantibacillus paraplantarum* L-ZS9 in kimchi (Park et al., 2016). Thermal treatment is also highly relevant to food processing and whilst its effect on all QSM is not known, AI-2 concentrations are diminished by pasteurisation/ultra-heat-treatment (UHT; Lu et al., 2004).

An important limitation is that many studies report QSM production by strains isolated from foods, rather than quantifying QSM *in situ*, thereby only estimating the potential prevalence of QS in foods. A further confounding factor is the use of biosensors that may not distinguish between various enantiomers of QSM or between bacterial QSM and host-derived molecular mimics.

Biofilms within food and food industries as environments for QS

Around one quarter of food waste is attributed to microbial processes (Huis in 't Veld, 1996), with implications for food safety and quality at a consumer level, economic losses at an industrial level and resource wastage in the context of sustainability. Microbial load and community composition are influenced by the nature and origin of raw materials, processing methods, transport and storage conditions (Jarvis et al., 2018; Van Reckem et al., 2020; Zwirzitz et al., 2020) and may fluctuate in accordance with the conditions of the niche. Food processing typically employs several physico-chemical hurdles to mitigate undesirable microbial growth such as thermal treatment, high pressure processing, use of acids, bacteriocins or other additives as well as regular sanitisation (Khan et al., 2017). Cumulatively, it has been proposed that this process could select for resistant strains that persist in the processing environment, particularly within biofilms, in turn re-contaminating finished foods (Walsh and Fanning, 2008).

Biofilms can be formed at many points in the food production process (Maes et al., 2019; Wagner et al., 2020), beginning with colonisation of raw plant materials and animal tissues during primary production. Biofilms can also form on man-made materials such as plastic or steel food-contact surfaces through preconditioning with biomolecules which facilitate attachment and extracellular matrix production by bacteria. Biofilm dwelling can provide a degree of shielding and protection from physical forces such as desiccation and shear, or biocides, facilitating greater resistance, particularly in mixed biofilms (Giaouris et al., 2015).

Biofilm formation has traditionally been viewed as a negative bacterial trait in the food industry, due to its association with specific spoilage organisms (SSO) and pathogenic bacteria that can re-contaminate foods post-processing, resulting in food spoilage and outbreaks of food-borne illness, as well as acceleration of ablation and corrosion of food-contact surfaces. The impact microbial transmission from biofilms into finished food products is of particular concern given the rising popularity of minimally processed and ready-to-eat foods (Meireles et al., 2018). Further, biofilms are increasingly recognised to promote antimicrobial tolerance (Uruén et al., 2020) as well as act as focal points for HGT between members of the population contained within (Abe, Nomura and Suzuki, 2020), potentially exacerbating the challenge of AMR.

However, biofilms also underpin and drive many key biotransformations in food and QS plays a role in at least some of these. Biofilm formation is thought to be crucial for the growth of milk kefir grains, which is catalysed by autoaggregation between LAB such as *L. lactis, Leuconostoc mesenteroides, Lentilactobacillus kefiri*, and *Lentilactobacillus sunkii* followed by synergistic kefiran production (EPS) by LAB and acetic acid bacteria (AAB), with cross-kingdom networking by yeasts such as *Kluyveromyces marxianus* (Wang et al., 2012; Han et al., 2018). Water kefir has received less attention than its dairy counterpart, but likely recapitulates this paradigm, with dextran-producing LAB thought to play a key role in grain growth (Fels et al., 2018; Guzel-Seydim et al., 2021). QS is likely to receive increased attention in this area, both for its relevance to the production of fermented foods with a biofilm quality such as kefirs, as well as its broader technological relevance in modulating the production of microbially synthesised extracellular polysaccharides.

Freeze-drying survival rates are also a concern in the commercial production of probiotic products. Notably, modulation of osmotic stress exposure in *L. plantarum* LIP-1 was found to enhance AI-2 production and promote biofilm formation by the strain, enabling it to better withstand the freeze-drying process (Jingjing et al., 2021). As subsequently outlined in the context of the human gut, biofilm formation and linked traits such as EPS production are increasingly being proposed as probiotic traits as they may enhance the survival of probiotic strains throughout gastrointestinal transit (Kelly et al., 2020).

Bacteriocin production

Amongst the bacterial processes regulated by QS in foods, bacteriocin production has received particular attention due to its application in the production of food and feed, as well as

antimicrobial therapy. Bacteriocins are a group of ribosomally synthesised peptides with antimicrobial activity, notably mediating interspecies competition due to immunity genes in the producer strain (Cotter et al., 2005). It has been approved as a natural biopreservative in foods by both the FDA in the US and EFSA in the EU and extensively investigated for applications in dairy foods, as well as meat, seafood and vegetable-based foods (Gharsallaoui et al., 2016).

As outlined previously, some AIP fulfil a dual role as both QSM and antimicrobial peptides, including lantibiotics (class I bacteriocins) such as nisin and lacticin 481, produced by some strains of *Lactococcus lactis* and subtilin, produced by specific strains of *B. subtilis* (Kleerebezem, 2004; Gobbetti et al., 2007). In the case of class II bacteriocins, such as certain plantaricins in *Lactiplantibacillus plantarum,* salivaricins in *Ligilactobacillus salivarius* and some carnobacteriocins produced by members of the genus *Carnobacterium*, a dedicated peptide pheromone is responsible for regulating transcription of the bacteriocin genes, forming a three-component system (Leisner et al., 2007; Maldonado-Barragán et al., 2009).

Bacteriocin production is by now well-established as an attractive feature in potential probiotic strains. In the context of interspecies interactions and microbial succession, bacteriocin production is proposed to enhance the viability of producer strains, particularly in complex ecosystems (Maldonado-Barragán et al., 2013). *In-situ* production of certain bacteriocins within foods can control the growth of spoilage and pathogenic microorganisms due to their specificity of action and non-toxic effect on the host (Dobson et al., 2012). Moreover, QS systems offer the potential to fine-tune the dynamics of bacteriocin synthesis. Future studies could examine in greater detail the dynamics of co-culture induction in complex communities, as reported in a strain-specific manner in *L. plantarum* (Maldonado-Barragán et al., 2013), with a view to optimising *in-situ* production of bacteriocins.

Quorum sensing in the human gut microbiome

As previously described, the relatively high microbial load in the gut as well as the associations between the gut microbiome and health have made it a point of focus for human microbiome studies. The gut microbiome refers broadly to the gastrointestinal tract, primarily comprising the stomach, small and large intestine, sometimes also including the oral cavity and the microbial communities that become established within. The niches provided by the various compartments are highly dynamic with respect to changes in pH, oxygenation, nutrient availability, host–microbe interactions and microbial load, rendering community assemblage an incredibly complex ecological process (Donaldson et al., 2016). Additional spatial organisation is conferred by the distinct microenvironments provided by the gut lumen, mucin layer, intestinal crypts and mucosal epithelium.

Recent studies have highlighted the biofilm-like structure of mucus-associated bacterial communities in the gut lumen (Duncan et al., 2021), suggesting the likely prevalence of QS considering its previously established link with biofilms. Studies in this field are challenging due to the well-established inter-individual variation present even between 'healthy' individuals (Jones et al., 2018). Gaps remain in understanding the relative significance and importance of changes in composition and functionality of microbiomes as well as the ecological forces influencing assembly, maintenance and temporal fluctuation.

Perhaps the clearest instance of an interaction between microbiota present in a consumed food and the gut microbiome is food-borne illness. Many hurdles are mounted against invading bacterial pathogens, both from the resident microbiome (a phenomenon termed 'colonisation resistance') as well as host cells and immune mechanisms, all of which must be overcome to establish infection (Buffie and Pamer, 2013). In this delicate balance between colonisation, invasion and regulation, many bacterial pathogens utilise QS, at least in part, to regulate the expression of clinically relevant virulence factors that are metabolically costly and less strategic at low population densities (Rutherford and Bassler, 2012). Indeed, certain components of the human immune system are primed to detect and respond to pathogens and their virulence factors, which will be discussed below.

Quorum sensing molecules detected in the human gut microbiome

Relatively few studies have evaluated the presence of QSM within the human gut microbiome, due to the technical challenges associated with chromatography on luminal samples and low abundance of the molecules (Xue et al., 2021). Sampling of AHL-QSM at relevant temporal and spatial points is challenging due to their propensity to degrade at biological pH shortly after secretion, either spontaneously to tetramic acid, or by enzymatic hydrolysis of the lactone ring, leading their concentration to reflect temporal rather than historic population information (Peyrottes et al., 2020). Figure 3 provides an overview of the findings reported to date regarding QSM in the human gut.

With respect to the oral cavity, high-performance liquid chromatography-coupled mass spectrometry (HPLC-MS) has been used to detect AHL-QSM in extracted teeth and saliva samples, with C8-HSL being most abundant and present in all saliva samples and most of the extracted teeth, whilst C14-HSL and C18-HSL were present at lower levels (Muras et al., 2020).

Mass Spectrometry (MS) has been used to detect the novel QSM 3-oxo-C12:2, a derivative of the AHL 3-oxo-C12 bearing 2 unsaturations, in human faeces (Landman et al., 2018). It was detected at higher levels in both healthy control and Inflammatory Bowel Disease (IBD) patients in remission versus those in active flare and was correlated with higher abundances of Bacillota, especially *Faecalibacterium prausnitzii*, and lower abundances of

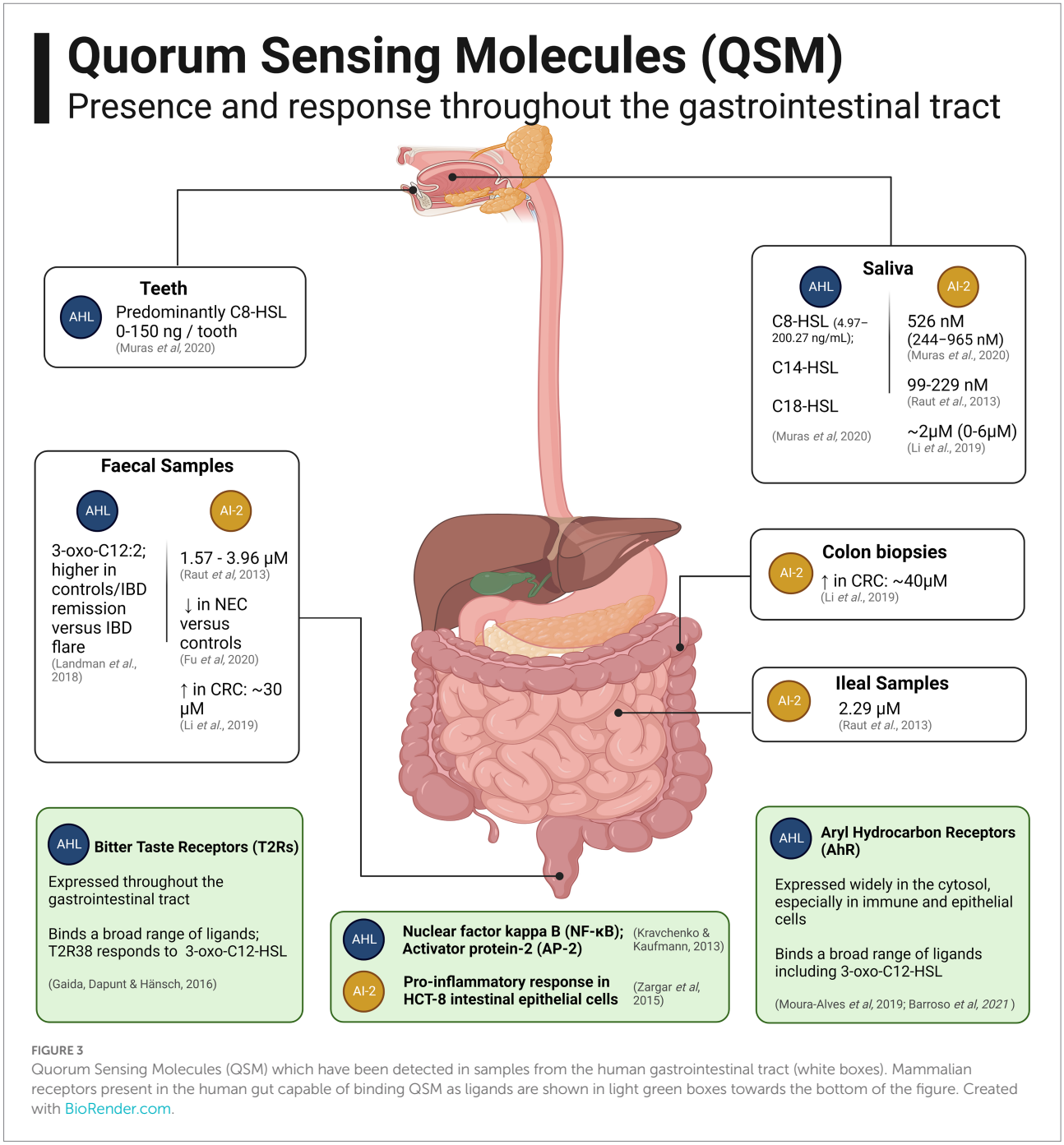

FIGURE 3
Quorum Sensing Molecules (QSM) which have been detected in samples from the human gastrointestinal tract (white boxes). Mammalian receptors present in the human gut capable of binding QSM as ligands are shown in light green boxes towards the bottom of the figure. Created with BioRender.com.

E. coli. 3-oxo-C12:2 also displayed anti-inflammatory properties and an ability to limit cytokine-induced tight junction disruption in a Caco-2/TC7 model when compared with the native 3-oxo-C12 from *P. aeruginosa* (Aguanno et al., 2020). The presence and presumptive bioactivity in the human gut microbiome of AHLs bearing such unsaturations is intriguing, as unsaturated pheromones are generally uncommon and their production had otherwise only been reported in the marine *Roseobacter* clade (Ziesche et al., 2015; Peyrottes et al., 2020). The producer of the precursor AHL and unsaturations, as well as its precise biological effects, remain unidentified to this date. A novel UPLC-MS/MS method has recently been developed to detect AHL-QSM in caecal, sera and liver samples of germ-free, conventional and *Citrobacter rodentium*-infected mice (Xue et al., 2021). This study demonstrated the translocation of bacterial AHL-QSM across the intestinal barrier throughout host tissues and the perturbation in AHL profiles provoked by *C. rodentium* infection.

Relatively few studies have investigated AI-2 levels in the gut microbiome. Liquid chromatography–tandem mass spectrometry was used to detect AI-2 produced by the oral microbiota in saliva samples (Campagna et al., 2009) *via* the linear precursor molecule 4,5-dihydroxy-2,3-pentanedione (DPD). Concentrations

fluctuated considerably between participants (average 526 nM, range 244–965 nM), potentially highlighting inter-individual variation or temporal fluctuations in the oral microbiome (Rickard et al., 2008). AI-2 also appears to mediate inter-kingdom interactions in the human mouth in that, for example, hyphal development in the fungal pathogen *Candida albicans* is inhibited by AI-2 produced by *Aggregatibacter actinomycetemcomitans* (Bachtiar et al., 2014). Beyond the oral cavity, AI-2 has been detected in ileal and rectal samples taken during endoscopy from participants with and without IBD (Raut et al., 2013). In the gut, one study found diminished AI-2 levels in the acute phase of Necrotising Enterocolitis (NEC), a serious gastrointestinal disease primarily affecting infants, consequentially proposing the QSM as a potential biomarker for early detection and prophylaxis (Fu et al., 2020). In contrast, AI-2 levels were observed to be significantly higher in faecal samples and biopsies from patients with Colorectal Cancer (CRC) versus those of adenomas/healthy controls (Li et al., 2019a,b).

AI-3 is the most recently described QSM thought to be found in the gut. AI-3 family pyrazinones are produced by a wide range of bacteria relevant to the gut microbiome, as well as in pathogen-free mice colonised with *E. coli* BW25113, although human microbiome samples have not been interrogated to date using analytical techniques (Kim et al., 2020). Similarly, although direct quantification of other QS systems has not to our knowledge been reported, *in silico* predictions *via* the QSHGM database (Wu et al., 2021b) reveal presence of photopyrone, dialkylresorcinol and DSF genetic circuits in a wide range of gut microbes, although this remains to be evaluated using analytical techniques.

Taken together, QS systems appear to be active at various points of the human gut microbiome as are several distinct strategies by the eukaryotic host to monitor and respond to bacterial QSM. Future studies leveraging novel sampling approaches can further clarify the relative importance and clinical significance of the various systems, particularly regarding the interactions between commensals and opportunistic pathogens introduced to the gut microbiome.

Qs influence on collective bacterial behaviours in the gut

Lifestyle switching, through environmental and quorum sensing, has been proposed to favour the survival and colonisation of introduced species in the human gut (Mukherjee and Bassler, 2019). QS can also facilitate the establishment of collective behaviours of microbial populations and communities within the gastrointestinal tract, potentially affecting community assemblage and host physiology. AI-2 systems are most commonly implicated in this context, in both positive and negative senses.

Vibrio cholerae provides one of the clearest examples of lifestyle switching in order to adapt to and survive harsh environmental conditions in the environment and in the gut using QS. It forms aggregates of biofilms when surrounded by other *V. cholerae* cells and switches to a dispersal strategy to escape the matrix when surrounded by high numbers of 'other' non-*V. cholerae* cells. (March and Bentley, 2004; Bari et al., 2013; Bridges and Bassler, 2021). It has recently been proposed that *V. cholerae* senses its own quorum *via* CAI-1 QSM in conjunction with the biogenic amine norspermidine, which is relatively specific to *V. cholera*, whilst other populations are monitored using AI-2 and spermidine, a ubiquitous biogenic amine found throughout the human gut (Bridges and Bassler, 2021). CAI-1 has also been demonstrated to enhance the virulence of the non-producer Enteropathogenic *E. coli* (EPEC), possibly contributing to co-infection of the host (Gorelik et al., 2019). AI-2 also modulates sporulation and biofilm formation in the pathogenic *Clostridium difficile,* facilitating switching between dormancy, vegetative growth, virulence, immune evasion and antibiotic tolerance (Đapa et al., 2013; Desai and Kenney, 2019; Tijerina-Rodríguez et al., 2019). Additionally, *C. difficile* uses an *agr* system mediated by thiolactone QSM to regulate production of the toxins TcdA and TcdB which compromise the host epithelial barrier in *C. difficile* infection (CDI; Darkoh et al., 2015). Certain *C. difficile* phage appear to bear and disseminate *agr* variants amongst their hosts, highlighting the complexity of microbiome dynamics and the difficulty in limiting investigations to single kingdoms (Hargreaves et al., 2014). This also supports the recent implication of bacterial QS as a broad mediator of phage-host interactions in the gut (León-Félix and Villicaña, 2021). Such insights certainly require additional scrutiny, but could prove significant in the development of phage therapy.

There are also many instances where QS activity is associated with positive compositions or outputs from microbial communities. One standout study found that increasing local levels of AI-2 in a mouse model of antibiotic treatment promoted the recovery of Bacillota (previously known as Firmicutes) whilst hindering the expansion of Bacteroidota (previously known as Bacteroidetes; Thompson et al., 2015). As previously described for food-borne probiotic strains, AI-2 QS was also shown to positively influence colonisation of a probiotic *Bifidobacterium breve* UCC2003 in the gut (Christiaen et al., 2014). Indeed, *luxS*-deficient *Streptococcus mutans* mutants incapable of producing AI-2 were found to upregulate carbohydrate metabolism and ABC transporters, highlighting the potential for QS to govern individual behaviours as well as collective ones (Yuan et al., 2021) and underlining the necessity for systems biology approaches when evaluating proposed therapeutic applications of QSI.

Detection of bacterial QS by the human host

Bacterial quorum sensing may also contribute to host–microbe interactions as evidenced by the existence of pathways in eukaryotic multicellular organisms to detect and even interfere with microbial communications (Aframian and Eldar, 2020).

Indeed, the broader field of microbial endocrinology abounds with examples of crosstalk between host hormones and bacterial signalling systems, perhaps unsurprisingly considering the hormone-like properties of bacterial QSM (Neuman et al., 2015; Li et al., 2019a). Taken together, this is suggestive of co-evolution and adaptation by the eukaryotic host to monitor for AHL production and coordinate a defensive response.

AHL-QSM are small, lipophilic molecules and although poorly soluble in water, their diffusion into eukaryotic cells has recently been demonstrated, with interaction with intracellular targets also considered possible (Kamaraju et al., 2011; Peyrottes et al., 2020). Molecular self-assembly in aqueous solution into micelles and vesicles has been observed for 3-oxo-C8-AHL, 3-oxo-C12-AHL, C12-AHL and C16-AHL, which may guide our understanding of the kinetics of secreted QSM (Gahan et al., 2020). Bacterial outer membrane vesicles (OMVs) have also been proposed to traffic quorum sensing molecules within and between bacterial microcolonies, circumventing the issue of hydrophobicity (Toyofuku et al., 2017). OMVs have also been detected in host blood, heart and urine samples, being able to cross the mucus layer and epithelium of the gut (Stentz et al., 2015). Whilst OMVs have been studied to the greatest extent in the context of Gram-negative pathogens, attention is turning to their significance in probiotic and commensal strains, including *E. coli* Nissle 1917 and ECOR63, respectively (Alvarez et al., 2016), however more precise characterisation of their composition and relevance to QS is required.

Bitter taste receptors (T2Rs) belong to the G protein-coupled receptor group and were initially studied in the context of taste, being highly expressed on the tongue. However they have been found to be expressed in a variety of other sites including the upper respiratory tract and gastrointestinal tract, suggesting a broader role (Verbeurgt et al., 2017). Indeed, there is evidence of variable interaction of these receptors with numerous bacterial metabolites including AHLs. T2R38 is one example that is expressed throughout the gastrointestinal tract on intestinal epithelial cells (Behrens and Meyerhof, 2011; Karlsson et al., 2012) and activated by the AHL-QSM 3-oxo-C12-HSL in myeloid cells, enhancing phagocytic activities (Gaida et al., 2016) – although the myeloid cells in the latter study were derived from patient biopsies of osteomyelitis. Yet another study, using a heterologous expression system, found that T2R38 did not respond to 3-oxo-C12 HSL nor the cyclic AIP Agr-D1 thiolactone and CSP-1, but was activated by a range of bacterial metabolites including acetone, 2-butanone, 2-pentanone, 2-methylpropanal, dimethyl disulphide, methylmercaptan, and γ-butyrolactone (Verbeurgt et al., 2017). Methodological differences between the studies may account for this discordance.

Pro-inflammatory cascades have also been reported by AHL interaction with nuclear factor kappa B (NF-κB) and activator protein-2 (AP-2) receptors (Kravchenko and Kaufmann, 2013). The human aryl hydrocarbon receptor (AhR) is present in the human gut and interacts with a wide array of microbial metabolites and was shown to detect and react to relative abundances of AHLs, quinolones and phenazines produced by *P. aeruginosa* to manage immune response over the course of infection (Moura-Alves et al., 2019; Barroso et al., 2021).

In contrast to AHL-QSM, unmodified AI-2 is hydrophilic and does not appear to penetrate the plasma membrane, although heptyl modifications increase its affinity (Kamaraju et al., 2011). *In vitro* exposure of HCT-8 intestinal epithelial cells to AI-2 was found to provoke an inflammatory response (Zargar et al., 2015); this interaction could be studied in a more representative model system such as intestinal organoids or *in vivo*. Recent evidence suggests that mammalian epithelial cells can produce an AI-2 analogue that may mimic and interfere with bacterial QS, although the structure has yet to be determined (Ismail et al., 2016).

Quorum sensing inhibition in food microbiomes

Given the association between QS and bacterial biofilm formation and food spoilage activity, QSI has been proposed as a potential strategy to positively regulate bacterial phenotypes and improve food safety and quality. In fact, many foods themselves exhibit QSI activity associated with defence systems in plant/animal tissue or with the presence of microorganisms that have developed mechanisms to interfere with QS activity of neighbouring species.

Quorum sensing systems are interdependent and complex—the field of QSI can generally benefit from the application of a systems biology approach to understand the network of interactions occurring within a particular microbiome. As applied to food production systems, QSI interventions may need to be timed to suppress bacterial QS at critical control points in the food chain, as opposed to their constitutive deployment, or targeted against specific bacterial species implicated in spoilage or pathogenesis whilst maintaining the structure of the overall food microbiome.

QSI produced in microbe-microbe interactions in food microbiomes

Several instances of QSI activity in foods are attributed to members of food microbiomes. Many quorum quenching (QQ) enzymes belonging to AHL lactonase, acylase and oxidoreductase families have been identified, for the most part being isolated in soil and marine metagenomes, plant symbionts and pathogenic bacteria (Bijtenhoorn et al., 2011; Fetzner, 2015). Figure 4 provides an overview of the source and structures of some prominent examples of QQ enzymes and QSI compounds. The majority of QSI discovered to date are active against AHL-QSM; to our knowledge, only one AI-2 QQ enzyme has been identified to date, originating in a soil metagenomic bank and hypothesised to

reduce an AI-2 precursor, 4-hydroxy-2,3-pentanedione-5-phosphate, to the inactive derivative 3,4,4-trihydroxy-2-pentanone-5-phosphate (Weiland-Bräuer et al., 2016). For an extensive list of microbially derived QQ enzymes, the reader is directed to a comprehensive review (Sikdar and Elias, 2020).

With that being said, food microbiomes have yielded some novel QSI agents in recent years, particularly QQ enzymes as shown in Figure 3. An AHL acylase with was recently characterised in a *Komagataeibacter europaeus* strain isolated from grape vinegar (Werner et al., 2021), complementing an earlier report of another putative AHL acylase in a *S. epidermidis* strain isolated from fermented soybean curd (Mukherji and Prabhune, 2015). In the latter, the authors propose QQ as a possible probiotic trait in food fermentations to reduce overall concentrations of AHL-QSM. Another study demonstrated the potential of *in silico* screening through mining of a Mao-tofu metagenome, discovering a novel AHL lactonase (aii810) active at low temperatures (Fan et al., 2017).

As AHL-QS producers account for a large proportion of the burden of spoilage and pathogenesis in aquaculture, this area has received significant attention and yielded an array of novel AHL-QQ enzymes. Aquaculture and fish gut microbiome isolates including *Bacillus* sp. QSI-1, *Bacillus licheniformis* T-1 and *Enterococcus faecium* QQ12 have been identified as potential probiotic feed ingredients due to their potential modulatory role for the AHL-QSM profile of the fish gut microbiome (Chu et al., 2014) and protecting against *A. hydrophila* infection through AHL lactonase activity of YtnP (Peng et al., 2021) and autoinducer inactivation (*aiiA*) homologues (Vadassery and Pillai, 2020). Another study found widespread AHL-QQ activity in bacterial isolates from rainbow trout tissue, including members of the genera *Bacillus*, *Enterobacter*, *Citrobacter*, *Acinetobacter*, *Agrobacterium*, *Pseudomonas* and *Stenotrophomonas*. Characterisation showed variability in both enzymatic and non-enzymatic modes of action, highlighting the diversity of QQ activity observed in the comparably simple fish gut microbiome, as well as a propensity for cell-bound activity rather than secretion (Torabi Delshad et al., 2018).

Metagenomic studies have revealed the presence of potential quorum quenching determinants in dairy products and production plants (Alexa Oniciuc et al., 2020); food microbiomes may represent in this sense a relatively untapped reservoir for novel QSI determinants. Indeed, there are numerous reports of culture extracts from specific LAB strains exerting anti-biofilm, anti-virulence and QSI effects on other bacterial species; for instance, cell free supernatants of LAB isolated from fermented grape interfere with AI-2 quorum sensing and biofilm formation in *Salmonella* Typhi and S. Typhimurium (Pelyuntha et al., 2019) and supernatants of LAB strains isolated from beef and cow's milk inhibited pyocyanin production in a *P. aeruginosa* isolate of rancid butter and diminished violacein production in *C. violaceum* (Aman et al., 2021). The molecular mechanism of this widespread yet strain-specific activity remains unelucidated to date, but is thought to involve, at least in part, acid production along with small molecules secreted by the LAB strains. Indeed, another study evaluated both acidic and neutralised supernatants of LAB strains, finding that neutralised supernatants more weakly inhibited biofilm formation in *P. aeruginosa* compared with acidic fractions; moreover, only acidic supernatants interfered with the *las* and *rhl* quorum sensing systems (Rana et al., 2020).

Intriguingly, many examples of QSI arise amongst eukaryotic members of food microbiomes, specifically fungi. AI-2 QSI activity of brown algae has been attributed not to the plant cells but rather to bacterial and fungal endophytes (Tourneroche et al., 2019). Recently, a novel QSI compound (tryptophol acetate) was discovered to be produced by the yeast *Kluyveromyces marxianus* present in a Tibetan milk kefir (Malka et al., 2021). It was found to interfere with bacterial AHL and CAI-1 signalling, with possible applications for bioprotection of foods and prevention of proliferation of enteric pathogens such as *V. cholerae* (CAI-1). Again, this highlights the need for systems biology approaches that encompass all relevant kingdoms of life, not solely bacteria, when studying QS in a microbiome context.

Lastly, purified microbially derived enzymes can be incorporated into food formulations or cleaning protocols for food processing plants. To our knowledge, just one study has examined the use of enzymes with quorum quenching activity in foods. In this case, it was found that treatment with a commercial preparation of 7 peptidases and 1 amylase (Flavourzyme) decreased the relative expression of genes involved in quorum sensing (Nahar et al., 2021). However, this study only examined AI-2 related transcription, which could be due to suppression of the AMC (Activated Methyl Cycle) as a result of global metabolic perturbation. Treating raw sturgeon with AiiAAI96 (AHL lactonase) and nisin (bacteriocin) prior to vacuum packaging extended the product shelf life by 5 days (Gui et al., 2021), showing promise as a biopreservative targeting both Gram-positive and negative SSO. Heterologous expression of QQ enzymes *in situ* offers another potential route for biotechnological applications, as exemplified by the use of a *Lacticaseibacillus casei* strain, often used in the dairy industry, to express the AHL lactonase AiiK which can attenuate virulence in *Aeromonas hydrophila* (Dong et al., 2020) and *P. aeruginosa* (Dong et al., 2018).

QSI By components of food matrices

In addition to microbially produced QSI molecules, it has been established that many components of food matrices can, to some degree, modulate bacterial QS. A brief overview of prominent examples are provided in Table 2. In some cases, such as the organic acids, they may affect the stability of the QSM themselves or downregulate their synthesis by the producer strain due to acid stress. In other instances, such as fatty acids, the QSI phenomenon is thought to arise due to their structural similarity to the fatty-acid-derived QSM including AHLs and DSF. Indeed,

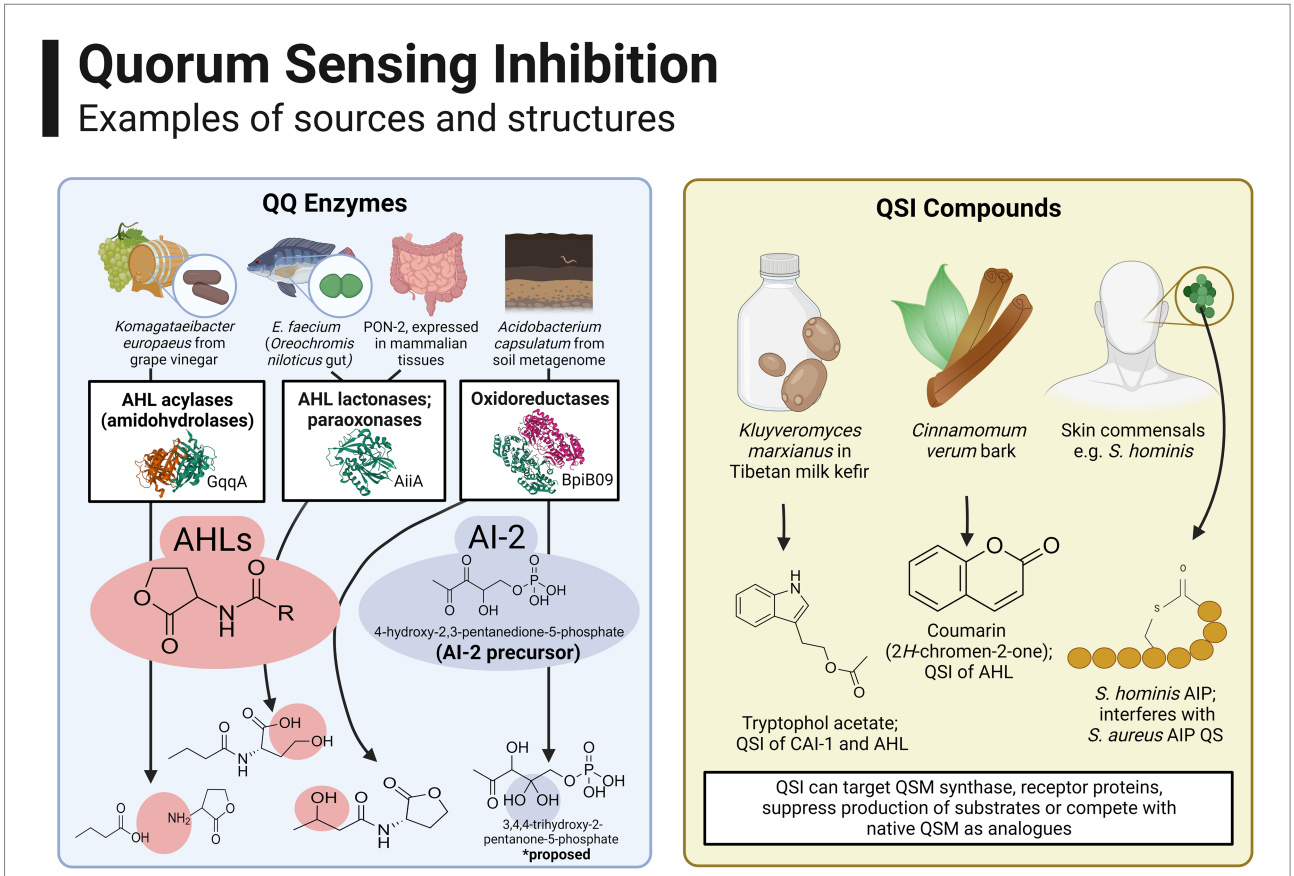

FIGURE 4
Overview of the source and structures of some prominent examples of QQ enzymes and QSI compounds. Many QQ enzymes have been described for AHLs, such as the AHL acylase GqqA reported in *Komagataeibacter europaeus* isolated from grape vinegar [Werner et al., 2021; Image from the RCSB PDB (rcsb.org) of PDB ID 7ALZ], AHL lactonases such as AiiA from *E. faecium* isolated from the gut of *Oreochromis niloticus* [Vadassery and Pillai, 2020; Image from the RCSB PDB (rcsb.org) of PDB ID 7L5F] and paraoxonase enzymes which are expressed widely in mammalian tissues (Peyrottes et al., 2020). Oxidoreductase enzymes have been isolated from environments such as soil and activity has been reported against AHLs (Bijtenhoorn et al., 2011; Image from the RCSB PDB (rcsb.org) of PDB ID 3RKR) as well as AI-2 (Weiland-Bräuer et al., 2016). Examples of non-enzymatic QSI include tryptophol acetate, active against CAI-1 and AHLs (Malka et al., 2021), coumarin and derivatives, which can interfere with AHL-QS (Gutiérrez-Barranquero et al., 2015) and AIP analogues produced by closely related staphylococcal species (Peng et al., 2019). Created with BioRender.com.

in the case of ascorbic acid (vitamin C) the mechanism of action could arise due to its effect on pH or due to the structural similarity between it (5*S*)-5-[(1*R*)-1,2-Dihydroxyethyl]-3,4-dihydroxy-2(5*H*)-furanone) and other furanones – such disambiguation will be critical for harnessing it as a potential QSI agent.

Generally, plant-based foods do not appear to support bacterial quorum sensing activity to the same extent as animal-based ones (Medina-Martínez et al., 2006). This phenomenon is hypothesised to arise from co-evolutionary forces between plants and microorganisms and is primarily mediated by inhibitory plant secondary metabolites including furanones, phenolics and other bioactives that can act as QSM analogues (Rodrigues et al., 2016; Zaytseva et al., 2019; Pun et al., 2021). This could suggest the potential for plant-derived ingredients to generally disrupt bacterial QS activity or support their incorporation in food formulations to modulate the food microbiome of the product. However due to the general bioactivity of plant secondary metabolites, possible off-target effects should be assessed and effective QSI activity established in the context of the matrix effects and digestion.

Whilst food matrix-derived peptides may be similar in size and sequence to known QS AIP, no QSI peptides have been described to date in foods. Bioactive peptides are intriguing due to their small size, which allows them to diffuse relatively easily through food matrices and biofilms; additionally, they are amenable to bioengineering against resistance as they are gene-encoded (Bhutia and Maiti, 2008; Field et al., 2019). QSI AIP have been described in coagulase-negative staphylococci in the skin microbiome with activity against *S. aureus* (Peng et al., 2019) – this could suggest that intra-genus competition within food microbiomes represents an opportunity for future mining and discovery of potential therapeutic agents with direct applications in food production.

This provides a new perspective on food processing and formulation and the impact of ingested foods on the gut

TABLE 2 Overview of components of food matrices which can mediate bacterial Quorum Sensing Inhibition (QSI) or related phenotypes, such as biofilm inhibition and sporulation.

Food component	Examples	QS system or phenotype affected	Bacteria affected	Concentration	References
Organic acids	Lactic acid	AHL; Anti-biofilm	*Chromobacterium violaceum* CV026; *E. coli*; *Salmonella* sp.	0.2–1%	Amrutha, Sundar and Shetty, (2017)
	Acetic acid	AHL; Anti-biofilm	*C. violaceum* CV026; *E. coli*; *Salmonella* sp.	1–1.5%	
	Citric acid	AHL; Anti-biofilm	*C. violaceum CV026, E. coli*; *Salmonella* sp.	1.5–2%	
	Malic acid	AI-2	*E. coli O157:H7*; *S.* Typhimurium	4%	Almasoud et al., (2016)
	Ascorbic acid (vitamin C)	AHL	*P. aeruginosa*	5–12·5 mg/ml	El-Mowafy, Shaaban and Abd El Galil, (2014); Pandit et al., 2017)
		Sporulation; AI-2	*C. perfringens,*	10 to 30 mM (sporulation); 300 mM (AI-2)	Novak and Fratamico, (2006)
		AI-2	*E. coli* EMC17	125 mM	Shivaprasad et al., (2021)
		AIP (ComC)	*B. subtilis*	10 to 40 mM	Pandit et al., (2017)
Long Chain Fatty Acids	Mono-unsaturated palmitoleic myristoleic acids	AHL	*Acinetobacter baumannii*	0.02 mg/ml	Nicol et al., (2018)
(LCFAs)	Linoleic acid	DSF	*P. aeruginosa*	10 µM	Kim et al., (2021)
	Fatty acids produced by fungal endophyte of *Coriandrum sativum*	Anti-biofilm	*S. mutans*	31.3 mg/l	Abdel-Aziz, Emam and Raafat, (2020)
	Oleic acid (Cis-9-octadecenoic acid)	Anti-biofilm	*S. aureus*	0.1% v/v	Stenz et al., (2008)
		AHL	*C. violaceum* CV026;	3.696 mg/ml	Singh et al., (2013)
	Palmitic acid (C16:0), Stearic acid (C18:0), Oleic acid (C18:1ω9), Linoleic acid (C18:2ω6)	AI-2	*V. harveyi, E. coli*	1–10 mM	Soni et al., (2008)
Endocannabinoids	Endocannabinoid 2-AG (arachidonic acid derivative)	AI-3 (*via* QseC)	EHEC, *Citrobacter rodentium*	Not quantified – 2-AG levels were elevated in intervention group *via* knockout of monoacylglycerol lipase (Mgll)	Ellermann et al., (2021)
Furanones	Brominated, halogenated and natural forms in seaweeds, tomatoes, strawberries and other berries; synthetic derivatives	AHL	*P. aeruginosa*	3.125–50 µM	Colin Slaughter, (1999); Manefield et al., (1999); Proctor, McCarron and Ternan, (2020)
		AI-2	*Vibrio harveyi, Vibrio parahaemolyticus*	20 mg/l	Defoirdt et al., (2006)
		Anti-biofilm	*S.* Typhimurium; *L. monocytogenes;*	10 to 15 µM (*S.* Typhimurium); 0.05 mmol/l at 24 h, 2 mmol/l at 48 h (*L. monocytogenes*)	Janssens et al., (2008); Rodríguez-López et al., (2019)
Coumarin	Dihydrocoumarin	Anti-biofilm	*Hafnia alvei*	3.2 mM	Hou et al., (2017)
		AHL	*C. violaceum* CV026	6.3 mM	
	Coumarin from *Cinnamomum verum*	AHL	*P. aeruginosa* (*pqsA, rhlI, lasI*)	1.36 mM	Gutiérrez-Barranquero et al., (2015)
Vitamin B2	Riboflavin and derivatives	AHL (LasR system)	*P. aeruginosa*	200 µM (effective soluble concentration)	Rajamani et al., (2008)
Steviol glycosides	Steviol	AHL (*las* / *rhl* systems)	*E. coli* K802NR-pSB1075 (*las*); *P. aeruginosa*	0.26–0.52 mM (*las*); 0.0325–0.52 mM (*rhl*)	Markus et al., (2020)
	Reb A		PAO-JP2 (pKD-rhlA) (*rhl*)	0.019375–0.31 mM (*rhl*)	
	Stevioside			0.5–1.0 mM (*las*); 1 mM (*rhl*)	

10.3389/fmicb.2022.1002185

microbiome. Whilst many components pertain to raw food ingredients derived from plants and animals, many of these such as organic acids, fatty acids and vitamins can themselves be microbially synthesised and are of interest in their own right in the context of human nutrition. Aromatic and volatile compounds are overrepresented, with many QSI compounds also having a role in flavouring such as Maillard reaction-derived furanones (Wang and Ho, 2008) and lactone derivatives such as coumarins. Understanding the directionality of these effects, particularly with respect to stability and efficacy in food matrices and withstanding transit through the digestive tract, will be of key importance in the development of applications in the food formulation space.

Quorum sensing inhibition in the human gut microbiome

As previously outlined, quorum sensing has been implicated in the onset of pathogenesis in infections and is thought to influence community composition in other human-associated microbiomes such as those of the oral cavity, lung, skin, urinary and reproductive tracts (Bradshaw and Sobel, 2016; Cole et al., 2018; Scoffone et al., 2019; Williams et al., 2019). As some pathogenic bacteria utilise QS to time their deployment of virulence factors, it has been proposed that QS activities of neighbouring bacteria in the gut microbiome could interfere with this timing, either by QSI or by prematurely inducing the quorum level with species-agnostic QSM (Cho et al., 2021). Unsurprisingly, many instances of QSI activity can be observed in the crosstalk between host and microbe and in communications within bacterial communities.

QSI enzymes in host tissue

Paraoxonase (PON) enzymes are expressed widely across human tissues, including the intestines and can inactivate AHL-QSM through hydrolysis of the lactone ring moiety (Camps et al., 2011; Peyrottes et al., 2020). Like many QQ enzymes, PON have a broad substrate specificity and can also inactivate esters, e.g. oestrogen esters, lactones or organophosphates, highlighting the need to consider off-target effects in evaluation of QS-based therapies.

QSI produced in microbe-microbe interactions in the human gut

Microbe-microbe interactions in the human gut can involve cooperation, through sharing of resources and cross-feeding, as well as antagonism, in efforts to outcompete neighbouring cells. Just as in food microbiomes, QS appears to be widespread amongst bacteria in human gut microbiomes and likely, to some degree, mediates interspecies interactions therein. Indeed, AI-2 was shown to orchestrate both cross-feeding and also QSI in co-culture of *C. acetobutylicum* and *D. vulgaris* Hildenborough, depending on the extent of nutrient limitation in the system (Ranava et al., 2021), highlighting the conditionality which can be present in bacterial cooperation.

Overall, there are relatively fewer instances of QQ enzymes or QSI compounds being reported from the gut microbiome, possibly due to the focus of bioprospecting efforts on natural environments, as well as the difficulty in successfully culturing gut commensals *in vitro*. However, QSI potential has been established by some studies, for example, in the oral microbiome 60% of recovered bacteria in dental plaque and saliva exhibited AHL-degradation capacity and treatment of mock communities with the broad-spectrum AHL-lactonase Aii20J reduced biofilm formation and altered the overall community composition (Muras et al., 2020). Penicillin V acylases are microbially produced enzymes within the choloylglycine hydrolase family able to inactivate AHL-QSM due to structural similarity with the functional residues of native AHL acylases (Liu et al., 2012; Mukherji and Prabhune, 2015; Daly et al., 2021). To date, however, there are scarce reports of their presence in human gut microbiomes wherein bile salt hydrolases predominate. This highlights the importance of substrate specificity and receptor promiscuity when potentially targeting QS in complex microbiomes such as those of foods and the gut.

In addition to enzymatic QQ, there are several reports of QSM produced by one species acting as analogues for other species, potentially mediating microbe-microbe interactions. Whilst, to our knowledge, no direct examples exist pertaining to the human gut microbiome, there are examples from the human skin and anaerobic waste digestion microbiomes. AIP produced by skin commensals such as coagulase-negative staphylococci including *Staphylococcus hominis* can inhibit the *agr* system of *S. aureus,* reducing the expression of phenol-soluble modulin α (PSMα) which undermines skin barrier integrity (Williams et al., 2019).

Whilst, to our knowledge, no clinical trials have been conducted to date in humans, engineered probiotics are being evaluated to harness QS to promote human health and wellbeing. An *E. coli* Nissle 1917 strain designed to respond to the AHL-QSM $3OC_{12}HSL$ was shown to eliminate and prevent *P. aeruginosa* gastrointestinal infections in animal models (Hwang et al., 2017). In another study using a rational design approach, expression of small peptides resembling LuxS active sites reduced AI-2 activity of aquaculture pathogens *Edwardsiella tarda*, *A. hydrophila* and *V. harveyi* (Sun and Zhang, 2016). Given the ubiquity of AI-2 signalling, this approach clearly offers broad cross-disciplinary applicability.

Another approach involves direct oral administration of purified QQ enzymes such as AHL-lactonase, which resisted digestion and attenuated virulence of *A. hydrophila* in a zebrafish model (Cao et al., 2012). Studies examining feasibility of QSI therapies as applied to human gut microbiomes must take digestive processes into account to ensure delivery to the site of action, as well as evaluating the impact on the structure and composition

microbiome. *Ex vivo* modelling of the human gut offers great promise in modelling the effect of QQ enzyme treatment on the functional and taxonomical composition of the gut microbiome.

Conclusion

The field of quorum sensing research has seen a shift from fundamental to translational science in the past two decades. Nevertheless, despite a preponderance of newly discovered and/or bioengineered quorum sensing inhibitors, several important gaps remain to be addressed so that the therapeutic targeting of quorum sensing systems for the modulation of food and human gut microbiomes may expand as a field.

Firstly, analytical techniques must continue to be developed to augment our capacity to monitor quorum sensing activity and efficacy of quorum sensing inhibitory interventions, particularly for AIP-QS systems and QS within complex matrices such as foods and luminal samples from the human gut. Continued innovation with respect to bioinformatic approaches in particular can further potentiate our understanding of the significance of QS within microbiomes generally, not restricted to those discussed in this review. In this sense, an important consideration in future study design will be the disambiguation of QS gene presence/absence and QS functionality in food and gut microbiomes. Whilst biofilms pose challenges with respect to modelling in a meaningful manner, their ubiquity and potential to act as reservoirs for AMR genetic determinants, food-borne pathogens and specific spoilage organisms are likely to drive efforts to better understand, manage and harness biofilms in foods and in the human gut.

Secondly, many interventions such as specific strains, probiotics, prebiotics and phage, are being investigated with a view to the modulation of complex microbiomes such as those of foods and the human gut. As described earlier, quorum sensing-regulated biofilm production has been shown to improve the survival of probiotic strains during food processing, food fermentations and transit through the human gut. We propose that future studies in this field may consider quorum sensing activity in specific strains as a probiotic trait, where supported by evidence and subject to requisite evaluation. Similarly, strains with QS inhibitory activity could be investigated for their potential clinical or biotechnological applications.

Thirdly, our ability to address AMR can be augmented by better understanding the role of QS in disseminating AMR genes, as well as evaluating QSI agents with a view to the development of anti-virulence therapies and combinatorial agents to enhance the efficacy of existing antibiotics. Here, harnessing systems biology and synthetic ecology approaches will be critical to ensure only the most effective and promising hits are brought through to the preclinical stage.

In conclusion, over the span of a little over 50 years, the field of quorum sensing research has been founded and come to be regarded to be of key importance with respect to microbial physiology in the context of social interactions. Whilst food and human gut microbiomes have received relatively less attention, the accumulated literature points to the presence of quorum sensing molecules and regulated behaviours in these contexts. Further, the abundance and diversity of host receptors to survey bacterial QSM, in addition to the numerous examples of QSI systems across kingdoms of life and environmental niches, has likely arisen due to the ubiquity and evolutionary importance of QS within microbiome science. Addressing the knowledge gaps identified above will help in the critical evaluation of proposed QS and QSI interventions in these contexts, with the potential to positively impact human, animal and ecosystem health.

Author contributions

AF, AA-O, CG, and PC conceived the manuscript. KF wrote the manuscript. AA-O, CG, AF, and PC contributed to the final preparation. All authors contributed to the article and approved the submitted version.

Funding

This research was conducted with the financial support of Science Foundation Ireland (SFI) under Grant Number SFI/12/RC/2273 P2.

Acknowledgments

The authors acknowledge Gloria Spampinato for her contribution towards the manuscript, as well as the constructive feedback received from reviewers during peer review.

Conflict of interest

The authors declare that the research was conducted in the absence of any commercial or financial relationships that could be construed as a potential conflict of interest.

Publisher's note

References

Abdel-Aziz, M. M., Emam, T. M., and Raafat, M. M. (2020). Hindering of cariogenic biofilm by fatty acid Array derived from an endophytic strain. *Biomol. Ther.* 10:811. doi: 10.3390/biom10050811

Abe, K., Nomura, N., and Suzuki, S. (2020). Biofilms: hot spots of horizontal gene transfer (HGT) in aquatic environments, with a focus on a new HGT mechanism. *FEMS Microbiol. Ecol.* 96. doi: 10.1093/femsec/fiaa031

Aframian, N., and Eldar, A. (2020). A bacterial tower of babel: quorum-sensing signaling diversity and its evolution. *Annu. Rev. Microbiol.* 74, 587–606. doi: 10.1146/annurev-micro-012220-063740

Aguanno, D., Coquant, G., Postal, B. G., Osinski, C., Wieckowski, M., Stockholm, D., et al. (2020). The intestinal quorum sensing 3-oxo-C12:2 acyl homoserine lactone limits cytokine-induced tight junction disruption. *Tissure Barr.* 8:1832877. doi: 10.1080/21688370.2020.1832877

Alexa Oniciuc, E. A., Walsh, C. J., Coughlan, L. M., Awad, A., Simon, C. A., Ruiz, L., Crispie, F., et al. (2020) 'Dairy Products and Dairy-Processing Environments as a Reservoir of Antibiotic Resistance and Quorum-Quenching Determinants as Revealed through Functional Metagenomics *mSystems*, 5, e00723-19. doi:10.1128/mSystems.00723-19 2379-5077.

Allen, R. C., McNally, L., Popat, R., and Brown, S. P. (2016). Quorum sensing protects bacterial co-operation from exploitation by cheats. *ISME J.* 10, 1706–1716. doi: 10.1038/ismej.2015.232

Almasoud, A., Hettiarachchy, N., Rayaprolu, S., Babu, D., Kwon, Y. M., Mauromoustakos, A., et al. (2016). Inhibitory effects of lactic and malic organic acids on autoinducer type 2 (AI-2) quorum sensing of Escherichia coli O157:H7 and salmonella typhimurium. *Science* 66, 560–564. doi: 10.1016/j.lwt.2015.11.013

Alvarez, C.-S., Badia, J., Bosch, M., Giménez, R., and Baldomà, L. (2016). Outer membrane vesicles and soluble factors released by probiotic Nissle 1917 and commensal ECOR63 enhance barrier function by regulating expression of tight junction proteins in intestinal epithelial cells. *Front. Microbiol.* 7:1981. doi: 10.3389/fmicb.2016.01981

Alvarez-Ordóñez, A., Coughlan, L. M., Briandet, R., and Cotter, P. D. (2019). Biofilms in food processing environments: challenges and opportunities. *Annu. Rev. Food Sci. Technol.* 10, 173–195. doi: 10.1146/annurev-food-032818-121805

Aman, M., Aneeqha, N., Bristi, K., Deeksha, J., Afza, N., Sindhuja, V., et al. (2021). Lactic acid bacteria inhibits quorum sensing and biofilm formation of Pseudomonas aeruginosa strain JUPG01 isolated from rancid butter. *Biocatal. Agric. Biotechnol.* 36. doi: 10.1016/j.bcab.2021.102115

Amrutha, B., Sundar, K., and Shetty, P. H. (2017). Study on and biofilms from fresh fruits and vegetables. *J. Food Sci. Technol.* 54, 1091–1097. doi: 10.1007/s13197-017-2555-2

Bachtiar, E. W., Bachtiar, B. M., Jarosz, L. M., Amir, L. R., Sunarto, H., Ganin, H., et al. (2014). AI-2 of Aggregatibacter actinomycetemcomitans inhibits Candida albicans biofilm formation. *Front. Cell. Infect. Microbiol.* 4:94. doi: 10.3389/fcimb.2014.00094

Bari, S. M. N., Roky, M. K., Mohiuddin, M., Kamruzzaman, M., Mekalanos, J. J., and Faruque, S. M., et al. (2013). Quorum-sensing autoinducers resuscitate dormant vibrio cholerae in environmental water samples. *Proc. Natl. Acad. Sci. U. S. A.* 110, 9926–9931. doi: 10.1073/pnas.1307697110

Barroso, A., Mahler, J. V., Fonseca-Castro, P. H., and Quintana, F. J. (2021). The aryl hydrocarbon receptor and the gut-brain axis. *Cell. Mol. Immunol.* 18, 259–268. doi: 10.1038/s41423-020-00585-5

Behrens, M., and Meyerhof, W. (2011). Gustatory and extragustatory functions of mammalian taste receptors. *Physiol. Behav.* 105, 4–13. doi: 10.1016/j.physbeh.2011.02.010

Benítez-Cabello, A., Calero-Delgado, B., Rodríguez-Gómez, F., Bautista-Gallego, J., Garrido-Fernández, A., et al. (2020). The use of multifunctional yeast-lactobacilli starter cultures improves fermentation performance of Spanish-style green table olives. *Food Microbiol.* 91:103497. doi: 10.1016/j.fm.2020.103497

Bez, C., Covaceuszach, S., Bertani, I., Choudhary, K. S., and Venturi, V. (2021). LuxR Solos from Environmental Fluorescent Pseudomonads. *mSphere* 6, e01322–e01320. doi: 10.1128/mSphere.01322-20

Bhutia, S. K, Maiti, T. K. (2008). Targeting tumors with peptides from natural sources. *Trends Biotechnol* 26, 210–217.

Bijtenhoorn, P., Mayerhofer, H., Müller-Dieckmann, J., Utpatel, C., Schipper, C., Hornung, C., et al. (2011). A novel metagenomic short-chain dehydrogenase/reductase attenuates Pseudomonas aeruginosa biofilm formation and virulence on Caenorhabditis elegans. *PLoS One* 6:e26278. doi: 10.1371/journal.pone.0026278

Billot, R., Plener, L., Jacquet, P., Elias, M., Chabrière, E., and Daudé, D., et al. (2020). Engineering acyl-homoserine lactone-interfering enzymes toward bacterial control. *J. Biol. Chem.* 295, 12993–13007. doi: 10.1074/jbc.REV120.013531

Blana, V. A., Doulgeraki, A. I., and Nychas, G.-J. E. (2011). Autoinducer-2-like activity in lactic acid bacteria isolated from minced beef packaged under modified atmospheres. *J. Food Prot.* 74, 631–635. doi: 10.4315/0362-028X.JFP-10-276

Bofinger, M. R., de Sousa, L. S., Fontes, J. E. N., and Marsaioli, A. J. (2017). Diketopiperazines as cross-communication - quorum- sensing signals between Cronobacter sakazakii and Bacillus cereus. *ACS Omega* 2, 1003–1008. doi: 10.1021/acsomega.6b00513

Brachmann, A. O., Brameyer, S., Kresovic, D., Hitkova, I., Kopp, Y., Manske, C., et al. (2013, 2013). Pyrones as bacterial signaling molecules. *Nat. Chem. Biol.* 9, 573–578. doi: 10.1038/nchembio.1295

Bradshaw, C. S., and Sobel, J. D. (2016). Current treatment of bacterial vaginosis-limitations and need for innovation. *J. Infect. Dis.* 214, S14–S20. doi: 10.1093/infdis/jiw159

Brameyer, S., Kresovic, D., Bode, H. B., and Heermann, R. (2015). Dialkylresorcinols as bacterial signaling molecules. *Proc. Natl. Acad. Sci. U. S. A.* 112, 572–577. doi: 10.1073/pnas.1417685112

Bridges, A. A., and Bassler, B. L. (2021). Inverse regulation of biofilm dispersal by polyamine signals. *elife* 10:e65487. doi: 10.7554/eLife.65487

Bronesky, D., Wu, Z., Marzi, S., Walter, P., Geissmann, T., Moreau, K., et al. (2016). Staphylococcus aureus RNAIII and its regulon link quorum sensing, stress responses, metabolic adaptation, and regulation of virulence gene expression. *Annu. Rev. Microbiol.* 70, 299–316. doi: 10.1146/annurev-micro-102215-095708

Buffie, C. G., and Pamer, E. G. (2013). Microbiota-mediated colonization resistance against intestinal pathogens. *Nat. Rev. Immunol.* 13, 790–801. doi: 10.1038/nri3535

Campagna, S. R., Gooding, J. R., and May, A. L. (2009). Direct quantitation of the quorum sensing signal, autoinducer-2, in clinically relevant samples by liquid chromatography-tandem mass spectrometry. *Anal. Chem.* 81, 6374–6381. doi: 10.1021/ac900824j

Camps, J., Pujol, I., Ballester, F., Joven, J., and Simó, J. M. (2011). Paraoxonases as potential antibiofilm agents: their relationship with quorum-sensing signals in gram-negative bacteria. *Antimicrob. Agents Chemother.* 55, 1325–1331. doi: 10.1128/AAC.01502-10

Cao, Y., He, S., Zhou, Z., Zhang, M., Mao, W., Zhang, H., et al. (2012). Orally administered thermostable N-acyl homoserine lactonase from bacillus sp. strain AI96 attenuates Aeromonas hydrophila infection in zebrafish. *Appl. Environ. Microbiol.* 78, 1899–1908. doi: 10.1128/AEM.06139-11

Cho, J. Y., Liu, R., Macbeth, J. C., and Hsiao, A. (2021). The Interface of and the gut microbiome. *Gut Microbes* 13:1937015. doi: 10.1080/19490976.2021.1937015

Christiaen, S. E. A., O'Connell Motherway, M., Bottacini, F., Lanigan, N., Casey, P. G., Huys, G., et al. (2014). Autoinducer-2 plays a crucial role in gut colonization and probiotic functionality of Bifidobacterium breve UCC2003. *PLoS One* 9:e98111. doi: 10.1371/journal.pone.0098111

Chu, W., Zhou, S., Zhu, W., and Zhuang, X. (2014). Quorum quenching bacteria bacillus sp. QSI-1 protect zebrafish (Danio rerio) from Aeromonas hydrophila infection. *Sci. Rep.* 4:5446. doi: 10.1038/srep05446

Clarke, M. B., Hughes, D. T., Zhu, C., Boedeker, E. C., and Sperandio, V. (2006). The QseC sensor kinase: a bacterial adrenergic receptor. *Proc. Natl. Acad. Sci. U. S. A.* 103, 10420–10425. doi: 10.1073/pnas.0604343103

Cole, S. J., Hall, C. L., Schniederberend, M., Farrow III, J. M., Goodson, J. R., Pesci, E. C., et al. (2018). Host suppression of quorum sensing during catheter-associated urinary tract infections. *Nat. Commun.* 9:4436. doi: 10.1038/s41467-018-06882-y

Colin Slaughter, J. (1999). The naturally occurring furanones: formation and function from pheromone to food. *Biol. Rev. Camb. Philos. Soc.* 74, 259–276. doi: 10.1017/S0006323199005332

Cook, L. C., and Federle, M. J. (2014). Peptide pheromone signaling in streptococcus and enterococcus. *FEMS Microbiol. Rev.* 38, 473–492. doi: 10.1111/1574-6976.12046

Cornforth, D. M., Popat, R., McNally, L., Gurney, J., Scott-Phillips, T. C., Ivens, A., et al. (2014). Combinatorial quorum sensing allows bacteria to resolve their social and physical environment. *Proc. Natl. Acad. Sci. U. S. A.* 111, 4280–4284. doi: 10.1073/pnas.1319175111

Cotter, P. D., Hill, C., and Ross, R. P. (2005). Bacteriocins: developing innate immunity for food. *Nat. Rev. Microbiol.* 3, 777–788. doi: 10.1038/nrmicro1273

Cutignano, A. (2019). Analytical approaches for the identification of quorum sensing molecules. in *Quorum Sensing* . ed. G. Tommaro (London: Academic Press), 29–53.

Daly, J. W., Keely, S. J., and Gahan, C. G. M. (2021). Functional and phylogenetic diversity of BSH and PVA enzymes. *Microorganisms* 9:732. doi: 10.3390/microorganisms9040732

Đapa, T., Leuzzi, R., Ng, Y. K., Baban, S. T., Adamo, R., Kuehne, S. A., et al. (2013). Multiple factors modulate biofilm formation by the anaerobic pathogen Clostridium difficile. *J. Bacteriol.* 195, 545–555. doi: 10.1128/JB.01980-12

Darkoh, C., DuPont, H., Norris, S. J., and Kaplan, H. B. (2015). Toxin synthesis by Clostridium difficile is regulated through quorum signaling. *MBio* 6:e02569. doi: 10.1128/mBio.02569-14

de Almeida, O. G. G., Vitulo, N., de Martinis, E. C. P., and Felis, G. E. (2021). Pangenome analyses of LuxS-coding genes and enzymatic repertoires in cocoa-related lactic acid bacteria. *Genomics* 113, 1659–1670. doi: 10.1016/j.ygeno.2021.04.010

De Filippis, F., Parente, E., and Ercolini, D. (2018). Recent past, present, and future of the food microbiome. *Annu. Rev. Food Sci. Technol.* 9, 589–608. doi: 10.1146/annurev-food-030117-012312

Defoirdt, T. (2018). Quorum-sensing systems as targets for Antivirulence therapy. *Trends Microbiol.* 26, 313–328. doi: 10.1016/j.tim.2017.10.005

Defoirdt, T., Crab, R., Wood, T. K., Sorgeloos, P., Verstraete, W., and Bossier, P., et al. (2006). Quorum sensing-disrupting brominated furanones protect the gnotobiotic brine shrimp Artemia franciscana from pathogenic Vibrio harveyi, Vibrio campbellii, and Vibrio parahaemolyticus isolates. *Appl. Environ. Microbiol.* 72, 6419–6423. doi: 10.1128/AEM.00753-06

Delalande, L. (2005). N-hexanoyl-L-homoserine lactone, a mediator of bacterial quorum-sensing regulation, exhibits plant-dependent stability and may be inactivated by germinating Lotus corniculatus seedlings. *FEMS Microbiol. Ecol.* 52, 13–20. doi: 10.1016/j.femsec.2004.10.005

Deng, Z., Luo, X. M., Liu, J., and Wang, H. (2020). Quorum sensing, biofilm, and intestinal mucosal barrier: involvement the role of probiotic. *Front. Cell. Infect. Microbiol.* 10:538077. doi: 10.3389/fcimb.2020.538077

Desai, S. K., and Kenney, L. J. (2019). Switching lifestyles is an adaptive strategy of bacterial pathogens. *Front. Cell. Infect. Microbiol.* 9:421. doi: 10.3389/fcimb.2019.00421

Dinh, C. V., and Prather, K. L. J. (2019). Development of an autonomous and bifunctional quorum-sensing circuit for metabolic flux control in engineered Escherichia coli. *Proc. Natl. Acad. Sci. U. S. A.* 116, 25562–25568. doi: 10.1073/pnas.1911144116

Dobson, A., Cotter, P. D., Ross, R. P., and Hill, C. (2012). Bacteriocin production: a probiotic trait? *Appl. Environ. Microbiol.* 78, 1–6. doi: 10.1128/AEM.05576-11

Donaldson, G. P., Lee, S. M., and Mazmanian, S. K. (2016). Gut biogeography of the bacterial microbiota. *Nat. Rev. Microbiol.* 14, 20–32. doi: 10.1038/nrmicro3552

Dong, W., Cai, Y., Xu, Z., Fu, B., Chen, Q., Cui, Y., et al. (2020). Heterologous expression of AHL lactonase AiiK by lactobacillus casei MCJΔ1 with great quorum quenching ability against Aeromonas hydrophila AH-1 and AH-4. *Microb. Cell Factories* 19:191. doi: 10.1186/s12934-020-01448-4

Dong, W., Zhu, J., Guo, X., Kong, D., Zhang, Q., Zhou, Y., et al. (2018). Characterization of AiiK, an AHL lactonase, from Kurthia huakui LAM0618 and its application in quorum quenching on Pseudomonas aeruginosa PAO1. *Sci. Rep.* 8:6013. doi: 10.1038/s41598-018-24507-8

Duncan, K., Carey-Ewend, K., and Vaishnava, S. (2021). Spatial analysis of gut microbiome reveals a distinct ecological niche associated with the mucus layer. *Gut Microbes* 13:1874815. doi: 10.1080/19490976.2021.1874815

Eickhoff, M. J., and Bassler, B. L. (2018). SnapShot: bacterial quorum sensing. *Cells* 174, 1328–1328.e1. doi: 10.1016/j.cell.2018.08.003

Ellermann, M., Jimenez, A. G., Pifer, R., Ruiz, N., and Sperandio, V. (2021). The canonical long-chain fatty acid sensing machinery processes arachidonic acid to inhibit virulence in Enterohemorrhagic *Escherichia coli*. *MBio* 12, e03247–e03220. doi: 10.1128/mBio.03247-20

El-Mowafy, S. A., Shaaban, M. I., and Abd El Galil, K. H. (2014). Sodium ascorbate as a quorum sensing inhibitor of Pseudomonas aeruginosa. *J. Appl. Microbiol.* 117, 1388–1399. doi: 10.1111/jam.12631

Fan, X., Liang, M., Wang, L., Chen, R., Li, H., and Liu, X., et al. (2017). Aii810, a novel cold-adapted -Acylhomoserine lactonase discovered in a metagenome, can strongly attenuate virulence factors and biofilm formation. *Front. Microbiol.* 8:1950. doi: 10.3389/fmicb.2017.01950

Fels, L., Jakob, F., Vogel, R. F., and Wefers, D. (2018). Structural characterization of the exopolysaccharides from water kefir. *Carbohydr. Polym.* 189, 296–303. doi: 10.1016/j.carbpol.2018.02.037

Field, D., et al (2019). Bioengineering nisin to overcome the nisin resistance protein. *Mol. Microbiol.* 111, 717–731.

Fetzner, S. (2015). Quorum quenching enzymes. *J. Biotechnol.* 201, 2–14. doi: 10.1016/j.jbiotec.2014.09.001

Flavier, A. B., Clough, S. J., Schell, M. A., and Denny, T. P. (1997). Identification of 3-hydroxypalmitic acid methyl ester as a novel autoregulator controlling virulence in Ralstonia solanacearum. *Mol. Microbiol.* 26, 251–259. doi: 10.1046/j.1365-2958.1997.5661945.x

Flemming, H.-C., Wingender, J., Szewzyk, U., Steinberg, P., Rice, S. A., and Kjelleberg, S., et al. (2016). Biofilms: an emergent form of bacterial life. *Nat. Rev. Microbiol.* 14, 563–575. doi: 10.1038/nrmicro.2016.94

Fu, H., Elena, R. C., and Marquez, P. H. (2019). The roles of small RNAs: insights from bacterial quorum sensing. *ExRNA* 1:32. doi: 10.1186/s41544-019-0027-8

Fu, C.-Y., Li, L. Q., Yang, T., She, X., Ai, Q., Wang, Z. L., et al. (2020). Autoinducer-2 May be a new biomarker for monitoring neonatal necrotizing enterocolitis. *Front. Cell. Infect. Microbiol.* 10:140. doi: 10.3389/fcimb.2020.00140

Fuqua, C., Parsek, M. R., and Greenberg, E. P. (2001). Regulation of gene expression by cell-to-cell communication: acyl-homoserine lactone quorum sensing. *Annu. Rev. Genet.* 35, 439–468. doi: 10.1146/annurev.genet.35.102401.090913

Gahan, C. G., Patel, S. J., Boursier, M. E., Nyffeler, K. E., Jennings, J., Abbott, N. L., et al. (2020). Bacterial quorum sensing signals self-assemble in aqueous media to form micelles and vesicles: an integrated experimental and molecular dynamics study. *J. Phys. Chem. B* 124, 3616–3628. doi: 10.1021/acs.jpcb.0c00496

Gaida, M. M., Dapunt, U., and Hänsch, G. M. (2016). Sensing developing biofilms: the bitter receptor T2R38 on myeloid cells. *Patho. Dis.* 74:ftw004. doi: 10.1093/femspd/ftw004

Garcia-Gutierrez, E., and Cotter, P. D. (2021). Relevance of organ(s)-on-a-chip systems to the investigation of food-gut microbiota-host interactions. *Crit. Rev. Microbiol.* 48, 463–488. doi: 10.1080/1040841X.2021.1979933

Gharsallaoui, A., Oulahal, N., Joly, C., and Degraeve, P. (2016). Nisin as a food preservative: part 1: physicochemical properties, antimicrobial activity, and Main uses. *Crit. Rev. Food Sci. Nutr.* 56, 1262–1274. doi: 10.1080/10408398.2013.763765

Giaouris, E., Heir, E., Desvaux, M., Hébraud, M., Møretrø, T., Langsrud, S., et al. (2015). Intra- and inter-species interactions within biofilms of important foodborne bacterial pathogens. *Front. Microbiol.* 6:841. doi: 10.3389/fmicb.2015.00841

Gobbetti, M., de Angelis, M., di Cagno, R., Minervini, F., and Limitone, A. (2007). Cell-cell communication in food related bacteria. *Int. J. Food Microbiol.* 120, 34–45. doi: 10.1016/j.ijfoodmicro.2007.06.012

Gorelik, O., Levy, N., Shaulov, L., Yegodayev, K., Meijler, M. M., Sal-Man, N., et al. (2019). Vibrio cholerae autoinducer-1 enhances the virulence of enteropathogenic Escherichia coli. *Sci. Rep.* 9:4122. doi: 10.1038/s41598-019-40859-1

Gori, K., Moslehi-Jenabian, S., Purrotti, M., and Jespersen, L. (2011). Autoinducer-2 activity produced by bacteria found in smear of surface ripened cheeses. *Int. Dairy J.* 21, 48–53. doi: 10.1016/j.idairyj.2010.06.009

Gui, M., Liu, L., Wu, R., Hu, J., Wang, S., Li, P., et al. (2018). Detection of new quorum sensing n-acyl homoserine lactones from aeromonas veronii. *Front. Microbiol.* 9:1712. doi: 10.3389/fmicb.2018.01712

Gui, M., Zhang, Y., Gao, L., and Li, P. (2021). Effect of AHL-lactonase and nisin on microbiological, chemical and sensory quality of vacuum packaged sturgeon storage at 4°C. *Int. J. Food Prop.* 24, 222–232. doi: 10.1080/10942912.2021.1872621

Gutiérrez-Barranquero, J. A., Reen, F. J., McCarthy, R. R., and O'Gara, F. (2018). Deciphering the role of coumarin as a novel quorum sensing inhibitor suppressing virulence phenotypes in bacterial pathogens. *Appl. Microbiol. Biotechnol.* 99, 3303–16. doi: 10.1007/s00253-015-6436-1

Guzel-Seydim, Z. B., Gökırmaklı, Ç., and Greene, A. K. (2021). A comparison of milk kefir and water kefir: physical, chemical, microbiological and functional properties. *Trends Food Sci. Technol.* 113, 42–53. doi: 10.1016/j.tifs.2021.04.041

Han, X., Zhang, L. J., Wu, H. Y., Wu, Y. F., and Zhao, S. N. (2018). Investigation of microorganisms involved in kefir biofilm formation. *Antonie Van Leeuwenhoek* 111, 2361–2370. doi: 10.1007/s10482-018-1125-6

Hargreaves, K. R., Kropinski, A. M., and Clokie, M. R. J. (2014). What does the talking?: quorum sensing signalling genes discovered in a bacteriophage genome. *PLoS One* 9:e85131. doi: 10.1371/journal.pone.0085131

Hawver, L. A., Jung, S. A., and Ng, W.-L. (2016). Specificity and complexity in bacterial quorum-sensing systems. *FEMS Microbiol. Rev.* 40, 738–752. doi: 10.1093/femsre/fuw014

Heilmann, S., Krishna, S., and Kerr, B. (2015). Why do bacteria regulate public goods by quorum sensing?-how the shapes of cost and benefit functions determine the form of optimal regulation. *Front. Microbiol.* 6:767. doi: 10.3389/fmicb.2015.00767

Hengge, R., Häussler, S., Pruteanu, M., Stülke, J., Tschowri, N., Turgay, K., et al. (2019). Recent advances and current trends in nucleotide second messenger signaling in bacteria. *J. Mol. Biol.* 431, 908–927. doi: 10.1016/j.jmb.2019.01.014

Hense, B. A., Kuttler, C., Müller, J., Rothballer, M., Hartmann, A., Kreft, J. U., et al. (2007). Does efficiency sensing unify diffusion and quorum sensing? *Nat. Rev. Microbiol.* 5, 230–239. doi: 10.1038/nrmicro1600

Hickey, A., Pardo, L. M., Reen, F. J., and McGlacken, G. P. (2021). Pyrones identified as LuxR signal molecules in Photorhabdus and their synthetic analogues

can Alter multicellular phenotypic behavior of bacillus atropheaus. *ACS Omega* 6, 33141–33148. doi: 10.1021/acsomega.1c05508

Hou, H. M., Jiang, F., Zhang, G. L., Wang, J. Y., Zhu, Y. H., Liu, X. Y., et al. (2017). Inhibition of hafnia alvei H4 biofilm formation by the food additive Dihydrocoumarin. *J. Food Prot.* 80, 842–847. doi: 10.4315/0362-028X.JFP-16-460

Hu, X., Wang, Y., Gao, L., Jiang, W., Lin, W., Niu, C., et al. (2018). The impairment of methyl metabolism from luxS mutation of Streptococcus mutans. *Front. Microbiol.* 9:404. doi: 10.3389/fmicb.2018.00404

Hughes, D. T., and Sperandio, V. (2008). Inter-kingdom signalling: communication between bacteria and their hosts. *Nat. Rev. Microbiol.* 6, 111–120. doi: 10.1038/nrmicro1836

Huis in 't Veld, J. H. (1996). Microbial and biochemical spoilage of foods: an overview. *Int. J. Food Microbiol.* 33, 1–18. doi: 10.1016/0168-1605(96)01139-7

Hurley, A., and Bassler, B. L. (2017). Asymmetric regulation of quorum-sensing receptors drives autoinducer-specific gene expression programs in vibrio cholerae. *PLoS Genet.* 13:e1006826. doi: 10.1371/journal.pgen.1006826

Hwang, I. Y., Koh, E., Wong, A., March, J. C., Bentley, W. E., Lee, Y. S., et al. (2017). Engineered probiotic Escherichia coli can eliminate and prevent Pseudomonas aeruginosa gut infection in animal models. *Nat. Commun.* 8:15028. doi: 10.1038/ncomms15028

Ismail, A. S., Valastyan, J. S., and Bassler, B. L. (2016). A host-produced Autoinducer-2 mimic activates bacterial quorum sensing. *Cell Host Microbe* 19, 470–480. doi: 10.1016/j.chom.2016.02.020

Jagadeesan, B., Gerner-Smidt, P., Allard, M. W., Leuillet, S., Winkler, A., Xiao, Y., et al. (2019). The use of next generation sequencing for improving food safety: translation into practice. *Food Microbiol.* 79, 96–115. doi: 10.1016/j.fm.2018.11.005

Janssens, Y., Nielandt, J., Bronselaer, A., Debunne, N., Verbeke, F., Wynendaele, E., et al. (2018). Disbiome database: linking the microbiome to disease. *BMC Microbiol.* 18:50. doi: 10.1186/s12866-018-1197-5

Janssens, J. C. A., Steenackers, H., Robijns, S., Gellens, E., Levin, J., Zhao, H., et al. (2008). Brominated furanones inhibit biofilm formation by salmonella enterica serovar typhimurium. *Appl. Environ. Microbiol.* 74, 6639–6648. doi: 10.1128/AEM.01262-08

Jarvis, K. G., Daquigan, N., White, J. R., Morin, P. M., Howard, L. M., Manetas, J. E., et al. (2018). Microbiomes associated with foods from plant and animal sources. *Front. Microbiol.* 9:2540. doi: 10.3389/fmicb.2018.02540

Jingjing, E., Rongze, M., Zichao, C., Caiqing, Y., Ruixue, W., Qiaoling, Z., et al. (2021). Improving the freeze-drying survival rate of lactobacillus plantarum LIP-1 by increasing biofilm formation based on adjusting the composition of buffer salts in medium. *Food Chem.* 338:128134. doi: 10.1016/j.foodchem.2020.128134

Johansen, P., and Jespersen, L. (2017). Impact of quorum sensing on the quality of fermented foods. *Curr. Opin. Food Sci.* 13, 16–25. doi: 10.1016/j.cofs.2017.01.001

Jones, R. B., Zhu, X., Moan, E., Murff, H. J., Ness, R. M., Seidner, D. L., et al. (2018). Inter-niche and inter-individual variation in gut microbial community assessment using stool, rectal swab, and mucosal samples. *Sci. Rep.* 8:4139. doi: 10.1038/s41598-018-22408-4

Joshi, J. R., Khazanov, N., Charkowski, A., Faigenboim, A., Senderowitz, H., Yedidia, I., et al. (2021). Interkingdom signaling interference: the effect of plant-derived small molecules on quorum sensing in plant-pathogenic bacteria. *Annu. Rev. Phytopathol.* 59, 153–190. doi: 10.1146/annurev-phyto-020620-095740

Kalia, V. C. (2013). Quorum sensing inhibitors: an overview. *Biotechnol. Adv.* 31, 224–245. doi: 10.1016/j.biotechadv.2012.10.004

Kalkum, M., Lyon, G. J., and Chait, B. T. (2003). Detection of secreted peptides by using hypothesis-driven multistage mass spectrometry. *Proc. Natl. Acad. Sci. U. S. A.* 100, 2795–2800. doi: 10.1073/pnas.0436605100

Kamaraju, K., Smith, J., Wang, J., Roy, V., Sintim, H. O., Bentley, W. E., et al. (2011). Effects on membrane lateral pressure suggest permeation mechanisms for bacterial quorum signaling molecules. *Biochemistry* 50, 6983–6993. doi: 10.1021/bi200684z

Kang, Y., Kim, H., Goo, E., Jeong, H., An, J. H., Hwang, I., et al. (2019). Unraveling the role of quorum sensing-dependent metabolic homeostasis of the activated methyl cycle in a cooperative population of Burkholderia glumae. *Sci. Rep.* 9:11038. doi: 10.1038/s41598-019-47460-6

Kareb, O., and Aïder, M. (2020). Quorum sensing circuits in the communicating mechanisms of bacteria and its implication in the biosynthesis of Bacteriocins by lactic acid bacteria: a review. *Probiot. Antimicro. Proteins* 12, 5–17. doi: 10.1007/s12602-019-09555-4

Karlsson, T., Turkina, M. V., Yakymenko, O., Magnusson, K. E., and Vikström, E. (2012). The Pseudomonas aeruginosa N-acylhomoserine lactone quorum sensing molecules target IQGAP1 and modulate epithelial cell migration. *PLoS Pathog.* 8:e1002953. doi: 10.1371/journal.ppat.1002953

Kelly, S. M., Lanigan, N., O'Neill, I. J., Bottacini, F., Lugli, G. A., Viappiani, A., et al. (2020). Bifidobacterial biofilm formation is a multifactorial adaptive phenomenon in response to bile exposure. *Sci. Rep.* 10:11598. doi: 10.1038/s41598-020-68179-9

Kendall, M. M., and Sperandio, V. (2016). What a dinner party! Mechanisms and functions of Interkingdom signaling in host-pathogen associations. *MBio* 7:e01748. doi: 10.1128/mBio.01748-15

Khan, I., Tango, C. N., Miskeen, S., Lee, B. H., and Oh, D. H. (2017). Hurdle technology: a novel approach for enhanced food quality and safety – a review. *Food Control* 73, 1426–1444. doi: 10.1016/j.foodcont.2016.11.010

Kim, H.-S., Cha, E., Ham, S. Y., Park, J. H., Nam, S. J., Kwon, H., et al. (2021). Linoleic acid inhibits Pseudomonas aeruginosa biofilm formation by activating diffusible signal factor-mediated quorum sensing. *Biotechnol. Bioeng.* 118, 82–93. doi: 10.1002/bit.27552

Kim, C. S., Gatsios, A., Cuesta, S., Lam, Y. C., Wei, Z., Chen, H., et al. (2020). Characterization of Autoinducer-3 structure and biosynthesis in *E. coli*. *ACS Central Sci.* 6, 197–206. doi: 10.1021/acscentsci.9b01076

Kim, I. H., Kim, S. Y., Park, N. Y., Wen, Y., Lee, K. W., Yoon, S. Y., et al. (2018). Cyclo-(l -Phe- l -pro), a quorum-sensing signal of Vibrio vulnificus, induces expression of Hydroperoxidase through a ToxR-LeuO-HU-RpoS signaling pathway to confer resistance against oxidative stress. *Infect. Immun.* 86, e00932–e00917. doi: 10.1128/iai.00932-17

Kleerebezem, M. (2004). Quorum sensing control of lantibiotic production; nisin and subtilin autoregulate their own biosynthesis. *Peptides* 25, 1405–1414. doi: 10.1016/j.peptides.2003.10.021

Kleerebezem, M., Quadri, L. E. N., Kuipers, O. P., and de Vos, W. M. (1997). Quorum sensing by peptide pheromones and two-component signal-transduction systems in gram-positive bacteria. *Mol. Microbiol.* 24, 895–904. doi: 10.1046/j.1365-2958.1997.4251782.x

Kravchenko, V. V., and Kaufmann, G. F. (2013). Bacterial inhibition of inflammatory responses via TLR-independent mechanisms. *Cell. Microbiol.* 15, 527–536. doi: 10.1111/cmi.12109

Lade, H., Paul, D., and Kweon, J. H. (2014). Quorum quenching mediated approaches for control of membrane biofouling. *Int. J. Biol. Sci.* 10, 550–565. doi: 10.7150/ijbs.9028

Landman, C., Grill, J. P., Mallet, J. M., Marteau, P., Humbert, L., le Balc'h, E., et al. (2018). Inter-kingdom effect on epithelial cells of the N-acyl homoserine lactone 3-oxo-C12:2, a major quorum-sensing molecule from gut microbiota. *PLoS One* 13:e0202587. doi: 10.1371/journal.pone.0202587

Leisner, J. J., Laursen, B. G., Prévost, H., Drider, D., and Dalgaard, P. (2007). Carnobacterium: positive and negative effects in the environment and in foods. *FEMS Microbiol. Rev.* 31, 592–613. doi: 10.1111/j.1574-6976.2007.00080.x

León-Félix, J., and Villicaña, C. (2021). The impact of quorum sensing on the modulation of phage-host interactions. *J. Bacteriol.* 203, e00687–e00620. doi: 10.1128/JB.00687-20

Li, Q., Peng, W., Wu, J., Wang, X., Ren, Y., Li, H., et al. (2019a). Autoinducer-2 of gut microbiota, a potential novel marker for human colorectal cancer, is associated with the activation of TNFSF9 signaling in macrophages. *Onco. Targets. Ther.* 8:e1626192. doi: 10.1080/2162402X.2019.1626192

Li, Q., Ren, Y., and Fu, X. (2019b). Inter-kingdom signaling between gut microbiota and their host. *Cell. Mol. Life Sci.* 76, 2383–2389. doi: 10.1007/s00018-019-03076-7

Li, Y.-H., and Tian, X. (2012). Quorum sensing and bacterial social interactions in biofilms. *Sensors* 12, 2519–2538. doi: 10.3390/s120302519

Lin, J., Cheng, J., Wang, Y., and Shen, X. (2018). The quinolone signal (PQS): not just for quorum sensing anymore. *Front. Cell. Infect. Microbiol.* 8:230. doi: 10.3389/fcimb.2018.00230

Lindsay, A., and Ahmer, B. M. M. (2005). Effect of sdiA on biosensors of N-acylhomoserine lactones. *J. Bacteriol.* 187, 5054–5058. doi: 10.1128/JB.187.14.5054-5058.2005

Liu, L., Chen, X., Skogerbø, G., Zhang, P., Chen, R., He, S., et al. (2012). The human microbiome: a hot spot of microbial horizontal gene transfer. *Genomics* 100, 265–270. doi: 10.1016/j.ygeno.2012.07.012

Liu, L., Li, T., Cheng, X. J., Peng, C. T., Li, C. C., He, L. H., et al. (2018b). Structural and functional studies on Pseudomonas aeruginosa DspI: implications for its role in DSF biosynthesis. *Sci. Rep.* 8:3928. doi: 10.1038/s41598-018-22300-1

Liu, C., Di Sun, J. Z., and Liu, W. (2018a). Two-component signal transduction systems: a major strategy for connecting input stimuli to biofilm formation. *Front. Microbiol.* 9:3279. doi: 10.3389/fmicb.2018.03279

Lu, L., Hume, M. E., and Pillai, S. D. (2004). Autoinducer-2-like activity associated with foods and its interaction with food additives. *J. Food Prot.* 67, 1457–1462. doi: 10.4315/0362-028X-67.7.1457

Lu, Y., Zeng, J., Wu, B., E, S., Wang, L., Cai, R., et al. (2017). Quorum sensing N-acyl Homoserine lactones-SdiA suppresses Escherichia coli- Pseudomonas

aeruginosa conjugation through inhibiting traI expression. *Front. Cell. Infect. Microbiol.* 7:7. doi: 10.3389/fcimb.2017.00007

Lyons, T., Gahan, C. G., and O'Sullivan, T. P. (2020). Structure-activity relationships of furanones, dihydropyrrolones and thiophenones as potential quorum sensing inhibitors. *Future Med. Chem.* 12, 1925–1943. doi: 10.4155/fmc-2020-0244

Machado Ribeiro, T. R., Salgaço, M. K., Adorno, M. A. T., da Silva, M. A., Piazza, R. M. F., Sivieri, K., et al. (2021). Human microbiota modulation via QseC sensor kinase mediated in the Escherichia coli O104:H4 outbreak strain infection in microbiome model. *BMC Microbiol.* 21:163. doi: 10.1186/s12866-021-02220-3

Maes, S., Heyndrickx, M., Vackier, T., Steenackers, H., Verplaetse, A., Reu, K. D. E., et al. (2019). Identification and spoilage potential of the remaining dominant microbiota on food contact surfaces after cleaning and disinfection in different food industries. *J. Food Prot.* 82, 262–275. doi: 10.4315/0362-028X.JFP-18-226

Maldonado-Barragán, A., Caballero-Guerrero, B., Lucena-Padrós, H., and Ruiz-Barba, J. L. (2013). Induction of bacteriocin production by coculture is widespread among plantaricin-producing lactobacillus plantarum strains with different regulatory operons. *Food Microbiol.* 33, 40–47. doi: 10.1016/j.fm.2012.08.009

Maldonado-Barragán, A., Ruiz-Barba, J. L., and Jiménez-Díaz, R. (2009). Knockout of three-component regulatory systems reveals that the apparently constitutive plantaricin-production phenotype shown by lactobacillus plantarum on solid medium is regulated via quorum sensing. *Int. J. Food Microbiol.* 130, 35–42. doi: 10.1016/j.ijfoodmicro.2008.12.033

Malka, O., Kalson, D., Yaniv, K., Shafir, R., Rajendran, M., Ben-David, O., et al. (2021). Cross-kingdom inhibition of bacterial virulence and communication by probiotic yeast metabolites. *Microbiome* 9:70. doi: 10.1186/s40168-021-01027-8

Manefield, M., de Nys, R., Naresh, K., Roger, R., Givskov, M., Peter, S., et al. (1999). Evidence that halogenated furanones from Delisea pulchra inhibit acylated homoserine lactone (AHL)-mediated gene expression by displacing the AHL signal from its receptor protein. *Microbiology* 145, 283–291. doi: 10.1099/13500872-145-2-283

March, J. C., and Bentley, W. E. (2004). Quorum sensing and bacterial cross-talk in biotechnology. *Curr. Opin. Biotechnol.* 15, 495–502. doi: 10.1016/j.copbio.2004.08.013

Markus, V., Share, O., Teralı, K., Ozer, N., Marks, R. S., Kushmaro, A., et al. (2020). Anti-quorum sensing activity of stevia extract, Stevioside, Rebaudioside a and their Aglycon Steviol. *Molecules* 25:5480. doi: 10.3390/molecules25225480

Medina-Martínez, M. S., Uyttendaele, M., Demolder, V., and Debevere, J. (2006). Influence of food system conditions on N-acyl-L-homoserine lactones production by Aeromonas spp. *Int. J. Food Microbiol.* 112, 244–252. doi: 10.1016/j.ijfoodmicro.2006.04.025

Meireles, A., Faia, S., Giaouris, E., and Simões, M. (2018). Antimicrobial susceptibility and sessile behaviour of bacteria isolated from a minimally processed vegetables plant. *Biofouling* 34, 1150–1160. doi: 10.1080/08927014.2018.1554742

Michael, B., Smith, J. N., Swift, S., Heffron, F., and Ahmer, B. M. M. (2001). SdiA of salmonella enterica is a LuxR homolog that detects mixed microbial communities. *J. Bacteriol.* 183, 5733–5742. doi: 10.1128/JB.183.19.5733-5742.2001

Miller, C., and Gilmore, J. (2020). Detection of quorum-sensing molecules for pathogenic molecules using cell-based and cell-free biosensors. *Antibiotics* 9:259. doi: 10.3390/antibiotics9050259

Mole, B. M., Baltrus, D. A., Dangl, J. L., and Grant, S. R. (2007). Global virulence regulation networks in phytopathogenic bacteria. *Trends Microbiol.* 15, 363–371. doi: 10.1016/j.tim.2007.06.005

Monnet, V., Juillard, V., and Gardan, R. (2016). Peptide conversations in gram-positive bacteria. *Crit. Rev. Microbiol.* 42, 339–351. doi: 10.3109/1040841X.2014.948804

Moura-Alves, P., Puyskens, A., Stinn, A., Klemm, M., Guhlich-Bornhof, U., Dorhoi, A., et al. (2019). Host monitoring of quorum sensing during infection. *Science* 366:eaaw1629. doi: 10.1126/science.aaw1629

Mukherjee, S., and Bassler, B. L. (2019). Bacterial quorum sensing in complex and dynamically changing environments. *Nat. Rev. Microbiol.* 17, 371–382. doi: 10.1038/s41579-019-0186-5

Mukherji, R., and Prabhune, A. (2015). Possible correlation between bile salt hydrolysis and AHL Deamidation: Staphylococcus epidermidis RM1, a potent quorum quencher and bile salt hydrolase producer. *Appl. Biochem. Biotechnol.* 176, 140–150. doi: 10.1007/s12010-015-1563-9

Muras, A., Otero-Casal, P., Blanc, V., and Otero, A. (2020). Acyl homoserine lactone-mediated quorum sensing in the oral cavity: a paradigm revisited. *Sci. Rep.* 10:9800. doi: 10.1038/s41598-020-66704-4

Murugayah, S. A., and Gerth, M. L. (2019). Engineering quorum quenching enzymes: progress and perspectives. *Biochem. Soc. Trans.* 47, 793–800. doi: 10.1042/BST20180165

Nahar, S., Jeong, H. L., Kim, Y., Ha, A. J. W., Roy, P. K., Park, S. H., et al. (2021). Inhibitory effects of Flavourzyme on biofilm formation, quorum sensing, and virulence genes of foodborne pathogens salmonella typhimurium and Escherichia coli. *Food Res. Int.* 147:110461. doi: 10.1016/j.foodres.2021.110461

Nahar, S., Mizan, M. F. R., Ha, A. J. W., and Ha, S. D. (2018). Advances and future prospects of enzyme-based biofilm prevention approaches in the food industry. *Compr. Rev. Food Sci. Food Saf.* 17, 1484–1502. doi: 10.1111/1541-4337.12382

Nealson, K. H., Platt, T., and Woodland Hastings, J. (1970). Cellular control of the synthesis and activity of the bacterial luminescent system. *J. Bacteriol.* 104, 313–322. doi: 10.1128/jb.104.1.313-322.1970

Neuman, H., Debelius, J. W., Knight, R., and Koren, O. (2015). Microbial endocrinology: the interplay between the microbiota and the endocrine system. *FEMS Microbiol. Rev.* 39, 509–521. doi: 10.1093/femsre/fuu010

Ng, W.-L., and Bassler, B. L. (2009). Bacterial quorum-sensing network architectures. *Annu. Rev. Genet.* 43, 197–222. doi: 10.1146/annurev-genet-102108-134304

Nicol, M., Alexandre, S., Luizet, J. B., Skogman, M., Jouenne, T., Salcedo, S., et al. (2018). Unsaturated fatty acids affect quorum sensing communication system and inhibit motility and biofilm formation of *Acinetobacter baumannii*. *Int. J. Mol. Sci.* 19:214. doi: 10.3390/ijms19010214

Nogueira, F., Sharghi, S., Kuchler, K., and Lion, T. (2019). Pathogenetic impact of bacterial-fungal interactions. *Microorganisms* 7:459. doi: 10.3390/microorganisms7100459

Novak, J. S., and Fratamico, P. M. (2006). Evaluation of ascorbic acid as a quorum-sensing analogue to control growth, sporulation, and enterotoxin production in Clostridium perfringens. *J. Food Sci.* 69, FMS72–FMS78. doi: 10.1111/j.1365-2621.2004.tb13374.x

Novick, R. P., and Muir, T. W. (1999). Virulence gene regulation by peptides in staphylococci and other gram-positive bacteria. *Curr. Opin. Microbiol.* 2, 40–45. doi: 10.1016/S1369-5274(99)80007-1

One Health High-Level Expert Panel (OHHLEP)Adisasmito, W. B., Almuhairi, S., Behravesh, C. B., Bilivogui, P., Bukachi, S. A., et al. (2022). One health: a new definition for a sustainable and healthy future. *PLoS Pathog.* 18:e1010537. doi: 10.1371/journal.ppat.1010537

Pandit, S., Ravikumar, V., Abdel-Haleem, A. M., Derouiche, A., Mokkapati, V. R. S. S., Sihlbom, C., et al. (2017). Low concentrations of vitamin C reduce the synthesis of extracellular polymers and destabilize bacterial biofilms. *Front. Microbiol.* 8:2599. doi: 10.3389/fmicb.2017.02599

Papenfort, K., and Bassler, B. L. (2016). Quorum sensing signal-response systems in gram-negative bacteria. *Nat. Rev. Microbiol.* 14, 576–588. doi: 10.1038/nrmicro.2016.89

Park, H., Shin, H., Lee, K., and Holzapfel, W. (2016). Autoinducer-2 properties of kimchi are associated with lactic acid bacteria involved in its fermentation. *Int. J. Food Microbiol.* 225, 38–42. doi: 10.1016/j.ijfoodmicro.2016.03.007

Pasolli, E., de Filippis, F., Mauriello, I. E., Cumbo, F., Walsh, A. M., Leech, J., et al. (2020). Large-scale genome-wide analysis links lactic acid bacteria from food with the gut microbiome. *Nat. Commun.* 11:2610. doi: 10.1038/s41467-020-16438-8

Pelyuntha, W., Chaiyasut, C., Kantachote, D., and Sirilun, S. (2019). Cell-free supernatants from cultures of lactic acid bacteria isolated from fermented grape as biocontrol against Typhi and typhimurium virulence via autoinducer-2 and biofilm interference. *PeerJ* 7:e7555. doi: 10.7717/peerj.7555

Penesyan, A., Nagy, S. S., Kjelleberg, S., Gillings, M. R., and Paulsen, I. T. (2019). Rapid microevolution of biofilm cells in response to antibiotics. *NPJ Bio. Microbio.* 5:34. doi: 10.1038/s41522-019-0108-3

Peng, P., Baldry, M., Gless, B. H., Bojer, M. S., Espinosa-Gongora, C., Baig, S. J., et al. (2019). Effect of co-inhabiting coagulase negative staphylococci on quorum sensing, host factor binding, and biofilm formation. *Front. Microbiol.* 10:2212. doi: 10.3389/fmicb.2019.02212

Peng, M., Tong, W., Zhao, Z., Xiao, L., Wang, Z., Liu, X., et al. (2021). Attenuation of Aeromonas hydrophila infection in Carassius auratus by YtnP, a -acyl Homoserine lactonase from bacillus licheniformis T-1. *Antibiotics* 10:631. doi: 10.3390/antibiotics10060631

Pereira, C. S., Thompson, J. A., and Xavier, K. B. (2013). AI-2-mediated signalling in bacteria. *FEMS Microbiol. Rev.* 37, 156–181. doi: 10.1111/j.1574-6976.2012.00345.x

Pérez, P. D, and Hagen, S. J. (2010). Heterogeneous response to a quorum-sensing signal in the luminescence of individual Vibrio fischeri. *PLoS One*, 5: e15473. doi: 10.1371/journal.pone.0015473

Perpetuini, G., Pham-Hoang, B. N., Scornec, H., Tofalo, R., Schirone, M., Suzzi, G., et al. (2016). In lactobacillus pentosus, the olive brine adaptation genes are required for biofilm formation. *Int. J. Food Microbiol.* 216, 104–109. doi: 10.1016/j.ijfoodmicro.2015.10.002

Peyrottes, A., Coquant, G., Brot, L., Rainteau, D., Seksik, P., Grill, J. P., et al. (2020). Anti-inflammatory effects of analogues of N-acyl Homoserine lactones on eukaryotic cells. *Int. J. Mol. Sci.* 21:9448. doi: 10.3390/ijms21249448

Plummer, P. J. (2012). LuxS and quorum-sensing in campylobacter. *Front. Cell. Infect. Microbiol.* 2:22. doi: 10.3389/fcimb.2012.00022

Prescott, R. D., and Decho, A. W. (2020). Flexibility and adaptability of quorum sensing in nature. *Trends Microbiol.* 28, 436–444. doi: 10.1016/j.tim.2019.12.004

Proctor, C. R., McCarron, P. A., and Ternan, N. G. (2020). Furanone quorum-sensing inhibitors with potential as novel therapeutics against Pseudomonas aeruginosa. *J. Med. Microbiol.* 69, 195–206. doi: 10.1099/jmm.0.001144

Pun, M., Khazanov, N., Galsurker, O., Weitman, M., Kerem, Z., Senderowitz, H., et al. (2021). Phloretin, an apple Phytoalexin, affects the virulence and fitness of Pectobacterium brasiliense by interfering with quorum-sensing. *Front. Plant Sci.* 12:671807. doi: 10.3389/fpls.2021.671807

Qian, Y., Kando, C. K., Thorsen, L., Larsen, N., and Jespersen, L. (2015). Production of autoinducer-2 by aerobic endospore-forming bacteria isolated from the west African fermented foods. *FEMS Microbiol. Lett.* 362:fnv186. doi: 10.1093/femsle/fnv186

Qian, Y., Ye, J.-X., Yang, S.-P., Lin, Z.-Q., Cao, W., Xie, J., et al. (2018). Evaluation of the spoilage potential of Shewanella putrefaciens, Aeromonas hydrophila, and Aeromonas sobria isolated from spoiled Pacific white shrimp (*Litopenaeus vannamei*) during cold storage. *J. Food Saf.* 38:e12550. doi: 10.1111/jfs.12550

Quintieri, L., Caputo, L., de Angelis, M., and Fanelli, F. (2020). Genomic analysis of three cheese-borne pseudomonas lactis with biofilm and spoilage-associated behavior. *Microorganisms* 8:1208. doi: 10.3390/microorganisms8081208

Rahmati, S., Yang, S., Davidson, A. L., and Zechiedrich, E. L. (2002). Control of the AcrAB multidrug efflux pump by quorum-sensing regulator SdiA. *Mol. Microbiol* 43, 677–85. doi: 10.1046/j.1365-2958.2002.02773.x

Rajamani, S., Bauer, W. D., Robinson, J. B., Farrow, J. M. III, Pesci, E. C., Teplitski, M., et al. (2008). The vitamin riboflavin and its derivative lumichrome activate the LasR bacterial quorum-sensing receptor. *Mol. Plant Microbe Interact.* 21, 1184–1192. doi: 10.1094/MPMI-21-9-1184

Rampioni, G., Falcone, M., Heeb, S., Frangipani, E., Fletcher, M. P., Dubern, J. F., et al. (2016). Unravelling the genome-wide contributions of specific 2-Alkyl-4-quinolones and PqsE to quorum sensing in Pseudomonas aeruginosa. *PLoS Pathog.* 12:e1006029. doi: 10.1371/journal.ppat.1006029

Rana, S., Bhawal, S., Kumari, A., Kapila, S., and Kapila, R. (2020). pH-dependent inhibition of AHL-mediated quorum sensing by cell-free supernatant of lactic acid bacteria in Pseudomonas aeruginosa PAO1. *Microb. Pathog.* 142:104105. doi: 10.1016/j.micpath.2020.104105

Ranava, D., Backes, C., Karthikeyan, G., Ouari, O., Soric, A., Guiral, M., et al. (2021). Metabolic exchange and energetic coupling between nutritionally stressed bacterial species: role of quorum-sensing molecules. *MBio* 12, e02758–e02720. doi: 10.1128/mBio.02758-20

Raut, N., Pasini, P., and Daunert, S. (2013). Deciphering bacterial universal language by detecting the quorum sensing signal, autoinducer-2, with a whole-cell sensing system. *Anal. Chem.* 85, 9604–9609. doi: 10.1021/ac401776k

Rezzonico, F., Smits, T. H. M., and Duffy, B. (2012). Detection of AI-2 receptors in genomes of Enterobacteriaceae suggests a role of type-2 quorum sensing in closed ecosystems. *Sensors* 12, 6645–6665. doi: 10.3390/s120506645

Rickard, A. H., Campagna, S. R., and Kolenbrander, P. E. (2008). Autoinducer-2 is produced in saliva-fed flow conditions relevant to natural oral biofilms. *J. Appl. Microbiol.* 105, 2096–2103. doi: 10.1111/j.1365-2672.2008.03910.x

Rodrigues, A. C., D'Ávila de OLIVEIRA, B., da SILVA, E. R., SACRAMENTO, N. T. B., BERTOLDI, M. C., and PINTO, U. M. (2016). Anti-quorum sensing activity of phenolic extract from Eugenia brasiliensis (*Brazilian cherry*). *Food Sci. Tech.* 36, 337–343. doi: 10.1590/1678-457X.0089

Rodríguez-López, P., Barrenengoa, A. E., Pascual-Sáez, S., and Cabo, M. L. (2019). Efficacy of synthetic Furanones on biofilm formation. *Foods* 8:647. doi: 10.3390/foods8120647

Ruparell, A., Dubern, J. F., Ortori, C. A., Harrison, F., Halliday, N. M., Emtage, A., et al. (2016). The fitness burden imposed by synthesising quorum sensing signals. *Sci. Rep.* 6:33101. doi: 10.1038/srep33101

Rutherford, S. T., and Bassler, B. L. (2012). Bacterial quorum sensing: its role in virulence and possibilities for its control. *Cold Spring Harb. Perspect. Med.* 2:a012427. doi: 10.1101/cshperspect.a012427

Rutherford, S. T., van Kessel, J. C., Shao, Y., and Bassler, B. L. (2011). AphA and LuxR/HapR reciprocally control quorum sensing in vibrios. *Genes Dev.* 25, 397–408. doi: 10.1101/gad.2015011

Scoffone, V. C., Trespidi, G., Chiarelli, L. R., Barbieri, G., and Buroni, S. (2019). Quorum sensing as Antivirulence target in cystic fibrosis pathogens. *Int. J. Mol. Sci.* 20:1838. doi: 10.3390/ijms20081838

Sender, R., Fuchs, S., and Milo, R. (2016). Revised estimates for the number of human and bacteria cells in the body. *PLoS Biol.* 14:e1002533. doi: 10.1371/journal.pbio.1002533

Sepehr, S., Rahmani-Badi, A., Babaie-Naiej, H., and Soudi, M. R. (2014). Unsaturated fatty acid, cis-2-decenoic acid, in combination with disinfectants or antibiotics removes pre-established biofilms formed by food-related bacteria. *PLoS One* 9:e101677. doi: 10.1371/journal.pone.0101677

Shivaprasad, D. P., Taneja, N. K., Lakra, A., and Sachdev, D. (2021). In vitro and in situ abrogation of biofilm formation in *E. coli* by vitamin C through ROS generation, disruption of quorum sensing and exopolysaccharide production. *Food Chem.* 341:128171. doi: 10.1016/j.foodchem.2020.128171

Sikdar, R., and Elias, M. (2020). Quorum quenching enzymes and their effects on virulence, biofilm, and microbiomes: a review of recent advances. *Expert Rev. Anti-Infect. Ther.* 18, 1221–1233. doi: 10.1080/14787210.2020.1794815

Silpe, J. E., and Bassler, B. L. (2019). A host-produced quorum-sensing autoinducer controls a phage lysis-Lysogeny decision. *Cells* 176, 268–280.e13. doi: 10.1016/j.cell.2018.10.059

Singh, V. K., Kavita, K., Prabhakaran, R., and Jha, B. (2013). Cis-9-octadecenoic acid from the rhizospheric bacterium Stenotrophomonas maltophilia BJ01 shows quorum quenching and anti-biofilm activities. *Biofouling* 29, 855–867. doi: 10.1080/08927014.2013.807914

Skandamis, P. N., and Nychas, G.-J. E. (2012). Quorum sensing in the context of food microbiology. *Appl. Environ. Microbiol.* 78, 5473–5482. doi: 10.1128/AEM.00468-12

Solano, C., Echeverz, M., and Lasa, I. (2014). Biofilm dispersion and quorum sensing. *Curr. Opin. Microbiol.* 18, 96–104. doi: 10.1016/j.mib.2014.02.008

Soni, K. A., Jesudhasan, P., Cepeda, M., Widmer, K., Jayaprakasha, G. K., Patil, B. S., et al. (2008). Identification of ground beef-derived fatty acid inhibitors of autoinducer-2-based cell signaling. *J. Food Prot.* 71, 134–138. doi: 10.4315/0362-028X-71.1.134

Stentz, R., Horn, N., Cross, K., Salt, L., Brearley, C., Livermore, D. M., et al. (2015). Cephalosporinases associated with outer membrane vesicles released by Bacteroides spp. protect gut pathogens and commensals against β-lactam antibiotics. *J. Antimicrob. Chemother.* 70, 701–709. doi: 10.1093/jac/dku466

Stenz, L., FranÃ§ois, P., Fischer, A., Huyghe, A., Tangomo, M., Hernandez, D., et al. (2008). Impact of oleic acid (cis-9-octadecenoic acid) on bacterial viability and biofilm production in Staphylococcus aureus. *FEMS Microbiol. Lett.* 287, 149–155. doi: 10.1111/j.1574-6968.2008.01316.x

Stephens, K., and Bentley, W. E. (2020). Synthetic biology for manipulating quorum sensing in microbial consortia. *Trends Microbiol.* 28, 633–643. doi: 10.1016/j.tim.2020.03.009

Striednig, B., and Hilbi, H. (2022). Bacterial quorum sensing and phenotypic heterogeneity: how the collective shapes the individual. *Trends Microbiol.* 30, 379–389. doi: 10.1016/j.tim.2021.09.001

Subramoni, S., and Venturi, V. (2009). LuxR-family "solos": bachelor sensors/regulators of signalling molecules. *Microbiology* 155, 1377–1385. doi: 10.1099/mic.0.026849-0

Sun, B., and Zhang, M. (2016). Analysis of the antibacterial effect of an Edwardsiella tarda LuxS inhibitor. *Springerplus* 5:92. doi: 10.1186/s40064-016-1733-4

Swaggerty, C. L., Genovese, K. J., He, H., Byrd J. A. Jr, and Kogut, M. H. (2018). Editorial: mechanisms of persistence, survival, and transmission of bacterial foodborne pathogens in production animals. *Front. Vet. Sci.* 5. doi: 10.3389/fvets.2018.00139

Teng, S.-W., Schaffer, J. N., Tu, K. C., Mehta, P., Lu, W., Ong, N. P., et al. (2011). Active regulation of receptor ratios controls integration of quorum-sensing signals in Vibrio harveyi. *Mol. Syst. Biol.* 7:491. doi: 10.1038/msb.2011.30

Thompson, J. A., Oliveira, R. A., Djukovic, A., Ubeda, C., and Xavier, K. B. (2015). Manipulation of the quorum sensing signal AI-2 affects the antibiotic-treated gut microbiota. *Cell Rep.* 10, 1861–1871. doi: 10.1016/j.celrep.2015.02.049

Tijerina-Rodríguez, L., Villarreal-Treviño, L., Baines, S. D., Morfín-Otero, R., Camacho-Ortíz, A., Flores-Treviño, S., et al. (2019). High sporulation and overexpression of virulence factors in biofilms and reduced susceptibility to vancomycin and linezolid in recurrent clostridium [Clostridioides] difficile infection isolates. *PLoS One* 14:e0220671. doi: 10.1371/journal.pone.0220671

Torabi Delshad, S., Soltanian, S., Sharifiyazdi, H., Haghkhah, M., and Bossier, P. (2018). Identification of N-acyl homoserine lactone-degrading bacteria isolated from rainbow trout (Oncorhynchus mykiss). *J. Appl. Microbiol.* 125, 356–369. doi: 10.1111/jam.13891

Tourneroche, A., Lami, R., Hubas, C., Blanchet, E., Vallet, M., Escoubeyrou, K., et al. (2019). Bacterial-fungal interactions in the kelp Endomicrobiota drive Autoinducer-2 quorum sensing. *Front. Microbiol.* 10:1693. doi: 10.3389/fmicb.2019.01693

Toyofuku, M., Morinaga, K., Hashimoto, Y., Uhl, J., Shimamura, H., Inaba, H., et al. (2017). Membrane vesicle-mediated bacterial communication. *ISME J.* 11, 1504–1509. doi: 10.1038/ismej.2017.13

Uruén, C., Chopo-Escuin, G., Tommassen, J., Mainar-Jaime, R. C., and Arenas, J. (2020). Biofilms as promoters of bacterial antibiotic resistance and tolerance. *Antibiotics* 10:3. doi: 10.3390/antibiotics10010003

Vadassery, D. H., and Pillai, D. (2020). Quorum quenching potential of enterococcus faecium QQ12 isolated from gastrointestinal tract of Oreochromis niloticus and its application as a probiotic for the control of Aeromonas hydrophila infection in goldfish Carassius auratus (Linnaeus 1758). *Brazilian J. Microbiol.* 51, 1333–1343. doi: 10.1007/s42770-020-00230-3

Van Reckem, E., Charmpi, C., Van der Veken, D., Borremans, W., De Vuyst, L., Weckx, S., et al. (2020). Application of a high-throughput amplicon sequencing method to chart the bacterial communities that are associated with European fermented meats from different origins. *Foods* 9, 9:1247. doi: 10.3390/foods9091247

Verbeke, F., de Craemer, S., Debunne, N., Janssens, Y., Wynendaele, E., van de Wiele, C., et al. (2017). Peptides as quorum sensing molecules: measurement techniques and obtained levels in vitro and in vivo. *Front. Neurosci.* 11:183. doi: 10.3389/fnins.2017.00183

Verbeurgt, C., Veithen, A., Carlot, S., Tarabichi, M., Dumont, J. E., Hassid, S., et al. (2017). The human bitter taste receptor T2R38 is broadly tuned for bacterial compounds. *PLoS One* 12:e0181302. doi: 10.1371/journal.pone.0181302

Wagner, E. M., Pracser, N., Thalguter, S., Fischel, K., Rammer, N., Pospíšilová, L., et al. (2020). Identification of biofilm hotspots in a meat processing environment: detection of spoilage bacteria in multi-species biofilms. *Int. J. Food Microbiol.* 328:108668. doi: 10.1016/j.ijfoodmicro.2020.108668

Walsh, C., and Fanning, S. (2008). Antimicrobial resistance in foodborne pathogens--a cause for concern? *Curr. Drug Targets* 9, 808–815. doi: 10.2174/138945008785747761

Walter, J., Armet, A. M., Finlay, B. B., and Shanahan, F. (2020). Establishing or exaggerating causality for the gut microbiome: lessons from human microbiota-associated rodents. *Cells* 180, 221–232. doi: 10.1016/j.cell.2019.12.025

Walters, M., and Sperandio, V. (2006). Autoinducer 3 and epinephrine signaling in the kinetics of locus of enterocyte effacement gene expression in enterohemorrhagic Escherichia coli. *Infect. Immun.* 74, 5445–5455. doi: 10.1128/IAI.00099-06

Wang, S.-Y., Chen, K. N., Lo, Y. M., Chiang, M. L., Chen, H. C., Liu, J. R., et al. (2012). Investigation of microorganisms involved in biosynthesis of the kefir grain. *Food Microbiol.* 32, 274–285. doi: 10.1016/j.fm.2012.07.001

Wang, J., Ding, L., Li, K., Huang, H., Hu, H., Geng, J., et al. (2018). Estimation of spatial distribution of quorum sensing signaling in sequencing batch biofilm reactor (SBBR) biofilms. *Sci. Total Environ.* 612, 405–414. doi: 10.1016/j.scitotenv.2017.07.277

Wang, Y., and Ho, C.-T. (2008). Formation of 2,5-dimethyl-4-hydroxy-3(2H)-furanone through methylglyoxal: a Maillard reaction intermediate. *J. Agric. Food Chem.* 56, 7405–7409. doi: 10.1021/jf8012025

Wang, S., Payne, G. F., and Bentley, W. E. (2020). Quorum sensing communication: molecularly connecting cells, their neighbors, and even devices. *Ann. Rev. Chem. Biomol. Eng.* 11, 447–468. doi: 10.1146/annurev-chembioeng-101519-124728

Wang, X.-Y., and Xie, J. (2020). Quorum sensing system-regulated proteins affect the spoilage potential of co-cultured Acinetobacter johnsonii and Pseudomonas fluorescens from spoiled bigeye tuna (*Thunnus obesus*) as determined by proteomic analysis. *Front. Microbiol.* 11:940. doi: 10.3389/fmicb.2020.00940

Weiland-Bräuer, N., Kisch, M. J., Pinnow, N., Liese, A., and Schmitz, R. A. (2016, 2016). A highly effective inhibition of biofilm formation by the first metagenome-derived AI-2 quenching enzyme. *Front. Microbiol.* 7:1098. doi: 10.3389/fmicb.2016.01098

Wellington, S., and Greenberg, E. P. (2019). Quorum sensing signal selectivity and the potential for interspecies cross talk. *MBio* 10, e00146–e00119. doi: 10.1128/mBio.00146-19

Wen, K. Y., Cameron, L., Chappell, J., Jensen, K., Bell, D. J, Kelwick, R., et al. (2017). A cell-free biosensor for detecting quorum sensing molecules in P. aeruginosa-infected respiratory samples. *ACS Synthetic Biol.* 6, 2293–2301. doi: 10.1021/acssynbio.7b00219

Werner, N., Petersen, K., Vollstedt, C., Garcia, P. P., Chow, J., Ferrer, M., et al. (2021). The Komagataeibacter europaeus GqqA is the prototype of a novel bifunctional N-acyl-homoserine lactone acylase with prephenate dehydratase activity. *Sci. Rep.* 11:12255. doi: 10.1038/s41598-021-91536-1

Whiteley, M., Diggle, S. P., and Greenberg, E. P. (2017). Progress in and promise of bacterial quorum sensing research. *Nature* 551, 313–320. doi: 10.1038/nature24624

Whon, T. W., Ahn, S. W., Yang, S., Kim, J. Y., Kim, Y. B., Kim, Y., et al. (2021). ODFM, an omics data resource from microorganisms associated with fermented foods. *Sci Data* 8. doi: 10.1038/s41597-021-00895-x

Wilbert, S. A., Mark Welch, J. L., and Borisy, G. G. (2020). Spatial ecology of the human tongue dorsum microbiome. *Cell Rep.* 30, 4003–4015.e3. doi: 10.1016/j.celrep.2020.02.097

Williams, M. R., Costa, S. K., Zaramela, L. S., Khalil, S., Todd, D. A., Winter, H. L., et al. (2019). Quorum sensing between bacterial species on the skin protects against epidermal injury in atopic dermatitis. *Sci. Transl. Med.* 11:eaat8329. doi: 10.1126/scitranslmed.aat8329

Wolfe, B. E., and Dutton, R. J. (2015). Fermented foods as experimentally tractable microbial ecosystems. *Cells* 161, 49–55. doi: 10.1016/j.cell.2015.02.034

Wu, S., Feng, J., Liu, C., Wu, H., Qiu, Z., Ge, J., et al. (2021b). Machine learning aided construction of the quorum sensing communication network for human gut microbiota. *Nat. Commun.* 13:3079. doi: 10.1038/s41467-022-30741-6

Wu, S., Xu, C., Liu, J., Liu, C., and Qiao, J. (2021a). Vertical and horizontal quorum-sensing-based multicellular communications. *Trends Microbiol.* 29, 1130–1142. doi: 10.1016/j.tim.2021.04.006

Wynendaele, E., Bronselaer, A., Nielandt, J., D'Hondt, M., Stalmans, S., Bracke, N., et al. (2013). Quorumpeps database: chemical space, microbial origin and functionality of quorum sensing peptides. *Nucleic Acids Res.* 41, D655–D659. doi: 10.1093/nar/gks1137

Wynn, D., Raut, N., Joel, S., Pasini, P., Deo, S. K., and Daunert, S. (2018). Detection of bacterial contamination in food matrices by integration of quorum sensing in a paper-strip test. *Analyst* 143, 4774–4782. doi: 10.1039/C8AN00878G

Xue, J., Chi, L., Tu, P., Lai, Y., Liu, C. W., Ru, H., et al. (2021). Detection of gut microbiota and pathogen produced N-acyl homoserine in host circulation and tissues. *NPJ Bio. Microbio.* 7:53. doi: 10.1038/s41522-021-00224-5

Yap, M., Ercolini, D., Álvarez-Ordóñez, A., O'Toole, P. W., O'Sullivan, O., Cotter, P. D., et al. (2022). Next-generation food research: use of meta-Omic approaches for characterizing microbial communities along the food chain. *Annu. Rev. Food Sci. Technol.* 13, 361–384. doi: 10.1146/annurev-food-052720-010751

Yu, H., Li, J., Han, Y., Shi, G., Liu, Z., and Zeng, M. (2019). AHLs-produced bacteria in refrigerated shrimp enhanced the growth and spoilage ability of Shewanella baltica. *J. Food Sci. Technol.* 56, 114–121. doi: 10.1007/s13197-018-3464-8

Yuan, K., Hou, L., Jin, Q., Niu, C., Mao, M., Wang, R., et al. (2021). Comparative transcriptomics analysis of Streptococcus mutans with disruption of LuxS/AI-2 quorum sensing and recovery of methyl cycle. *Arch. Oral Biol.* 127:105137. doi: 10.1016/j.archoralbio.2021.105137

Yuan, L., Sadiq, F. A., Burmølle, M., Liu, T., and He, G. (2018). Insights into bacterial Milk spoilage with particular emphasis on the roles of heat-stable enzymes, biofilms, and quorum sensing. *J. Food Prot.* 81, 1651–1660. doi: 10.4315/0362-028X.JFP-18-094

Zargar, A., Quan, D. N., Carter, K. K., Guo, M., Sintim, H. O., Payne, G. F., et al. (2015). Bacterial secretions of nonpathogenic Escherichia coli elicit inflammatory pathways: a closer investigation of interkingdom signaling. *MBio* 6:e00025. doi: 10.1128/mBio.00025-15

Zaytseva, Y. V., Sidorov, A. V., Marakaev, O. A., and Khmel, I. A. (2019). Plant-microbial interactions involving quorum sensing regulation. *Microbiology* 88, 523–533. doi: 10.1134/S0026261719040131

Zhou, L., Zhang, L. H., Cámara, M., and He, Y. W. (2017). The DSF family of quorum sensing signals: diversity, biosynthesis, and turnover. *Trends Microbiol.* 25, 293–303. doi: 10.1016/j.tim.2016.11.013

Ziesche, L., Bruns, H., Dogs, M., Wolter, L., Mann, F., Wagner-Döbler, I., et al. (2015). Homoserine lactones, methyl Oligohydroxybutyrates, and other extracellular metabolites of macroalgae-associated bacteria of the Roseobacter clade: identification and functions. *Chembiochem: Eur. J. Chem. Biol.* 16, 2094–2107. doi: 10.1002/cbic.201500189

Zink, K. E., Ludvik, D. A., Lazzara, P. R., Moore, T. W., Mandel, M. J., Sanchez, L. M., et al. (2021). A small molecule coordinates symbiotic behaviors in a host organ. *MBio* 12, e03637–e03620. doi: 10.1128/mBio.03637-20

Zwirzitz, B., Wetzels, S. U., Dixon, E. D., Stessl, B., Zaiser, A., Rabanser, I., et al. (2020). The sources and transmission routes of microbial populations throughout a meat processing facility. *NPJ Bio. Microbio.* 6:26. doi: 10.1038/s41522-020-0136-z

10.3389/fmicb.2022.1002185

Glossary

agr	Accessory gene regulator system
AHL	Acylated homoserine lactone
AhR	Aryl hydrocarbon receptor
AI	Autoinducer
AIP	Autoinducer peptide
AMC	Activated methyl cycle
AMR	Antimicrobial resistance
ATP	Adenosine triphosphate
CAI-1	Cholera autoinducer
cAMP	Cyclic adenosine monophosphate
c-di-GMP	Cyclic diguanylate (c-di-GMP)
CRC	Colorectal cancer
DKP	Diketopiperazines
DPD	4,5-dihydroxy-2,3-pentanedione
DPO	3,5-dimethylpyrazin-2-one
DSF	Diffusible signal factor
EHEC	Enterohemorrhagic *Escherichia coli*
EPEC	Enteropathogenic *E. coli* (EPEC)
EPS	Exopolysaccharide
HGT	Horizontal gene transfer
HPLC	High-performance liquid chromatography
HSL	Homoserine lactone
IBD	Inflammatory bowel disease
LAB	Lactic acid bacteria
LEE	Locus of enterocyte effacement
miRNAs	micro RNAs
MS	Mass spectrometry
NEC	Necrotising enterocolitis
OMV	Outer membrane vesicles
QQ	Quorum quenching
Qrr sRNAs	Quorum regulatory sRNAs
QS	Quorum sensing
QSM	Quorum sensing molecules
R-THMF	(*2R,4S*)-2-methyl-2,3,3,4-tetrahydroxytetrahydro-furan)
SAH	S-adenosylhomocysteine
SAM	S-adenosyl-L-methionine
siRNAs	Small Inhibitory RNAs
SRH	S-ribosyl-homocysteine
SSO	Specific spoilage organisms
S-THMF	(*2S,4S*)-2-methyl-2,3,3,4-tetra-hydroxytetrahydrofuran
TCS	Two-component systems

frontiers | Frontiers in Microbiology

TYPE Original Research
PUBLISHED 02 December 2022
DOI 10.3389/fmicb.2022.1001700

OPEN ACCESS

EDITED BY
Agapi Doulgeraki,
Institute of Technology of Agricultural Products, Greece

REVIEWED BY
Sudhir K. Shukla,
Bhabha Atomic Research Centre (BARC), India
Georgios Efthimiou,
University of Hull, United Kingdom

*CORRESPONDENCE
Melesio Gutiérrez-Lomelí
melesio.gutierrez@academicos.udg.mx

SPECIALTY SECTION
This article was submitted to Food Microbiology, a section of the journal Frontiers in Microbiology

RECEIVED 23 July 2022
ACCEPTED 10 November 2022
PUBLISHED 02 December 2022

CITATION
Avila-Novoa MG, Solis-Velazquez OA, Guerrero-Medina PJ, González-Gómez J-P, González-Torres B, Velázquez-Suárez NY, Martínez-Chávez L, Martínez-Gonzáles NE, De la Cruz-Color L, Ibarra-Velázquez LM, Cardona-López MA, Robles-García MÁ and Gutiérrez-Lomelí M (2022) Genetic and compositional analysis of biofilm formed by *Staphylococcus aureus* isolated from food contact surfaces. *Front. Microbiol.* 13:1001700. doi: 10.3389/fmicb.2022.1001700

Genetic and compositional analysis of biofilm formed by *Staphylococcus aureus* isolated from food contact surfaces

María Guadalupe Avila-Novoa[1], Oscar Alberto Solis-Velazquez[1], Pedro Javier Guerrero-Medina[1], Jean-Pierre González-Gómez[2], Berenice González-Torres[2], Noemí Yolanda Velázquez-Suárez[1], Liliana Martínez-Chávez[3], Nanci Edid Martínez-Gonzáles[3], Lucia De la Cruz-Color[1], Luz María Ibarra-Velázquez[1], Marco Antonio Cardona-López[1], Miguel Ángel Robles-García[1] and Melesio Gutiérrez-Lomelí[1]*

[1]Centro de Investigación en Biotecnología Microbiana y Alimentaria, Departamento de Ciencias Básicas, Centro Universitario de la Ciénega, Universidad de Guadalajara, Ocotlán, Jalisco, Mexico, [2]Laboratorio Nacional para la Investigación en Inocuidad Alimentaria (LANIIA), Centro de Investigación en Alimentación y Desarrollo, A.C. (CIAD), Culiacán, Sinaloa, Mexico, [3]Laboratorio de Microbiología e Inocuidad de Alimentos, Departamento de Farmacología, Centro Universitario de Ciencias Exactas e Ingenierías, Universidad de Guadalajara, Guadalajara, Jalisco, Mexico

Introduction: *Staphylococcus aureus* is an important pathogen that can form biofilms on food contact surfaces (FCS) in the dairy industry, posing a serious food safety, and quality concern. Biofilm is a complex system, influenced by nutritional-related factors that regulate the synthesis of the components of the biofilm matrix. This study determines the prevalence of biofilm-associated genes and evaluates the development under different growth conditions and compositions of biofilms produced by *S. aureus*.

Methods: Biofilms were developed in TSB, TSBG, TSBNaCl, and TSBGNaCl on stainless-steel (SS), with enumeration at 24 and 192 h visualized by epifluorescence and scanning electron microscopy (SEM). The composition of biofilms was determined using enzymatic and chemical treatments and confocal laser scanning microscopy (CLSM).

Results and discussion: A total of 84 *S. aureus* (SA1–SA84) strains were collected from 293 dairy industry FCS (FCS-stainless steel [n = 183] and FCS-polypropylene [n = 110]) for this study. The isolates harbored the genes *sigB* (66%), *sar* (53%), *agrD* (52%), *clfB/clfA* (38%), *fnbA/fnbB* (20%), and *bap* (9.5%). 99. In particular, the biofilm formed by *bap*-positive *S. aureus* onto SS showed a high cell density in all culture media at 192 h in comparison with the biofilms formed at 24 h ($p < 0.05$). Epifluorescence microscopy and SEM revealed the metabolically active cells and the different stages of biofilm formation. CLSM analysis detected extracellular polymeric of *S. aureus* biofilms on SS,

such as eDNA, proteins, and polysaccharides. Finally, the level of detachment on being treated with DNase I (44.7%) and NaIO 4(42.4%) was greater in the biofilms developed in TSB compared to culture medium supplemented with NaCl at 24 h; however, there was no significant difference when the culture medium was supplemented with glucose. In addition, after treatment with proteinase K, there was a lower level of biomass detachment (17.7%) of the biofilm developed in TSBNaCl ($p < 0.05$ at 24 h) compared to that in TSB, TSBG, and TSBGNaCl (33.6, 36.9, and 37.8%, respectively). These results represent a deep insight into the composition of *S. aureus* biofilms present in the dairy industry, which promotes the development of more efficient composition-specific disinfection strategies.

KEYWORDS

***Staphylococcus aureus*, biofilms, extracellular matrix, food contact surface, genotypic characterization**

Introduction

Staphylococcus aureus has various implications within nosocomial diseases and foodborne illnesses in terms of public health and economic effect. *S. aureus* has caused 1,681 illnesses and 86 hospitalizations reported in the foodborne-associated outbreaks in the United States (Dewey-Mattia et al., 2018); decreased animal production and milk production caused by clinical and subclinical mastitis in dairy animals; and increased use of antimicrobials for the treatment and prevention of mastitis and numerous diseases, including abscesses, septicemia, and pneumonia, which could lead to the emergence of antimicrobial resistance (Kumar et al., 2010; Akanbi et al., 2017; Abdi et al., 2018; Elsayed et al., 2019; Zhang et al., 2020). In addition, *S. aureus* can form biofilm and could be involved in 65–85% of microbial and chronic infections that are associated with biofilm formation reported by the National Institutes of Health (Flemming et al., 2016; Jamal et al., 2018).

Staphylococcus aureus can produce biofilm using different strategies, including (i) expression of the polysaccharide intercellular adhesin (PIA) by the *icaADBC* operon; (ii) release of extracellular DNA (eDNA); and (iii) expression of numerous surface proteins including MSCRAMMs (microbial surface components recognizing adhesive matrix molecules) (Archer et al., 2011; Dakheel et al., 2016). *S. aureus* produces a variety of MSCRAMMs such as fibronectin-binding proteins (FnBPs), *S. aureus* surface protein G (SasG), clumping factors A and B (ClfA, ClfB), the serine/aspartate-rich (Sdr) protein family, and biofilm-associated protein (Bap), which are protein components of the microbial surface that mediate the initial attachment to the surface proteins of host cells or binding to abiotic surfaces generate biofilms (Arciola et al., 2005; Renner and Weibel, 2011; Gutiérrez et al., 2012; Otto, 2018; Schllcher and Horswill, 2020).

Subsequently, the amounts of individual components of the extracellular matrix of S. *aureus* biofilms such as polysaccharides, glycoproteins, cell-surface-secreted bacterial proteinaceous adhesins, eDNA, and teichoic acids are influenced by different environmental conditions such as the culture medium, different *S. aureus* isolates, and interaction between different species and the surface (Flemming and Wingender, 2010; Schwartz et al., 2016; Singh et al., 2017; Liu et al., 2018; Sugimoto et al., 2018; Solis-Velazquez et al., 2021).

Staphylococcus aureus can produce biofilm in food processing environments and on equipment, including food contact surfaces (FCSs) (both food contact and non-food contact), pipelines, pasteurizers, and raw milk storage tanks, in the dairy industry (Gutiérrez et al., 2012; Di Ciccio et al., 2015; Avila-Novoa et al., 2018b). The persistence of biofilm in food processing environments is due to equipment designs that are difficult to clean and disinfect, ineffective cleaning of the food manufacturing environment, or interaction of antimicrobials and disinfectants with the extracellular matrix, decreasing their effectiveness, which has hindered strategies for the control of biofilms within the industry (Brooks and Flint, 2008; Bridier et al., 2015; Hall and Mah, 2017).

Biofilm is a potential source of direct and indirect contamination among food products and responsible for damaged equipment or drinking-water distribution, more expensive energy costs, and outbreaks (Møretrø and Langsrud, 2017; Alvarez-Ordóñez et al., 2019; Avila-Novoa et al., 2021; Carrascosa et al., 2021). Biofilms generate major food safety problems and economic losses for the food industry.

Hence, there is a need for knowledge about the factors that regulate the components in the extracellular matrix and the development or growth of biofilms, such as environmental conditions and phenotypic and genotypic characterization of biofilm-forming *S. aureus* that differ from those in planktonic conditions and which contribute to better adaptation of pathogens in a food processing environment, to establish control measures for the removal of biofilms. Therefore, the main objectives of this research were as follows: (i) to determine the prevalence of biofilm-associated genes in the *S. aureus* isolates

and (ii) to provide useful data about the biofilm development under different growth conditions and the composition of biofilms formed by *S. aureus*.

Materials and methods

Bacterial strains

A total of 84 *S. aureus* strains were recovered from FCS in the dairy industry of Jalisco. In brief, 35.7% of enterotoxigenic *S. aureus* harbored 2–4 enterotoxin genes (*sea*, *seb*, *sec*, *sed*, *see*, *seh*, *sei*, and *sej*) (Avila-Novoa et al., 2018a) and 52.3% of the *S. aureus* contained the *icaADBC* gene that synthesizes PIA (Avila-Novoa et al., 2018b). Stocks were stored in tryptic soy broth (TSB; Becton Dickinson Bioxon, Le Pont de Claix, France) containing 30% glycerol at 80°C. Working cultures were maintained in TSB for 24 h at 37°C.

Presence of *Staphylococcus aureus* adhesion and biofilm-related genes

Genomic DNA was extracted from *S. aureus* strains using a Bacteria DNA Preparation Kit (Jena Bioscience, Dortmund, Germany) according to the manufacturer's instructions. All *S. aureus* strains were investigated for the detection of *clfB*, *clfA*, *fnbA*, *fnbB*, and *bap genes* by PCR using the protocol of Tang et al. (2013); *agrD*, *sar*, and *sigB* in the DNA were also determined (Kim et al., 2016). The amplification conditions used were as follows: 5 min at 95°C; 35 cycles of 40 s at 95°C, 50 s at different temperatures for different genes (**Supplementary Table 3**) and 50 s at 72°C; followed by a final extension of 10 min at 72°C. After that, the PCR products were electrophoresed on 1% agarose gel (UltraPure agarose, Invitrogen, Carlsbad, CA, USA), containing green gel loading buffer (Jena Bioscience, Dortmund, Germany) and visualized by transillumination under UV light (UVP, DigiDoc-It Darkroom, Upland, CA, USA). *S. aureus* ATCC 25923 was used as the positive control.

Evaluation of cell viability and matrix characterization of biofilms under various environmental conditions

Surface preparation and quantification of biofilm formation

Stainless-steel (SS) coupons (AISI 316, 0.8 × 2.0 × 0.1 cm; CIMA Inoxidable, Jalisco, Mexico), prepared as described by Marques et al. (2007), were used as the surfaces for biofilms formation. In brief, the individual sterile SS coupons were introduced into a polypropylene tube (15 ml Centrifuge Tube, Corning CentriStar) containing 10 ml of TSB, TSB + 0.4% glucose (Golden Bell, Zapopan, México) (TSBG), TSB + 4% NaCl (Golden Bell, Zapopan, México) (TSBNaCl), or TSB + 0.4% glucose + 4% NaCl (TSBGNaCl) and then inoculated with 100 μl of the corresponding strain (~10^8 cfu/ml). Next, the polypropylene tubes were incubated at 37°C for 24 and 192 h, allowing the formation of biofilm. Bacterial enumeration of biofilms after incubation was conducted as previously described by Avila-Novoa et al. (2021). Three replicates were performed for each strain. *S. aureus* ATCC 25923 was used as the positive control.

Epifluorescence microscopy and scanning electron microscopy

After 24 and 192 h of incubation, the SS coupons were removed from the polypropylene test tubes containing 10 ml of TSB, TSBG, TSBNaCl, or TSBGNaCl, and the non-adhered cells were eliminated with PBS and vortexed for 10 s. In brief, cell viability was examined by staining cells with 5 (6)-carboxyfluorescein diacetate (CFDA, 10 μg/ml; Sigma-Aldrich, St. Louis, MO, USA) as described by Avila-Novoa et al. (2018b). Epifluorescence microscopy was performed using a Nikon Eclipse E400, a 100x oil immersion lens, and a blue excitation filter (BA 515 B-2A), at an emission wavelength of 450–490 nm. Scanning electron microscopy (SEM) was performed on the SS coupons after 24 and 192 h of incubation using the protocols described by Borucki et al. (2003) and Fratesi et al. (2004). Biofilms were observed using a TESCAN Mira3 LMU scanning electron microscope (Tezcan, Prague, Czech Republic).

Evaluation of biofilms with composition by confocal laser scanning microscopy and detachment assays

Confocal laser scanning microscopy

After incubation at 37°C for 24 and 192 h, the SS coupons were thoroughly rinsed with PBS and vortexed for 10 s to eliminate the non-adhered cells. Then, for observation, the components of the biofilm were exposed to the following three dyes: (i) SYTO 9® Green-Fluorescent Nucleic Acid Stain (Invitrogen, Eugene, OR, USA) (excitation, 476 nm; emission, 500–520 nm) which stains nucleic acids, (ii) FilmTracer™ SYPRO® Ruby Biofilm Matrix Stain (Invitrogen, Eugene, OR, USA) (excitation, 405 nm; emission, 655–755 nm) which labels most classes of proteins, and (iii) WGA, wheat germ agglutinin conjugated with Oregon Green (Invitrogen, Eugene, OR, USA) (excitation, 459 nm; emission, 505–540 nm) which stains *N*-acetyl-D-glucosamine residues (Oniciuc et al., 2016). Subsequently, microscopic observation and image analysis of biofilms were performed with a Zeiss LSM 700 confocal laser

scanning microscope (Carl Zeiss, Germany) and ZEN 2009 V 5.5 Software (Carl Zeiss®, Jena, Germany).

Matrix characterization

Biofilm detachment assays were carried out as described by Oniciuc et al. (2016) and Avila-Novoa et al. (2021). Mature biofilms were treated with (i) proteinase K (PROMEGA, Madison, WI, USA) (0.1 mg ml^{-1} in 20 mM Tris-HCl: 1 mM $CaCl_2$), (ii) 40 mM $NaIO_4$ in double-distilled H_2O, or (iii) 0.5 mg ml^{-1} DNase I (Roche, Mannheim, Germany) in 5 mM $MgCl_2$, for 2 and 24 h at 37°C. Previously, the mature biofilms were cultivated in TSB, TSBG, TSBNaCl, or TSBGNaCl (37°C for 192 h) and subsequently washed with 0.9% NaCl for treatment. Biomass quantification was performed by measuring the optical density (OD) at 492 nm (OD_{492}) using a Multiskan FC (Thermo Fisher Scientific Inc., Madison, WI, USA). All experiments were performed in triplicate.

Statistical analysis

All experiments were evaluated using analysis of variance (ANOVA), followed by a least significant difference (LDS) test, in the Statgraphics Centurion XVI software program (StatPoint Technologies, Inc., Warrenton, VA, USA). Values of $p < 0.05$ were considered statistically significant.

Results

Of all isolates, 66% (56/84) harbored *sigB*, 53% (45/84) *sar*, 52% (44/84) *agrD*, 38% (32/84) *clfB*, 38% (32/84) *clfA*, 20% (17/84) f*nbA*, 20% (17/84) f*nbB*, and 9.5% (8/84) *bap*. Of the 22 isolates, *agrD*, *sigB,* and *sar* were detected in 26%, and *clfA*, *clfB*, *fnbA,* and *fnbB* were detected in 13% (**Table 1**). Subsequently, a selection of three strains of *S. aureus* (SA-4, SA-33, SA-41) was based on the genotypic and phenotypic characteristics associated with the formation of biofilm, in addition to the risks associated with the consumer by the detection of enterotoxigenic genes involved in food poisoning in previous publications (Avila-Novoa et al., 2018a,b; **Table 2**). All the tested microorganisms (*bap*-positive *S. aureus* [SA-4, SA-33, SA-41]) showed a strong ability to develop biofilms in TSB (8.30–9.04 log_{10} cfu/cm^2), TSBG (7.91–8.53 log_{10} cfu/cm^2), and TSBGNaCl (8.28–8.94 log_{10} cfu/cm^2), compared to TSBNaCl (7.84–8.52 log_{10} cfu/cm^2; $p < 0.05$) at 24 h; however, the development of the biofilm *S. aureus* was favored at 192 h ($p < 0.05$) (**Figure 1**). Generally, *S. aureus* formed a higher cellular density biofilm in TSBGNaCl (9.14–9.56 log_{10} cfu/cm^2) in comparison with TSBNaCl (8.25–8.89 log_{10} cfu/cm^2; $p < 0.05$) and TSBG (8.34–9.47 log_{10} cfu/cm^2; $p < 0.05$) at 192 h. Besides that, *S. aureus* biofilm had a lower biomass biofilm in TSBNaCl in comparison with TSB (8.94–9.35 log_{10} cfu/cm^2; $p < 0.05$); there was no difference between TSBNaCl and TSBG ($p > 0.05$), TSBG and TSB ($p > 0.05$), and TSB and TSBGNaCl ($p > 0.05$) at 192 h (**Figure 1**). Furthermore, there was no significant difference in the biofilm formation capacity of SA-4, SA-33, SA-41, and *S. aureus* ATCC 25923 in unsupplemented TSB (24–192 h; $p > 0.05$). A comparison of supplemented media showed that TSBG decreased the cell density (<1 log_{10} cfu/cm^2) of SA-33 and SA-41 (TSBG; $p < 0.05$); TSBGNaCl decreased that of SA-4, SA-41, and *S. aureus* ATCC 25923 ($p < 0.05$), and TSBNaCl that of SA-33 and *S. aureus* ATCC 25923 ($p < 0.05$) at 24 h. The cellular density of biofilm of SA-4, SA-33, and SA-41 on TSBG ($p < 0.05$) and that of SA-33 on TSBNaCl ($p < 0.05$) was decreased compared to the cell density of SA-41 which increased (>1 log_{10} cfu/cm^2) on TSBGNaCl ($p < 0.05$) at 192 h. Epifluorescence micrographs showed adhered-embedded cells in possible extracellular polymeric substances (EPS) and microcolonies made up of metabolically active cells (**Figures 2A–C**). In addition, SEM analysis showed the different stages of biofilm formation with adhered cells,

TABLE 1 Frequency of *agrD*, *sar*, *sigB,* and *adhesin genes* in *Staphylococcus aureus* isolates from food contact surfaces (FCSs) in the dairy industry.

Genotype	No. (%) of *S. aureus* strain isolated
clfA-clfB-fnbpA-fnbpB-bap-agrD-sigB-sar	4 (4.76)
clfA-clfB-fnbpA-fnbpB-agrD-sigB-sar	1 (1.19)
clfA-clfB-fnbpA-fnbpB-sigB-sar	1 (1.19)
clfA-clfB-fnbpA-fnbpB-agrD-sar	1 (1.19)
fnbpA-fnbpB-agrD-sigB-sar	4 (4.76)
clfA-clfB-fnbpA-fnbpB-agrD	1 (1.19)
clfA-clfB-fnbpA-fnbpB-sar	1 (1.19)
clfA-clfB-fnbpA-fnbpB-sigB	1 (1.19)
clfA-clfB-fnbpA-fnbpB-bap	1 (1.19)
clfA-clfB-agrD-sigB-sar	1 (1.19)
clfA-clfB-bap-agrD-sigB	1 (1.19)
clfA-clfB-agrD-sigB	6 (7.14)
agrD-sigB-sarA-bap	1 (1.19)
clfA-clfB-sar	1 (1.19)
clfA-clfB-agrD	2 (2.38)
clfA-clfB-sigB	4 (4.76)
agrD-sigB-sar	12 (14.28)
sigB-sarA-bap	1 (1.19)
fnbpA-fnbpB-agrD	1 (1.19)
fnbpA-fnbpB-sigB	1 (1.19)
clfA-clfB	6 (7.14)
agrD-sigB	8 (9.52)
sigB-sar	7 (8.33)
AgrD	5 (5.95)
SigB	3 (3.57)
Sar	2 (2.38)

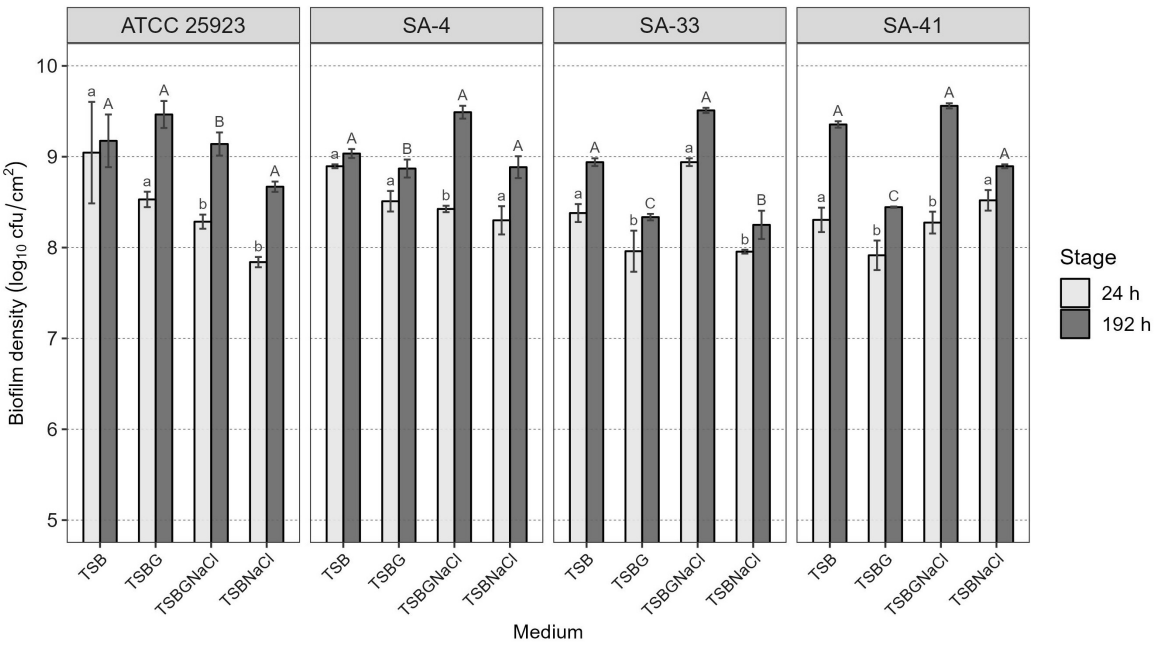

FIGURE 1
Cell density of *S. aureus* biofilms developed in different enriched media at 24 and 192 h of maturity. Different lowercase letters indicate significant differences between S. aureus strains on the same growth medium at 24 h of development and uppercase letters at 192 h, according to the Tukey test ($p < 0.05$). TSB, Tryptic soy broth; TSBG, TSB + 0.4% Glucose; TSBNaCl, TSB + 4% NaCl; TSBGNaCl, TSB + 0.4% Glucose + 4% NaCl.

forming microcolonies embedded in EPS, or maturation and dispersal of cells, highlighting the rheological structure of the biofilm (**Figures 2D–F**).

Additionally, the components of the SA-4, SA-33, and SA-41 biofilms were determined by the detachment of the biofilm according to the medium in which it was developed (**Figure 3**). The level of the detachment of the biofilms developed after the treatments with $NaIO_4$, DNase I, and proteinase *K* with an exposure time of 2 h was lower compared to that at 24 h ($p < 0.05$). After treatment with $NaIO_4$ and proteinase *K*, there was a lower level of the detachment of the biomass of the biofilm developed in TSBNaCl ($p < 0.05$ at 2 h) compared to TSBG; however, there was no significant difference after treatment with DNase I in the biofilms developed in TSB, TSBG, TSBNaCl, and TSBGNaCl ($p > 0.05$ at 2 h). In general, after treatment with DNase I, the level of biomass detachment was greater (44.7%) of the biofilm developed in TSB compared to TSBNaCl and TSBGNaCl (20.5 and 33.1%, respectively) ($p < 0.05$ at 24 h). The effects with $NaIO_4$ was a greater level of biomass detachment (42.4%) of the biofilm developed in TSB compared to TSBNaCl (17.9%; $p < 0.05$ at 24 h); however, there was a significant difference in detached biofilm biomass generated between TSBG and TSBNaCl ($p < 0.05$ at 24 h) and TSBNaCl and TSBGNaCl ($p < 0.05$ at 24 h). In addition, after treatment with proteinase *K*, there was a lower level of biomass detachment (17.7%) of the biofilm developed in TSBNaCl ($p < 0.05$ at 24 h) compared to that in TSB, TSBG, and TSBGNaCl (33.6, 36.9, and 37.8%, respectively). SA-33 and SA-41 showed less detachment of biofilm biomass after the treatments with $NaIO_4$, DNase I, and proteinase *K* compared to SA-4 ($p < 0.05$, at 2–24 h). Confocal laser scanning microscopy (CLSM) analysis in conjugation with three different fluorescent dyes was used to observe the biofilm production of *S. aureus*, and the results indicated that these biofilms were composed of bacterial cells and EPS. Biofilm matrices of SA-4, SA-33, and SA-41 were formed by different *S. aureus* and EPS such as eDNA (**Figures 4A–D**), proteins (**Figures 4E–H**), and polysaccharides adhesin (**Figures 4I–L**).

Discussion

Staphylococcus aureus can generate biofilms on FCS within the dairy industry, affecting the quality and safety of food products. In brief, this pathogen causes outbreaks of foodborne illnesses associated with the consumption of milk and dairy products, and cow clinical and subclinical mastitis, which leads to huge economic losses.

In this study, the prevalence of genes encoding for the adhesion factors revealed 20% for (*fnbA/fnbB*) and 38% for (*clfA/clfB*) in the 84 *S. aureus* strains recovered from FCS in the dairy industry of Jalisco (Avila-Novoa et al., 2018a). Similar observations have also been reported by other investigators (Tang et al., 2013; Gogoi-Tiwari et al., 2015; Azara et al., 2017;

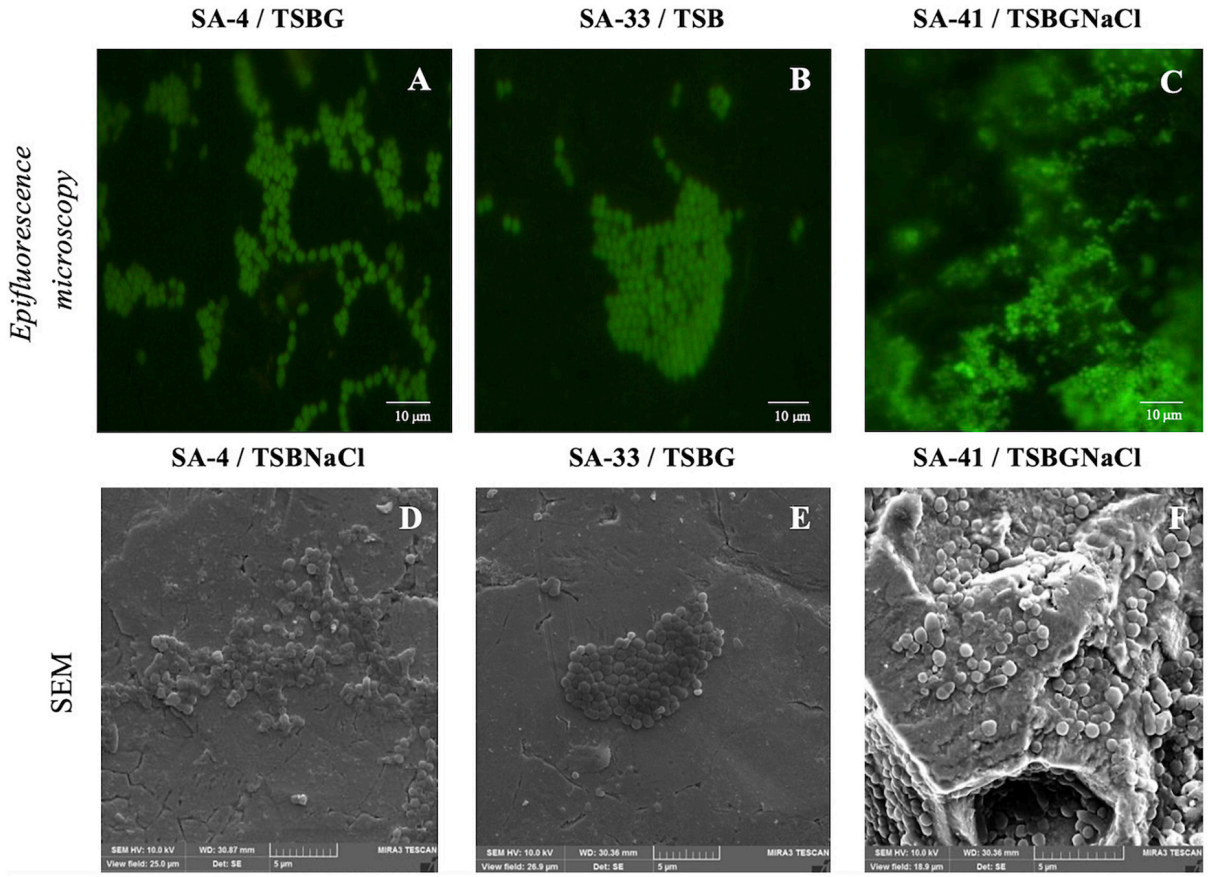

FIGURE 2
Biofilms of isolates *S. aureus* [SA-4 **(A,D)**, SA-33 **(B,E)**, and SA-41 **(C,F)**] from food contact surfaces (FCS). Biofilms were developed on stainless steel through 192 h of incubation in different medium at 37°C and visualized with epifluorescence microscopy (top row) and SEM (bottom row). SA, *S. aureus*; TSB, Tryptic soy broth; TSBG, TSB + 0.4% Glucose; TSBNaCl, TSB + 4% NaCl; TSBGNaCl, TSB + 0.4% Glucose + 4% NaCl.

Azmi et al., 2019; Liu et al., 2020; Zaatout et al., 2020) who reported similar percentages (*clfA* [2.3–41.6%], *clfB* [4.6%], *fnbA* [0–54.5%], and *fnbB* [1.3–68.7%]) for the prevalence of some of the adhesion genes. Also, Azara et al. (2017); Vergara et al. (2017), and Zhang et al. (2020) found no evidence of the *fnbA* or *fnbB* genes in *S. aureus*. Additionally, 9.5% of the *S. aureus* isolates had *bap* which has been associated with *S. aureus* of bovine mastitis origin and with *ica*-independent biofilm formation (Arciola et al., 2001; O'Gara, 2007; Archer et al., 2011; Salgado-Ruiz et al., 2015; Aslantaş and Demir, 2016).

In contrast, a considerably greater prevalence of *clfA* (50–100%), *clfB* (80.2–100%), *fnbA* (72.8–100%), and *fnbB* (80.3–100%) genes have been found in *S. aureus* isolates collected from milk samples from cows with clinical and subclinical mastitis, pasteurized milk, chicken, food poisoning outbreaks, pork, and slaughtered goats (Tang et al., 2013; Aslantaş and Demir, 2016; Pereyra et al., 2016; Azara et al., 2017; Vergara et al., 2017; Dai et al., 2019; Liu et al., 2020; Zhang et al., 2020). Also, the *bap* gene was not detected in isolates of S. *aureus* by Tang et al. (2013); Pereyra et al. (2016), and Liu et al. (2020).

This suggests that a variety of virulence factors such as ClfA, ClfB, FnbA, FnbB, and Bap are involved in the initial attachment to the surface proteins of host cells and colonization of the mammary gland by *S. aureus*. Besides, binding to abiotic surfaces such as FCS, these virulence factors are involved in the initial stage of biofilm formation or with components inside EPS to give biofilm stability.

Nevertheless, the variation in the prevalence of *S. aureus* virulence factors in this study could be associated with the genetic diversity of strains, epidemiological factors where different sources or mechanisms of contamination in the food processing environment are involved in each of the developed countries, and the source and sizes of samples or their geographic locations. Some virulence factors of *S. aureus* are encoded in plasmids or phages which can be transferred between bacteria by horizontal gene transfer where the exchange and transfer of genes are facilitated by biofilm formation (Fueyo et al., 2005; Beceiro et al., 2013; Derakhshan et al., 2021).

Biofilm formation by *S. aureus* not only involves the *icaADBC* operon, *agr* locus, and quorum-sensing mechanisms

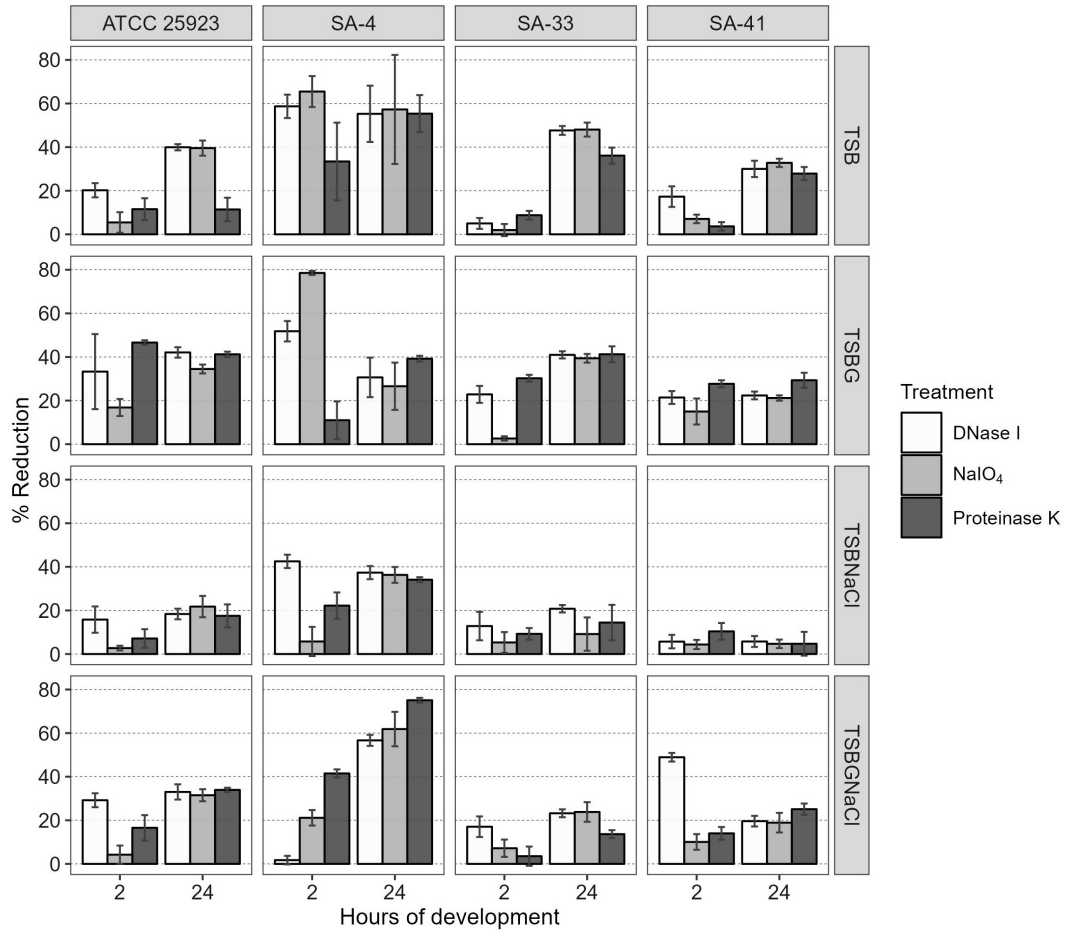

FIGURE 3
Percentage reduction of *S. aureus* biofilms after treatment with DNase I, NaIO4, or proteinase K at 2 and 24 h of maturity. SA, *S. aureus*; TSB, Tryptic soy broth; TSBG, TSB + 0.4% Glucose; TSBNaCl, TSB + 4% NaCl; TSBGNaCl, TSB + 0.4% Glucose + 4% NaCl.

(QS) but also other biofilm-associated genes such as *arlRS*, *bap*, *hla*, *rbf*, *sar*, *sigB*, *tcaR*, and *trap* (Tsang et al., 2008; Ciftci et al., 2009; Aslantaş and Demir, 2016; Kim et al., 2016; Sankar Ganesh et al., 2019). Following other studies (Kim et al., 2016; Avila-Novoa et al., 2021), we found that the presence of *sigB*, *sar*, and *agrD* genes was associated with the regulation and formation of biofilms; also, *agr* regulates the production of biofilms, including the detachment of biofilm, and then the expression of virulence-associated gene expression helps in dissemination of *S. aureus* (Boles and Horswill, 2008; Paharik and Horswill, 2016). However, the absence of regulators such as *sigB*, *agrD*, and *sar* in isolates *S. aureus* could be for the presence of other regulators such as MgrA and ArIRS have also been linked to biofilm formation. Hence, three strains of different *bap*-positive *S. aureus* were investigated for evaluation of cell viability and matrix characterization of biofilms under various environmental conditions. In this study, we also found that the cell density of *bap*-positive *S. aureus* biofilms is higher in medium supplements with glucose (8.34–9.47 $\log_{10}$ cfu/cm^2 in TSBG) or glucose and NaCl (9.14–9.56 $\log_{10}$ cfu/cm^2 in TSBGNaCl) at 192 h ($p < 0.05$). Besides, the cell density of a biofilm is lower in TSBNaCl (24–192 h; $p < 0.05$) (**Figure 1**). The observations emphasize the fact that the ability to form biofilm is complex when using medium supplements (TSBG, TSBNaCl, and TSBGNaCl) compared to TSB. Similar observations have also been reported by other investigators (O'Neill et al., 2007; Croes et al., 2009; Srey et al., 2013): the evidence of glucose or NaCl induce biofilm formation for *S. aureus*. This could be associated with the fact that the supplements favor the pre-conditioning of the surface and irreversible adhesion for the formation of the biofilm and are associated with the genotypic characteristics of *S. aureus* (**Table 2**). Likewise, Cucarella et al. (2001) reported that *bap*-positive *S. aureus* can form biofilm even though its *icaADBC* operon was disrupted. Also, pre-conditioning influences the chemical and physical properties of the substrate/fluid interface making it a more favorable environment for bacterial adhesion (Chmielewski and Frank, 2003; Lorite et al., 2011).

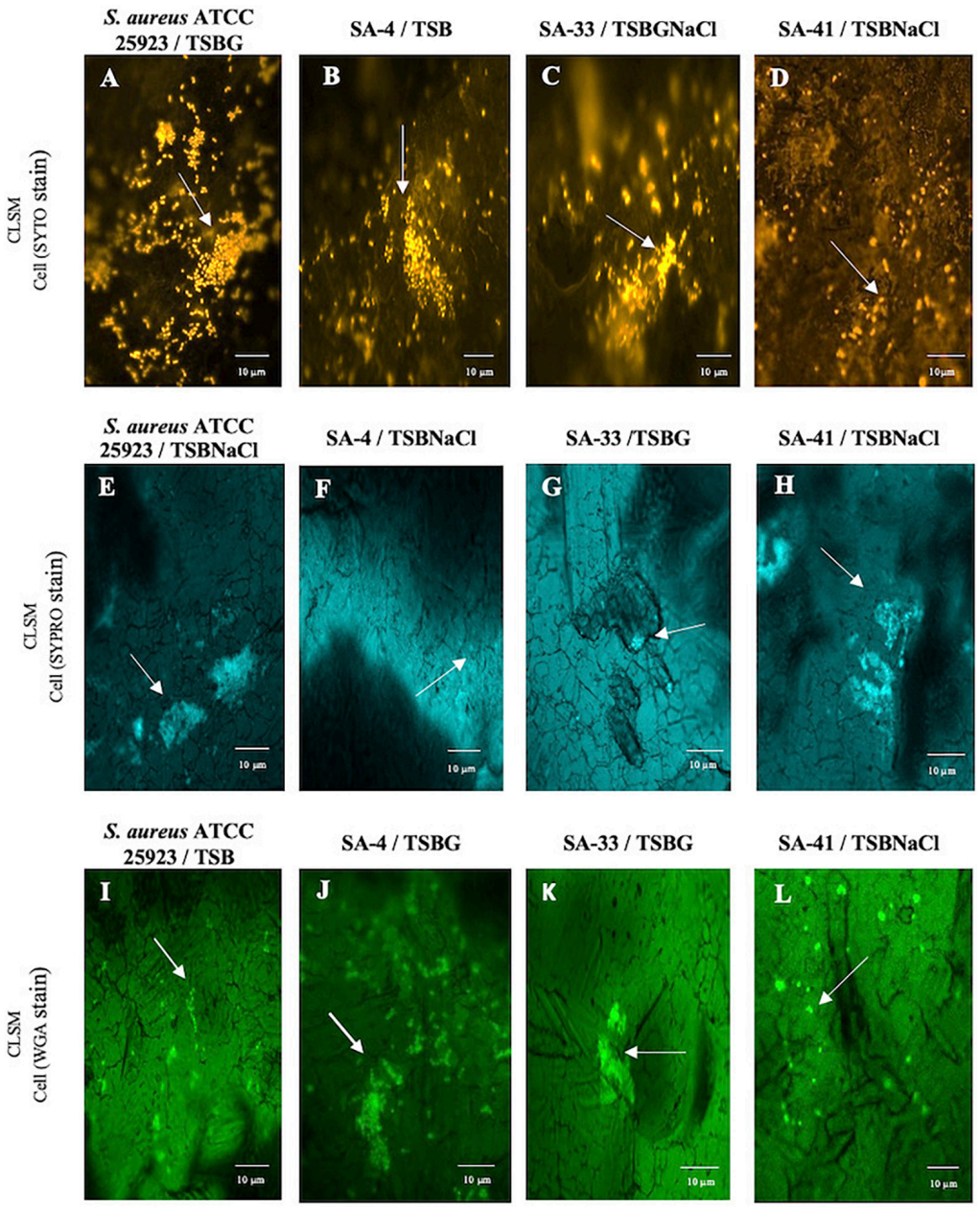

FIGURE 4
Biofilm matrix structures obtained from CLSM observation of *S. aureus* ATCC 25923 **(A,E,I)**, SA-4 **(B,F,J)**, SA-33 **(C,G,K)**, and SA-41 **(D,H,L)** isolates from FCS on stainless steel through h of incubation in 37°C for 192 h in different medium. SA, *S. aureus*; TSB, Tryptic soy broth; TSBG, TSB + 0.4% Glucose; TSBNaCl, TSB + 4% NaCl; TSBGNaCl, TSB + 0.4% Glucose + 4% NaCl.

TABLE 2 Characteristics associated with biofilm formation of *Staphylococcus aureus* in this study.

Bacterial strain	[a]SE's/ [b]*icaADBC*	Genotypes biofilm related							
		clfA	*clfB*	*fnbpA*	*fnbpB*	*bap*	*agrD*	*sigB*	*sar*
SA-4	*sec* + *sed* + *seg* + *sej/icaADBC*	+	+	+	+	+	+	+	+
SA-33	*sej/icaADBC*	–	+	+	+	+	+	+	+
SA-41	–/icaAD	–	+	+	+	+	+	+	+

[a], [b] Avila-Novoa et al. (2018a,b).

The presence of high concentrations of glucose in the medium decreases pH due to catabolism; however, this represses *agr*-locus favoring the biofilm formation of *S. aureus* (O'Neill et al., 2007; McCarthy et al., 2015; Paharik and Horswill, 2016). Taglialegna et al. (2016) determined the expression of *bap* and the formation of the biofilm of *S. aureus* V329 (Bap-positive) in LB-glucose, concluding that Bap promotes the aggregation de Bap-positive strains and the development of the biofilm, where the pH decreases (pH < 5) due to the growth of *S. aureus* in the LB-glucose medium. Likewise, Sugimoto et al. (2018) argue that low pH limits the production of extracellular proteases, inducing the association of surface proteins in the extracellular matrix and promoting the formation of biofilms. Lade et al. (2019) determined differences in biofilm formation when there are NaCl supplements (1–2%) to the TSB and they associate it with the loose attachment of *S. aureus* biofilms to the surface due to an excess of NaCl. There is an association between methicillin-sensitive *S. aureus* (MSSA) or methicillin-resistant *S. aureus* (MSRA) and *ica*-dependent biofilm. O'Neill et al. (2007) determined that NaCl-induced biofilm development was significantly more prevalent in MSSA clinical isolates compared with MRSA; however, various external signals, such as pH, incubation temperatures, ingredients composition (glucose, sodium chloride, ethanol, caseins, serum albumin, fibrin, and dilution rate of media), and CO_2, (Kumar et al., 2017; Miao et al., 2017; Solis-Velazquez et al., 2021), can alter the regulation and the expression of biofilm-associated genes and regulators and/or biofilm development.

Overall, biofilm *S. aureus* matrix presented greater detachment of biofilm after DNase I (44.7%) and $NaIO_4$ (42.4%) treatment in TSB as compared to low detachment of biofilm in TSBNaCl ($p < 0.05$ at 24 h) (**Figure 3**). Dakheel et al. (2016) and Oniciuc et al. (2016) reported similar percentages of polysaccharide levels (20–52%) for *S. aureus* isolates from different systemic infections, dairy products, fish and fish products, and meat and meat products. In contrast, other researchers, Fredheim et al. (2009) and Solis-Velazquez et al. (2021), have reported low biofilm detachment after DNase I treatment in *S. epidermidis* (20%) and *S. aureus* (7.95%).

In addition, after treatment with proteinase *K*, there was a lower level of biomass detachment (17.7%) of the biofilm developed in TSBNaCl ($p < 0.05$ at 24 h) compared to that in TSB, TSBG, and TSBGNaCl (33.6, 36.9, and 37.8, respectively) in this study. A similar observation was also reported by Dakheel et al. (2016) and Oniciuc et al. (2016), who showed detachment of biofilm for *S. aureus* strains isolated from isolates of different systemic infections and food sources after proteinase *K* treatment (39–70%). Likewise, Shukla and Rao (2017) showed that *bap*-positive *S. aureus* V329 and other *S. aureus* (SA7, SA10, SA33, and SA352) bovine mastitis isolates had a biofilm detachment of about 60–84% after proteinase *K* treatment. In contrast, Fredheim et al. (2009) and Solis-Velazquez et al. (2021) have reported low biofilm detachment after proteinase *K* treatment in *S. epidermidis* (10%) and *S. aureus* (12.5%). However, proteinase *K* treatment did not affect the *bap*-mutant *S. aureus* M556 or *bap*-negative *S. aureus* biofilm (Shukla and Rao, 2013, 2017).

Our data showed that the different levels of polysaccharide, proteins, and eDNA after treatments may be associated with the expression or regulation of the *icaADBC* operon, *agr*-locus, etc., in *S. aureus,* biofilm age, environmental factors, and conditions of treatment enzymatic such as concentration, period of contact, type surface etc. Bai et al. (2021) argue that the surface materials, growth conditions, and biofilm maturity affected the composition of complex extracellular matrixes (ECMs) of *S. aureus.* Clearly, eDNA is one of the main components of the biofilm in this study; however, eDNA plays several roles such as bacterium surface adhesion by modulation of charge and hydrophobicity interactions between the bacteria and the abiotic surface (Nguyen et al., 2016) and chelates divalent cations, which triggers a genetic response to increase pathogenicity and resistance to antimicrobials (Okshevsky and Meyer, 2015). Abdallah et al. (2014) argue that the increase in the biofilm age also promoted increases in the proteins and carbohydrates in the matrix of the *S. aureus* biofilm.

$NaIO_4$ can modify PIA/poly N-acetylglucosamine (PNGA) polymer chains by cleaving C3-C4 bonds in exopolysaccharide residues and oxidizing carbons to produce vicinal hydroxyl groups (Chaignon et al., 2007). Nevertheless, the low or high level of exopolysaccharides after $NaIO_4$ treatment in MRSA may be due to differences both in the amount of O-linked acetates with succinate and acetylation levels of amino groups (Spiliopoulou et al., 2012; Dakheel et al., 2016). Besides, polysaccharides are not the only component within the biofilm matrix, there are other components such as eDNA, proteins, and lipids, that interact with each other and can affect detachment. Likewise, Oniciuc et al. (2016) proved that protein-based matrices are of prime importance for the structure of biofilms formed by *S. aureus* strain isolates from food sources; however, the biofilms are composed of different types of proteins, which may vary from one *S. aureus* strain to another (Chaignon et al., 2007). The results obtained by CLSM allowed visual analysis of the concurrent distribution of eDNA, protein, and polysaccharide components within the biofilms and SEM enable observation of the biofilm architecture (EPS and embedded bacterial cells) (**Figures 2**, **4**). The heterogeneity of the biofilm matrix limits the effect of the biocides and/or by quenching their action (Araújo et al., 2013; Lutskiy et al., 2015). However, in this study, it is suggested that proteinase *K* and DNase I allow the dispersion of the biofilm, or they could be facilitating the penetration of other biocides into the biofilm. The proteinase *K* has a synergistic effect when associated with antibiotics, and DNase I has anti-biofilm activity against *S. aureus* biofilm (Kaplan et al., 2012; Shukla and Rao, 2013, 2017). Consequently, it is very urgent and significant to establish control strategies and prevention methods in food industries where they have

incorporated the use of two or several successive treatments that may be necessary for a sufficient remotion of biofilm produced by *S. aureus*.

Conclusion

Most of the *S. aureus* strains isolated from FCS in the dairy industry of Jalisco harbored virulence-associated genes, and in addition, they carried genes associated with the formation of biofilms. The biofilms formed with the selected strains showed different compositions of EPS. Our study showed that the proportion components that make up the extracellular matrix are associated with factors such as culture media and genetic characteristics of the *S. aureus* isolates. Determining the virulence potential of *S. aureus* is important in terms of public health, as is risk identification in milk and dairy products because they provide critical information for microbiological and chemical risk assessment.

Data availability statement

The original contributions presented in this study are included in the article/**Supplementary material**, further inquiries can be directed to the corresponding author.

Author contributions

MA-N and MG-L: conceptualization, resources and funding acquisition, supervision, and project administration. OS-V, J-PG-G, and BG-T: methodology and investigation. NV-S, LM-C, NM-G, and LD: validation and formal analysis. LI-V, MC-L, and MR-G: original draft preparation. MA-N, PG-M, and MG-L: writing—review and editing. All authors have read and agreed to the published version of the manuscript.

Conflict of interest

The authors declare that the research was conducted in the absence of any commercial or financial relationships that could be construed as a potential conflict of interest.

Publisher's note

All claims expressed in this article are solely those of the authors and do not necessarily represent those of their affiliated organizations, or those of the publisher, the editors and the reviewers. Any product that may be evaluated in this article, or claim that may be made by its manufacturer, is not guaranteed or endorsed by the publisher.

Supplementary material

The Supplementary Material for this article can be found online at: https://www.frontiersin.org/articles/10.3389/fmicb.2022.1001700/full#supplementary-material

References

Abdallah, M., Chataigne, G., Ferreira-Theret, P., Benoliel, C., Drider, D., Dhulster, P., et al. (2014). Effect of growth temperature, surface type and incubation time on the resistance of *Staphylococcus aureus* biofilms to disinfectants. *Appl. Microbiol. Biotechnol.* 98, 2597–2607. doi: 10.1007/s00253-013-5479-4

Abdi, R. D., Gillespie, B. E., Vaughn, J., Merrill, C., Headrick, S. I., Ensermu, D. B., et al. (2018). Antimicrobial resistance of *Staphylococcus aureus* isolates from dairy cows and genetic diversity of resistant isolates. *Foodborne Pathog. Dis.* 15, 449–458. doi: 10.1089/fdp.2017.23612

Akanbi, O. E., Njom, H. A., Fri, J., Otigbu, A. C., and Clarke, A. M. (2017). Antimicrobial susceptibility of *Staphylococcus aureus* isolated from recreational waters and beach sand in Eastern Cape Province of South Africa. *Int. J. Environ. Res. Public Health* 14:1001. doi: 10.3390/ijerph14091001

Alvarez-Ordóñez, A., Coughlan, L. M., Briandet, R., and Cotter, P. D. (2019). Biofilms in food processing environments: Challenges and opportunities. *Annu. Rev. Food Sci. Technol.* 10, 173–195. doi: 10.1146/annurev-food-032818-121805

Araújo, P. A., Lemos, M., Mergulhão, F., Melo, L., and Simões, M. (2013). The influence of interfering substances on the antimicrobial activity of selected quaternary ammonium compounds. *Int. J. Food Sci.* 2013:2237581.

Archer, N. K., Mazaitis, M. J., Costerton, J. W., Leid, J. G., Powers, M. E., and Shirtliff, M. E. (2011). *Staphylococcus aureus* biofilms. *Virulence* 2, 445–459. doi: 10.4161/virus.2.5.17724

Arciola, C. R., Baldassarri, L., and Montanaro, L. (2001). Presence of *icaA* and *icaD* genes and slime production in a collection of staphylococcal strains from catheter-associated infections. *J. Clin. Microbiol.* 39, 2151–2156. doi: 10.1128/JCM.39.6.2151-2156.2001

Arciola, C. R., Campoccia, D., Gamberini, S., Baldassarri, L., and Montanaro, L. (2005). Prevalence of cna, fnbA and fnbB adhesin genes among *Staphylococcus aureus* isolates from orthopedic infections associated to different types of implant. *FEMS Microbiol. Lett.* 246, 81–86. doi: 10.1016/j.femsle.2005.03.035

Aslantaş, Ö, and Demir, C. (2016). Investigation of the antibiotic resistance and biofilm-forming ability of *Staphylococcus aureus* from subclinical bovine mastitis cases. *J. Dairy Sci.* 99, 8607–8613. doi: 10.3168/jds.2016-11310

Avila-Novoa, M. G., González-Gómez, J. J., Guerrero-Medina, P. J., Cardona-López, M. A., Ibarra-Velazquez, L. M., Velazquez-Suarez, N. Y., et al. (2021). *Staphylococcus aureus* and methicillin-resistant S. aureus (MRSA) strains isolated from dairy products: Relationship of ica-dependent / independent and components of biofilms produced *in vitro*. *Int. Dairy J.* 119:105066. doi: 10.1016/j.idairyj.2021.105066

Avila-Novoa, M. G., Iñiguez-Moreno, M., González-Gómez, J. P., Zacarías-Castillo, E., Guerrero-Medina, P. J., Padilla-Frausto, J. J., et al. (2018a). Detection of enterotoxin genes of *Staphylococcus aureus* isolates from food contact surfaces in the dairy industry of Jalisco, Mexico. *Biotecnia* 20, 72–78. doi: 10.18633/biotecnia.v20i2.602

Avila-Novoa, M. G., Iñíguez-Moreno, M., Solís-Velázquez, O. A., González-Gómez, J. P., Guerrero-Medina, P. J., and Gutiérrez-Lomelí, M. (2018b). Biofilm formation by *Staphylococcus aureus* isolated from food contact surfaces in the dairy industry of Jalisco, Mexico. *J. Food Qual.* 2018b, 72–78.

Azara, E., Longheu, C., Sanna, G., and Tola, S. (2017). Biofilm formation and virulence factor analysis of *Staphylococcus aureus* isolates collected from ovine mastitis. *J. Appl. Microbiol.* 123, 372–379. doi: 10.1111/jam.13502

Azmi, K., Qrei, W., and Abdeen, Z. (2019). Screening of genes encoding adhesion factors and biofilm production in methicillin resistant strains of *Staphylococcus aureus* isolated from Palestinian patients. *BMC Genom.* 20:578. doi: 10.1186/s12864-019-5929-1

Bai, X., Nakatsu, C. H., and Bhunia, A. K. (2021). Bacterial biofilms and their implications in pathogenesis and food safety. *Foods* 10:2117.

Beceiro, A., Tomás, M., and Bou, G. (2013). Antimicrobial resistance and virulence: A successful or deleterious association in the bacterial world? *Clin. Microbiol. Rev.* 26, 185–230. doi: 10.1128/CMR.00059-12

Boles, B. R., and Horswill, A. R. (2008). Agr-mediated dispersal of *Staphylococcus aureus* biofilms. *PLoS Pathog.* 4:e1000052. doi: 10.1371/journal.ppat.1000052

Borucki, M. K., Peppin, J. D., White, D., Loge, F., and Call, D. R. (2003). Variation in biofilm formation among strains of *Listeria monocytogenes*. *Appl. Environ. Microbiol.* 69, 7336–7342. doi: 10.1128/AEM.69.12.7336-7342.2003

Bridier, A., Sanchez-Vizuete, P., Guilbaud, M., Piard, J. C., Naïtali, M., and Briandet, R. (2015). Biofilm-associated persistence of food-borne pathogens. *Food Microbiol.* 45, 167–178. doi: 10.1016/j.fm.2014.04.015

Brooks, J. D., and Flint, S. H. (2008). Biofilms in the food industry: Problems and potential solutions. *Int. J. Food Sci. Technol.* 43, 2163–2176. doi: 10.1111/j.1365-2621.2008.01839.x

Carrascosa, C., Raheem, D., Ramos, F., Saraiva, A., and Raposo, A. (2021). Microbial biofilms in the food industry–a comprehensive review. *Int. J. Environ. Res. Public Health* 18:2014. doi: 10.3390/ijerph18042014

Chaignon, P., Sadovskaya, I., Ragunah, C., Ramasubbu, N., Kaplan, J. B., and Jabbouri, S. (2007). Susceptibility of staphylococcal biofilms to enzymatic treatments depends on their chemical composition. *Appl. Microbiol. Biotechnol.* 75, 125–132. doi: 10.1007/s00253-006-0790-y

Chmielewski, R. A. N., and Frank, J. F. (2003). Biofilm formation and control in food processing facilities. *Compr. Rev. Food Sci. Food Saf.* 2, 22–32. doi: 10.1111/j.1541-4337.2003.tb00012.x

Ciftci, A., Findik, A., Onuk, E. E., and Savasan, S. (2009). Detection of methicillin resistance and slime factor production of *Staphylococcus aureus* in bovine mastitis. *Braz. J. Microbiol.* 40, 254–261.

Croes, S., Deurenberg, R. H., Boumans, M. L. L., Beisser, P. S., Neef, C., and Stobberingh, E. E. (2009). *Staphylococcus aureus* biofilm formation at the physiologic glucose concentration depends on the S. aureus lineage. *BMC Microbiol.* 9:229. doi: 10.1186/1471-2180-9-229

Cucarella, C., Solano, C., Valle, J., Amorena, B., Lasa, I., and Penadés, J. R. (2001). Bap, a *Staphylococcus aureus* surface protein involved in biofilm formation. *J. Bacteriol.* 183, 2888–2896. doi: 10.1128/JB.183.9.2888-2896.2001

Dai, J., Wu, S., Huang, J., Wu, Q., Zhang, F., and Zhang, J. (2019). Prevalence and characterization of *Staphylococcus aureus* isolated from pasteurized milk in China. *Front. Microbiol.* 10:641. doi: 10.3389/fmicb.2019.00641

Dakheel, K. H., Rahim, R. A., Neela, V. K., Al-obaidi, J. R., Hun, T. G., and Yusoff, K. (2016). Methicillin-resistant *Staphylococcus aureus* biofilms and their influence on bacterial adhesion and cohesion. *Biomed. Res. Int.* 2016:4708425. doi: 10.1155/2016/4708425

Derakhshan, S., Navidinia, M., and Haghi, F. (2021). Antibiotic susceptibility of human-associated *Staphylococcus aureus* and its relation to agr typing, virulence genes, and biofilm formation. *BMC Infect. Dis.* 21:627. doi: 10.1186/s12879-021-06307-0

Dewey-Mattia, D., Manikonda, K., Hall, A. J., Wise, M. E., and Crowe, S. J. (2018). Surveillance for foodborne disease outbreaks–United States, 2009-2015. *MMWR Surveill. Summ.* 67, 1–11. doi: 10.15585/mmwr.ss6710a1

Di Ciccio, P., Vergara, A., Festino, A. R., Paludi, D., Zanardi, E., Ghidini, S., et al. (2015). Biofilm formation by *Staphylococcus aureus* on food contact surfaces: Relationship with temperature and cell surface hydrophobicity. *Food Control.* 50, 930–936. doi: 10.1016/j.foodcont.2014.10.048

Elsayed, M. S. A. E., Roshdey, T., Salah, A., Tarabees, R., Younis, G., and Eldeep, D. (2019). Phenotypic and genotypic methods for identification of slime layer production, efflux pump activity, and antimicrobial resistance genes as potential causes of the antimicrobial resistance of some mastitis pathogens from farms in Menoufia, Egypt. *Mol. Biol. Rep.* 46, 6533–6546. doi: 10.1007/s11033-019-05099-6

Flemming, H. C., and Wingender, J. (2010). The biofilm matrix. *Nat. Rev. Microbiol.* 8, 623–633. doi: 10.1038/nrmicro2415

Flemming, H. C., Wingender, J., Szewzyk, U., Steinberg, P., Rice, S. A., and Kjelleberg, S. (2016). Biofilms: An emergent form of bacterial life. *Nat. Rev. Microbiol.* 14, 563–575. doi: 10.1038/nrmicro.2016.94

Fratesi, S. E., Lynch, F. L., Kirkland, B. L., and Brown, L. R. (2004). Effects of SEM preparation techniques on the appearance of bacteria and biofilms in the carter sandstone. *J. Sedimen. Res.* 74, 858–867. doi: 10.1306/042604740858

Fredheim, E. G. A., Klingenberg, C., Rohde, H., Frankenberger, S., Gaustad, P., Flægstad, T., et al. (2009). Biofilm formation by *Staphylococcus haemolyticus*. *J. Clin. Microbiol.* 47, 1172–1180. doi: 10.1128/JCM.01891-08

Fueyo, J. M., Mendoza, M. C., Rodicio, M. R., Mun, J., and Alvarez, M. A. (2005). Cytotoxin and pyrogenic toxin superantigen gene profiles of *Staphylococcus aureus* associated with subclinical mastitis in dairy cows and relationships with macrorestriction genomic profiles. *J. Clin. Microbiol.* 43, 1278–1284. doi: 10.1128/JCM.43.3.1278-1284.2005

Gogoi-Tiwari, J., Waryah, C. B., Eto, K. Y., Tau, M., Wells, K., Costantino, P., et al. (2015). Relative distribution of virulence-associated factors among Australian bovine *Staphylococcus aureus* isolates: Potential relevance to development of an effective bovine mastitis vaccine. *Virulence* 6, 419–423. doi: 10.1080/21505594.2015.1043508

Gutiérrez, D., Delgado, S., Vázquez-Sánchez, D., Martínez, B., Cabo, M. L., Rodríguez, A., et al. (2012). Incidence of *Staphylococcus aureus* and analysis of associated bacterial communities on food industry surfaces. *Appl. Environ. Microbiol.* 78, 8547–8554. doi: 10.1128/AEM.02045-12

Hall, C. W., and Mah, T. F. (2017). Molecular mechanisms of biofilm-based antibiotic resistance and tolerance in pathogenic bacteria. *FEMS Microbiol. Rev.* 41, 276–301. doi: 10.1093/femsre/fux010

Jamal, M., Ahmad, W., Andleeb, S., Jalil, F., Imran, M., Nawaz, M. A., et al. (2018). Bacterial biofilm and associated infections. *J. Chin. Med. Assoc.* 81, 7–11. doi: 10.1016/j.jcma.2017.07.012

Kaplan, J. B., LoVetri, K., Cardona, S. T., Madhyastha, S., Sadovskaya, I., Jabbouri, S., et al. (2012). Recombinant human DNase I decreases biofilm and increases antimicrobial susceptibility in staphylococci. *J. Antibiot.* 65, 73–77.

Kim, B. R., Bae, Y. M., and Lee, S. Y. (2016). Effect of environmental conditions on biofilm formation and related characteristics of *Staphylococcus aureus*. *J. Food Saf.* 36, 412–422. doi: 10.1111/jfs.12263

Kumar, A., Alam, A., Rani, M., Ehtesham, N. Z., and Hasnain, S. E. (2017). Biofilms: Survival and defense strategy for pathogens. *Int. J. Med. Microbiol.* 307, 481–489. doi: 10.1016/j.ijmm.2017.09.016

Kumar, R., Yadav, B. R., and Singh, R. S. (2010). Genetic determinants of antibiotic resistance in *Staphylococcus aureus* isolates from milk of mastitic crossbred cattle. *Curr. Microbiol.* 60, 379–386. doi: 10.1007/s00284-009-9553-1

Lade, H., Park, J. H., Chung, S. H., Kim, I. H., Kim, J. M., Joo, H. S., et al. (2019). Biofilm formation by *Staphylococcus aureus* clinical isolates is differentially affected by glucose and sodium chloride supplemented culture media. *J. Clin. Med.* 8:1853. doi: 10.3390/jcm8111853

Liu, H., Shang, W., Hu, Z., Zheng, Y., Yuan, J., Hu, Q., et al. (2018). A novel SigB(Q225P) mutation in *Staphylococcus aureus* retains virulence but promotes biofilm formation. *Emerg. Microbes Infect.* 7:72. doi: 10.1038/s41426-018-0078-1

Liu, K., Tao, L., Li, J., Fang, L., Cui, L., Li, J., et al. (2020). Characterization of *Staphylococcus aureus* isolates from cases of clinical bovine mastitis on large-scale Chinese dairy farms. *Front. Vet. Sci.* 7:580129. doi: 10.3389/fvets.2020.580129

Lorite, G. S., Rodrigues, C. M., Souza, A. A., De Kranz, C., Mizaikoff, B., and Cotta, M. A. (2011). The role of conditioning film formation and surface chemical changes on *Xylella fastidiosa* adhesion and biofilm evolution. *J. Colloid Interface Sci.* 359, 289–295. doi: 10.1016/j.jcis.2011.03.066

Lutskiy, M. Y., Avneri-Katz, S., Zhu, N., Itsko, M., Ronen, Z., Arnusch, C. J., et al. (2015). A microbiology-based assay for quantification of bacterial early stage biofilm formation on reverse-osmosis and nanofiltration membranes. *Sep. Purif. Technol.* 141, 214–220. doi: 10.1016/j.seppur.2014.12.003

Marques, S. C., Silva-Rezende, J. G., de Freitas-Alves, L. P., Cassia-Silva, B., Alves, E., de Abreu, L. R., et al. (2007). Formation of biofilms by *Staphylococcus aureus* on stainless steel and glass surfaces and its resistance to some selected chemical sanitiziers. *Braz. J. Microbiol.* 38, 538–543. doi: 10.1590/S1517-83822007000300029

McCarthy, H., Rudkin, J. K., Black, N. S., Gallagher, L., O'Neill, E., and O'Gara, J. P. (2015). Methicillin resistance and the biofilm phenotype in *Staphylococcus aureus*. *Front. Cell. Infect. Microbiol.* 5:1. doi: 10.3389/fcimb.2015.00001

Miao, J., Liang, Y., Chen, L., Wang, W., Wang, J., Li, B., et al. (2017). Formation and development of *Staphylococcus* biofilm: With focus on food safety. *J. Food Saf.* 37:e12358. doi: 10.1111/jfs.12358

Møretrø, T., and Langsrud, S. (2017). Residential bacteria on surfaces in the food industry and their implications for food safety and quality. *Compr. Rev. Food Sci. Food Saf.* 16, 1022–1041. doi: 10.1111/1541-4337.12283

Nguyen, V. H., Klai, N., Nguyen, T. D., and Tyagi, R. D. (2016). Impact of extraction methods on bio-flocculants recovered from backwashed sludge of bio-filtration unit. *J. Environ. Manage.* 180, 344–350.

O'Gara, J. P. (2007). Ica and beyond: Biofilm mechanisms and regulation in *Staphylococcus epidermidis* and *Staphylococcus aureus*. *FEMS Microbiol. Lett.* 270, 179–188. doi: 10.1111/j.1574-6968.2007.00688.x

O'Neill, E., Pozzi, C., Houston, P., Smyth, D., Humphreys, H., Robinson, D. A., et al. (2007). Association between methicillin susceptibility and biofilm regulation in *Staphylococcus aureus* isolates from device-related infections. *J. Clin. Microbiol.* 45, 1379–1388. doi: 10.1128/JCM.02280-06

Okshevsky, M., and Meyer, R. L. (2015). The role of extracellular DNA in the establishment, maintenance and perpetuation of bacterial biofilms. *Crit. Rev. Microbiol.* 41, 341–352. doi: 10.3109/1040841X.2013.841639

Oniciuc, E. A., Cerca, N., and Nicolau, A. I. (2016). Compositional analysis of biofilms formed by *Staphylococcus aureus* isolated from food sources. *Front. Microbiol.* 7:390. doi: 10.3389/fmicb.2016.00390

Otto, M. (2018). Staphylococcal biofilms. *Microbiol. Spectr.* 6, 1–26. doi: 10.1128/microbiolspec.GPP3-0023-2018

Paharik, A. E., and Horswill, A. R. (2016). The staphylococcal biofilm: Adhesin, regulation, and host response. *Microbiol. Spectr.* 4, 1–48. doi: 10.1128/microbiolspec.VMBF-0022-2015

Pereyra, E. A. L., Picech, F., Renna, M. S., Baravalle, C., Andreotti, C. S., Russi, R., et al. (2016). Detection of *Staphylococcus aureus* adhesion and biofilm-producing genes and their expression during internalization in bovine mammary epithelial cells. *Vet. Microbiol.* 183, 69–77. doi: 10.1016/j.vetmic.2015.12.002

Renner, L. D., and Weibel, D. B. (2011). Physicochemical regulation of biofilm formation. *MRS Bull.* 36, 347–355. doi: 10.1557/mrs.2011.65

Salgado-Ruiz, T. B., Rodríguez, A., Gutiérrez, D., Martínez, B., García, P., Espinoza-Ortega, A., et al. (2015). Molecular characterization and antimicrobial susceptibility of *Staphylococcus aureus* from small-scale dairy systems in the highlands of Central México. *Dairy Sci. Technol.* 95, 181–196. doi: 10.1007/s13594-014-0195-0

Sankar Ganesh, P., Krishnamurthy, V., ISwamy, K., Suvaithenamudhan, S., Amuthan, M., Vimali, I., et al. (2019). Biofilm-associated agr and sar quorum sensing systems of methicillin-resistant *Staphylococcus aureus* are inhibited by fruit extracts of *Illicium verum*. *Preprints* 2019:2019080096. doi: 10.20944/preprints201908.0096.v1

Schllcher, K., and Horswill, A. (2020). *Staphylococcal* biofilm development: Structure, regulation, and treatment strategies. *Microbiol. Mol. Biol. Rev.* 84, e26–e19. doi: 10.1128/MMBR.0026-19

Schwartz, K., Ganesan, M., Payne, D. E., Solomon, M. J., and Boles, B. R. (2016). Extracellular DNA facilitates the formation of functional amyloids in *Staphylococcus aureus* biofilms. *Mol. Microbiol.* 99, 123–134. doi: 10.1111/mmi.13219

Shukla, S. K., and Rao, T. S. (2013). Dispersal of bap-mediated *Staphylococcus aureus* biofilm by proteinase K. *J. Antibiot.* 66, 55–60. doi: 10.1038/ja.2012.98

Shukla, S. K., and Rao, T. S. (2017). *Staphylococcus aureus* biofilm removal by targeting biofilm-associated extracellular proteins. *Indian J. Med. Res.* 146, S1–S8. doi: 10.4103/ijmr.IJMR_410_15

Singh, S., Singh, S. K., Chowdhury, I., and Singh, R. (2017). Understanding the mechanism of bacterial biofilms resistance to antimicrobial agents. *Open Microbiol. J.* 11, 53–62. doi: 10.2174/1874285801711010053

Solis-Velazquez, O. A., Gutiérrez-Lomelí, M., Guerreo-Medina, P. J., Rosas-García, M. L., Iñiguez-Moreno, M., and Avila-Novoa, M. G. (2021). Nosocomial pathogen biofilms on biomaterials: Different growth medium conditions and components of biofilms produced *in vitro*. *J. Microbiol. Immunol. Infect.* 54, 1038–1047. doi: 10.1016/j.jmii.2020.07.002

Spiliopoulou, A. I., Krevvata, M. I., Kolonitsiou, F., Harris, L. G., Wilkinson, T. S., Davies, A. P., et al. (2012). An extracellular *Staphylococcus epidermidis* polysaccharide: Relation to polysaccharide intercellular adhesin and its implication in phagocytosis. *BMC Microbiol.* 12:76. doi: 10.1186/1471-2180-12-76

Srey, S., Jahid, I. K., and Ha, S. D. (2013). Biofilm formation in food industries: A food safety concern. *Food Control.* 31, 572–585. doi: 10.1016/j.foodcont.2012.12.001

Sugimoto, S., Sato, F., Miyakawa, R., Chiba, A., Onodera, S., Hori, S., et al. (2018). Broad impact of extracellular DNA on biofilm formation by clinically isolated Methicillin-resistant and -sensitive strains of *Staphylococcus aureus*. *Sci. Rep.* 8:2254. doi: 10.1038/s41598-018-20485-z

Taglialegna, A., Navarro, S., Ventura, S., Garnett, J. A., Matthews, S., Penades, J. R., et al. (2016). *Staphylococcal* bap proteins build amyloid scaffold biofilm matrices in response to environmental signals. *PLoS Patho.* 12:e1005711. doi: 10.1371/journal.ppat.1005711

Tang, J., Chen, J., Li, H., Zeng, P., and Li, J. (2013). Characterization of adhesin genes, staphylococcal nuclease, hemolysis, and biofilm formation among *Staphylococcus aureus* strains isolated from different sources. *Foodborne Pathog. Dis.* 10, 757–763. doi: 10.1089/fpd.2012.1474

Tsang, L. H., Cassat, J. E., Shaw, L. N., Beenken, K. E., and Smeltzer, M. S. (2008). Factors contributing to the biofilm-deficient phenotype of *Staphylococcus aureus* sarA mutants. *PLoS One.* 3:e3361. doi: 10.1371/journal.pone.0003361

Vergara, A., Normanno, G., Di Ciccio, P., Pedonese, F., Nuvoloni, R., Parisi, A., et al. (2017). Biofilm formation and its relationship with the molecular characteristics of food-related methicillin-resistant *Staphylococcus aureus* (MRSA). *J. Food Sci.* 82, 2364–2370. doi: 10.1111/1750-3841.13846

Zaatout, N., Ayachi, A., and Kecha, M. (2020). Epidemiological investigation of subclinical bovine mastitis in Algeria and molecular characterization of biofilm-forming *Staphylococcus aureus*. *Trop. Anim. Health Prod.* 52, 283–292. doi: 10.1007/s11250-019-02015-9

Zhang, D. X., Li, Y., Yang, X. Q., Su, H. Y., Wang, Q., Zhang, Z. H., et al. (2020). *In vitro* antibiotic susceptibility, virulence genes distribution and biofilm production of *Staphylococcus aureus* isolates from bovine mastitis in the Liaoning province of China. *Infect. Drug Resist.* 13, 1365–1375. doi: 10.2147/IDR.S247765

Frontiers in Microbiology

Explores the habitable world and the potential of microbial life

The largest and most cited microbiology journal which advances our understanding of the role microbes play in addressing global challenges such as healthcare, food security, and climate change.

Discover the latest Research Topics

See more →

Frontiers

Avenue du Tribunal-Fédéral 34
1005 Lausanne, Switzerland
frontiersin.org

Contact us

+41 (0)21 510 17 00
frontiersin.org/about/contact